Option Pricing and Hedging Analysis under Regime-switching Models

by

Chao Qiu

A thesis
presented to the University of Waterloo
in fulfillment of the
thesis requirement for the degree of
Doctor of Philosophy
in
Actuarial Science

Waterloo, Ontario, Canada, 2013

I hereby declare that I am the sole author of this thesis. This is a true copy of the thesis, including any required final revisions, as accepted by my examiners.

I understand that my thesis may be made electronically available to the public.

Chao Qiu

Abstract

This thesis explores option pricing and hedging in a discrete time regime-switching environment. If the regime risk cannot be hedged away, then we cannot ignore this risk and use the Black-Scholes pricing and hedging framework to generate a unique pricing and hedging measure. We develop a risk neutral pricing measure by applying an Esscher Transform to the real world asset price process, with the focus on the issue of incompleteness of the market. The Esscher transform turns out to be a convenient and effective tool for option pricing under the discrete time regime switching models. We apply the pricing measure to both single variate European options and multivariate options. To better understand the effect of the pricing method, we also compared the results with those generated from two other risk neutral methods: the Black-Scholes model, and the natural equivalent martingale method.

We further investigate the difference in hedging associated with different pricing measures. This is of interest when the choice of pricing method is uncertain under regime switching models. We compare four hedging strategies: delta hedging for the three risk neutral pricing methods under study, and mean variance hedging. We also develop a more general tool of tail ordering for hedging analysis in a general incomplete market with the uncertainty of the risk neutral measures. As a result of the analysis, we propose that pricing and hedging using the Esscher transform may be an effective strategy for a market where the regime switching process brings uncertainty.

Acknowledgements

First and foremost, I would like to express my deepest gratitude to my supervisors Professor Mary Hardy, who has kindly advised me into this interesting, challenging, and rewarding research area. Thanks also to Professor Chengguo Weng and Professor Joseph Kim for their continuous supports, guidance and encouragement throughout the courses of this thesis. Besides my supervisors, I also sincerely thank the rest of my thesis committee: Professor Ken Seng Tan, Professor David Saunders, Professor Rogemar Mamon, and Professor Margaret Insley for their insightful comments and valuable suggestions.

Table of Contents

List of Tables

List of Figures

Chapter 1

Pricing European Options under Markov Regime-switching Models with the Esscher Transform

1.1 Introduction

The regime switching framework for modeling econometric series provides an intuitive and transparent way to capture market behaviors under different economic conditions. Markov regime switching process have been widely used in econometrics since the pioneering work of Hamilton (1989). In actuarial applications, Hardy (2001) used a discrete time regime switching process for modeling long term index prices and pricing derivatives, and in Hardy (2003) and Hardy et al (2006), the model was used for risk management of maturity guarantees in equity linked insurance. Many other authors, including Duan et al. (2002), Bollen (1998), Mamon and Rodrigo (2005), Elliott et al. (2005), and Liew and Siu (2010) have considered option pricing under various different Markov regime switching models, while Boyle and Liew (2007) and Till (2011) investigated the optimization of hedge fund asset allocation under a regime switching economic model.

My thesis explores an option pricing approach and conducts delta hedging anal-

ysis in a discrete time regime switching environment. The object of this chapter is the pricing of a European option in a market where there is one risky asset and one risk free asset. We focus on the issue of market incompleteness associated with the regime switching process. We develop a martingale pricing scheme, where the equivalent martingale probability measure is identified using the Esscher Transform technique. To do this, we will first specify the market model, discuss the incompleteness issue, and review some well-documented risk neutral pricing methods developed for the regime switching environment in the literature and distinguish our work from them.

For readers' convenience, I denote the source of cited definitions, lemmas, and propositions in my thesis, and use the annotation CQ to indicate my contribution to this work.

1.1.1 Model

A regime switching model can be expressed as a bivariate process, say $\{\rho_t, Y_t\}$, where ρ_t denotes the regime process and Y_t represents the process, whose conditional distribution at time t depends on the time t regime, ρ_t (Hamilton, 1989). In some cases, the distribution of Y_t is solely determined by the regime at time t. In these cases, we may label the distribution with the single regime state ρ_t. That is, conditional on ρ_t, $Y_t \sim F_{\rho_t}$, where F_{ρ_t} represents the conditional distribution function determined by ρ_t. The structure of this model is illustrated in Figure 1.1. In more complicated models, the distribution of Y_t may depend on other information, such as the lagged values of Y_t. In this thesis, we focus on the former one with a discrete time Markov regime switching process. Although some of the results may be generalized, for example, to regime switching auto-regressive processes, this development is left for future research.

The underlying model in our study is

$$(B_t, S_t)_{0 \le t \le T}, \tag{1.1.1}$$

where B_t and S_t denote respectively the prices of a bond and a stock index at time

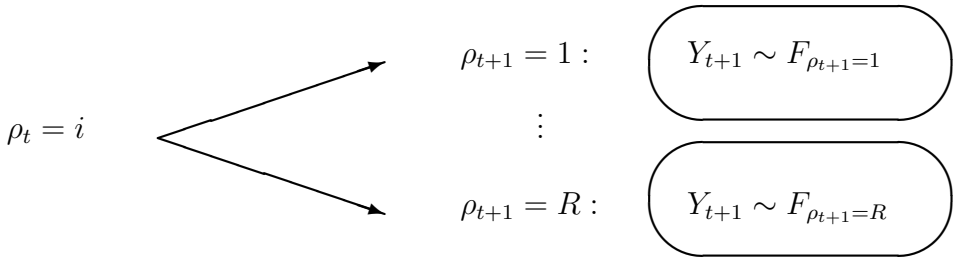

Figure 1.1: Decomposition of uncertainty for Y_{t+1} under regime switching models

t. Assume a constant risk free rate of return r is associated with the bond. Then, the price processes of the assets are

$$\begin{cases} B_t &= B_0\, e^{rt} \\ S_t &= S_0\, \exp(\sum_{1\le s\le t} Y_s), \end{cases} \tag{1.1.2}$$

where the return process e^{Y_s} follows a Markov regime switching model with, say, R regimes, where R is a positive integer. Let $\mathcal{F}_t^Y$ and $\mathcal{F}_t^\rho$ denote the $\mathbb{P}$-augmentation of the natural filtrations generated by the yield process $\{Y_s\}_{s=0}^t$ and the regime process $\{\rho_s\}_{s=0}^t$, separately. Then, we write $\mathcal{F}_t = \mathcal{F}_t^Y \vee \mathcal{F}_t^\rho$ representing the minimal sigma algebra containing $\mathcal{F}_t^Y$ and $\mathcal{F}_t^\rho$. It is worth noting that we assume here that we can observe ρ_t given the filtration $\mathcal{F}_t$. We do not consider (ρ_t) as a hidden Markov chain process, although this is a more realistic assumption for applications. In practice, assuming a hidden Markov regime switching model, we may use the historical data of the underlying asset to calibrate the model and identify ρ_t. For a detailed discussion, see, for example, Till (2011). Alternatively, the model for regimes may be specified under $\mathbb{Q}$ measure, after identifying the model for regimes under the $\mathbb{Q}$ measure and calibrating the model using the corresponding derivative data in the market. In this thesis, the Markov model is specified under measure $\mathbb{P}$ and $\rho_t \in \mathcal{F}_t$. Based on the filtration, we have the following additional assumptions for $t = 1, \ldots, T$.

(A1) ρ_t follows a finite state Markov chain process;

(A2) Y_t is a continuous random variable; and the distribution of Y_t conditional on ρ_t is independent of $\rho_s, s \neq t$.

(A3) $\operatorname{ess\,inf} Y_t < r < \operatorname{ess\,sup} Y_t$; and the moment generating function exists for Y_t under $\mathbb{P}$ measure.

If we do not consider the model with $Y_t \equiv r$, then the condition $\operatorname{ess\,inf} Y_t < r < \operatorname{ess\,sup} Y_t$ in (A3) is necessary for a non-trivial arbitrage free model. The existence of moment generating function is a necessary condition for our pricing method.

1.1.2 Incompleteness of the Markets under the Regime Switching Models

We first analyze the randomness of log return random variables Y_t, and then discuss the issue of market incompleteness. As illustrated in Figure 1.1, the randomness of Y_{t+1} under a Markov regime switching model can be decomposed into two parts: the part from the regime switching process and the part within each regime. In view of the above decomposition on the log return, we may price a European option, as the discounted expected payoff under a chosen equivalent martingale measure $\mathbb{Q}$, through the law of iterated expectation as follows. Recall that $\mathcal{F}_t = \mathcal{F}_t^Y \vee \mathcal{F}_t^\rho$. Based on the filtration $\mathcal{F}_t$, the price of a European option with payoff $H(S_T)$ is

$$P_t := P_t(H(S_T)) \quad = \quad e^{-r(T-t)} \mathsf{E}^{\mathbb{Q}}[\, H(S_T) \,|\, \mathcal{F}_t^Y \vee \mathcal{F}_t^\rho \,], \tag{1.1.3}$$

where $\mathsf{E}^{\mathbb{Q}}$ denotes the expectation under $\mathbb{Q}$ measure. We will specify $\mathsf{E}^{\mathbb{Q}}$ in our pricing method later. Based on the Markov property of the regime switching process $(\rho_t)_{t=0}^T$, equation (1.1.3) can be rewritten, using the law of iterated expectation, as

$$P_t = e^{-r} \mathsf{E}^{\mathbb{Q}} \left[\mathsf{E}^{\mathbb{Q}} \left[H(S_T) \,|\, \{Y_s\}_{s=1}^t, \rho_{t+1} \right] \,|\{Y_s\}_{s=1}^t, \rho_t \right] \tag{1.1.4}$$

In (1.1.4), there are two pricing steps related to the two parts of the randomness of Y_t. In step one, conditional on ρ_{t+1}, the price $\mathsf{E}^{\mathbb{Q}} \left[H(S_T) | \mathcal{F}_t^Y, \rho_{t+1} \right]$ is determined.

Then in step two, the price P_t is obtained by averaging over regimes ρ_{t+1}. The filtration for the out expectation is $\mathcal{F}_t$ while the $\sigma-$field for the inner expectation at time t is $\sigma(\mathcal{F}_t \vee \{\rho_{t+1}\})$

It is also worth noting that no perfect replication strategy exists for the option pricing process under our model, since it is assumed that there is no replicating process available for regime switching. As an illustration, Figure 1.2 uses a simplified pricing tree for a two-state regime switching model, with different payoffs under different regimes. In the tree, the only opportunity to replicate the payoffs is at the square box. Assume that we have different replicating strategies with respect to different regimes ρ_{t+1}. In this case, even if the replicating can be perfect conditional on ρ_{t+1}, with the uncertainty of the regime switching, the payoff cannot be replicated. Thus, this market must be incomplete. In my thesis, we assume a continuous random variable Y_t in a discrete time model; the conditional distribution of Y_t given the filtration $\mathcal{F}_t$ reflects both the uncertainty of regime switching and the uncertainty within each regime.

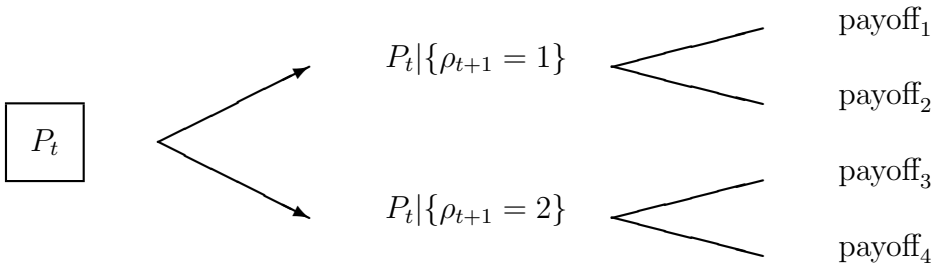

Figure 1.2: Illustration of the uncertainty for pricing under regime switching models

1.1.3 Distinction of Our Approach

This chapter addresses option pricing and hedging under discrete time Markov regime switching models. This section briefly distinguishes our pricing approach from those in the existing literature. The pricing approach used by previous authors can be expressed as a double expectation, with the inner expectation conditional on the

physical path of regime transition, as follows

$$P_t = e^{-r\,(T-t)}\,\mathsf{E}_t^{\mathbb{P}}(\,\mathsf{E}_t^{\mathbb{Q}}[\,H(S_T)\,|\,\rho_s, s = t+1,\ldots,T\,]\,), \tag{1.1.5}$$

where $H(S_T)$ represents the contingent claim of the derivative, $\mathsf{E}_t^{\mathbb{P}} = \mathsf{E}^{\mathbb{P}}(\cdot\,|\,\mathcal{F}_t)$ represents the expectation under the physical probability measure given information by time t, and $\mathsf{E}_t^{\mathbb{Q}} = \mathsf{E}^{\mathbb{Q}}(\cdot\,|\,\mathcal{F}_t)$ represents the expectation under the risk neutral probability measure $\mathbb{Q}$, given information by time t. In (1.1.5), the formula uses $\mathbb{P}$-measure to specify the probability distribution associated with the future regime switching paths $(\rho_s)_{s=t+1}^{T}$. An example of this distribution is given as the distribution of sojourn in each regime along a regime switching path; see, for example, Hardy (2001) for more details. Under $\mathbb{Q}$-measure in (1.1.5), the log-return process in each regime is adjusted to be risk neutral, i.e.,

$$\mathsf{E}^{\mathbb{Q}}(e^{Y_t}|\rho_t) = e^{r}.$$

We will term this pricing formula (1.1.5) for *the natural equivalent martingale measure method* (NEMM). You can find this pricing method in Hardy (2001), Elliott et al. (2005) and Liew and Siu (2010), and many others. In this formula, there is no satisfactory explanation for using the $\mathbb{P}$ measure for the outer expectation. Assuming (as we do) that the regime switching risk is non-diversifiable, and that it is non-replicable, there should be a price of this risk, and the use of the $\mathbb{P}$-measure for the expectation fails to allow for the price of regime switching risk. For more discussion on the pricing of the outer expectation, see, for example, Siu (2011), which supports the case that this approach does not price the systemic regime risk.

An alternative approach to option pricing is through identifying an equivalent martingale measure (EMM), taking account of the joint risk factors (ρ_t) and (Y_t). Some pricing measures have been explored using this approach. Two interesting examples proposed in the literature are as follows.

For a continuous time Markov regime switching model, Naik (1993) proposed an equivalent martingale measure assuming there are state prices associated with regime

switching. However, this approach does not seem to have been developed further, and identifying the state prices remains a challenge.

Another equivalent martingale measure in an incomplete market model is the so–called minimal martingale measure (Föllmer and Schweizer, 1991), found by minimizing the quadratic function of hedging errors. However, Elliott and Madan (1998) show that the minimal martingale measure is not a practical measure since its existence requires that S_t is restrictively bounded from above. Usually S_t (and, hence Y_t) are assumed unbounded, for example, assuming a normal distribution for Y_t. In this situation, the minimization of quadratic functions of hedging errors will not avoid arbitrage opportunities.

Therefore, the measures used in the above two examples are not practical measures. In this chapter, we identify an equivalent martingale measure under discrete time Markov regime switching models by applying the Esscher Transform. The Esscher transform has previously been applied to the pricing formula (1.1.5) by Elliott et al. (2005). However, their method implicitly assumes that the regime switching risk is diversifiable. In this work, we use the Esscher transform to identify the $\mathbb{Q}$ measure, with the incorporation of the non-diversifiable regime risk, and derive option prices that are therefore different from the NEMM prices.

The Esscher Transform is a convenient tool for tilting a distribution, which has a long history of application in actuarial science (eg, Kahn, 1962). It has been used to determine the risk premium in insurance, as in Bühlmann (1980, 1983) and Bühlmann et al. (1996, 1998). Gerber and Shiu (1994) pioneered its application in identifying the risk neutral measure to value options for Lévy processes. Its application in incomplete market financial problems highlights the important role of actuarial methods in risk management.

In the remaining part of the present chapter, we will identify the equivalent martingale measure and deduce the resulting distribution of the underlying asset prices; then, we specifically derive the European option prices under the two state regime switching lognormal (RSLN2) models. The Esscher transform can be justified theoretically as the measure which maximizes an expected power utility, but in the option pricing context, it is not clear exactly what this means, compared with prices

generated by different EMMs. By developing the Esscher transform pricing formula, we can compare the price and the implied hedge strategy with other EMMs.

1.2 No-arbitrage Pricing Approach by Using the Esscher Transform

In an incomplete market model, any martingale measure which is equivalent to the physical measure, is a potential pricing measure. We employ the Esscher transform to identify a specific equivalent martingale measure (EMM), from the range of EMMs, and use the resulting measure to price options. The obtained prices are compared with two other related risk neutral approaches: the Black–Scholes formula (BS) and the natural equivalent martingale measure method (NEMM).

We will first recall the general framework of a martingale approach for no-arbitrage pricing under discrete time models, and then introduce the Esscher Transform. The absence of arbitrage opportunities in a discrete time multiperiod model is defined similar to the definition in a single period model as follows (see Föllmer and Schied (2004) chapter one). Consider a market of one risk free asset S_t^0 with constant rate of return r and m risky assets. Denote $\mathbf{S}_t = (S_t^0, \ldots, S_t^m)$; the price process $(\mathbf{S}_t)_{0 \le t \le N}$ is adapted to a filtration $(\mathcal{F}_t)_{0 \le t \le T}$. Let $\xi = (\xi_t)_{0 \le t \le T}$ denote a trading strategy, where ξ_t is $\mathcal{F}_t$-measurable and $\xi_t = (\xi_t^0, \ldots, \xi_t^m)$ with ξ_t^i representing the units of asset i in the strategy at time t.

Definition 1.2.1. (Resnick, 1999) A strategy ξ is a self-financing trading strategy if

$$\xi_t \cdot \mathbf{S}_{t+1} = \xi_{t+1} \cdot \mathbf{S}_{t+1}, \qquad 0 \le t \le T-1$$

That is, the changes of the portfolio is due to the change of the underlying stock prices.

Definition 1.2.2. (Panjer, H. (Ed.), 1998) In a multi-period securities market

model, an arbitrage opportunity is a self-financing strategy (ξ_t) such that

$$\xi_0 \cdot \mathbf{S}_0 \leq 0, \quad \text{and} \quad \xi_T \cdot \mathbf{S}_T \geq 0 \quad \text{with} \quad \mathbb{P}(\xi_T \cdot \mathbf{S}_T > 0) > 0. \tag{1.2.6}$$

A securities market model is no-arbitrage if there is no arbitrage opportunities.

The no-arbitrage condition of a market model is achieved through the existence of the so-called equivalent risk-neutral measure, or equivalent martingale measure. In the context of the relationship between numéraires and measure changes, the risk neutral measure in our case is associated with the money market account as the numéraire.

Definition 1.2.3. (Föllmer and Schied 2004) A risk-neutral measure is a probability measure $\mathbb{Q}$ satisfying $\mathsf{E}^{\mathbb{Q}}(S_t) < \infty$ and

$$S_t^i = \mathsf{E}^{\mathbb{Q}}\left(e^{-r} S_{t+1}^i | \mathcal{F}_t\right), \quad i = 0, \ldots, m; \; t = 0, 1, \ldots$$

Two probability measures $\mathbb{Q}$ and $\mathbb{P}$ defined on a same measurable space $(\Omega, \mathcal{F})$ are said to be equivalent, denoted as $\mathbb{Q} \sim \mathbb{P}$, if, for $A \in \mathcal{F}$, $\mathbb{Q}(A) = 0$ if and only if $\mathbb{P}(A) = 0$. Based on Definition 1.2.3, we define the set of equivalent martingale measures (EMM) as follows

$$\mathcal{Q} = \{\mathbb{Q} \,|\, \mathbb{Q} \text{ is a risk-neutral measure with } \mathbb{Q} \sim \mathbb{P}\}, \tag{1.2.7}$$

where $\mathbb{P}$ is the physical probability measure. Based on the EMMs, we have the following well-known results known as the Fundamental Theorem of Asset Pricing.

Lemma 1.2.1. *(Föllmer and Schied 2004) A market model is arbitrage-free if and only if $\mathcal{Q}$ is a nonempty set.*

Proof. See the proof of Theorem 1.6 in Föllmer and Schied (2004). □

A European derivative on the underlying assets $S_T^i, i = 0, \ldots m$ has a payoff $H = g(S_T^0, \ldots, S_T^m)$, where g is a measurable function on R^{m+1}. After introducing

the derivative for a price at time t, denoted by $P_t(H)$, the market is expanded by having a new asset with the initial price at time t as follows:

$$S_t^{m+1} := P_t(H) \tag{1.2.8}$$

We intent to identify the price $P_t(H)$ which does not generate arbitrage opportunities in the expanded market.

Definition 1.2.4. (Föllmer and Schied 2004) We call the real number $P_t(H) \geq 0$ a no-arbitrage price of the derivative with payoff H, if this expanded market through (1.2.8) is arbitrage-free.

Then, the set of no-arbitrage prices of the derivatives are as follows.

Lemma 1.2.2. *(Föllmer and Schied 2004) Assume that the set $\mathcal{Q}$ of equivalent martingale measures, defined in (1.2.7), for the market model is non-empty. Then the set of arbitrage-free prices at time t, denoted by $\mathcal{P}_t(H)$, of a contingent claim H is non-empty and*

$$\mathcal{P}_t(H) = \left\{ E^{\mathbb{Q}}\left(e^{-r(T-t)}H \,|\, \mathcal{F}_t\right) \middle|\, \mathbb{Q} \in \mathcal{Q} \,\text{such that}\, E^{\mathbb{Q}}(H \,|\, \mathcal{F}_t) < \infty \; a.s. \right\}$$

Proof. See proof of Theorem 1.30 in Föllmer and Schied (2004). □

Next, we introduce the tool to identifying the EMM: the Esscher transform of a random variable Y, defined as

$$\mathcal{E} := \frac{e^{h\,Y}}{\mathsf{E}^{\mathbb{P}}[e^{h\,Y}]}, \tag{1.2.9}$$

where $\mathsf{E}^{\mathbb{P}}$ denotes the expectation under the physical probability measure $\mathbb{P}$. In (1.2.9), $\mathsf{E}^{\mathbb{P}}[e^{h\,Y}]$ is the moment generating function of Y under $\mathbb{P}$–measure, if it exists, for some constant h, named the Esscher transform parameter. We always assume, throughout the chapter, that the moment generating functions $\mathsf{E}^{\mathbb{P}}[e^{hY_t}]$ exist over their corresponding domains. For a discrete time adapted process $\{Y_t, \mathcal{F}_t\}_{t=1}^{T}$, we use

conditional Esscher transform (Bühlmann et al., 1996) as defined below:

$$\tilde{\mathcal{E}} := \prod_{t=1}^{T} \frac{e^{h_t Y_t}}{\mathsf{E}^{\mathbb{P}}[e^{h_t Y_t} | \mathcal{F}_{t-1}]}, \tag{1.2.10}$$

where $\{h_t\}_{t=1}^{T}$ is a sequence of random variables, with h_t adapted to $\mathcal{F}_{t-1}$, treated as parameters in the transform. Using the conditional Esscher transform with appropriately chosen parameters $\{h_t\}_{t=1}^{T}$, we can generate an EMM (denoted by $\mathbb{Q}$) from the physical probability measure $\mathbb{P}$ as we will specify later on.

Now, we apply the conditional Esscher transform to the Markov regime switching models. Recall that S_t denotes the price of the stock on which the option under consideration is written, and the log-returns

$$Y_t = \log \frac{S_t}{S_{t-1}}, \text{ for } t = 1, \ldots, T,$$

where T denotes the expiration date of the option; the filtration $\mathcal{F}_t := \mathcal{F}_t^Y \vee \mathcal{F}_t^\rho$ with $\mathcal{F}_t^Y$ and $\mathcal{F}_t^\rho$ being the $\mathbb{P}$-augmentation of the natural filtrations generated by the log-return process $\{Y_s\}_{s=0}^{t}$ and the regime process $\{\rho_s\}_{s=0}^{t}$ respectively. Based on Lemma 1.2.2, the price of the option, with a payoff $H(S_T)$, at time s for $s = 1, \ldots, T$, is given by

$$P_s(H(S_T)) \;=\; e^{-r(T-s)} \mathsf{E}^{\mathbb{Q}}[\, H(S_T) \,|\, \mathcal{F}_s], \tag{1.2.11}$$

where $\mathsf{E}^{\mathbb{Q}}$ means the expectation under an equivalent martingale measure $\mathbb{Q}$. We define $\mathbb{Q}$-measure through the following Radon-Nikodym derivative with respect to $\mathbb{P}$ on $\mathcal{F}_s$:

$$\left.\frac{d\mathbb{Q}}{d\mathbb{P}}\right|_{\mathcal{F}_s} \;=\; \prod_{t=1}^{s} \frac{e^{h_t^* Y_t}}{\mathsf{E}^{\mathbb{P}}[e^{h_t^* Y_t} |\, \mathcal{F}_{t-1}]}, \tag{1.2.12}$$

where the parameter h_t^* is a $\mathcal{F}_{t-1}$-measurable random variable satisfying

$$e^r = \frac{\mathsf{E}^{\mathbb{P}}[e^{(h_t^*+1)\,Y_t} \mid \mathcal{F}_{t-1}]}{\mathsf{E}^{\mathbb{P}}[e^{h_t^*\,Y_t} \mid \mathcal{F}_{t-1}]}, \quad \text{for } t = 1, \ldots, s. \tag{1.2.13}$$

It is worth noting that, for $s' < s$,

$$\left.\frac{d\mathbb{Q}}{d\mathbb{P}}\right|_{\mathcal{F}_{s'}} = \mathsf{E}^{\mathbb{P}}\left[\left(\left.\frac{d\mathbb{Q}}{d\mathbb{P}}\right|_{\mathcal{F}_s}\right)\middle|\,\mathcal{F}_{s'}\right].$$

Hereafter, we call the probability measure $\mathbb{Q}$ obtained through equation (1.2.12) conditional Esscher transform $\mathbb{Q}$ measure (abbreviated ET-$\mathbb{Q}$), as the right hand side of (1.2.12) is a conditional Esscher transform.

As we can see shortly in Proposition 1.2.1, the ET-$\mathbb{Q}$ is a uniquely determined EMM. To establish such a result, we first need to recall the definition of stochastic ordering and some of its properties.

Definition 1.2.5. (Ross, 1996) (a). Let Y be a random variable with support $[a, b]$ under two equivalent probability measures $\mathbb{Q}_1$ and $\mathbb{Q}_2$. Y is said to be stochastically larger under $\mathbb{Q}_1$ than under $\mathbb{Q}_2$, denoted $\mathbb{Q}_1 \geq_{st} \mathbb{Q}_2$, if

$$\mathbb{Q}_1(Y > y) \geq \mathbb{Q}_2(Y > y), \quad \forall\ y \in \mathbb{R}. \tag{1.2.14}$$

(b). Y is strictly larger under $\mathbb{Q}_1$ than under $\mathbb{Q}_2$, denoted by $\mathbb{Q}_1 >_{st} \mathbb{Q}_2$, if (1.2.14) holds with "$\geq$" replaced by "$>$" for some y.

Lemma 1.2.3. *(Ross, 1996) If $\mathbb{Q}_1 \geq_{st} \mathbb{Q}_2$ for a random variable Y, then*

$$E^{\mathbb{Q}_1}[\,g(Y)\,] \geq E^{\mathbb{Q}_2}[\,g(Y)\,] \tag{1.2.15}$$

for any increasing function g defined on the support of Y.

Proof. See proposition 9.1.2 in Ross (1996). □

We can also characterize stochastic ordering between two probability measures by their Radon Nikodym derivative as shown in the next lemma.

Lemma 1.2.4. *(**CQ**) Let Y be a random variable with support $[a, b]$, where $a, b \in \mathbb{R}$ and a and b can be $-\infty$ and ∞ respectively. Assume that under two probability measures $\mathbb{Q}_1$ and $\mathbb{Q}_2$, a continuous random variable Y has positive density functions $f^{\mathbb{Q}_1}(y)$ and $f^{\mathbb{Q}_2}(y)$ with regard to the Lebesgue measure, respectively. If the densities satisfy $f^{\mathbb{Q}_1}(y) = g(y)\, f^{\mathbb{Q}_2}(y)$ for a continuous non-negative and strictly increasing function g, then $\mathbb{Q}_1 >_{st} \mathbb{Q}_2$.*

Proof. First note that there must exist a constant $y_0 \in (a, b)$ such that

$$\begin{cases} g(y) < 1, & y < y_0, \\ g(y) > 1, & y > y_0. \end{cases} \tag{1.2.16}$$

Otherwise, if $g(y) > 1$ for all $y \in \mathbb{R}$, then we must have

$$\int_a^b f^{\mathbb{Q}_1}(y)\, dy > \int_a^b f^{\mathbb{Q}_2}(y)\, dy,$$

which contradicts the assumption that both $f^{\mathbb{Q}_1}$ and $f^{\mathbb{Q}_2}$ are density functions and hence both integrals in the last display are equal to one. Similarly, we could achieve a contradiction by assuming $g(y) < 1$ for all $y \in \mathbb{R}$. Thus, taking into account the continuous and strictly increasing properties of g, we immediately know that the claim in (1.2.16) is true.

Next, we shall show that $\mathbb{Q}_1(\, Y > y_1\,) > \mathbb{Q}_2(\, Y > y_1\,)$ holds for all $y_1 \in (a, b)$. We prove this by considering the following mutually exclusive cases, with regard to the position of y_1, respectively as below.

(i) If $y_1 \leq y_0$. Then, $0 < g(y) < 1$ for $a < y < y_1$. Hence,

$$\int_a^{y_1} g(y) f^{\mathbb{Q}_2}(y)\, dy < \int_a^{y_1} f^{\mathbb{Q}_2}(y)\, dy,$$

which immediately implies that $\mathbb{Q}_1(\, Y > y_1\,) > \mathbb{Q}_2(\, Y > y_1\,)$ for all $a < y_1 \leq y_0$. If $a < y_1 < y_0$, then $f(y_1) > 0$.

(ii) If $y_0 < y_1 < b$. Then, $g(y) > 1$ for $y_1 < y < b$; and hence

$$\int_{y_1}^{b} g(y) f^{\mathbb{Q}_2}(y)\, dy > \int_{y_1}^{b} f^{\mathbb{Q}_2}(y)\, dy,$$

which immediately implies that $\mathbb{Q}_1(\, Y > y_1\,) > \mathbb{Q}_2(\, Y > y_1\,)$ for all $y_1 \in (y_0, b)$.

□

Remark 1.2.1. In the following proposition, we state the result of identify a unique (up to almost surely) $\mathcal{F}_{t-1}$-measurable random variable h_t^* through solving the equation (1.2.13). To make the proof easy to carry out, we focus on the regime switching models with the filtration specified by $\mathcal{F}_t = \mathcal{F}_t^Y \vee \mathcal{F}_t^\rho$, even though the proof can be extended to other filtration.

Proposition 1.2.1. *(CQ) Suppose $\mathcal{F}_t = \mathcal{F}_t^Y \vee \mathcal{F}_t^\rho$. Define conditional cumulant generating functions*

$$\Psi_{t-1}(h_t) = \log \mathbb{E}^{\mathbb{P}}\left[e^{h_t Y_t} | \mathcal{F}_{t-1}\right], \text{ for } t = 1, \ldots, T, \text{ and } h_t \in \mathbb{R}.$$

Assume that the domain of $\Psi_{t-1}(h_t)$ is non-empty with the boundaries (u_1, u_2), where $u_1 + 1 < u_2$ and u_1 and u_2 can be $-\infty$ and ∞ respectively. Assume $\Psi_{t-1}(h_t)$ tends to infinity at the boundary u_1 if $-\infty < u_1$, and at the boundary u_2 if $u_2 < \infty$, almost surely, and suppose that for each t, $\Psi_{t-1}(h_t)$ is strictly convex and twice differentiable almost surely. Furthermore, we assume that $\mathbb{P}(Y_t > r|\mathcal{F}_{t-1}) > 0$ and $\mathbb{P}(Y_t < r|\mathcal{F}_{t-1}) > 0$ hold almost surely for all $t = 1, 2, \ldots, T$. Then, we have the following results:

(a) There exists a unique (up to almost surely) $\mathcal{F}_{t-1}$-measurable random variable h_t^* satisfying equation (1.2.13).

(b) The probability measure $\mathbb{Q}$ defined by the Radon-Nikodym derivative (1.2.12) with condition (1.2.13) is an EMM.

Proof. (a). For notational convenience, in this proof, denote $\mathcal{F}_{t-1} := (Y_1, \ldots, Y_{t-1}, \rho_0, \ldots, \rho_{t-1})$ in this proof. Similarly, $f(y_t|\mathcal{F}_{t-1}) = f(y_t|Y_1, \ldots, Y_{t-1}, \rho_0, \ldots, \rho_{t-1})$, as the

density defined for the random variable Y_t conditional on $Y_1, \ldots, Y_{t-1}, \rho_0, \ldots, \rho_{t-1}$. To show that there is a unique solution h_t^* given $\mathcal{F}_{t-1}$ in (1.2.13), let

$$f^{h_t}(y_t|\mathcal{F}_{t-1}) = \frac{e^{h_t y_t}}{\mathsf{E}^{\mathbb{P}}(e^{h_t Y_t}|\mathcal{F}_{t-1})} f(y_t|\mathcal{F}_{t-1}) \tag{1.2.17}$$

be the Esscher Transformed density generated from $f(y_t|\mathcal{F}_{t-1})$, the physical density of Y_t conditional on $\mathcal{F}_{t-1}$. Accordingly, we will use $\mathsf{E}^{h_t}(\cdot|\mathcal{F}_{t-1})$ to denote the expectation under the above density in (1.2.17) with parameter h_t. Then, equation (1.2.13) can be expressed as

$$e^r = \mathsf{E}^{h_t^*}[e^{Y_t}|\mathcal{F}_{t-1}]$$

Consequently, it would be sufficient if we could establish the following results: (i) $\mathsf{E}^{h_t}(e^{Y_t}|\mathcal{F}_{t-1})$ is a strictly increasing function of h_t almost surely; (ii) $\mathsf{E}^{h_t}(e^{Y_t}|\mathcal{F}_{t-1})$ is a continuous function of h_t almost surely; (iii) $\inf_{h_t} \mathsf{E}^{h_t}(e^{Y_t}|\mathcal{F}_{t-1}) \leq e^r \leq \sup_{h_t} \mathsf{E}^{h_t}(e^{Y_t}|\mathcal{F}_{t-1})$ almost surely. For notational convenience, without confusion, we omit the term "almost surely" in the following proof.

Results (i) and (ii) can be proved in a completely parallel way as in Proposition 1.2 of Christoffersen et al. (2010). Indeed, result (i) follows from the assumption that $\log \mathsf{E}^{\mathbb{P}}[e^{h_t Y_t}|\mathcal{F}_{t-1}]$ is strictly convex in h_t, and result (ii) is the direct result of the twice differentiable assumption on the $\Psi = \log \mathsf{E}^{\mathbb{P}}[e^{h_t Y_t}|\mathcal{F}_{t-1}]$. To show result (iii), we consider the following four distinct cases separately, with regard to the range of domain of Ψ.

Case 1: Assume the domain of $\Psi_{t-1}(h_t)$ is $h_t \in (-\infty, \infty)$. We show that

$$\lim_{h_t \to -\infty} \mathsf{E}^{h_t}(e^{Y_t}|\mathcal{F}_{t-1}) \leq e^r \leq \lim_{h_t \to \infty} \mathsf{E}^{h_t}(e^{Y_t}|\mathcal{F}_{t-1}), \text{ a.s.} \tag{1.2.18}$$

To prove (1.2.18), we first express $\mathsf{E}^{h_t}(e^{Y_t}|\mathcal{F}_{t-1})$ as follows:

$$\begin{aligned}\mathsf{E}^{h_t}(e^{Y_t}|\mathcal{F}_{t-1}) &= \int_{-\infty}^{\infty} e^{y_t} f^{h_t}(y_t \,|\, F_{t-1})\, dy_t = \frac{\int_{-\infty}^{\infty} e^{y_t} e^{h_t y_t} f(y_t \,|\, F_{t-1})\, dy_t}{\mathsf{E}^{\mathbb{P}}(e^{h_t Y_t}|\mathcal{F}_{t-1})} \\ &=: I_1(h_t) + I_2(h_t),\end{aligned}$$

where

$$I_1(h_t) = \frac{\int_{r}^{\infty} e^{y_t} e^{h_t y_t} f(y_t \,|\, F_{t-1})\, dy_t}{\mathsf{E}^{\mathbb{P}}(e^{h_t Y_t}|\mathcal{F}_{t-1})} \quad \text{and} \quad I_2(h_t) = \frac{\int_{-\infty}^{r} e^{y_t} e^{h_t y_t} f(y_t \,|\, F_{t-1})\, dy_t}{\mathsf{E}^{\mathbb{P}}(e^{h_t Y_t}|\mathcal{F}_{t-1})}$$

Clearly, for any $h_t \in \mathbb{R}$

$$I_1(h_t) \geq e^r \int_{r}^{\infty} f^{h_t}(y_t \,|\, F_{t-1})\, dy_t, = e^r \Pr{}^{h_t}(Y_t > r|\mathcal{F}_{t-1}),$$

and therefore

$$\mathsf{E}^{h_t}(e^{Y_t}|\mathcal{F}_{t-1}) \geq e^r \Pr{}^{h_t}(Y_t > r|\mathcal{F}_{t-1}) \quad \forall\, h_t \in \mathbb{R} \tag{1.2.19}$$

If we show that $\lim_{h_t \to \infty} \Pr^{h_t}(Y_t > r|\mathcal{F}_{t-1}) = 1$, then we have $\lim_{h_t \to \infty} \mathsf{E}^{h_t}(e^{Y_t}|\mathcal{F}_{t-1}) \geq e^r$.
In addition, since

$$I_2(h_t) \leq e^r \overset{h_t}{\Pr}(Y \leq r \,|\, \mathcal{F}_{t-1}) \leq e^r, \quad \forall h_t \in \mathbb{R}$$

If we show that $\lim_{h_t \to -\infty} I_1(h_t) = 0$ and $\lim_{h_t \to -\infty} I_1 h_t = 0$, then we have

$$\lim_{h_t \to -\infty} \mathsf{E}^{h_t}(e^{Y_t}|\mathcal{F}_{t-1}) = \lim_{h_t \to -\infty} I_1(h_t) + I_2(h_t) \leq e^r$$

Then, it would be sufficient if we could establish the following two conditions.

1. Limiting probabilities:

$$\Pr{}^{h_t}(Y_t > r|\mathcal{F}_{t-1}) \to 1 \text{ and } \Pr{}^{h_t}(Y_t \leq r|\mathcal{F}_{t-1}) \to 0, \text{ as } h_t \to \infty; \tag{1.2.20}$$

$$\Pr^{h_t}(Y_t > r|\mathcal{F}_{t-1}) \to 0 \text{ and } \Pr^{h_t}(Y_t \le r|\mathcal{F}_{t-1}) \to 1, \text{ as } h_t \to -\infty \quad (1.2.21)$$

2. Limiting expectation conditions:

$$\lim_{h_t \to -\infty} I_1 h_t = 0$$

Regarding the limiting probabilities, we will prove the case $h_t \to \infty$ only, as it can be similarly proved for $h_t \to -\infty$. Let $R = \mathbb{P}(Y_t > r|\mathcal{F}_{t-1})$. Then, the given conditions imply that $0 < R \le 1$ almost surely. Therefore, given $\mathcal{F}_{t-1}$, there exists a constant $y' > r$ such that $\mathbb{P}(Y_t > y'|\mathcal{F}_{t-1}) > \frac{R}{N}$ for some positive integer N. Let $\Delta = y' - r$. We have, $\forall\, h_t > 0$,

$$\begin{aligned}
\Pr^{h_t}(Y_t > r|\mathcal{F}_{t-1}) &\ge \Pr^{h_t}(Y_t > y'|\mathcal{F}_{t-1}) \\
&= \int_{y'}^{\infty} \frac{e^{h_t y_t}}{\mathsf{E}^{\mathbb{P}}(e^{h_t Y_t}|\mathcal{F}_{t-1})} f(y_t|\mathcal{F}_{t-1})\, dy_t \\
&\ge \frac{e^{h_t y'}}{\mathsf{E}^{\mathbb{P}}(e^{h_t Y_t}|\mathcal{F}_{t-1})} \int_{y'}^{\infty} f(y_t|\mathcal{F}_{t-1})\, dy_t \\
&\ge \frac{e^{h_t y'}}{\mathsf{E}^{\mathbb{P}}(e^{h_t Y_t}|\mathcal{F}_{t-1})} \frac{R}{N} \\
&= \frac{e^{h_t \Delta}\, e^{h_t r}}{\mathsf{E}^{\mathbb{P}}(e^{h_t Y_t}|\mathcal{F}_{t-1})} \frac{R}{N},
\end{aligned} \quad (1.2.22)$$

and

$$\begin{aligned}
\Pr^{h_t}(Y_t \le r|\mathcal{F}_{t-1}) &= \int_{-\infty}^{r} \frac{e^{h_t y_t}}{\mathsf{E}^{\mathbb{P}}(e^{h_t Y_t}|\mathcal{F}_{t-1})} f(y_t|\mathcal{F}_{t-1})\, dy_t \\
&\le \frac{e^{h_t r}}{\mathsf{E}^{\mathbb{P}}(e^{h_t Y_t}|\mathcal{F}_{t-1})} \int_{-\infty}^{r} f(y_t|\mathcal{F}_{t-1})\, dy_t \\
&= \frac{e^{h_t r}}{\mathsf{E}^{\mathbb{P}}(e^{h_t Y_t}|\mathcal{F}_{t-1})} (1 - R).
\end{aligned} \quad (1.2.23)$$

Combining (1.2.23) and (1.2.22), we get

$$\Pr^{h_t}(Y_t \le r|\mathcal{F}_{t-1}) \le \frac{\Pr^{h_t}(Y_t \le r|\mathcal{F}_{t-1})}{\Pr^{h_t}(Y_t > r|\mathcal{F}_{t-1})} \le (1 - R) \Big/ \left(e^{h_t \Delta} \frac{R}{N} \right),$$

whereby,

$$\lim_{h_t \to \infty} \Pr^{h_t}(Y_t \leq r | \mathcal{F}_{t-1}) \leq \lim_{h_t \to \infty} (1 - R) \Big/ \left(e^{h_t \Delta} \frac{R}{N} \right) = 0.$$

This immediately implies the limits in (1.2.20).

Regarding the limiting expectation condition, we consider $h_t < 0$, since the condition is required for $h_t \to -\infty$. Define

$$g(y_t) = \frac{e^{h_t y_t} f(y_t | \mathcal{F}_{t-1})}{\mathsf{E}^{\mathbb{P}}(e^{h_t Y_t} | \mathcal{F}_{t-1}) \Pr^{h_t}(Y_t > r | \mathcal{F}_{t-1})}, \text{ and } q(y_t) = \frac{f(y_t | \mathcal{F}_{t-1})}{\mathbb{P}(Y_t > r | \mathcal{F}_{t-1})}.$$

which can be considered as two density functions for Y_t with the same support of (r, ∞). In addition, the ratio $q(y_t)/g(y_t) = \dfrac{e^{-h_t y_t} \mathsf{E}^{\mathbb{P}}(e^{h_t Y_t} | \mathcal{F}_{t-1}) \Pr^{h_t}(Y_t > r | \mathcal{F}_{t-1})}{\mathbb{P}(Y_t > r | \mathcal{F}_{t-1})}$ is strictly increasing in y_t for a fixed $h_t < 0$. According to Lemma 1.2.4, Y_t is stochastically larger under probability measure with density $q(y_t)$ than under $g(y_t)$, given a fixed $h_t < 0$. Then, based on Lemma1.2.3,

$$\int_r^\infty e^{y_t} g(y_t)\, dy_t \leq \int_r^\infty e^{y_t} q(y_t)\, dy_t, \qquad \forall\ h_t < 0. \tag{1.2.24}$$

Consequently,

$$\begin{aligned} \int_r^\infty e^{y_t} \frac{e^{h_t y_t} f(y_t | \mathcal{F}_{t-1})}{\mathsf{E}^{\mathbb{P}}(e^{h_t Y_t} | \mathcal{F}_{t-1}) \Pr^{h_t}(Y_t > r | \mathcal{F}_{t-1})}\, dy_t &\leq \int_r^\infty e^{y_t} f(y_t | \mathcal{F}_{t-1}) / \mathbb{P}(Y_t > r | \mathcal{F}_{t-1})\, dy_t \\ &\leq \mathsf{E}^{\mathbb{P}}(e^{Y_t} | \mathcal{F}_{t-1}) / \mathbb{P}(Y_t > r | \mathcal{F}_{t-1}), \end{aligned} \tag{1.2.25}$$

where the second inequality is due to (1.2.24). From the arbitrariness of $h_t < 0$, we also have, with $\mathbb{P}(Y_t > r | \mathcal{F}_{t-1}) = R$,

$$e^r \leq \int_r^\infty e^{y_t} \frac{e^{h_t y_t} f(y_t | \mathcal{F}_{t-1})}{\mathsf{E}^{\mathbb{P}}(e^{h_t Y_t} | \mathcal{F}_{t-1}) \Pr^{h_t}(Y_t > r | \mathcal{F}_{t-1})}\, dy_t \leq \mathsf{E}^{\mathbb{P}}(e^{Y_t} | \mathcal{F}_{t-1}) / R. \tag{1.2.26}$$

Thus, with the boundary results in (1.2.26), the limiting expectation condition is

satisfied, since

$$\lim_{h_t\to-\infty} I_2(h_t) = \lim_{h_t\to-\infty} \Pr{}^{h_t}(Y_t > r|\mathcal{F}_{t-1}) \int_r^\infty e^{y_t} \frac{e^{h_t\, y_t} f(y_t|\mathcal{F}_{t-1})}{\mathsf{E}^{\mathbb{P}}(e^{h_t\, Y_t}|\mathcal{F}_{t-1}) \Pr^{h_t}(Y_t > r|\mathcal{F}_{t-1})}\, dy_t = 0,$$

as $\lim_{h_t\to-\infty} \Pr^{h_t}(Y_t > r|\mathcal{F}_{t-1}) = 0$.

Case 2: Assume the domain of $\Psi_{t-1}(h_t)$ is $-\infty < a < h_t < b < \infty$, where $a+1 < b$.

Based on the assumption that $\Psi_{t-1} = \log \mathsf{E}^{\mathbb{P}}\left[e^{h_t Y_t}|\mathcal{F}_{t-1}\right]$ is twice differentiable with regard to h_t, and tends to infinity at the finite boundaries of its domain of h_t almost surely, we have the following result. As $h_t \to a$, $\mathsf{E}^{\mathbb{P}}\left[e^{h_t Y_t}|\mathcal{F}_{t-1}\right]$ tends to infinity at the boundary of its domain of h_t almost surely, while $\mathsf{E}^{\mathbb{P}}(e^{(h_t+1)\, Y_t}|\mathcal{F}_{t-1}) < \infty$. Thus,

$$\lim_{h_t\to a} \mathsf{E}^{h_t}(e^{Y_t}|\mathcal{F}_{t-1}) = \lim_{h_t\to a} \frac{\mathsf{E}^{\mathbb{P}}(e^{(h_t+1)\, Y_t}|\mathcal{F}_{t-1})}{\mathsf{E}^{\mathbb{P}}(e^{h_t\, Y_t}|\mathcal{F}_{t-1})} = 0 \tag{1.2.27}$$

Similarly, as $h_t \to b$,

$$\lim_{h_t\to b-1} \mathsf{E}_t^h(e^{Y_t}|\mathcal{F}_{t-1}) = \lim_{h_t\to b-1} \frac{\mathsf{E}^{\mathbb{P}}(e^{(h_t+1)\, Y_t}|\mathcal{F}_{t-1})}{\mathsf{E}^{\mathbb{P}}(e^{h_t\, Y_t}|\mathcal{F}_{t-1})} = \infty \tag{1.2.28}$$

As a result, we have $\lim_{h_t\to-\infty} \mathsf{E}^{h_t}(e^{Y_t}|\mathcal{F}_{t-1}) \le e^r \le \lim_{h_t\to h'} \mathsf{E}^{h_t}(e^{Y_t}|\mathcal{F}_{t-1})$.

Case 3: Assume the domain of $\Psi_{t-1}(h_t)$ is $h_t \in (-\infty, b)$. Based on the result from (1.2.18) and (1.2.28), we have

$$\lim_{h_t\to-\infty} \mathsf{E}^{h_t}(e^{Y_t}|\mathcal{F}_{t-1}) \le e^r \le \lim_{h_t\to b-1} \mathsf{E}^{h_t}(e^{Y_t}|\mathcal{F}_{t-1}), \text{ a.s.}$$

Case 4: Assume the domain of $\Psi_{t-1}(h_t)$ is $h_t \in (a, \infty)$. Similarly, we have

$$\lim_{h_t\to a} \mathsf{E}^{h_t}(e^{Y_t}|\mathcal{F}_{t-1}) \le e^r \le \lim_{h_t\to\infty} \mathsf{E}^{h_t}(e^{Y_t}|\mathcal{F}_{t-1}), \text{ a.s.}$$

(b). We need to show $\mathsf{E}^{\mathbb{Q}}\left[\frac{S_t}{e^{rt}}\middle|\mathcal{F}_{t-1}\right]=\frac{S_{t-1}}{e^{r(t-1)}}$, or equivalently $\mathsf{E}^{\mathbb{Q}}\left[\frac{S_t}{S_{t-1}}\middle|\mathcal{F}_{t-1}\right]=e^r$, for $t=1,\ldots,T$. In fact, by part (a), h_t^* is uniquely determined given $\mathcal{F}_{t-1}$ and hence, it follows from the tower rule for the conditional expectation that

$$\begin{aligned}\mathsf{E}^{\mathbb{Q}}\left[\frac{S_t}{S_{t-1}}\middle|\mathcal{F}_{t-1}\right] &= \mathsf{E}^{\mathbb{P}}\left[e^{Y_t}\frac{\frac{d\mathbb{Q}}{d\mathbb{P}}|_{\mathcal{F}_t}}{\frac{d\mathbb{Q}}{d\mathbb{P}}|_{\mathcal{F}_{t-1}}}\middle|\mathcal{F}_{t-1}\right] \\ &= \mathsf{E}^{\mathbb{P}}\left[\frac{e^{(h_t^*+1)Y_t}}{\mathsf{E}^{\mathbb{P}}[e^{h_t^*Y_t}|\mathcal{F}_{t-1}]}\middle|\mathcal{F}_{t-1}\right]=e^r,\end{aligned} \tag{1.2.29}$$

where the last equality is due to condition (1.2.13) with $s=t$. □

Remark 1.2.2. It is worth noting that the conditions in Proposition 1.2.1 are quite mild in that they are satisfied by many popular regime switching models in finance, and therefore the ET-$\mathbb{Q}$ can be used as a valid EMM in option pricing for a wide range of models. To demonstrate this fact, we analyze the well-known regime switching lognormal models in Example 1 and the regime switching auto-regressive model in Example 2 below.

Example 1. In the regime switching lognormal models with R regimes, Y_t only depends on ρ_t and $Y_t|\rho_t\sim N(\mu_{\rho_t},\,\sigma^2_{\rho_t})$ under $\mathbb{P}$–measure. Therefore,

$$\Psi_{t-1}(h)\equiv\log\mathsf{E}^{\mathbb{P}}\left[e^{hY_t}|\mathcal{F}_{t-1}\right]=\log\mathsf{E}^{\mathbb{P}}\left[e^{hY_t}|\rho_{t-1}\right],$$

and for any i from the regime state space,

$$\begin{aligned}\log\mathsf{E}^{\mathbb{P}}\left[e^{hY_t}|\rho_{t-1}=i\right] &= \log\left(\sum_{j=1}^{R}\left(\mathsf{E}^{\mathbb{P}}\left[e^{hY_t}|\rho_t=j\right]\cdot\mathbb{P}(\rho_t=j|\rho_{t-1}=i)\right)\right) \\ &= \log\sum_{j=1}^{R}\exp\left(\mu_j h+\frac{1}{2}\sigma_j^2h^2+\log p_{ij}\right),\end{aligned}$$

where $p_{ij}=\mathbb{P}(\rho_t=j|\rho_{t-1}=i)$. Obviously, the above conditional cumulant generating function is twice differentiable and tends to infinity as h tends to either $-\infty$

or ∞. Next we show the strict convexity of $\log \mathsf{E}^{\mathbb{P}}\left[e^{hY_t}|\rho_{t-1}=i\right]$ as a function of h. Indeed, $g_{ij}(h) := \mu_j h + \frac{1}{2}\sigma_j^2 h^2 + \log p_{ij}$ is obviously strictly convex as a function of h so that its second derivative $g''_{ij}(h) > 0$ for all $h \in \mathbb{R}$, and therefore

$$\begin{aligned}
& \frac{\partial^2 \log \mathsf{E}^{\mathbb{P}}\left[e^{hY_t}|\rho_{t-1}=i\right]}{\partial h^2} \\
= & \frac{1}{\left(\sum_{j=1}^R e^{g_{ij}(h)}\right)^2}\left[\left(\sum_{j=1}^R \left(\, e^{g_{ij}(h)}[g''_{ij}(h)+(g'_{ij})^2]\,\right)\right)\left(\sum_{j=1}^R \left(e^{g_{ij}(h)}\right)\right) - \left(\sum_{j=1}^R e^{g_{ij}(h)} g'_{ij}(h)\right)^2\right] \\
> & \frac{1}{\left(\sum_{j=1}^R e^{g_{ij}(h)}\right)^2}\left[\left(\sum_{j=1}^R \left(\, e^{g_{ij}(h)}(g'_{ij})^2\,\right)\right)\left(\sum_{j=1}^R \left(e^{g_{ij}(h)}\right)\right) - \left(\sum_{j=1}^R e^{g_{ij}(h)} g'_{ij}(h)\right)^2\right] \\
\geq & 0,
\end{aligned}$$

where the last step is due to Hölder's inequality.

The above analysis implies that, with probability one, $\Psi_{t-1}(h)$ is strictly convex, twice differentiable and tends to infinity as h tends to either $-\infty$ or ∞. Therefore,the conditions in Proposition 1.2.1 are satisfied. □

Example 2. In this example, we consider the the following regime switching AR(1) model $(Y_t, \rho_t)_{t=0}^T$, where the log-return Y_t depends on not only the regime state ρ_t but also the log-return in the previous period:

$$Y_t = \mu_{\rho_t} + \alpha Y_{t-1} + \sigma_{\rho_t}\varepsilon_t, \;\; t = 1, \ldots, T, \tag{1.2.30}$$

where $(\varepsilon_t)_{t=1}^T$ is a sequence of white noises with $\varepsilon_t \sim N(0,1)$ under $\mathbb{P}$–measure. From (1.2.30) and the Markov property of $(\rho_t)_{t=0}^T$,

$$\Psi_{t-1}(h) \equiv \log \mathsf{E}^{\mathbb{P}}\left[e^{hY_t}|\mathcal{F}_{t-1}\right] = \log \mathsf{E}^{\mathbb{P}}\left[e^{hY_t}|Y_{t-1}, \rho_{t-1}\right],$$

and for any i from the regime state space and real number y,

$$\begin{aligned} & \log \mathsf{E}^{\mathbb{P}}\left[e^{hY_t}|Y_{t-1}=y,\rho_{t-1}=i\right] \\ = & \log\left(\sum_{j=1}^{R}\mathsf{E}^{\mathbb{P}}\left[e^{hY_t}|Y_{t-1}=y,\rho_t=j\right]\cdot\mathbb{P}(\rho_t=j|\rho_{t-1}=i)\right) \\ = & \log\sum_{j=1}^{R}\exp\left((\mu_i+\alpha y)h+\frac{1}{2}\sigma_j^2h^2+\log p_{ij}\right), \end{aligned}$$

where $p_{ij}=\mathbb{P}(\rho_t=j|\rho_{t-1}=i)$. Following exactly the same argument as in Example 1, we can easily show that the above function of h satisfies all the conditions in Proposition 1.2.1. □

Remark 1.2.3. Although the analysis in Examples 1 and 2 is quite straightforward, it has very important implications. For instance, Example 1 indicates that, when the log-return Y_t only depends on ρ_t, to verify the conditions in Proposition 1.2.1, it is sufficient to investigate whether they are satisfied by the conditional cumulant generating function $\log \mathsf{E}^{\mathbb{P}}\left[e^{hY_t}|\rho_{t-1}=i\right]$ for each regime state i. This provides us with a very transparent method for verification, and more importantly, by this fact we can easily show that conditions in Proposition 1.2.1 are indeed satisfied for many other distributions besides the normal distribution. The verification approach conducted in Example 2 can be extended to AR models with a higher order and even other more sophisticated models such as regime switching ARCH and GARCH models.

1.2.1 Distributions under the Risk Neutral Measure

In the previous section, we have established an EMM $\mathbb{Q}$ measure through the Radon-Nikodym derivative given in (1.2.12) with conditions (1.2.13). In this section, we consider the $\mathbb{Q}$ measure distribution of the underlying asset price in an R state Markov regime switching model. First, we derive the distribution of Y_t conditional on $\mathcal{F}_{t-1}$; then, we consider the joint distribution of $Y_t,\ldots,Y_T$. Let u_t denote a real number at which the moment generating function of Y_t conditional on $\mathcal{F}_{t-1}$

exists. Then, similar to (1.2.29), the moment generating function for the conditional distribution of Y_t given $\mathcal{F}_{t-1}$ can be written as follows:

$$\begin{aligned} \mathsf{E}^{\mathbb{Q}}\left[e^{u_t Y_t}\middle|\,\mathcal{F}_{t-1}\right] &= \mathsf{E}^{\mathbb{P}}\left[e^{u_t Y_t}\frac{\frac{d\mathbb{Q}}{d\mathbb{P}}\big|_{\mathcal{F}_t}}{\frac{d\mathbb{Q}}{d\mathbb{P}}\big|_{\mathcal{F}_{t-1}}}\middle|\,\mathcal{F}_{t-1}\right] \\ &= \frac{\mathsf{E}^{\mathbb{P}}\left[e^{(u_t+h_t^*)Y_t}\middle|\,\mathcal{F}_{t-1}\right]}{\mathsf{E}^{\mathbb{P}}[e^{h_t^* Y_t}|\,\mathcal{F}_{t-1}]}. \end{aligned} \tag{1.2.31}$$

Recall $\mathcal{F}_t = \mathcal{F}_t^Y \vee \mathcal{F}_t^\rho$ under regime switching models. Based on the filtration $\mathcal{F}_t$ and the Markov property of the regime process imposed in section 1.1.1, we can replace the result in (1.2.31) by

$$\mathsf{E}^{\mathbb{Q}}(e^{s\,Y_t}|\,\mathcal{F}_{t-1}^Y \bigcap \{\rho_{t-1}=i\}) = \frac{\mathsf{E}^{\mathbb{P}}\left[e^{(s+h_t^*)Y_t}\middle|\,\mathcal{F}_{t-1}^Y \bigcap \{\rho_{t-1}=i\}\right]}{\mathsf{E}^{\mathbb{P}}[e^{h_t^* Y_t}|\,\mathcal{F}_{t-1}^Y \bigcap \{\rho_{t-1}=i\}]}. \tag{1.2.32}$$

For the simplicity of the computation, we further set up the following independence assumption, which is common in the literature.

(A4) $Y_1, \ldots, Y_T$ are independent given $\{\rho_t\}_{t=0}^T$.

red Assumption (A4) rules out the dependent models like Autoregressive-moving-average (ARMA) models. Based on assumptions (A1) to (A4), (1.2.31) implies

$$\mathsf{E}^{\mathbb{Q}}(e^{s\,Y_t}|\,\rho_{t-1}=i) = \frac{\mathsf{E}^{\mathbb{P}}\left[e^{(s+h_t^*)Y_t}\middle|\,\rho_{t-1}=i\right]}{\mathsf{E}^{\mathbb{P}}[e^{h_t^* Y_t}|\,\rho_{t-1}=i]}. \tag{1.2.33}$$

So we may condition on the regime process only, and no longer need the full $\mathcal{F}_{t-1}$, when we consider the distribution of the underlying asset price under $\mathbb{Q}$ measure.

Proposition 1.2.1 applied to the regime switching model implies that h_t^* is the unique $\sigma(\rho_{t-1})$-measurable random variable such that

$$e^r = \frac{\mathsf{E}^{\mathbb{P}}[e^{(h_t^*+1)\,Y_t}\,|\rho_{t-1}]}{\mathsf{E}^{\mathbb{P}}[e^{h_t^*\,Y_t}\,|\,\rho_{t-1}]} \tag{1.2.34}$$

This means that under the RSLN framework with R regimes there are R possible values for h_t^*, depending on the regime at time $t-1$. Let $h^{(i)}$ be the unique value of h_t^* conditional on $\rho_{t-1} = i$. {As we assume that the state space of ρ_{t-1} is finite. }

Expanding (1.2.33) with $h^{(i)}$, the density function of Y_t under the Esscher transformed $\mathbb{Q}$ measure (ET-$\mathbb{Q}$ density) conditional on $\{\rho_{t-1} = i, \rho_t = j\}$ is

$$f_{ij}^{\mathbb{Q}}(y_t) = \frac{e^{h^{(i)}y_t}\, f^{\mathbb{P}}(y_t|\rho_t = j)}{\mathsf{E}^{\mathbb{P}}\left[e^{h^{(i)}Y_t}|\rho_{t-1} = i, \rho_t = j\right]} \tag{1.2.35}$$

and similarly, the $\mathbb{Q}$ density of Y_t conditional on $\{\rho_{t-1} = i\}$,

$$f_{i}^{\mathbb{Q}}(y_t) = \frac{e^{h^{(i)}y_t}\, f^{\mathbb{P}}(y_t|\rho_{t-1} = i)}{\mathsf{E}^{\mathbb{P}}\left[e^{h^{(i)}Y_t}|\rho_{t-1} = i\right]}, \tag{1.2.36}$$

where $f^{\mathbb{P}}$ denotes the corresponding density function of Y_t under the $\mathbb{P}$-measure. The following proposition shows that $f_i^{\mathbb{Q}}$ can be expressed as a mixture of the $f_{ij}^{\mathbb{Q}}$ functions.

Proposition 1.2.2. *The ET-$\mathbb{Q}$ density of Y_t conditional on $\{\rho_{t-1} = i\}$ is a mixed density,*

$$f_{i}^{\mathbb{Q}}(y_t) = \sum_{j=1}^{R} q_{ij}\, f_{ij}^{\mathbb{Q}}(y_t), \tag{1.2.37}$$

where

$$q_{ij} = \frac{p_{ij}\, \mathsf{E}^{\mathbb{P}}(e^{h^{(i)}\,Y_t}\,|\,\rho_{t-1} = i, \rho_t = j)}{\mathsf{E}^{\mathbb{P}}(e^{h^{(i)}\,Y_t}\,|\,\rho_{t-1} = i)}, \quad i, j \in \{1, \ldots, R\}, \tag{1.2.38}$$

Proof. The proof follows from the fact that

$$f^{\mathbb{P}}(y_t|\rho_{t-1} = i) = \sum_{j=1}^{R} p_{ij}\, f^{\mathbb{P}}(y_t|\rho_t = j).$$

Indeed, substituting the above into (1.2.35) and using (1.2.36), we immediately have

$$\begin{aligned} f_i^{\mathbb{Q}}(y_t) &= \frac{e^{h^{(i)}\, y_t}\, f^{\mathbb{P}}(y_t|\rho_{t-1}=i)}{\mathsf{E}^{\mathbb{P}}[e^{h^{(i)}\, Y_t}\,|\rho_{t-1}=i]} \\ &= \frac{e^{h^{(i)}\, y_t}\, \sum_{j=1}^{R} p_{ij}\, f^{\mathbb{P}}(y_t|\rho_t=j)}{\mathsf{E}^{\mathbb{P}}[e^{h^{(i)}\, Y_t}\,|\rho_{t-1}=i]} \\ &= \sum_{j=1}^{R} \left(\frac{p_{ij}\, \mathsf{E}^{\mathbb{P}}[e^{h^{(i)}\, Y_t}\,|\,\rho_{t-1}=i,\rho_t=j]}{\mathsf{E}^{\mathbb{P}}[e^{h^{(i)}\, Y_t}\,|\rho_{t-1}=i]} \right) \frac{e^{h^{(i)}\, y_t}\, f^{\mathbb{P}}(y_t|\rho_t=j)}{\mathsf{E}^{\mathbb{P}}[e^{h^{(i)}\, Y_t}\,|\,\rho_{t-1}=i,\rho_t=j]} \\ &= \sum_{j=1}^{R} q_{ij} f_{ij}^{\mathbb{Q}}(y_t). \end{aligned}$$

Clearly, $\sum_{j=1}^{R} q_{ij} = 1$, since

$$\mathsf{E}^{\mathbb{P}}[e^{h^{(i)}Y_t}|\rho_{t-1}=i] = \sum_{j=1}^{R} p_{ij}\mathsf{E}^{\mathbb{P}}[e^{h^{(i)}Y_t}|\rho_{t-1}=i,\rho_t=j]. \tag{1.2.39}$$

□

Remark 1.2.4. Using Proposition 1.2.2, we can represent the distribution law of the process of (S_t) under the ET-$\mathbb{Q}$ measure by a new Markov regime switching process denoted by (S_t^*) and specified as follows. Let (ρ_t^*) denote a regime process with R^2 states $\{[ij] : i,j = 1,\ldots,R\}$, where $\rho_t^* = [ij]$ corresponds to the event of the physical regime process $\{\rho_{t-1}=i,\rho_t=j\}$. Then the regime transition probabilities under $\mathbb{Q}$ measure are

$$\mathbb{Q}\left(\rho_{t+1}^* = [ij]\big|\rho_t^* = [kl]\right) = \begin{cases} 0 & i \neq l \\ q_{ij} & i = l \end{cases} \tag{1.2.40}$$

Having obtained the conditional distribution of Y_t given $\mathcal{F}_{t-1}$ with densities expressed from (1.2.35) to (1.2.38), we further investigate the joint density of $Y_1,\ldots,Y_T$. We observe from equation (1.2.35) that, conditional on $\{\rho_t^*\}_{t=0}^T$, the distribution of Y_t is given as $f_{ij}^{\mathbb{Q}}$, which is independent of $Y_s, s \neq t$ under ET-$\mathbb{Q}$ measure. We

summarize in the following lemma.

Lemma 1.2.5. *Based on assumptions (A1) to (A4), $Y_1, \ldots, Y_T$ are conditionally independent under ET-$\mathbb{Q}$ measure given $\{\rho_t^*\}_{t=0}^T$.*

Proof. Based on assumptions (A1) to (A4), under ET-$\mathbb{Q}$ measure, the density of Y_t conditional on ρ_t^*, $f^{\mathbb{Q}}(y_t|\rho_t^*)$, is given in (1.2.35). According to assumption (A4), $Y_1, \ldots, Y_T$ conditional on $\{\rho_t\}_{t-0}^T$ are independent under $\mathbb{P}$-measure. Therefore, the term $f^{\mathbb{P}}(y_t|\rho_t = j)$ in (1.2.35) is independent of $Y_s, s \neq t$. Also, since the parameter $h_t^{(i)}$ is determined by $\rho_{t-1} = i$, the term $\mathsf{E}^{\mathbb{P}}\left[e^{h^{(i)}Y_t}|\rho_{t-1} = i, \rho_t = j\right]$ in (1.2.35) is jointly determined by ρ_t and ρ_{t-1}, i.e., independent of $Y_s, s \neq t$ and $\rho_s, s < t-1$. As a result,

$$f^{\mathbb{Q}}(y_t|\, y_1, \ldots, y_{t-1}; \rho_1^*, \ldots, \rho_t^*) = f^{\mathbb{Q}}(y_t|\rho_t^*), \tag{1.2.41}$$

by which we complete the proof. □

Lemma 1.2.6. *Based on assumptions (A1) to (A4), the distribution of Y_t conditional on ρ_t^*, under ET-$\mathbb{Q}$ measure, is independent of ρ_s^* for $s \neq t$.*

Proof. Based on the same argument for lemma 1.2.5. □

Based on Lemma 1.2.5 and Lemma 1.2.6, the distribution of Y_t is solely determined by ρ_t^* under the ET-$\mathbb{Q}$ measure.

It is worth noting that, in (1.2.35), to compute the probability associated with the path $\{\rho_t^*\}_{t=1}^T$ under the ET-$\mathbb{Q}$ measure, we need to sum over all the paths $\{\rho_t\}_{t=0}^T$ which generate the regime switching path $\{\rho_t^*\}_{t=1}^T$. In this study there is a one-to-one relationship between the paths $\{\rho_t^*\}_{t=1}^T$ and $\{\rho_t\}_{t=0}^T$ according to Remark 1.2.4. Therefore no sum is needed.

We can obtain the moment generating function of $Y_1, \ldots, Y_T$. Let $(u_1, \ldots, u_T)$ be a vector of real numbers such that the moment generating function $\mathsf{E}^{\mathbb{Q}}(e^{\sum_{t=1}^T u_t Y_t})$ exists. Then,

$$\mathsf{E}^{\mathbb{Q}}\left[e^{u_1Y_1+\cdots+u_TY_T}\right] = \mathsf{E}^{\mathbb{Q}}\left[\mathsf{E}^{\mathbb{Q}}\left(e^{u_1Y_1+\cdots+u_TY_T}\,|\,\{\rho_t^*\}_{t=1}^T\right)\right], \tag{1.2.42}$$

where

$$\begin{aligned} \mathsf{E}^{\mathbb{Q}}\left(e^{u_1Y_1+\cdots+u_TY_T}|\{\rho_t^*\}_{t=1}^T\right) &= \prod_{t=1}^T \mathsf{E}^{\mathbb{Q}}(e^{u_tY_t}\,|\,\rho_t^*) \\ &= \prod_{t=1}^T \frac{\mathsf{E}^{\mathbb{P}}(e^{(u_t+h_t)Y_t}|\,\rho_{t-1},\rho_t)}{\mathsf{E}^{\mathbb{P}}(e^{h_tY_t}|\,\rho_{t-1},\rho_t)}. \end{aligned} \tag{1.2.43}$$

The distribution of $\{\rho_t^*\}_{t=1}^T$ follows a Markov chain as described in Remark 1.2.4 with transition probabilities given in (1.2.38).

The distribution of $S_T = S_0\exp(\sum_{t=1}^T Y_t)$ given $(\rho_1^*,\rho_2^*\ldots,\rho_T^*)$ can be obtained in the same way as in (1.2.43). Let c be a constant such that the moment generating function of the log return $\sum_{t=1}^T Y_t$ exists conditional on $\{\rho_t^*\}_{t=1}^T$. Then,

$$\mathsf{E}^{\mathbb{Q}}\left(\exp\left[c\sum_{t=1}^T Y_t\right]\middle|\,\{\rho_t^*\}_{t=1}^T\right) = \prod_{t=1}^T \mathsf{E}^{\mathbb{Q}}(e^{cY_t}\,|\,\rho_t^*) \tag{1.2.44}$$

Next, we give an example to illustrate the result in Proposition 1.2.2.

Example 3. Assume a 2-state Markov regime switching models where Y_t follows the univariate natural exponential family within each regime. Under the ET-$\mathbb{Q}$ measure, the mixed density of Y_t given ρ_{t-1} under P-measure is

$$f(y_t\,|\,\rho_{t-1}=i) = p_{i1}\,g_1(y_t)\,\exp[\,\theta_1y_t - A_1(\theta_1)\,] + p_{i2}\,g_2(y_t)\,\exp[\,\theta_2y_t - A_2(\theta_2)\,]$$

where $g_j(y_t)$ and $A_j(\theta_j), j=1,2$ are given functions. $\theta_i, i=1,2$ are parameters. The moment generating function $E(e^{h_t^*Y}|\rho_{t-1}=i,\rho_t=j)$ is

$$\begin{aligned} & E(e^{h_t^*Y}|\rho_{t-1}=i,\rho_t=j) \\ = & \int_{Y_t} e^{h_t^*y}\,g_j(y_t)\,\exp[\theta_j\,y_t - A_j(\theta_j)]\,dy_t \\ = & \exp[A_j(\theta_j+h_t^*) - A_j(\theta_j)]. \end{aligned}$$

Two Esscher transform parameter h_t^*, denoted by $\{h^{[(1)}, h^{(2)}\}$ are uniquely determined by $\rho_{t-1} = 1$ or 2 through equation (1.2.13). From the proposition 1.2.2 (a), the resulting transition probabilities under the risk neutral measure are

$$q_{ij} = \frac{p_{ij}\ \exp[A_j(\theta_j + h^{(i)}) - A_j(\theta_j)]}{E(e^{h^{(i)}\, Y_t} \mid \rho_{t-1})} \quad i, j \in \{1, 2\}, \tag{1.2.45}$$

and the conditional density

$$f_{ij}^{\mathbb{Q}}(y_t) = g_j(y_t)\ \exp[\,(\theta_j + h^{(i)})y_t - A_j(\theta_j + h^{(i)})\,] \tag{1.2.46}$$

The maximum number of different $f_{ij}^{\mathbb{Q}}(y_t)$ is four. □

1.2.2 Calculating Option Prices

We consider the price at time t of a European option with a payoff function $H(S_T)$ at the expiration date T. The price under the ET-$\mathbb{Q}$ measure is

$$P_0(H(S_T)) = e^{-rT}\mathsf{E}^{\mathbb{Q}}[\,H(S_T)\,|\,\rho_0\,], \tag{1.2.47}$$

where $\mathsf{E}^{\mathbb{Q}}$ denotes the expectation under the ET-$\mathbb{Q}$ measure. We can compute this price by a two-step procedure, using iterated expectation. In the first step, we compute the prices of the option corresponding to each possible path of the regime switching process. In the second step, we calculate the expectation over all the possible paths of the regime switching process. In other words, we compute the price through the following iterated expectation:

$$P_0 \;=\; \mathsf{E}^{\mathbb{Q}}\left[\mathsf{E}^{\mathbb{Q}}\left[e^{-rT}H(S_T)|\{\rho_t^*\}_{t=1}^T\right]\right], \tag{1.2.48}$$

where (ρ_k^*) are the regimes defined by successive pairs of regimes under the original process.

Next let us briefly analyze the computation associated with the two expectations in equation (1.2.48). The inner expectation of equation (1.2.48) needs the distri-

bution of $S_T = S_0 \exp(\sum_{t=1}^{T} Y_t)$. We are given in (1.2.44) the moment generating function of $\sum_{t=1}^{T} Y_t$ conditional on $(\rho_1^*, \rho_2^* \ldots, \rho_T^*)$. The distribution of S_T is the averaged distribution over all paths of $\{\rho_t^*\}$. The outer expectation in equation (1.2.48) requires the average of the inner expectation over the Markov regime switching process $(\rho_1^*, \rho_2^*, \cdots, \rho_T^*)$; the associated issue is to compute the distribution of all scenarios of the regime switching. The computation time increases rapidly with the increase of the size of state space of regimes and the expiry date of target options. Hence, it is quite non–trivial when the expiration date T is large. To overcome this difficulty, we develop a solution illustrated under the regime switching lognormal models.

1.3 Pricing European Options using ET-Q under the RSLN2 Models

In the remaining part of this chapter we apply the distributions obtained through the risk neutral Esscher transform to price call and put options, with the focus on the option on a single risky asset under the Markov regime switching model with two regimes under the log-normal distributions (RSLN2). Our pricing approach can be applied to many other distribution families which are closed under n-fold convolution, and can be adapted for more than 2 regimes.

1.3.1 The RSLN2 Process under P–measure

As demonstrated by Hardy (2001), the RSLN2 model is a significant improvement over many other models in modeling long term stock returns. This model assumes that there are two economic regimes (bear or bull) behind the stock prices, and that the transition of regime variable, denoted by $\{\rho_t, t = 1, 2, \cdots, T\}$, from one period to the next follows a discrete time Markov chain with a transition matrix, denoted

by $\wp$, as follows:

$$\wp = \begin{array}{c} \\ 1 \\ 2 \end{array} \begin{array}{c} \begin{array}{cc} 1 & 2 \end{array} \\ \begin{pmatrix} p_{11} & p_{12} \\ p_{21} & p_{22} \end{pmatrix} \end{array} \tag{1.3.49}$$

Given the value (either 1 or 2) of the regime variable ρ_t for the tth period, the distribution of the log return Y_t is normally distributed:

$$Y_t|\rho_t \sim N(\mu_{\rho_t}, \sigma^2_{\rho_t}),$$

where different ρ_t results in different $\mu_{\rho_t}, \sigma^2_{\rho_t}$. The distribution of Y_t only depends on the regime variable ρ_t in the regime switching model. With the above specification, it is said that $(e^{Y_t})_{0\leq t\leq T}$ follows the RSLN2 model.

1.3.2 The Distribution under the Q-measure

The inner expectation of the right hand side is generally quite straightforward for each individual path, but the computation time increases rapidly with the number of time steps. To overcome this difficulty, we develop an algorithm for 2-regime lognormal models (RSLN-2). For details on the path reduction, see subsection 1.3.3.

For the RSLN-2 model, we have 6 parameters under the $\mathbb{P}$-measure; let μ_1 and μ_2, denote the means for the log-returns in regime 1 and regime 2 respectively, σ_1 and σ_2 denote the corresponding standard deviations, and p_{12} and p_{21} denote the transition probabilities. Then, the conditional density of Y_t conditional on $\rho_{t-1} = i$ under $\mathbb{P}$-measure is

$$f(y|\,\rho_{t-1} = i) = p_{i1}\,\frac{1}{\sigma_1}\,\phi\left(\frac{y-\mu_1}{\sigma_1}\right) + p_{i2}\,\frac{1}{\sigma_1}\,\phi\left(\frac{y-\mu_2}{\sigma_2}\right) \quad i = 1, 2 \tag{1.3.50}$$

where $\phi(\cdot)$ is the density of the standard normal distribution. We have, under this

model, for $i = 1, 2$,

$$\mathsf{E}^{\mathbb{Q}}[e^{s\,Y_t}|\{\rho_{t-1} = i,\ \rho_t = j\}] = \exp\left(\mu^*_{[i,j]}\,s + \frac{\sigma_j^2}{2}s^2\right) \tag{1.3.51}$$

and

$$\mathsf{E}^{\mathbb{Q}}[e^{s\,Y_t}|\,\rho_{t-1} = i] = q_{i1}\,\exp\left(\mu^*_{[i,1]}\,s + \frac{\sigma_1^2}{2}s^2\right) + q_{i2}\,\exp\left(\mu^*_{[i,2]}\,s + \frac{\sigma_2^2}{2}s^2\right)$$

where

$$\mu^*_{[ij]} = \mu_j + \sigma_j^2 h^{(i)} \tag{1.3.52}$$

$$q_{ij} = p_{ij}\,\frac{\mathsf{E}^{\mathbb{P}}[e^{Y_t\,h^{(i)}}\,|\rho_{t-1} = i,\ \rho_t = j]}{\mathsf{E}^{\mathbb{P}}[e^{Y_t\,h^{(i)}}\,|\rho_{t-1} = i]} \tag{1.3.53}$$

$$\mathsf{E}^{\mathbb{P}}[e^{h^{(i)}\,Y_t}|\rho_{t-1} = i] = p_{i1}\,\mathsf{E}^{\mathbb{P}}[e^{h^{(i)}\,Y_t}\,|\,\rho_t = 1] + p_{i2}\,\mathsf{E}^{\mathbb{P}}[e^{h^{(i)}\,Y_t}\,|\,\rho_t = 2]$$

$$\mathsf{E}^{\mathbb{P}}[e^{h^{(i)}\,Y_t}|\rho_{t-1} = i,\ \rho_t = j] = \exp\left(\mu_j\,h^{(i)} + \sigma_j^2(h^{(i)})^2/2\right)$$

The process $\{Y_t\}$, under the ET-$\mathbb{Q}$ measure, is a Markov regime switching Gaussian process with four regimes. The regime at t, $\rho_t^* = [ij]$, corresponds to a pair of consecutive regimes under the $\mathbb{P}$ measure as explained in Remark 1.2.4 in subsection 1.2.1. From (1.3.51), we see that $Y_t|\rho_t^* = [ij]$ has a normal distribution under $\mathbb{Q}$, with parameters $\mu^*_{[ij]}$ and σ_j^2.

Now, as the option that we are valuing is European, the price depends only on S_T, not on the path, $\{S_t\}_{t<T}$. Consider the time 0 price of a European option with payoff $H(S_T)|\boldsymbol{\rho}^*$ over a given path $\boldsymbol{\rho^*} = (\rho_1^*, \rho_2^*, \cdots, \rho_T^*)$ of the Markov chain regime switching process. Let N_{ij}, respectively denote the numbers of periods that the process spends in regime $[ij]$, for each pair $i, j = 1, 2$. Then, under $\mathbb{Q}$ measure,

$$\sum_{k=1}^{T} Y_k|(\rho_1^*, \ldots, \rho_T^*) \sim N\left(\sum_{i=1}^{2}\sum_{j=1}^{2} N_{ij}\mu^*_{[ij]},\ \sum_{j=1}^{2}(N_{1j} + N_{2j})\sigma_j^2\right), \tag{1.3.54}$$

where $\mu^*_{[ij]}$ are defined in (1.3.52), and σ_j^2 is the variance parameter for regime j under the $\mathbb{P}$-measure. This means that for each regime path, we can calculate the option cost using standard Black-Scholes analysis, which is particularly convenient for plain vanilla options. The final cost would be the weighted average of prices over all such paths, where the weight for each path is the $\mathbb{Q}$ measure probability for that path.

We also infer from (1.3.54) that different paths will generate the same option price, if the values of N_{ij} are the same for all i, j. Where the number of time steps is large, the process of determining the price and associated path probability for each possible path is computationally burdensome. In the following section, we demonstrate how similar paths can be grouped together to reduce the computation significantly for longer term options.

1.3.3 Reduction of Path Dimension

The regime process is demonstrated in the multi–period binomial tree in Figure 1.3. Given the starting regime at time zero, the process has two possible regimes at time one, and four possible regimes $[ij], i, j = 1, 2$ at time two. The four end points are

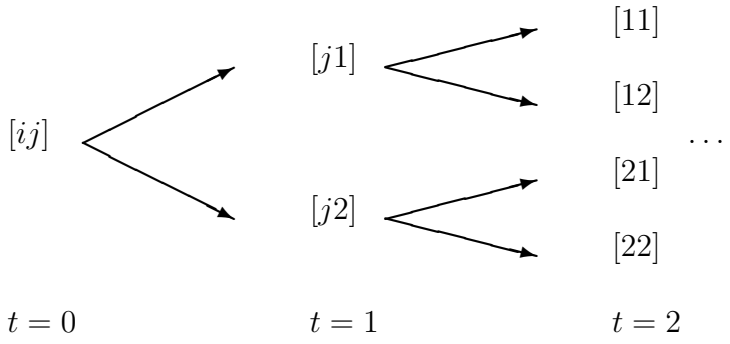

Figure 1.3: Regime Transition in the 4-Regime Model

distinct in this model, and the four paths cannot be recombined. The total number of paths in the tree increases exponentially with the number of time units for the problem, so for an n period tree there are 2^n paths, but, as mentioned above, there are not 2^n distinct option values.

We develop an iterative approach to reducing the dimension by adopting an idea from Hardy(2001), and using the fact that the inner conditional expectation in the option valuation, $\mathsf{E}^{\mathbb{Q}}[H(S_T)|\boldsymbol{\rho}^*]$ is the same for all paths that share the same values of N_{ij}, $i, j = 1, 2$.

To proceed, we need to introduce some notation. Let $\boldsymbol{\rho}^*(t, T)$ denote the set of all distinct pathes of the regime process $\boldsymbol{\rho}^*$ between times t and T for a regime process $\boldsymbol{\rho}^*$. The critical information about the path is encapsulated in the following vector process Π_t:

$$\Pi_t|_{\boldsymbol{\rho}^*(t,T)} = (\rho_t \quad N_{11}(t) \quad N_{12}(t) \quad N_{21}(t) \quad N_{22}(t))' \tag{1.3.55}$$

where $N_{ij}(t)$ represents the number of periods in state $[ij]$, between $t+1$ and T, for the regime process ρ^*. Recall that the process ρ^* is in $[ij]$ at t if and only if the process ρ_t is in regime i at $t-1$ and j at t.

The objective is to collect together, and count, all paths with identical values of Π_0. To this end, we work backwards from $T-1$. We construct recursively, all possible values of Π_t, as well as the count $N(\Pi_t)$, which denotes the number of paths sharing the same Π_t.

At $T-1$ there are four distinct paths, corresponding to the four possible combinations for ρ_{T-1} and ρ_T. For $t \leq T-2$, let

$$g(i, \Pi'_{t+1}) = \Pi'_t|_{\{\rho_t = i,\ \Pi_{t+1}\}},$$

where the subscript $\{\rho_t = i,\ \Pi_{t+1}\}$ takes the same role as $\boldsymbol{\rho}^*(t, T)$ does in (1.3.55) as they provide information in the same capacity needed for the functional Π. So, each Π_{t+1} generates two values for g, corresponding to $i = 1$ and $i = 2$. If $\rho_{t+1} = j$ then the N_{ij} element will increase by one from Π_{t+1} to $g(i, \Pi'_{t+1})$, and the other N_{kl}

values will remain the same. That is,

$$
\begin{aligned}
g(1,(1,a,b,c,d)) &= (1,a+1,b,c,d),\\
g(1,(2,a,b,c,d)) &= (1,a,b+1,c,d),\\
g(2,(1,a,b,c,d)) &= (2,a,b,c+1,d),\\
g(2,(2,a,b,c,d)) &= (2,a,b,c,d+1).
\end{aligned}
$$

This recursion generates 8 possible values for Π_{T-2}, and each is distinct, so the count for each feasible Π_{T-2} is 1.

We then generate 16 candidate values for Π_{T-3}, and find that there are only 14 distinct values; in two cases, 2 paths generate the same Π_{T-3}. These 14 values generate 22 distinct feasible values for Π_{T-4}.

We determine the count, $N(\Pi_t)$ for each distinct feasible value, by summing the counts of the associated values for Π_{t+1}. That is,

$$
N(\Pi_t) = \sum_{\{\Pi_{t+1} \,:\, g(j,\Pi_{t+1}) = \Pi_t\}} N(\Pi_{t+1}).
$$

where j denotes the value of ρ_t in the vector Π_t. We use the counts to determine the appropriate $\mathbb{Q}$ measure probabilities associated with each distinct path. Suppose we have summarized some paths of a T-period process in the vector

$$
\Pi_0 = (1, n_{11}, n_{12}, n_{21}, n_{22})' \quad \text{with count} \quad N(\Pi_0)
$$

Then

$$
\mathbb{Q}[\Pi_0 | \rho_0 = 1] = N(\Pi_0) \times q_{11}^{n_{11}} \times q_{12}^{n_{12}} \times q_{21}^{n_{21}} \times q_{22}^{n_{22}},
$$

where q_{ij} are given in (1.2.38).

If we know the starting regime, we can use only the paths with the correct ρ_0. If we do not, we generally assume the starting state is random, with probabilities from the stationary distribution of the Markov chain ρ_t under the physical $\mathbb{P}$-measure.

For longer options, this algorithm substantially reduces the computation time. As shown in Table 1.1, for a T-year option, there are 2^{T+1} possible paths for $\boldsymbol{\rho}^*$, and there are T^2+T+2 distinct values for Π_0; see Proposition 1.3.1. That means, for example, that for a 10-year option with monthly time steps, working through each path requires 2.6×10^{36} calculations, while using the algorithm above requires only 14,764 calculations. Proposition 1.3.1 states the total number of distinct path for Π_0. Let N^A denote the total number of path sets identified by (1.3.55) for T periods.

Table 1.1: Comparison of Path Numbers

T: Number of Period	Path after Iteration(T^2+T+2)	2^{T+1}(Multinomial Tree)
1	4	4
2	8	8
3	14	16
4	22	32
5	32	64
6	44	128
7	58	256
8	74	512
9	92	1024
10	112	2048
11	134	4096
12	158	8192
24	602	33554432
120	14522	2.66×10^{36}

Proposition 1.3.1. *(**CQ**)* $N^A = T^2+T+2$

Proof. To count N^A, we first set up a relationship between N_{12} and N_{21} as follows. Based on (1.2.40) and the relation between ρ_t^* and ρ_t for the RSLN2 models, we have the following transitions available: [11] $\rightarrow$ [11] or [12], with the same for [21]. We also have [12] $\rightarrow$ [21] or [22], with the same for [22]. As a result,

$$\begin{aligned} N_{21}+N_{11} &= N_{11}+N_{12}+c \\ N_{12}+N_{22} &= N_{21}+N_{22}+c, \end{aligned} \tag{1.3.56}$$

where $c \in \{-1, 0, 1\}$. Equation (1.3.56) is the same as

$$N_{21} \quad = \quad N_{12} + c. \tag{1.3.57}$$

Based on (1.3.57), we can show that, from

$$T = N_{11} + N_{12} + N_{21} + N_{22}, \tag{1.3.58}$$

if N_{11} and N_{22} are given, then the values of N_{12} and N_{21} are uniquely determined based on ρ_0 in Π_0. As a result, the value of $N(\Pi_t)$ is determined by the total number of combination of N_{11} and N_{22} within T periods. In the next step, we discuss the number of combination of N_{11} and N_{22} in three cases based on the value of N_{11}.

(i). Assume $N_{11} = 0$. We have the following relationships.

	Conditions				Resulting
	N_{11}	ρ_0	N_{22}	$\{N_{12}, N_{21}\}$	Relationships
T is even	$N_{11} = 0$	$\rho_0 = 1$	$N_{22} = T-1, \ldots, 0$	if N_{22} is even	$N_{21} = N_{12}$
				if N_{22} is odd	$N_{12} = N_{21} + 1$
T is odd	$N_{11} = 0$	$\rho_0 = 1$	$N_{22} = T-1, \ldots, 0$	if N_{22} is even	$N_{12} = N_{21} + 1$
				if N_{22} is odd	$N_{12} = N_{21}$

For example, if $\rho_0 = 1$, then the initial regime $\rho_1^* = [12]$ given $N_{11} = 0$. Also, since $N_{21} = N_{12} + c$ is satisfied for $c \in \{-1, 0, 1\}$, if N_{22} and T are even, then $N_{21} = N_{12}$; if N_{22} is odd and T is even, then $N_{21} = N_{12} + 1$. That is, for any $0 \leq N_{22} \leq T - 1$, we have a scenario available in the candidate path to represent the combination of N_{ij}, the regime occupations. As a result, if $N_{11} = 0$ and $\rho_0 = 1$, then the number of count for different combination of N_{ij} is T. Similarly, if $N_{11} = 0$ and $\rho_0 = 2$, the number of paths is $T + 1$.

(ii). Assume $N_{11} = T$. Then $N_{12} = N_{21} = N_{22} = 0$; the number of path is 1.

(iii). Assume $N_{11} = i, 1 \leq i \leq T - 1$, if $T \geq 2$. Since $[11] \rightarrow [22]$ does not occur, we

have $N_{22} = T - N_{11} - 1, \ldots, 0$. There are total $T - N_{11}$ different values of N_{22} corresponding to each N_{11}, based on $\rho_0 = 1$ or 2. In addition, we can show, in the similar way as in (i), that N_{12} and N_{21} are uniquely determined given I, N_{11}, N_{22}. Therefore, the total number of combination in (iii) is

$$2 \sum_{N_{11}=1}^{T-1} (T - N_{11} - 1) = T^2 - T. \tag{1.3.59}$$

Based on (i)-(iii), we have the total number of paths N^A is

$$N^A = (T + T + 1) + 1 + (T^2 - T) = T^2 + T + 2. \tag{1.3.60}$$

□

1.3.4 Calculating Option Prices

By the previous subsection, we can express the option price formula in terms of the vectors Π_0, and their associated probabilities. Given

$$\Pi_0 = (j, n_{11}, n_{12}, n_{21}, n_{22})$$

for a T-year RSLN process, the option price is the discounted expected value of the payoff, under the lognormal distribution with parameter values

$$\mu^*(\Pi_0) = \sum_{i=1}^{2} \sum_{j=1}^{2} n_{ij} \mu^*_{[ij]}$$

and

$$\sigma^*(\Pi_0) = \sqrt{\sum_{i=1}^{2} \sum_{j=1}^{2} n_{ij} \sigma^2 j}.$$

Then, summing over all feasible Π_0, we have the option price P, say, where

$$P = \sum_{\Pi_0} e^{-rT} E^{\mathbb{Q}_{\Pi_0}}[H(S_T)]\, q(\Pi_0)$$

where $E^{Q_{\Pi_0}}$ denotes expectation under the lognormal distribution with parameters $\mu^*(\Pi_0)$ and $\sigma^*(\Pi_0)$, and

$$q(\Pi_0) = \mathbb{Q}[\Pi_0|\rho_0 = j] \times \mathbb{Q}[\rho_0 = j]$$

For straightforward put and call options, the discounted price has the Black-Scholes format. For example, a put option with strike K on a non-dividend paying stock is

$$BSP(\Pi_0) = Ke^{-rT}\Phi(-d_2) - S_0 \exp\left(-rT + \mu'_k + \frac{\sigma'^2_k}{2}\right) \Phi(-d_1) \tag{1.3.61}$$

where

$$d_2 = \frac{\log(S_0/K) + \mu^*(\Pi_0)}{\sigma^*(\Pi_0)}; \qquad d_1 = d_2 + \sigma^*(\Pi_0) \tag{1.3.62}$$

and the price is

$$P = \sum_{\Pi_0} BSP(\Pi_0)\, q(\Pi_0) \tag{1.3.63}$$

1.4 Numerical Comparison of Esscher Transform, Black-Scholes and NEMM Method Option Prices

In this section, we calculate prices for European put options on non-dividend paying stocks. We use a range of strike values and terms. We compare the ET-$\mathbb{Q}$ measure prices with two other approaches used in the literature. The first is a naive Black-Scholes approach, which is used in Hardy (2003), where the hedge errors are separately accumulated under the RSLN-2 P-measure. The second is the approach

used in Bollen (1998) and Hardy (2001), and elsewhere, where the EMM is red constructed] by using the P measure regime switching process, adjusting parameters within each regime to ensure risk neutrality. This is a discrete analogue of the neutral equivalent martingale measure approach of Elliott et al. (2005).

We use parameters for the RSLN2 model from Hardy(2001), estimated from the monthly total returns on the Toronto Stock Exchange index from 1956 to 1999. The parameters are shown in Table 1.2. We also assume a risk free rate of return of

Table 1.2: RSLN2 Parameters

Regime 1	$\mu_1 = 0.012$	$\sigma_1 = 0.035$	$p_{12} = 0.037$
Regime 2	$\mu_2 = -0.016$	$\sigma_2 = 0.078$	$p_{21} = 0.210$

$r = 0.5\%$ per month, continuously compounded.

1.4.1 Esscher Transform Put Option Prices

To calculate the Esscher Transform prices, we solve the Esscher transform equations for $h^{(1)}$ and $h^{(2)}$, where

$$\begin{aligned} e^r &= \frac{\mathsf{E}^{\mathbb{P}}[e^{(h^{(1)}+1)Y_t}|\rho_{t-1}=1]}{\mathsf{E}^{\mathbb{P}}[e^{h^{(1)}Y_t}|\rho_{t-1}=1]} \\ &= \frac{p_{11}\, e^{\left(\mu_1(h^{(1)}+1)+\sigma_1^2(h^{(1)}+1)^2/2\right)} + p_{12}\, e^{\left(\mu_2(h^{(1)}+1)+\sigma_2^2(h^{(1)}+1)^2/2\right)}}{p_{11}\, e^{\left(\mu_1 h^{(1)}+\sigma_1^2(h^{(1)})^2/2\right)} + p_{12}\, e^{\left(\mu_2 h^{(1)}+\sigma_2^2(h^{(1)})^2/2\right)}} \end{aligned}$$

and similarly

$$\begin{aligned} e^r &= \frac{\mathsf{E}^{\mathbb{P}}[e^{(h^{(2)}+1)Y_t}|\rho_{t-1}=2]}{\mathsf{E}^{\mathbb{P}}[e^{h^{(2)}Y_t}|\rho_{t-1}=2]} \\ &= \frac{p_{21}\, e^{\left(\mu_1(h^{(2)}+1)+\sigma_1^2(h^{(2)}+1)^2/2\right)} + p_{22}\, e^{\left(\mu_2(h^{(2)}+1)+\sigma_2^2(h^{(2)}+1)^2/2\right)}}{p_{21}\, e^{\left(\mu_1 h^{(2)}+\sigma_1^2(h^{(2)})^2/2\right)} + p_{22}\, e^{\left(\mu_2 h^{(2)}+\sigma_2^2(h^{(2)})^2/2\right)}}. \end{aligned}$$

This leads to $h^{(1)} = -4.546$ and $h^{(2)} = 2.458$.

Table 1.3 reports the parameters for the 4-state regime switching process ρ_t^* under the ET-$\mathbb{Q}$ measure, corresponding to the $\mathbb{P}$-measure defined by the parameter values from Table 1.2. In the computation, we plug parameters $h^{(1)}$ and $h^{(2)}$ into equations (1.3.52) and (1.3.53) to obtain the $\mu^*_{[\rho_t^*]}$ and the transition probabilities. The values of $\sigma^*_{[\rho_t^*]}$ given $\rho_t^* = [ij]$ is equal to the physical volatilities in regime $\rho_t = j$.

Regime Parameters at t			Transition Probabilities given ρ_t^* under $\mathbb{Q}$ measure			
ρ_t^*	$\mu^*_{[\rho_t^*]}$	$\sigma^*_{[\rho_t^*]}$	$\rho^*_{t+1} = [11]$	$\rho^*_{t+1} = [12]$	$\rho^*_{t+1} = [21]$	$\rho^*_{t+1} = [22]$
[11]	0.0064	0.035	0.9561	0.0439	0.0000	0.0000
[12]	-0.0437	0.078	0.0000	0.0000	0.2191	0.7809
[21]	0.0150	0.035	0.9561	0.0439	0.0000	0.0000
[22]	-0.0010	0.078	0.0000	0.0000	0.2191	0.7809

Table 1.3: Regime and transition parameters under the ET-$\mathbb{Q}$ measure for the RSLN model.

Using these parameters, we apply the results in section 1.3.4 to calculate the exact prices for European put options (on a non-dividend paying stock), for a range of terms and strike prices. In the computation, we sum the conditional expected values of the contingent payoff given in (1.3.61) over all the distinct paths identified using the recursive algorithm from section 1.2. Some sample values are shown in Table 1.4.

K	$T = 120$	24	12	4
50	0.0687	0.0079	0.0010	0.0000
100	2.2155	3.9585	3.5686	2.5449
150	10.5673	34.1329	41.3789	47.0323
200	25.8436	77.4444	88.3556	96.0397

Table 1.4: Put option prices under the ET-$\mathbb{Q}$ measure. The starting stock price is \$100, T is term in months, and the risk free rate is $r = 0.5\%$ per month. Other parameters are from Tables 1.2 and 1.3.

1.4.2 The Black–Scholes Prices

We compare the ET-$\mathbb{Q}$ prices above with the Black-Scholes prices, with volatility equal to the stationary volatility of the RSLN2 model, which is

$$\sigma^2 = \mathsf{E}^{\mathbb{P}}[\mathsf{Var}[Y_t|\rho_t]] + \mathsf{Var}[\mathsf{E}^{\mathbb{P}}[Y_t|\rho_t]] = 0.045307^2, \tag{1.4.64}$$

where the variance is calculated under the physical $\mathbb{P}$-measure. As discussed at the beginning of this chapter, with the assumption that there is no replicating strategy available for the regime switching process, the risk neutral Gaussian measure assumed under the Black-Scholes method is not a desired equivalent martingale measure with the consideration of both risks associated with $\{\rho_t\}$ and $\{Y_t\}$. This method is used here for comparison purpose only, to measure the difference in pricing and hedging performance. The put option prices for the same range of terms and strikes as in Table 1.5.

K	$T = 120$	24	12	4
50	0.0364	0.0004	0.0000	0.0000
100	1.9837	3.8660	3.5984	2.6746
150	10.3495	34.2333	41.3553	47.0298
200	25.7897	77.4296	88.3530	96.0397

Table 1.5: Put option prices using the Black-Scholes formula. The starting stock price is \$100, T is term in months, the risk free rate is $r = 0.5\%$ per month, and the volatility is 4.5307% per month.

1.4.3 The NEMM Method

Hardy (2001) and Bollen (1998) use a simple transformation of the RSLN model $\mathbb{P}$–measure to a risk neutral $\mathbb{Q}$ measure, by changing the regime parameters such that each regime is risk neutral, that is

$$\mathsf{E}^{\mathbb{Q}}[e^{Y_t}|\rho_t = j] = e^r \quad \forall j$$

Then a European option payoff $H(S_T)$ can be valued at, say $t = 0$, by conditioning first on the $\mathbb{P}$-measure regime path, $\boldsymbol{\rho} = \{\rho_1, ..., \rho_T\}$, then by taking expectations over all regime paths, using the $\mathbb{P}$-measure transition matrix. That is,

$$e^{-rT}\, \mathsf{E}^{\mathbb{P}}[\mathsf{E}^{\mathbb{Q}}[H(S_T)|\boldsymbol{\rho}].$$

This is analogous to the natural equivalent martingale measure approach used by Elliott et al (2005) for the continuous time regime switching geometric Brownian motion model. More details of the implementation of this method are given in Hardy (2001).

In Table 1.6 we show prices for European put options, for the same range of strikes and terms, and using the same parameters, as in Tables 1.4 and 1.5.

K	$T = 120$	24	12	4
50	0.0383	0.0037	0.0005	0.0000
100	1.8341	3.5842	3.3058	2.4284
150	9.8757	34.1810	41.4195	47.0336
200	25.1952	77.4709	88.3579	96.0397

Table 1.6: Put option prices under the NEMM measure. The starting stock price is \$100, T is term in months, the risk free rate is $r = 0.5\%$ per month. Other parameters from table 1.6.

1.4.4 Remarks

It is interesting to note that there is no clear ordering of prices under these measures introduced in the previous three subsections. For the long term options, say T=120 months, the ET prices are greater than the Black Scholes prices for all strikes, but for shorter term options, the ET prices dip below the BS prices for options near to the money. Similarly, the ET prices exceed the NEMM prices for all strikes for long term options, but are slightly lower for in-the-money options for shorter terms. The price comparison at time t connects with the the comparison of the distributions of

$\sum_{s=t}^{T} Y_s$ under the respective $\mathbb{Q}$ measures, which we discuss in more details in chapter 4.

If we compare the three different $\mathbb{Q}$ measures more directly, we might gain some insight. Each $\mathbb{Q}$ measure comprises a number of Gaussian regimes, each regime having $\mu^{\mathbb{Q}}$ and $\sigma^{\mathbb{Q}}$ given below, corresponding to the lognormal parameters. We also show the stationary probabilities for the regimes.

Black Scholes:

One Regime

$\sigma^{\mathbb{Q}} = 0.0453 \quad \mu^{\mathbb{Q}} = 0.0040$

NEMM:

Two Regimes

$\sigma_1^{\mathbb{Q}} = 0.035 \quad \mu_1^{\mathbb{Q}} = 0.0044 \quad$ Probability 0.8502

$\sigma_2^{\mathbb{Q}} = 0.078 \quad \mu_2^{\mathbb{Q}} = 0.0020 \quad$ Probability 0.1498

ET:

Four Regimes

$\sigma_{[11]}^{\mathbb{Q}} = 0.035 \quad \mu_{[11]}^{\mathbb{Q}} = 0.0064 \quad$ Probability 0.7965

$\sigma_{[12]}^{\mathbb{Q}} = 0.078 \quad \mu_{[12]}^{\mathbb{Q}} = -0.0437 \quad$ Probability 0.0366

$\sigma_{[21]}^{\mathbb{Q}} = 0.035 \quad \mu_{[21]}^{\mathbb{Q}} = 0.015 \quad$ Probability 0.0366

$\sigma_{[22]}^{\mathbb{Q}} = 0.078 \quad \mu_{[22]}^{\mathbb{Q}} = -0.0010 \quad$ Probability 0.1303

Now, the paths for the NEMM process that result in a low stock price are those that are weighted more to Regime 2, and for the ET process are those that are weighted more to regimes [12] and [22]. The ET regimes are rather more adverse than the NEMM regimes, as the $\mu^{\mathbb{Q}}$ parameters are much lower. This would indicate higher option prices for out-of-the-money put options under ET compared with NEMM; similarly, ET regimes 2 and 4 would generate more weight for low stock prices compared with the BS model, with higher volatility and lower means. On the other hand, regimes 1 and 3 of the ET process have low variance and high mean, and will generate potentially heavier right tails for the stock price compared with the other two models.

However, the comparison of the distributions based on two moments are not sufficient to determine the levels of option prices. In Chapter 4, more analysis of the difference between two distributions under risk neutral measures are investigated, and the pricing and hedging performance are compared. Overall, there are no clear conclusions here. The ET prices are not consistently higher than the prices using two other measures for shorter terms; for longer terms, the impact of the two 'negative mean, high volatility' regimes in the ET process appears to generate higher prices for all the put options, compared with the other two processes. For shorter options there is no obvious intuition as to how the three prices will be ordered, and, in fact, selecting different terms and strikes from Tables 1.4, 1.5 and 1.6, we see that all possible orderings of prices from the three measures are achieved.

1.4.5 Preliminary Hedging Results

The price of an option is more meaningful when it is associated with a strategy for hedging the contingent claim. Here some preliminary numerical analysis is presented for the RSLN-2 prices in the section.

We simulated 10,000 paths for the underlying stock price, using the RSLN-2 $\mathbb{P}$-measure, with the parameters from Table 1.2. We also determined the delta hedge costs for each of the three measures, assuming monthly rebalancing. Because the underlying process is incomplete, and because the hedge is discretely rebalanced, the hedge will not be self financing. For each simulated path, we determine the present value of the hedging loss (PVHL), discounting at the risk free rate of interest, summing over all the months of the contract. The result is a Monte Carlo estimate of the distribution of the PVHL for each of the pricing measures. We consider a 12-month and a 120-month put option, and we assume the strike K and the starting asset price, S_0 are both 100.

We have summarized the effectiveness of the hedge using the following two measures:

1. The probability that the PVHL is positive – that is, that the hedge portfolio is insufficient overall, and

	K	Option Price	Pr[PVHL >0]	$\text{CTE}_{95\%}$(PVHL)
BS	100	1.9842	0.4155 (0.0049)	3.4172 (0.0777)
NEMM	100	1.8341	0.4406 (0.0050)	3.6800 (0.0812)
ET-Q	100	2.2155	0.3039 (0.0046)	3.1622 (0.0836)

Table 1.7: Present Value of Hedging Loss, 120 month Put Options, 10,000 simulations. Values inside brackets are the corresponding standard errors of Pr and the CTE.

	K	Option Price	Pr[PVHL >0]	$\text{CTE}_{95\%}$(PVHL)
BS	100	3.5983	0.3654 (0.0048)	6.4873 (0.1380)
NEMM	100	3.3058	0.3974 (0.0049)	6.9582 (0.1454)
ET-Q	100	3.5686	0.3148 (0.0046)	6.1543 (0.1243)

Table 1.8: Present Value of Hedging Loss, 12 month Put Options, 10,000 simulations. Values inside brackets are the corresponding standard errors of Pr and the CTE.

2. The 95% Conditional Tail Expectation (CTE) (or TailVaR) of the PVHL – that is, the average cost of the worst 5% of outcomes. The standard errors of the CTE are evaluated using the method suggested by Manistre and Hancock (2005).

In Table 1.7 we show the results for a 10-year at-the-money put option, where the probability and CTE are calculated under $\mathbb{P}$–measure. It appears from this experiment that the additional cost of the option under the ET method pays some benefits, in terms of a significantly reduced loss probability, and in a lower 95% CTE value. However, the reduction in the CTE, compared with the Black Scholes hedge, is only around \$0.25, and when that is compared with an additional option cost of \$0.23, it does not make a compelling argument for the ET hedge. The results for the 12-month option are more interesting, as summarized in Table 1.8. In this case, the Black-Scholes price is greater than the ET price, but the ET measure appears to create a more effective hedging strategy, both in terms of the probability of hedging loss, and with a lower CTE value. More research into whether these results apply

more generally with the ET price could be valuable.

1.5 Conclusions

The Esscher transform offers a pricing measure for discrete time regime switching models that differs from the natural equivalent martingale measure approach. This is intuitively attractive, as the regime switching risk is assumed to be undiversifiable.

The calculation of European option prices under regime switching models has been shown in this chapter to be relatively tractable – either through the dimension reduction algorithm, or, for more complex models (for example, with more regimes) through Monte Carlo pricing, once the full specification of the $\mathbb{Q}$ measure process is derived. In the next chapter, we extend the model to multivariate option pricing. The pricing is more complex, but the fundamental principles still follow the development in this chapter.

Pricing is only the first part of the story, however. Preliminary experiments with hedging indicate some potential for improved hedge performance using the ET measure. In later chapters, we analyze the ET hedge in more details.

Chapter 2

Esscher Transform Pricing of Multivariate Options under Discrete Time Regime Switching

2.1 Introduction

We proposed an approach, using the Esscher transform, to price univariate options under discrete time Markov regime switching models in Chapter 1. This chapter aims to extend this approach to the multivariate discrete time regime switching models. The Esscher transform has been a widely used tool for multivariate pricing in the literature, such as Bertholon et al. (2008) and Gourieroux and Monfrot (2007) for a general econometric asset pricing, Bühlmann (1980) for multivariate equilibrium pricing, Kajima (2006) and Wang (2007) for the links between distortion and the Esscher transform in multivariate equilibrium pricing, Song, et al. (2010) for multivariate option valuation under Markov chain models, and Ng and Li (2011) for the valuation of multivariate asset pricing annuity guarantees, among many others. Our work focuses on the market incompleteness due to regime uncertainty. Some

notation used in this chapter is listed as follows.

t		$t = 0, 1, \ldots, T$	the range of discrete time points
$S_{t,l}$		$t = 0, \ldots, T; l = 0, \ldots, N$	asset prices at time t for l^{th} asset
$Y_{t,l}$		$t = 1, \ldots, T; l = 1, \ldots, N$	log returns of asst prices at time t for l^{th} asset
$h_{t,l}$		$t = 1, \ldots, T; l = 1, \ldots, N$	Esscher transform parameters at t for l^{th} asset
$\mathbf{S}_{t,\bullet}$	=	$(S_{t,1}, \ldots, S_{t,N})'$	the column vector of $\mathbf{S}_{t,\bullet}$ at time t
$\mathbf{S}_{\bullet,l}$	=	$(S_{0,l}, \ldots, S_{T,l})$	the row vector of $\mathbf{S}_{\bullet,l}$ for l^{th} asset
$\mathbf{Y}_{t,\bullet}$	=	$(Y_{t,1}, \ldots, Y_{t,N})'$	the column vector of $\mathbf{Y}_{t,\bullet}$ at time t
$\mathbf{Y}_{\bullet,l}$	=	$(Y_{1,l}, \ldots, Y_{T,l})$	the row vector of $\mathbf{Y}_{\bullet,l}$ for l^{th} asset
$\mathbf{h}_{t,\bullet}$	=	$(h_{t,1}, \ldots, h_{t,N})'$	the column vector of $\mathbf{h}_{t,\bullet}$ at time t
ρ_t		$\rho_t = 1, \ldots R$	the undelying regimes

(2.1.1)

2.2 Market Models and Objective

Assume that there are N underlying risky assets in the market. The multivariate regime switching process can be represented as

$$(\rho_t, S_{t,0}, \ldots, S_{t,N})_{0 \le t \le T},$$

where $S_{t,l}$ is the price of asset l at time t, with $S_{t,0}$ representing the price of the risk free asset, and ρ_t represents the regime of the market at time t. For notational convenience, we use vector representation in this chapter. Define $\mathbf{S}_{t,\bullet} = (S_{t,1}, \ldots, S_{t,N})'$ and $\mathbf{S}_{\bullet,l} = (S_{0,l}, \ldots, S_{T,l})$. Similarly, we define vectors $\mathbf{Y}_{t,\bullet}$ and $\mathbf{Y}_{\bullet,l}$ for the log-returns of the underlying asset prices. The corresponding realized values are denoted by small letters, e.g., $\mathbf{y}_{t,\bullet} = (y_{t,1}, \ldots, y_{t,N})$ represents the realization of $\mathbf{Y}_{t,\bullet}$. Assume a

constant risk free rate r. Then, the market model is

$$\begin{cases} S_{t,0} &= S_{t-1,0}e^{rt} \\ S_{t,l} &= S_{t-1,l}e^{Y_{t,l}}, \quad l = 1, \ldots, N, \end{cases} \tag{2.2.2}$$

where $\{\mathbf{Y}_{t,\bullet}\}_{t=1}^{T}$ follows a regime switching process, i.e., the multivariate distribution of $\mathbf{Y}_{t,\bullet} = (Y_{t,1}, \ldots, Y_{t,N})$ depends on ρ_t.

The objective of this chapter is to price options written on the multiple risky assets. The pricing approach is illustrated for a European put options written on the geometric average of stock prices. We do not discuss hedging. Indeed, since the geometric average can be treated as a single risky asset price, the delta hedging for the put option can be conducted based on the delta of the portfolio which approximately replicates the geometric average. As a result, the hedging results for this European put option will be similar to the hedging results for a put option written on a single risky asset, as illustrated in Chapter 1.

Let $\mathcal{F}_t^Y$ and $\mathcal{F}_t^\rho$ denote the $\mathbb{P}$-augmentation of the filtration generated by $\{\mathbf{Y}_{s,\bullet}\}_{s=0}^{t}$ and $\{\rho_s\}_{s=0}^{t}$, respectively. We write $\mathcal{F}_t = \mathcal{F}_t^Y \vee \mathcal{F}_t^\rho$, representing the minimal sigma algebra containing $\mathcal{F}_t^Y$ and $\mathcal{F}_t^\rho$. Based on the filtration, we assume ρ_t is adapted to the filtration $\{\mathcal{F}_t\}$; that is, we can observe the state of ρ_t at time t. We do not assume, for our discrete time model, the predictability of ρ_t. Similar to chapter 1, we also impose the following assumptions for the market model (2.2.2).

(A1) The process $\{\rho_t\}_{t=0}^{T}$ follows a finite state Markov chain process, with a state space of R regimes. Assume the transition probability matrix $\wp = \{p_{ij}\}$, where $p_{ij} = \mathbb{P}(\rho_t = j \,|\, \rho_{t-1} = i)$, is time homogeneous.

(A2) The distribution of $\mathbf{Y}_{t,\bullet}$ conditional on ρ_t is independent of ρ_s and $\mathbf{Y}_{s,\bullet}$ for $s \neq t$.

The so-called MET-$\mathbb{Q}$ pricing measure is developed in section 2.3 of this chapter, and can be applied to option pricing for models such as the regime switching AR model, where the distribution of $\mathbf{Y}_{t,\bullet}$ conditional on ρ_t is dependent on $\mathbf{Y}_{s,\bullet}$, $s < t$. However,

for computational convenience, the independence of $\mathbf{Y}_{1,\bullet}, \ldots, \mathbf{Y}_{T,\bullet}$ conditional on $\{\rho_t\}$ is a assumed here.

(A3) $Y_{t,l}$ is a continuous random variable which satisfies $\operatorname{ess\,inf} Y_{t,l} < r < \operatorname{ess\,sup} Y_{t,l}$ for all $t = 1, \ldots, T$ and $l = 1, \ldots, N$;

(A4) $\mathsf{E}^{\mathbb{P}}(e^{\mathbf{h}'_{t,\bullet}\mathbf{Y}_{t,\bullet}}|\mathcal{F}_{t-1}) < \infty$ for all real vector $h_{t,\bullet} \in \mathbb{R}^N$.

Assumption (A3) is necessary in a no-arbitrage market. (A4) is a necessary condition for our pricing method.

2.3 Multivariate Esscher Transformed $\mathbb{Q}$ Measure

To conduct risk neutral pricing, we start with an equivalent risk neutral measure $\mathbb{Q}$ identified using the Esscher transform. This section further discusses the properties with the Esscher transform parameters and investigates the distribution under the identified $\mathbb{Q}$ measure.

2.3.1 Multivariate Esscher Transform

The Esscher transform is defined similarly as in Chapter 1, except that the single risky asset in the transform is replaced by multiple risky assets. If we let $H(\mathbf{S}_{T,\bullet})$ denote the payoff of the European option under consideration, then, after we identify the pricing measure $\mathbb{Q}$, the no-arbitrage price can be computed as the expectation of its discounted payoff, i.e.

$$P_t(H(\mathbf{S}_{T,\bullet})) \;=\; e^{-r(T-t)}\mathsf{E}^{\mathbb{Q}}[\, H(\mathbf{S}_{T,\bullet}) \,|\, \mathcal{F}_t \,], \tag{2.3.3}$$

where $\mathsf{E}^{\mathbb{Q}}[\cdot|\mathcal{F}_t]$ denotes the expectation conditional on $\mathcal{F}_t$ under the $\mathbb{Q}$ measure. In this study, the $\mathbb{Q}$ measure is identified by employing the conditional Esscher trans-

form introduced by Bühlmann (1996), and it is defined through the following Radon-Nikodym derivative

$$\left.\frac{d\mathbb{Q}}{d\mathbb{P}}\right|_{\mathcal{F}_t} = \prod_{s=1}^{t} \frac{e^{\mathbf{h}'_{s,\bullet}\mathbf{Y}_{s,\bullet}}}{\mathsf{E}^{\mathbb{P}}(e^{\mathbf{h}'_{s,\bullet}\mathbf{Y}_{s,\bullet}}|\,\mathcal{F}_{s-1})}, \quad t = 1, \ldots, T, \tag{2.3.4}$$

where the only parameters are the Esscher transform parameters $\mathbf{h}_{s,\bullet}$, and $\mathsf{E}^{\mathbb{P}}(\cdot|\mathcal{F}_{s-1})$ represents the conditional expectation under $\mathbb{P}$ measure. Equation (2.3.4) denotes the Radon-Nikodym derivative of $\mathbb{Q}$ over $\mathbb{P}$ on $\mathcal{F}_t$. To make the probability measure $\mathbb{Q}$ a risk neutral probability measure, the Esscher transform parameters in $\mathbf{h}_{s,\bullet} = (h_{s,1}, \ldots, h_{s,N})'$ in (2.3.4) must satisfy the following N equations

$$e^r = \frac{\mathsf{E}^{\mathbb{P}}[e^{\mathbf{h}'_{s,\bullet}\mathbf{Y}_{s,\bullet}+Y_{s,l}}|\,\mathcal{F}_{s-1}]}{\mathsf{E}^{\mathbb{P}}[e^{\mathbf{h}'_{s,\bullet}\mathbf{Y}_{s,\bullet}}|\,\mathcal{F}_{s-1}]}, \; l = 1, \ldots, N, \tag{2.3.5}$$

for all $s = 1, \ldots, T$. We call the measure $\mathbb{Q}$ obtained through $\left.\frac{d\mathbb{Q}}{d\mathbb{P}}\right|_{\mathcal{F}_t}$ defined by (2.3.4) and (2.3.5) the multivariate Esscher transform $\mathbb{Q}$ (MET$-\mathbb{Q}$) measure.

Proposition 2.3.1. *(**CQ**) The MET-$\mathbb{Q}$ measure identified through the Radon-Nikodym derivative (2.3.4) under conditions (2.3.5) is a risk neutral measure.*

Proof. As $h_{s,\bullet} \in \mathcal{F}_{t-1}$ for all $s \leq t$, we apply $\left.\frac{d\mathbb{Q}}{d\mathbb{P}}\right|_{\mathcal{F}_t}$, defined in (2.3.4) as follows:

$$\begin{aligned} \mathsf{E}^{\mathbb{Q}}\left(\frac{S_{t,l}}{S_{t-1,l}}\middle|\,\mathcal{F}_{t-1}\right) &= \mathsf{E}^{\mathbb{P}}\left[e^{Y_{t,l}}\frac{\left.\frac{d\mathbb{Q}}{d\mathbb{P}}\right|_{\mathcal{F}_t}}{\left.\frac{d\mathbb{Q}}{d\mathbb{P}}\right|_{\mathcal{F}_{t-1}}}\middle|\,\mathcal{F}_{t-1}\right] \\ &= \mathsf{E}^{\mathbb{P}}\left[e^{Y_{t,l}}\frac{e^{\mathbf{h}'_{t,\bullet}\mathbf{Y}_{t,\bullet}}}{\mathsf{E}^{\mathbb{P}}[e^{\mathbf{h}'_{t,\bullet}\mathbf{Y}_{t,\bullet}}|\mathcal{F}_{t-1}]}\middle|\,\mathcal{F}_{t-1}\right] = e^r \end{aligned} \tag{2.3.6}$$

where the last equation is due to the condition (2.3.5) with $s = t$. Thus, the MET-$\mathbb{Q}$ measure is a risk neutral measure. □

2.3.2 Identifiability of the Esscher Parameters

The Esscher transform parameters $h_{t,1}, \ldots, h_{t,N}$ are obtained by solving the system of nonlinear equations in (2.3.5). It is challenging to address the existence and uniqueness of the solution to the system, and we leave this issue for future research. In what follows, we will illustrate how to identify the Esscher transform parameters in some specific and yet important cases.

Example 4. Assume that, conditional on $\mathcal{F}_{t-1}$, $\mathbf{Y}_{t,\bullet}$ follows a multivariate normal MVN$(\boldsymbol{\mu}, \boldsymbol{\Sigma})$ with a mean vector $\boldsymbol{\mu} = (\mu_1, \ldots, \mu_N)'$ and a covariance matrix $\boldsymbol{\Sigma} = (\sigma_{ij})_{N\times N}$. Let $\mathbf{e}_l$ represent the column vector with one in the l^{th} coordinate and zeros in all the others. Then, condition (2.3.5) becomes

$$e^r = \frac{\exp\left((\mathbf{h}_{t,\bullet} + \mathbf{e}_l)'\boldsymbol{\mu} + \frac{1}{2}(\mathbf{h}_{t,\bullet} + \mathbf{e}_l)'\boldsymbol{\Sigma}(\mathbf{h}_{t,\bullet} + \mathbf{e}_l)\right)}{\exp\left(\mathbf{h}'_{t,\bullet}\boldsymbol{\mu} + \frac{1}{2}\mathbf{h}'_{t,\bullet}\Sigma\mathbf{h}_{t,\bullet}\right)}, \; l = 1, \ldots, N. \tag{2.3.7}$$

Equation (2.3.7) can be rewritten in a more concise form of

$$\boldsymbol{\Sigma}\mathbf{h}_{t,\bullet} = r\mathbf{1} - \boldsymbol{\mu} - \frac{1}{2}\mathbf{b},$$

where $\mathbf{1}$ denotes a vector with all elements equal to one, and $\mathbf{b} = (\sigma_{11}, \ldots, \sigma_{NN})'$. If the covariance matrix $\boldsymbol{\Sigma}$ is positive definite, then there is a unique $\mathbf{h}_{t,\bullet}$ satisfying (2.3.5) with $\mathbf{h}_{t,\bullet} = \Sigma^{-1}(r\mathbf{1} - \mu)$. □

Example 5. Assume that $Y_{t,1}, \ldots, Y_{t,N}$ are independent conditional on $\mathcal{F}_{t-1}$. Then,

$$\begin{aligned}
\mathsf{E}^{\mathbb{Q}}(e^{Y_{t,l}}|\mathcal{F}_{t-1}) &= \frac{\mathsf{E}^{\mathbb{P}}(e^{(h_{t,l}+1)Y_{t,l}}|\mathcal{F}_{t-1})}{\mathsf{E}^{\mathbb{P}}(e^{h_{t,l}Y_{t,l}}|\mathcal{F}_{t-1})} \prod_{k\neq 1} \frac{\mathsf{E}^{\mathbb{P}}(e^{h_{t,k}Y_{t,k}}|\mathcal{F}_{t-1})}{\mathsf{E}^{\mathbb{P}}(e^{h_{t,k}Y_{t,k}}|\mathcal{F}_{t-1})} \\
&= \frac{\mathsf{E}^{\mathbb{P}}(e^{(h_{t,l}+1)Y_{t,l}}|\mathcal{F}_{t-1})}{\mathsf{E}^{\mathbb{P}}(e^{h_{t,l}Y_{t,l}}|\mathcal{F}_{t-1})}, \qquad l = 1, \ldots, N.
\end{aligned}$$

As a result, the multivariate Esscher transforms are reduced to univariate Esscher transforms for $Y_{t,l}, l = 1, \ldots, N$, conditional on $\mathcal{F}_{t-1}$. □

Example 6. Assume that there are 2 risky assets in the market under a two-state

regime switching model, with the log return $Y_{t,\bullet}$ conditional on $\mathcal{F}_{t-1}$ following the mixed multivariate normal distribution $\sum_{j=1}^{2} p_{ij} MVN(\mu_j, \Sigma_j)$, where $p_{ij} = \mathbb{P}(\rho_t = j | \rho_{t-1} = i)$. We define a function $\mathbb{L}$ as below:

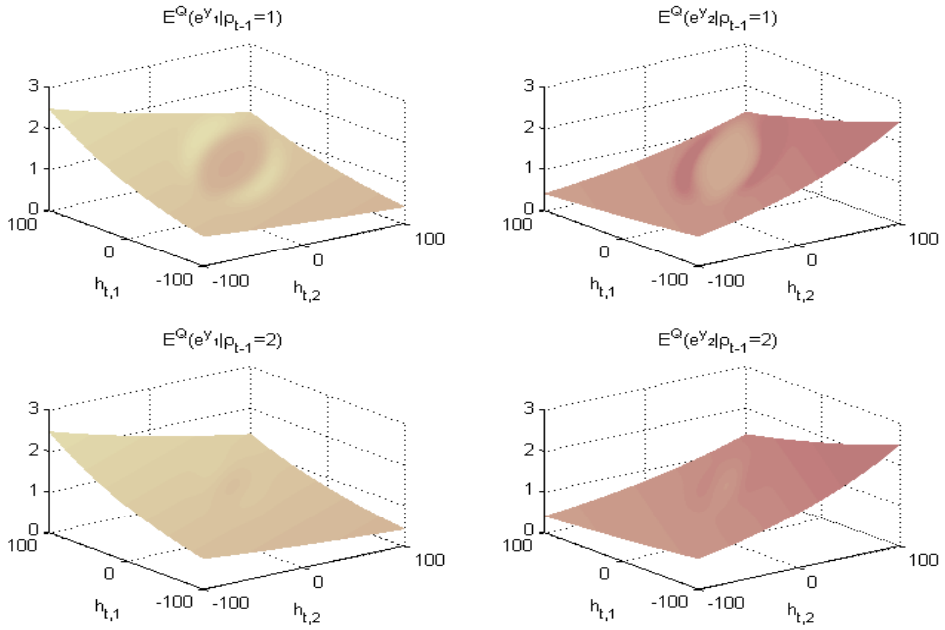

Figure 2.1: The surface of $\mathsf{E}^{\mathbb{Q}}[e^{h_{t,l} Y_{t,l}} | \rho_{t-1}]$ over the ranges of $h_{t,1}$ and $h_{t,2}$

$$\mathbb{L} = \left| e^r - \frac{\mathsf{E}^{\mathbb{P}}[e^{h'_{t,\bullet} Y_{t,\bullet} + Y_{t,1}} | \, \rho_{t-1}]}{\mathsf{E}^{\mathbb{P}}[e^{h'_{t,\bullet} Y_{t,\bullet}} | \, \rho_{t-1}]} \right| + \left| e^r - \frac{\mathsf{E}^{\mathbb{P}}[e^{h'_{t,\bullet} Y_{t,\bullet} + Y_{t,2}} | \, \rho_{t-1}]}{\mathsf{E}^{\mathbb{P}}[e^{h'_{t,\bullet} Y_{t,\bullet}} | \, \rho_{t-1}]} \right|$$

It is sufficient to investigate the solution to $\mathbb{L} = 0$ for the analysis of the existence and uniqueness of the solutions to (2.3.5). We conduct the analysis numerically, based on manipulated parameters for the multivariate RSLN2 models, assuming a positive covariance in one regime and negative covariance in the other. Parameters and correlation matrices on the joint distribution of $(Y_{t,1}, Y_{t,2})$ are given Table 2.5 and 2.6 in section 2.4.1, with three assets replaced by two assets.

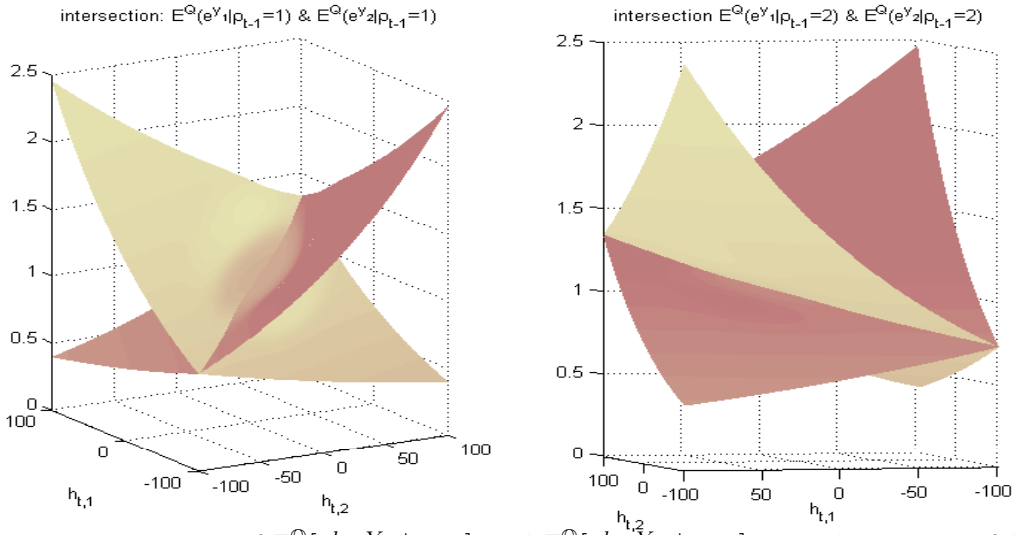

Figure 2.2: Intersection of $\mathsf{E}^{\mathbb{Q}}[e^{h_{t,l}Y_{t,l}}|\rho_{t-1}]$ and $\mathsf{E}^{\mathbb{Q}}[e^{h_{t,l}Y_{t,2}}|\rho_{t-1}]$ over the ranges of $h_{t,1}$ and $h_{t,2}$

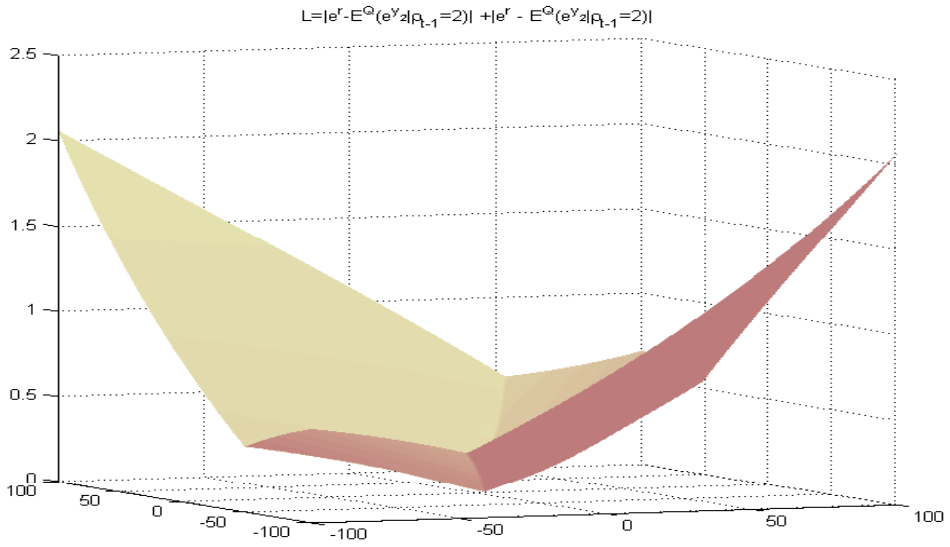

Figure 2.3: The surface of $\mathbb{L}$ over the ranges of $h_{t,1}$ and $h_{t,2}$

We first observe the surface of $\mathsf{E}^{\mathbb{Q}}[e^{h_{t,l}Y_{t,l}}|\rho_{t-1}]$ and $\mathsf{E}^{\mathbb{Q}}[e^{h_{t,l}Y_{t,2}}|\rho_{t-1}]$ over the range of $h_{t,1}$ and $h_{t,2}$ in Figure 2.1, and observe their intersection in Figure 2.2. We can see that the surface of $\mathsf{E}^{\mathbb{Q}}[e^{h_{t,l}Y_{t,l}}|\rho_{t-1}]$ and $\mathsf{E}^{\mathbb{Q}}[e^{h_{t,l}Y_{t,2}}|\rho_{t-1}]$ are not parallel, and they

intersect in an increasing curve. A point $(h_{t,1}, h_{t,2}, e^r)$ is in the curve. That is, there exist a pair of real numbers $h_{t,1}$ and $h_{t,2}$ at which e^r is a value of both functions $\mathsf{E}^{\mathbb{Q}}[e^{h_{t,l}Y_{t,l}}|\rho_{t-1}]$ and $\mathsf{E}^{\mathbb{Q}}[e^{h_{t,l}Y_{t,2}}|\rho_{t-1}]$. Figure 2.3 illustrates a surface of the values of $\mathbb{L}$ over the ranges of $h_{t,1}$ and $h_{t,2}$, for the RSLN2 model with the manipulated parameters. We can obtain the unique numerical value of $h_{t,\bullet}$ which makes $\mathbb{L} = 0$.

2.3.3 Distribution under the MET-$\mathbb{Q}$ Measure

Assume we identify the Esscher transform (2.3.4) satisfying conditions (2.3.5); then, we need to derive the distribution under the MET-$\mathbb{Q}$ measure of log-returns of the underlying asset prices, in order to conduct option pricing using the formula (2.3.3). We obtain the underlying distributions in a similar way as we do for the univariate models in section 1.2.1 of Chapter 1. Here we first derive the distribution of $\mathbf{Y}_{t,\bullet}$ conditional on $\mathcal{F}_{t-1}$, under the measure MET-$\mathbb{Q}$ identified by (2.3.4). Let $\mathbf{u} = (u_1, \ldots, u_N)'$ be a vector of real numbers such that $\mathsf{E}^{\mathbb{P}}(e^{\mathbf{u}'\mathbf{Y}_{t,\bullet}}|\,\mathcal{F}_{t-1}) < \infty$. Then, similar to (2.3.6), we have

$$\begin{aligned}
\mathsf{E}^{\mathbb{Q}}\left[e^{\mathbf{u}'\mathbf{Y}_{t,\bullet}}\middle|\,\mathcal{F}_{t-1}\right] &= \mathsf{E}^{\mathbb{P}}\left[e^{\mathbf{u}'\mathbf{Y}_{t,\bullet}}\frac{\frac{d\mathbb{Q}}{d\mathbb{P}}|_{\mathcal{F}_t}}{\frac{d\mathbb{Q}}{d\mathbb{P}}|_{\mathcal{F}_{t-1}}}\middle|\,\mathcal{F}_{t-1}\right] \\
&= \mathsf{E}^{\mathbb{P}}\left[e^{\mathbf{u}'\mathbf{Y}_{t,\bullet}}\frac{e^{h'_{t,\bullet}\mathbf{Y}_{t,\bullet}}}{\mathsf{E}^{\mathbb{P}}[e^{h'_{t,\bullet}\mathbf{Y}_{t,\bullet}}|\mathcal{F}_{t-1}]}\middle|\,\mathcal{F}_{t-1}\right]
\end{aligned} \tag{2.3.8}$$

Recall the notation $\mathcal{F}_t = \mathcal{F}_t^Y \vee \mathcal{F}_t^\rho$. As a result, the distribution of $\mathbf{Y}_{t,\bullet}$ conditional on $\mathcal{F}_{t-1}$, under the MET-$\mathbb{Q}$ measure, can be obtained through expanding the moment generating function (2.3.8). The density function of $Y_{t,\bullet}$ conditional on $\rho_t = j$ and $\mathcal{F}_{t-1}$, under the MET-$\mathbb{Q}$ measure, is

$$f^{\mathbb{Q}}(\mathbf{y}_{t,\bullet}|\mathcal{F}_{t-1}\bigcap\{\rho_t = j\}) = \frac{e^{\mathbf{h}'_{t,\bullet}\mathbf{y}_{t,\bullet}}f^{\mathbb{P}}(\mathbf{y}_{t,\bullet}|\mathcal{F}_{t-1}\bigcap\{\rho_t = j\})}{\mathsf{E}^{\mathbb{P}}[e^{\mathbf{h}'_{t,\bullet}\mathbf{Y}_{t,\bullet}}|\,\mathcal{F}_{t-1}\bigcap\{\rho_t = j\}]}. \tag{2.3.9}$$

For a Markov regime switching process assumed in assumptions (A1) and (A2),

(2.3.9) can be simplified as

$$f_{ij}^{\mathbb{Q}}(\mathbf{y}_{t,\bullet}) := f^{\mathbb{Q}}(\mathbf{y}_{t,\bullet}|\rho_{t-1}=i,\rho_t=j\}) = \frac{e^{\mathbf{h}'_{t,\bullet}\mathbf{y}_{t,\bullet}} f^{\mathbb{P}}(\mathbf{y}_{t,\bullet}|\rho_t=j\})}{\mathsf{E}^{\mathbb{P}}[e^{\mathbf{h}'_{t,\bullet}\mathbf{Y}_{t,\bullet}}|\,\rho_t=j]}. \tag{2.3.10}$$

We denote the density function of $\mathbf{Y}_{t,\bullet}$ given $\rho_{t-1}=i$ by $f_i^{\mathbb{Q}}(\mathbf{y}_{t,\bullet})$, i.e.,

$$f_i^{\mathbb{Q}}(\mathbf{y}_{t,\bullet}) = f^{\mathbb{Q}}(\mathbf{y}_{t,\bullet}|\rho_{t-1}=i).$$

Then, $f_i^{\mathbb{Q}}$ can be expressed as a mixture of those $f_{ij}^{\mathbb{Q}}$ as demonstrated in the following Proposition.

Proposition 2.3.2. *(**CQ**) Under assumptions (A1), (A2) and (A4) which we imposed in section 2.2, we have*

$$f_i^{\mathbb{Q}}(\mathbf{y}_{t,\bullet}) = \sum_{j=1}^{R} q_{ij}\, f_{ij}^{\mathbb{Q}}(\mathbf{y}_{t,\bullet}), \tag{2.3.11}$$

where

$$q_{ij} = \frac{p_{ij}\, \mathsf{E}^{\mathbb{P}}(e^{\mathbf{h}'_{t,\bullet}\mathbf{Y}_{t,\bullet}}\,|\,\rho_{t-1}=i,\rho_t=j)}{\mathsf{E}^{\mathbb{P}}(e^{\mathbf{h}'_{t,\bullet}\mathbf{Y}_{t,\bullet}}\,|\,\rho_{t-1}=i)}, \quad i,j\in\{1,\ldots,R\}, \tag{2.3.12}$$

Proof. The proof is completely parallel to that of Proposition 1.2.2, and hence omitted. □

Remark 2.3.1. Proposition 2.3.2 provides a way for us to compute the distribution of $\mathbf{S}_{t,\bullet}$ by introducing a new Markov process ρ_t^* with the following transition probabilities under the MET-$\mathbb{Q}$ measure:

$$\mathbb{Q}[\,\rho_t^*=[ij]\,|\,\rho_{t-1}^*=[kl]\,] = \begin{cases} 0, & i\neq l; \\ q_{ij}, & i=l. \end{cases}$$

where $\{\rho_t^*=[ij]\}=\{\rho_{t-1}=i,\rho_t=j\}$ for $t=1,2,\ldots,T$.

Lemma 2.3.1. *(**CQ**) Assume (A1) to (A4). Then, under the MET-$\mathbb{Q}$ measure, $\mathbf{Y}_{1,\bullet}, \ldots, \mathbf{Y}_{T,\bullet}$ are independent conditional on $\{\rho_t^*\}_{t=0}^T$, and the distribution of $\mathbf{Y}_{1,\bullet}$ conditional on ρ_t^* is independent of ρ_s^* for $s \neq t$.*

Proof. The proof is similar to the proof of Lemma 1.2.5 and Lemma 1.2.6 in Chapter 1. □

Remark 2.3.2. Based on Lemma 2.3.1, the distribution of $\mathbf{Y}_{t,\bullet}$ is solely determined by ρ_t^* under the ET-$\mathbb{Q}$ measure. As a result, the joint density of $(\mathbf{Y}_{1,\bullet}, \ldots, \mathbf{Y}_{T,\bullet})$ given $\{\rho_t^*\}_{t=0}^T$ is

$$f^{\mathbb{Q}}(\mathbf{y}_{1,\bullet}, \ldots, \mathbf{y}_{T,\bullet} | \{\rho_t^*\}_{t=0}^T) = \prod_{t=1}^T f^{\mathbb{Q}}(\mathbf{y}_{t,\bullet} | \rho_t^*).$$

Let $u_{t,\bullet} = (u_{t,1}, \ldots, u_{t,N})', t = 1, \ldots, T$, be the vectors of real numbers such that the moment generating function $\mathsf{E}^{\mathbb{Q}}(e^{\sum_{t=1}^T \mathbf{u}_{t,\bullet}' \mathbf{Y}_{t,\bullet}})$ exists. Then, based on the assumptions (A1) to (A4),

$$\begin{aligned} \mathsf{E}^{\mathbb{Q}}\left[e^{\mathbf{u}_{1,\bullet}'\mathbf{Y}_{1,\bullet}+\cdots+\mathbf{u}_{T,\bullet}'\mathbf{Y}_{T,\bullet}}\right] &= \mathsf{E}^{\mathbb{Q}}\left[\mathsf{E}^{\mathbb{Q}}\left(e^{\mathbf{u}_{1,\bullet}'\mathbf{Y}_{1,\bullet}+\cdots+\mathbf{u}_{T,\bullet}'\mathbf{Y}_{T,\bullet}} \mid \{\rho_t^*\}_{t=1}^T\right)\right] \\ &= \mathsf{E}^{\mathbb{Q}}\left[\prod_{t=1}^T \mathsf{E}^{\mathbb{Q}}(e^{\mathbf{u}_{t,\bullet}'\mathbf{Y}_{t,\bullet}} \mid \rho_t^*)\right], \end{aligned}$$

where the distribution of $\{\rho_t^*\}_{t=1}^T$ follows a Markov chain as discussed in Remark 2.3.1, with the transition probabilities under the MET-$\mathbb{Q}$ measure given in (2.3.12). Consequently, to identify the distribution of $(\mathbf{Y}_{1,\bullet}, \ldots, \mathbf{Y}_{T,\bullet})$, we may focus on its conditional moment generating function $\mathsf{E}^{\mathbb{Q}}\left(e^{\mathbf{u}_{t,\bullet}'\mathbf{Y}_{t,\bullet}} \mid \rho_t^*\right)$.

2.4 European Option Pricing for Multivariate Regime Switching Models under MET-$\mathbb{Q}$

In this section, we consider a European option with payoff $H(\mathbf{S}_{T,\bullet})$. Its price at time $t = 0$ can be computed as the following expectation

$$P_0(H(\mathbf{S}_{T,\bullet})) = e^{-r(T-t)}\mathsf{E}^{\mathbb{Q}}\left[\, H(\mathbf{S}_{T,\bullet}) \,|\, \rho_0 \,\right]. \tag{2.4.13}$$

where $\mathsf{E}^{\mathbb{Q}}[\cdot]$ denotes the expectation under MET-$\mathbb{Q}$ measure identified by the Radon-Nikodym derivative (2.3.4) and conditions (2.3.5). In section 2.3.3, we have shown that, based on the market model (2.2.2) and assumptions (A1) to (A4) described in section 2.2, under the MET-$\mathbb{Q}$ measure, $\mathbf{Y}_{t,\bullet}, t = 1, 2, \ldots$, follows a Markov regime switching process, and the distribution of Y_t is solely determined by ρ_t^*. The option pricing formula in (2.4.13) can then be computed as

$$P_0(H(\mathbf{S}_{T,\bullet})) = \mathsf{E}^{\mathbb{Q}}\left[\, \mathsf{E}^{\mathbb{Q}}\left[\, e^{-r(T-t)} H(\mathbf{S}_{T,\bullet}) \,|\, \{\rho_t^*\}_{t=1}^T \,\right]\right]. \tag{2.4.14}$$

In this formula, we compute the option price in two steps. In step one, we compute the time zero value of the payoff assuming the path of regime switching $\{\rho_t^*\}_{t=1}^T$. In step two, we take the average of the values obtained in step one over all regime paths under the MET-$\mathbb{Q}$ measure. If the option payoff is not path-dependent, such as the payoff of European call and put options, we can apply the path reduction algorithm we developed in section 1.3.3 to reduce the computation time for the outer expectation. In the following content of this section, we focus on computation of the inner expectation and the regime-transition probabilities of $\{\rho_t^*\}$. This section starts with the regime switching log-normal models; then discuss pricing under more general distributions using characteristic functions.

2.4.1 Pricing under the Multivariate RSLN Models

Assume a R-state multivariate regime switching lognormal (RSLN) model under $\mathbb{P}$ measure. Let the distribution of $\mathbf{Y}_{t,\bullet}$ given $\rho_t = j$ is MVN$(\boldsymbol{\mu}_j, \boldsymbol{\Sigma}_j)$, where $\boldsymbol{\mu}_j$

and $\boldsymbol{\Sigma}_j$ are the column vector of mean and covariance matrix for regime j. The moment generating function of $\mathbf{Y}_{t,\bullet}$ given ρ_t, denoted by $M(\mathbf{s})$ with a real vector $\mathbf{s} = (s_1, \ldots, s_N)'$, is

$$M(\mathbf{s}) = \exp\left(\mathbf{s}'\boldsymbol{\mu}_j + \frac{1}{2}\mathbf{s}'\boldsymbol{\Sigma}_j\mathbf{s}\right)$$

As we commented before, an European options can be priced by using the double expectation in (2.4.14). To compute the inner expectation in the equation, we first investigate the moment generating function of $\mathbf{Y}_{t,\bullet}$ given ρ_t^* under Q measure:

$$\begin{aligned}
& \mathsf{E}^{\mathbb{Q}}[\, e^{\mathbf{s}'\mathbf{Y}_{t,\bullet}} | \rho_t^* = [ij]\,] \\
= \;& \mathsf{E}^{\mathbb{P}}\left[e^{\mathbf{s}'\mathbf{Y}_{t,\bullet}} \frac{e^{\mathbf{h}_{t,\bullet}'\mathbf{Y}_{t,\bullet}}}{\mathsf{E}^{\mathbb{P}}(e^{\mathbf{h}_{t,\bullet}'\mathbf{Y}_{t,\bullet}} |\, \rho_t)} \,\middle|\, \rho_{t-1} = i, \rho_t = j \right] \\
= \;& \exp\left((\mathbf{s} + \mathbf{h}_{t,\bullet})'\boldsymbol{\mu}_j + \frac{1}{2}(\mathbf{s} + \mathbf{h}_{t,\bullet})'\boldsymbol{\Sigma}_j(\mathbf{s} + \mathbf{h}_{t,\bullet})\right) \exp\left(-\mathbf{h}_{t,\bullet}'\boldsymbol{\mu}_j - \frac{1}{2}\mathbf{h}_{t,\bullet}'\boldsymbol{\Sigma}_j\mathbf{h}_{t,\bullet}\right) \\
= \;& \exp\left(\mathbf{s}'(\boldsymbol{\mu}_j + h_{t,\bullet}'\boldsymbol{\Sigma}_j) + \frac{1}{2}\mathbf{s}'\boldsymbol{\Sigma}_j\mathbf{s}\right) \\
= \;& \exp\left(\mathbf{s}'\boldsymbol{\mu}_{[ij]}^* + \frac{1}{2}\mathbf{s}'\boldsymbol{\Sigma}_j\mathbf{s}\right), \quad i, j = 1, \ldots, R,
\end{aligned} \tag{2.4.15}$$

where

$$\boldsymbol{\mu}_{[ij]}^* = \boldsymbol{\mu}_j + \boldsymbol{\Sigma}_j\mathbf{h}_{t,\bullet}, \tag{2.4.16}$$

where $\mathbf{h}_{t,\bullet}$ is determined by equation (2.3.5). (2.4.15) implies that $\mathbf{Y}_{t,\bullet}$ given $\rho_t^* = [ij]$ follows a multivariate normal distribution with mean $\boldsymbol{\mu}_{[ij]}^*$ and covariance matrix $\boldsymbol{\Sigma}_j$ under the MET-$\mathbb{Q}$ measure. In addition, Let N_{ij} denote the frequency of the occurrence of $\rho_t^* = [ij]$ within the path $(\rho_1^*, \ldots, \rho_T^*)$. For notational convenience, let

$$\mathbf{Z} = (Z_1, \ldots, Z_N)', \;\text{ where }\; Z_l = \sum_{t=1}^{T} Y_{t,l}. \tag{2.4.17}$$

Then, the moment generating function of $\mathbf{Z}$ is as follows:

$$\begin{aligned}
\mathsf{E}^{\mathbb{Q}}\left(e^{\mathbf{s}'\mathbf{Z}}\middle|\ \{\rho_t^*\}_{t=1}^T\right) &= \mathsf{E}^{\mathbb{Q}}\left(\exp\left(s_1\sum_{t=1}^T Y_{t,1}+\cdots+s_N\sum_{t=1}^T Y_{t,N}\right)\middle|\ \{\rho_t^*\}_{t=1}^T\right)\\
&= \mathsf{E}^{\mathbb{Q}}\left(\exp\left(\sum_{l=1}^N s_l Y_{t,1}+\cdots+\sum_{l=1}^N s_l Y_{T,l}\right)\middle|\ \{\rho_t^*\}_{t=1}^T\right)\\
&= \prod_{t=1}^T \mathsf{E}^{\mathbb{Q}}\left(\exp\left(\sum_{l=1}^N s_l Y_{t,l}\right)\middle|\ \{\rho_t^*\}_{t=1}^T\right)\\
&= \exp\left(\mathbf{s}'\cdot\sum_{i=1}^R\sum_{j=1}^R N_{ij}\mu_{[ij]}+\frac{1}{2}\,\mathbf{s}'\cdot\sum_{i=1}^R\sum_{j=1}^R N_{ij}\Sigma_j\cdot\mathbf{s}\right)
\end{aligned}$$

The above display implies that $\mathbf{Z}$, conditional on $\{\rho_t^*\}_{t=1}^T$, is also a multivariate normal random variable under the MET-$\mathbb{Q}$ measure, i.e.,

$$(Z_1,\ldots,Z_N)|\,\{\rho_t^*\}_{t=1}^T \overset{Q}{\sim} \text{MVN}\left(\sum_{i=1}^R\sum_{j=1}^R N_{ij}\mu_{[ij]},\ \sum_{i=1}^R\sum_{j=1}^R N_{ij}\mathbf{\Sigma}_j\right). \tag{2.4.18}$$

To compute the outer expectation in (2.4.14), we can compute the regime transition probability as follows:

$$q_{ij}=p_{ij}\exp\left(\mathbf{h}'_{t,\bullet}\mu_j+\frac{1}{2}\,\mathbf{h}'_{t,\bullet}\Sigma_j\mathbf{h}_{t,\bullet}\right)\left(\sum_{l=1}^R p_{il}\exp\left(\mathbf{h}'_{t,\bullet}\mu_l+\frac{1}{2}\,\mathbf{h}'_{t,\bullet}\Sigma_l\mathbf{h}_{t,\bullet}\right)\right)^{-1} \tag{2.4.19}$$

After obtaining the distribution of $\left(\sum_{t=1}^T Y_{t,1},\ldots,\sum_{t=1}^T Y_{t,N}\right)$ under the MET-$\mathbb{Q}$ measure, we can then compute the price of European options by using the double expectation as defined in (2.4.13).

Geometric Average European Option

In the remaining sections of this chapter, we will illustrate how to compute the multivariate European options under the MET-$\mathbb{Q}$ measure by focusing on the so-

called geometric average European option. It is written on multiple underlying stocks and its payoff, with a strike price K, is given by

$$H(\mathbf{S}_{T,\bullet}) = \left(\prod_{l=1}^{N} \mathbf{S}_{T,l}^{\omega_l} - K \right)^+, \tag{2.4.20}$$

where ω_l is the geometric weight on the l^{th} asset with $\sum_{l=1}^{N} \omega_l = 1$ and $\omega_l > 0$ for $l = 1, \ldots, N$. The pricing of this option is usually used to approximate the value of the option written on the arithmetic average of the corresponding stock prices. See, for example, a review of the approximation in Musiela and Rutkowski (2004).

Based on the the MET$-\mathbb{Q}$ measure identified for the multivariate RSLN2 models, the geometric average $\prod_{l=1}^{N} S_{T,l}^{\omega_l}$ is log$-$normally distributed with parameters $(c\tilde{\mu}, c^2\tilde{\sigma}^2)$, where $\tilde{\mu} = \sum_{i=1}^{K}\sum_{j=1}^{K} N_{ij}\omega' \mu_{[ij]}$, $\tilde{\sigma}^2 = \sum_{i=1}^{K}\sum_{j=1}^{K} N_{ij}\omega'\Sigma_j\omega$ and $c = \prod_{l=1}^{N} S_{0,l}^{\omega_l}$. After obtaining the distribution of the geometric average $\prod_{l=1}^{N} S_{T,l}^{\omega_l}$ under the MET-$\mathbb{Q}$ measure, the price of $H(\mathbf{S}_{T,\bullet})$ can be computed as we did for a univariate option in Chapter 1.

2.4.2 Pricing under General Models Using Characteristic Functions

When the distribution of $\mathbf{Y}_{t,\bullet}$, conditional on ρ_t is not multivariate normal, the conditional distribution function of $\prod_{l=1}^{N} S_{T,l}^{\omega_l}$ may not have a closed form expression. In this case, the computation of the inner expectation in formula (2.4.14) is no longer the same as in Chapter 1. We have to develop a new method, and we propose a fast Fourier transform method in this section for option pricing in a more general multivariate case. The pioneer work of using the fast Fourier transform (FFT) method for option pricing is given by Carr and Madan (1999). In our studies, $(\mathbf{Y}_{t,\bullet})$ and (ρ_t) satisfy the assumptions in section 2.2, and we use the geometric average European call and put options to illustrate our method.

We first compute the characteristic function of $\mathbf{Z}$ under the MET$-\mathbb{Q}$ measure.

The characteristic function can be obtained based on the expectation of the characteristic functions of $\mathbf{Y}_{t,\bullet}, t = 1, \ldots, T$ under the MET$-\mathbb{Q}$ measure conditional on $\{\rho_t^*\}_{t=1}^T$. The corresponding conditional density of $\mathbf{Y}_{t,\bullet} = \mathbf{y}_{t,\bullet}$ is given in (2.3.10). Let $\mathbf{u} = (u_1, \ldots, u_N)'$ being a column of real numbers. Then, the characteristic function of $Y_{t,\bullet}$ under MET-$\mathbb{Q}$ measure, conditional on ρ_t^* is

$$\psi^{\mathbb{Q}}_{\mathbf{Y}_{t,\bullet}}(\mathbf{u} \,|\, \rho_t^*) = \int e^{i\mathbf{u}'\mathbf{y}_{t,\bullet}} f^{\mathbb{Q}}(\mathbf{y}_{t,\bullet}|\rho_t^*) d\,\mathbf{y}_{t,\bullet},$$

where $d\mathbf{y} = dy_{1,1} \cdots dy_{T,N}$. Consequently, the characteristic function of $\mathbf{Z}$ conditional on $\{\rho_t^*\}_{t=1}^T$ under MET$-\mathbb{Q}$ measure, denoted by $\psi^{\mathbb{Q}}_{\mathbf{Z}}(\mathbf{u} \,|\, \{\rho_t^*\}_{t=1}^T)$, is

$$\begin{aligned}
\psi^{\mathbb{Q}}_{\mathbf{Z}}(\mathbf{u} \,|\, \{\rho_t^*\}_{t=1}^T) &= \mathsf{E}^{\mathbb{Q}}\left(e^{i(u_1 Z_1 + \cdots + u_N Z_N)} | \{\rho_t^*\}_{t=1}^T\right) \\
&= \mathsf{E}^{\mathbb{Q}}\left(\exp\left[iu_1 \sum_{t=1}^T Y_{t,1} + \cdots + iu_N \sum_{t=1}^T Y_{t,N}\right] \middle| \{\rho_t^*\}_{t=1}^T\right) \\
&= \int \exp\left[iu_1 \sum_{t=1}^T y_{t,1} + \cdots + iu_N \sum_{t=1}^T y_{t,N}\right] \prod_{t=1}^T f^{\mathbb{Q}}_{ij}(\mathbf{y}_{t,\bullet}|\rho_t^*)\, d\mathbf{y} \\
&= \int \prod_{t=1}^T \left[\exp(iu_1 y_{t,1} + \cdots + iu_N y_{t,N}) \frac{e^{\mathbf{h}'_{t,\bullet}\mathbf{y}_{t,\bullet}}}{\mathsf{E}^{\mathbb{P}}[e^{\mathbf{h}'_{t,\bullet}\mathbf{y}_{t,\bullet}} |\, \rho_t]} f^{\mathbb{P}}(\mathbf{y}_{t,\bullet}|\rho_t)\right] d\mathbf{y} \\
&= \prod_{t=1}^T \frac{\mathsf{E}^{\mathbb{P}}(e^{i(\mathbf{u}+\mathbf{h}_{t,\bullet})'\mathbf{Y}_{t,\bullet}} |\, \rho_t)}{\mathsf{E}^{\mathbb{P}}(e^{\mathbf{h}'_{t,\bullet}\mathbf{Y}_{t,\bullet}} |\, \rho_t)} \\
&= \prod_{t=1}^T \psi^{\mathbb{Q}}_{Y_{t,\bullet}}(\mathbf{u} \,|\, \rho_t^*), \qquad (2.4.21)
\end{aligned}$$

where the parameters $h_{t,\bullet} = (h_{t,1}, \ldots, h_{t,N})$ are obtained by solving the N risk neutral equations (2.3.5). The unconditional characteristic function of $\mathbf{Z}$ is

$$\psi^{\mathbb{Q}}_{\mathbf{Z}}(\mathbf{u}) = \mathsf{E}^{\mathbb{Q}}\left[\psi^{\mathbb{Q}}_{\mathbf{Z}}(\mathbf{u} \,|\, \{\rho_t^*\}_{t=1}^T)\right], \qquad (2.4.22)$$

where the outer expectation can be obtained using the path reduction algorithm we developed in section 1.3.3 of Chapter 1, and the regime transition probability under MET-$\mathbb{Q}$ measure is given by (2.3.12).

Based on the characteristic function of $\mathbf{Z}$, we can evaluate a geometric average European call option, with payoff given in (2.4.20). Specifically, let

$$k = \log\left(\frac{K}{\prod_{l=1}^{N} S_{0,l}^{\omega_l}}\right).$$

Then, the option price is

$$P_c(k) := \int e^{-rT}\left(\prod_{l=1}^{N} S_{T,l}^{\omega_l} - \prod_{l=1}^{N} S_{0,l}^{\omega_l} e^{k}\right)^{+} f_{\mathbf{Z}}^{\mathbb{Q}}(\mathbf{z})d\mathbf{z}, \tag{2.4.23}$$

where $\mathbf{z} = (z_1, \ldots, z_N)$ and $f_{\mathbf{Z}}^{\mathbb{Q}}(\mathbf{z})$ denotes the density function of Z defined in (2.4.17). Based on $\psi_{\mathbf{Z}}^{\mathbb{Q}}(\mathbf{u})$ in (2.4.22), we can apply the FFT method from Carr and Madan (1999) to evaluate $P_c(k)$ in (2.4.23). To proceed, we first need to solve the issue regarding the convergence of the Fourier transform of option prices. As Carr and Madan (1999) pointed out, the pure Fourier transform

$$\tilde{\mathcal{L}} := \int_{-\infty}^{\infty} e^{ivk} P_c(k)dk$$

may not converge for a real number v, since the value of $P_c(k)$ does not vanish as $k \to -\infty$. Therefore, we use the modified call option price as follows. Let

$$\tilde{P}_c(k) = e^{\alpha k} P_c(k), \quad \alpha > 0. \tag{2.4.24}$$

Then,

$$\lim_{k\to-\infty} \tilde{P}_c(k) = 0. \tag{2.4.25}$$

Denote by $\mathcal{L}(v)$ the Fourier transform of the modified prices $\tilde{P}_c(k)$. Then,

$$\begin{aligned}
\mathcal{L}(v) &= \int_{-\infty}^{\infty} e^{ivk}\tilde{P}_c(k)dk \\
&= \int_{-\infty}^{\infty} e^{ivk}e^{\alpha k}\int_{\mathbf{z}} e^{-rT}\left(\prod_{l=1}^{N} S_{T,l}^{\omega_l} - K\right)^{+} f_{\mathbf{Z}}^{\mathbb{Q}}(\mathbf{z})d\mathbf{z}dk \\
&= \int_{\mathbf{z}} e^{-rT} f_{\mathbf{Z}}^{\mathbb{Q}}(\mathbf{z})\int_{-\infty}^{\infty} e^{ivk}e^{\alpha k}\left(\prod_{l=1}^{N} S_{0,l}^{\omega_l}e^{\omega_l z_l} - \prod_{l=1}^{N} S_{0,l}^{\omega_l}e^{k}\right)^{+} dkd\mathbf{z} \\
&= \prod_{l=1}^{N} S_{0,l}^{\omega_l}\int_{\mathbf{z}} e^{-rT} f_{\mathbf{Z}}^{\mathbb{Q}}(\mathbf{z})\int_{-\infty}^{\sum_{l=1}^{N}\omega_l z_l} e^{ivk}e^{\alpha k}\left(e^{c(z)} - e^{k}\right)dkd\mathbf{z} \\
&= \prod_{l=1}^{N} S_{0,l}^{\omega_l}\int_{\mathbf{z}} e^{-rT} f_{\mathbf{Z}}^{\mathbb{Q}}(\mathbf{z})\left(\frac{e^{(\alpha+1+iv)\sum_{l=1}^{N}\omega_l z_l}}{\alpha+iv} - \frac{e^{(\alpha+1+iv)\sum_{l=1}^{N}\omega_l z_l}}{\alpha+1+iv}\right)d\mathbf{z} \\
&= \prod_{l=1}^{N} S_{0,l}^{\omega_l}\frac{e^{-rT}}{(\alpha+1+iv)(\alpha+iv)}\int_{\mathbf{z}} f_{\mathbf{Z}}^{\mathbb{Q}}(\mathbf{z})e^{(\alpha+1+iv)\sum_{l=1}^{N}\omega_l z_l}d\mathbf{z} \qquad (2.4.26) \\
&= \prod_{l=1}^{N} S_{0,l}^{\omega_l}\frac{e^{-rT}}{(\alpha+1+iv)(\alpha+iv)}\psi_{\mathbf{Z}}^{\mathbb{Q}}\left((\omega_1(v-i\alpha-i),\ldots,\omega_N(v-i\alpha-i))'\right),
\end{aligned}$$

where $\psi_{\mathbf{Z}}^{\mathbb{Q}}(\cdot)$ is given in (2.4.22). Then, the option price can be computed by inverting the above formula $\mathcal{L}(v)$ as follows:

$$P_c(k) = e^{-\alpha k}\frac{1}{2\pi}\int_{-\infty}^{\infty} e^{-ivk}\mathcal{L}(v)dv \qquad (2.4.27)$$

It is worth noting that the Fourier transform method reduces the multiple integration for option pricing in (2.4.23) to a single integration in (2.4.27). The value of $P_c(k)$ in (2.4.27) can be computed numerically by applying the fast Fourier transform. The put option prices can be obtained in either of two ways. First, we can use the put-call parity; second, we can assume $a < -1$ and let

$$\tilde{P}_p(k) = e^{\alpha k}P_p(k),$$

where $P_p(k)$ is the put option price under consideration. Then, we can obtain the

put option price by following the same procedure as demonstrated in (2.4.26) and (2.4.27).

Example 7. Assume that $(Y_{t,1},\ldots,Y_{t,N})_{t=1}^{T}$ follows a multivariate Markov regime switching model with two regimes, where $Y_{t,1},\ldots,Y_{t,N}$ has a multivariate normal distribution conditional on ρ_t at regime one, and a multivariate Laplace distribution at regime two. The Laplace distribution has fatter tails than a normal distribution (Eltoft et al., 2006). The characteristic function of $\mathbf{Y}_{t,\bullet}$, conditional on $\rho_t = 1$, is

$$\psi^{\mathbb{P}}_{\mathbf{Y}_{t,\bullet}}(\mathbf{u}|\rho_t = 1) = \exp\left(i\mathbf{u}'\boldsymbol{\mu}_1 - \frac{1}{2}\mathbf{u}'\boldsymbol{\Sigma}_1\mathbf{u}\right),$$

where $\boldsymbol{\mu}_1$ is the mean vector, $\boldsymbol{\Sigma}_1$ is the covariance matrix of $\mathbf{Y}_{t,\bullet}$, and $\mathbf{u} = (u_1,\ldots,u_N)'$. The characteristic function of $\mathbf{Y}_{t,\bullet}$, conditional on $\rho_t = 2$, is

$$\psi^{\mathbb{P}}_{\mathbf{Y}_{t,\bullet}}(\mathbf{u}|\rho_t = 2) = \frac{1}{1+\lambda\frac{\mathbf{u}'\boldsymbol{\Sigma}_2\mathbf{u}}{2}},$$

where λ is a constant and $\boldsymbol{\Sigma}_2$ is the matrix parameter. The moment generating function of the Laplace distribution is given by

$$\mathsf{E}^{\mathbb{P}}\left(e^{\mathbf{u}'\mathbf{Y}_{t,\bullet}}|\rho_t = 2\right) = \frac{1}{1-\lambda\frac{\mathbf{u}'\Sigma_2\mathbf{u}}{2}}.$$

With these assumptions, condition (2.3.5) is equivalent to the following equations:

$$e^r = \frac{p_{i1}\mathsf{E}^{\mathbb{P}}\left(e^{\mathbf{h}'_{t,\bullet}\mathbf{Y}_{t,\bullet}+\mathbf{Y}_{t,l}}|\rho_{t-1}=i,\rho_t=1\right) + p_{i2}\mathsf{E}^{\mathbb{P}}\left(e^{\mathbf{h}'_{t,\bullet}\mathbf{Y}_{t,\bullet}+Y_{t,l}}|\rho_{t-1}=i,\rho_t=2\right)}{p_{i1}\mathsf{E}^{\mathbb{P}}\left(e^{\mathbf{h}'_{t,\bullet}\mathbf{Y}_{t,\bullet}}|\rho_{t-1}=i,\rho_t=1\right) + p_{i2}\mathsf{E}^{\mathbb{P}}\left(e^{\mathbf{h}'_{t,\bullet}\mathbf{Y}_{t,\bullet}}|\rho_{t-1}=i,\rho_t=2\right)}, \tag{2.4.28}$$

for $i = 1, 2$. Solving equations in (2.4.28), we can obtain the values of the Esscher transform parameters $\mathbf{h}_{t,\bullet} = (h_{t,1},\ldots,h_{t,N})$. The resulting Esscher transformed characteristic functions of $\mathbf{Y}_{t,\bullet}$ conditional on ρ_t^* under the MET-Q measure are used to

compute the characteristic function for multi-period, which as shown in (2.4.21) is

$$\psi^{\mathbb{Q}}_{\mathbf{Z}}(\mathbf{u}\,|\,\{\rho^*_t\}_{t=1}^T) = \prod_{t=1}^{T} \psi^{\mathbb{Q}}_{\mathbf{Y}_{t,\bullet}}(\mathbf{u}\,|\,\rho^*_t),$$

where

$$\psi^{\mathbb{Q}}_{\mathbf{Y}_{t,\bullet}}(\mathbf{u}\,|\,\rho^*_t) = \frac{\psi^{\mathbb{P}}_{\mathbf{Y}_{t,\bullet}}(\mathbf{u} - i\mathbf{h}_{t,\bullet}|\,\rho_{t-1},\rho_t)}{\mathsf{E}^{\mathbb{P}}(e^{\mathbf{h}'_{t,\bullet}\mathbf{Y}_{t,\bullet}}|\,\rho_{t-1},\rho_t)}.$$

As a result, under MET-$\mathbb{Q}$ measure, if $\rho^*_t = [i1], i = 1, 2$, then

$$\psi^{\mathbb{Q}}_{Y_{t,\bullet}}(\mathbf{u}\,|\,\rho^*_t = [i1]) = \exp\left(i\mathbf{u}'\boldsymbol{\mu}^*_{[i1]} - \frac{1}{2}\mathbf{u}'\boldsymbol{\Sigma}_1\mathbf{u}\right), \quad i = 1, 2$$

where $\boldsymbol{\mu}^*_{[i1]} = \boldsymbol{\mu}_1 + \boldsymbol{\Sigma}_1\mathbf{h}_{t,\bullet}$. If $\rho^*_t = [i2]$, then

$$\psi^{\mathbb{Q}}_{\mathbf{Y}_{t,\bullet}}(\mathbf{u}\,|\,\rho^*_t = [i2]) = \frac{2 - \lambda\mathbf{h}'_{t,\bullet}\boldsymbol{\Sigma}_2\mathbf{h}_{t,\bullet}}{2 + \lambda(\mathbf{u} - i\mathbf{h}_{t,\bullet})'\,\boldsymbol{\Sigma}_2\,(\mathbf{u} - i\mathbf{h}_{t,\bullet})}$$

The transition probability q_{ij} is

$$q_{ij} = \frac{p_{ij}\mathsf{E}^{\mathbb{P}}(e^{\mathbf{h}'_{t,\bullet}\mathbf{Y}_{t,\bullet}}|\,\rho_{t-1} = i, \rho_t = j)}{p_{i1}\,\mathsf{E}^{\mathbb{P}}(e^{\mathbf{h}'_{t,\bullet}\mathbf{Y}_{t,\bullet}}|\,\rho_{t-1} = i, \rho_t = 1) + p_{i2}\,\mathsf{E}^{\mathbb{P}}(e^{\mathbf{h}'_{t,\bullet}\mathbf{Y}_{t,\bullet}}|\,\rho_{t-1} = i, \rho_t = 2)} \tag{2.4.29}$$

□

2.5 Numerical Results of Option Pricing

In this section, we evaluate geometric average European call and put options written on multiple non-dividend paying stocks, for the Markov regime switching models discussed in the previous section. Specifically, we conduct the numerical computation for the multivariate RSLN2 model and for the Markov regime switching model with multivariate normal distribution in one regime and multivariate Laplace distribution in the other regime.

2.5.1 Prices under the Multivariate RSLN2 Model with Real Data

In this section, we use real stock data to fit the multivariate RSLN2 models. The data are from three sub-sectors of monthly S&P TSX indices during January 1988 and September 2011, obtained from the CHASS Data Center: Sector 10 (Energy) Monthly Total Return Index, denoted by $(S_{t,1})$; Sector 15 (Materials) Monthly Total Return Index, denoted by $(S_{t,2})$; and Sector 20 (Industrials) Monthly Total Return Index, denoted by $(S_{t,3})$.

We use the package RHmm in the software R to estimate the parameters of the underlying model. The transition probability matrix between the two regimes is

$$\wp = \begin{array}{c} \\ 1 \\ 2 \end{array} \begin{array}{c} \begin{array}{cc} 1 & 2 \end{array} \\ \begin{pmatrix} 0.774 & 0.226 \\ 0.033 & 0.967 \end{pmatrix} \end{array}.$$

The mean vectors and the covariance matrices of the multivariate Gaussian distributions within each regime are displayed in Table 2.1. From the results, we can denote

	State 1				State 2			
	mean	Covariance Matrix			mean	Covariance Matrix		
		$Y_{t,1}$	$Y_{t,2}$	$Y_{t,3}$		$Y_{t,1}$	$Y_{t,2}$	$Y_{t,3}$
$Y_{t,1}$	-0.0181	0.0079	0.0045	0.0051	0.0138	0.0015	0.0006	0.0010
$Y_{t,2}$	-0.0176	0.0045	0.0139	0.0034	0.0094	0.0006	0.0030	0.0011
$Y_{t,3}$	-0.0296	0.0051	0.0034	0.0094	0.0094	0.0010	0.0011	0.0019

Table 2.1: Distribution parameters within 2 regimes

the state one as the regime with a high volatility, and state two as the regime with a low volatility.

Let $\mathbf{e}_1 = (1, 0, 0)'$, and we define $\mathbf{e}_2$ and $\mathbf{e}_3$ in a similar way. Then, conditional

on $\rho_{t-1} = i$, the conditions (2.3.5) are equivalent to the following equations:

$$e^r = \sum_{j=1}^{2} q_{ij} \exp\left(\mathbf{e}_l'\left(\boldsymbol{\mu}_j + \boldsymbol{\Sigma}_j \mathbf{h}_{t,\bullet}\right) + \frac{1}{2}\mathbf{e}_l'\boldsymbol{\Sigma}_j\mathbf{e}_l\right), \quad l = 1, 2, 3, \tag{2.5.30}$$

where $\mathbf{h}_{t,\bullet} = (h_{t,1}, h_{t,2}, h_{t,3})$ and q_{ij} is given in (2.4.19). We solve (2.5.30) numerically, and obtain parameters $(h_{t,1}, h_{t,2}, h_{t,3})$ displayed in Table 2.2. There are four regimes,

ρ_{t-1}	$h_{t,1}$	$h_{t,2}$	$h_{t,3}$
1	0.0635	0.2429	2.6829
2	-5.4903	-0.7771	1.6278

Table 2.2: The Esscher transform parameters

denoted by $[ij]$ for $i, j \in \{1, 2\}$, under the MET-$\mathbb{Q}$ measure. The mean vectors of $\mathbf{Y}_{t,\bullet}$ within each regime and the regime transition probabilities under the MET-$\mathbb{Q}$ measure are reported in Table 2.3. The covariance matrix within regime $\rho_t^* = [ij]$ is the same as the physical covariance matrix $\boldsymbol{\Sigma}_j$ within regime $\rho_t = j$.

	Mean			T ransition Probabilities given ρ_t^* under $\mathbb{Q}$ measure			
$[ij]$		$\mu^*_{[ij]}$		$\rho^*_{t+1} = [11]$	$\rho^*_{t+1} = [12]$	$\rho^*_{t+1} = [21]$	$\rho^*_{t+1} = [22]$
[11]	-0.0030	-0.0050	-0.0031	0.7593	0.2407	0.0000	0.0000
[12]	0.0168	0.0132	0.0147	0.0000	0.0000	0.0403	0.9597
[21]	-0.0566	-0.0476	-0.0440	0.7593	0.2407	0.0000	0.0000
[22]	0.0066	0.0054	0.0059	0.0000	0.0000	0.0403	0.9597

Table 2.3: Regime and transition parameters under the MET$-\mathbb{Q}$ measure for the multivariate RSLN2 model.

To evaluate the option with the payoff $H(\mathbf{S}_{T,\bullet}) = \left(\prod_{i=1}^{3} S_{T,i}^{\omega_i} - K\right)^+$, we assume that $S_{0,i} = K = 100$ and $\omega_i = \frac{1}{3}$ for $i = 1, 2, 3$, and a constant risk free rate $r = 0.005$ per month. The computed option prices are displayed in Table 2.4, where we can see the difference between the option prices given different initial regimes. For example, the 4-month at-the-money option (K=100) is \$4.21 given $\rho_0 = 1$, and is only \$2.46 given $\rho_0 = 2$.

	$\rho_0 = 1$ High Volatility Regime				$\rho_0 = 2$ Low Volatility Regime			
K	$T = 120$	24	12	4	$T = 120$	24	12	4
50	0.1222	0.0183	0.0034	0.0001	0.1035	0.0090	0.0001	0.0000
100	3.1189	5.2816	5.0988	4.2110	2.8870	4.3042	3.6965	2.4633
150	13.2198	36.2435	42.6260	47.5542	12.7029	35.3598	42.0229	47.2389
200	30.2123	76.3208	89.4561	96.5514	29.5522	75.8546	89.0468	96.2485

Table 2.4: Prices of European put options on geometric averages on three assets

2.5.2 Price Comparison under Different Multivariate RSLN2 Models

It is of interest to investigate the connection between portfolio construction and the option price written on the portfolio. This section compares the prices of geometric average European options written on a portfolio of three assets, under the multivariate RLSN2 models with different assumptions on geometric weights for assets and the covariance matrix. We suppose three different covariance matrices of the underlying assets: all positively correlated, uncorrelated, and some negatively correlated. Assume that $S_{0,l} = 100$ for $l = 1, 2, 3$. Then, we compute option prices for four different portfolios. The first option is written on the portfolio with the geometric weights $\omega_1 = 0.5, \omega_2 = 0.1, \omega_3 = 0.4$ for assets with positive covariance as specified in Table 2.6. The other three options written on portfolios, with the same geometric weights, $\omega_1 = \omega_2 = \omega_3 = 1/3$, but different covariance matrices given in Table 2.6. The model parameters under $\mathbb{P}$ measure, including regime transition probabilities, mean vectors and correlation coefficient matrices of $(Y_{t,1}, Y_{t,2}, Y_{t,3})$ within each regime, are given in Table 2.5 and 2.6. The option prices under different combination of the above assumptions are respectively reported in Tables 2.7– 2.10.

We first compare prices of options written on portfolios with different geometric weights for the underlying assets. The option prices under two different portfolios are illustrated in Table 2.7, where the underlying portfolio has unequal geometric weights for assets, and in Table 2.8, where the underlying portfolio has equal weights. The tables show that out-of-money put options written on the former portfolio are

	Mean						p_{ij}	
ρ_t	$\mu_{t,1}$	$\mu_{t,3}$	$\mu_{t,3}$	$\sigma_{t,1}$	$\sigma_{t,3}$	$\sigma_{t,3}$	1	2
1	0.012	0.012	0.012	0.035	0.035	0.035	0.963	0.037
2	-0.016	-0.016	-0.016	0.078	0.078	0.078	0.21	0.79

Table 2.5: Means of $Y_{t,\bullet}$ conditional on ρ_t and transition probabilities under $\mathbb{P}$ measure

	Positive Correlated			Uncorrelated			Negative Correlated		
	$Y_{t,1}$	$Y_{t,2}$	$Y_{t,3}$	$Y_{t,1}$	$Y_{t,2}$	$Y_{t,3}$	$Y_{t,1}$	$Y_{t,2}$	$Y_{t,3}$
$Y_{t,1}$	1	0.5	0.5	1	0	0	1	0.5	-0.5
$Y_{t,2}$	0.5	1	0.5	0	1	0	-0.5	1	-0.5
$Y_{t,3}$	0.5	0.5	1	0	0	1	-0.5	0.5	1

Table 2.6: Conditional correlation matrices within each regime under $\mathbb{P}$ measure

K	$T = 120$	24	12	4
50	0.0255	0.0020	0.0002	0.0000
100	1.5453	3.1826	2.9315	2.1197
150	9.2487	33.5480	41.2998	47.0315
200	24.8305	77.3965	88.3532	96.0397

Table 2.7: European put option prices on geometric averages, with geometric weights (0.5, 0.1, 0.4) and positive covariance

K	$T = 120$	24	12	4
50	0.0206	0.0015	0.0001	0.0000
100	1.4305	3.0440	2.8184	2.0459
150	8.9946	33.4712	41.2922	47.0300
200	24.6297	77.3929	88.3531	96.0397

Table 2.8: European put option prices on geometric averages, with geometric weights (1/3, 1/3, 1/3) and positive covariance

cheaper than those written on the latter portfolio, while, on the contrary, most in-the-money put options prices are more expensive written on the former portfolio. This pricing difference arises from the fact that different geometric weights imply different

K	$T = 120$	24	12	4
50	0.0016	0.0000	0.0000	0.0000
100	0.6222	1.9451	1.9125	1.4346
150	6.9464	33.0891	41.2656	47.0298
200	23.3960	77.3842	88.3529	96.0397

Table 2.9: European put option prices on geometric averages, with geometric weights (1/3, 1/3, 1/3) and uncorrelated covariance

K	$T = 120$	24	12	4
50	0.0003	0.0000	0.0000	0.0000
100	0.3816	1.5353	1.5792	1.2125
150	6.1820	33.0475	41.2647	47.0298
200	23.2706	77.3841	88.3529	96.0397

Table 2.10: European put option prices on geometric averages, with geometric weights (1/3, 1/3, 1/3) and negative covariance

underlying processes ($\prod_{i=1}^{3} S_{T,i}^{\omega_i}$), which in turn imply different option prices. We illustrate in Table 2.11 the values of σ_t^p, the volatility of an imaged portfolio to represent the geometric average ($\prod_{i=1}^{3} S_{t,i}^{\omega_i}$) at time t given the current regime $\rho_t = i$, under two portfolios with different weights. For comparison, Table 2.11 also displays a so-called benchmark volatility σ defined as follows. From Table 2.5 we can see that the three assets have the same volatilities. If their correlation is 1, then the portfolio volatility achieve the maximum (the benchmark) and is equal to 0.0350 given $\rho_t = 1$ and 0.0780 given $\rho_t = 2$. This portfolio resembles a single asset ($S_{t,l}$).

	Portfolio 1	Portfolio 2	Benchmark σ (σ_t of a single asset $S_{t,l}$
σ_t^p given $\rho_t = 1$	0.0295	0.0286	0.0350
σ_t^p given $\rho_t = 2$	0.0657	0.0637	0.0780

Table 2.11: Different portfolios have different volatility σ_t^p. Suppose two portfolios represent the price process ($\prod_{i=1}^{3} S_{t,i}^{\omega_i}$). In this table, portfolio 1 denotes the underlying portfolio in Table 2.7 and has unequal geometric weights for assets; while portfolio 2 denotes the the portfolio in Table 2.7 and has equal geometric weights.

Second, Table 2.8 – 2.10 show that the option price also relies on the dependency

among the underlying assets for a geometric average European option. For an in-the-money put option, the prices derived from a mixture of positive and negative correlated underlying assets are smaller than those in the uncorrelated case, and the latter are in turn smaller than those under positive covariance.

We also compare the prices of the geometric average European put options with the prices of the univariate European put options, written on the single underlying asset $S_{0,1}$ with $S_{0,1} = 100$. It is worth noting that the multivariate option is usually cheaper than the univariate option. This is because that the option price increases with the dependence among assets in the underlying portfolio, and that a single underlying asset can be treated as a portfolio with perfect correlation among assets. The comparing between Table 2.12 and Table 2.7 implies such a conclusion.

K	$T = 120$	24	12	4
50	0.0687	0.0079	0.0010	0.0000
100	2.2155	3.9585	3.5686	2.5449
150	10.5673	34.1329	41.3789	47.0323
200	25.8436	77.4444	88.3556	96.0397

Table 2.12: Single variate put option prices under the ET-Q measure, with $S_0 = 100$, T the term in months, and $r = 0.5\%$ per month

2.5.3 Prices under Models with Multivariate Normal and Laplace distributions

In this section, we still consider 2 state regime switching models. However, we assume a multivariate normal distribution for $Y_{t,\bullet}$ under one regime, while a multivariate Laplace distribution under the other. We calculate the geometric average European option prices based on the results in Example 7 and the following assumptions.

1. Three risky assets are available in the market with initial prices $S_{0,l} = 100$; geometric weights are (1/3, 1/3, 1/3); the risk free rate is 0.005 per month.

2. Assume the multivariate Gaussian distribution within regime one; parameters include $\boldsymbol{\mu}_l = (0.012, 0.012, 0.012)', \sigma_{l,l} = 0.035$ for $l = 1, 2, 3$, and a positive correlation given in Table 2.6. Assume the Laplace distribution within regime two; parameters include $\sigma_{t,k} = 0.078$, a positive correlation in Table 2.6, and $\lambda = 2$.

We obtain the Esscher parameters by solving equations in (2.4.28) and transition probabilities under MET-$\mathbb{Q}$ measure using (2.4.29). Results are reported respectively in Table 2.13 and 2.14.

ρ^*_{t-1}	$h_{t,1}$	$h_{t,2}$	$h_{t,3}$
1	-2.730760533	-2.730701742	-2.730902478
2	0.21130023	0.211357128	0.211162703

Table 2.13: The Esscher transform parameters

Transition Probabilities given ρ^*_t under $\mathbb{Q}$ measure				
ρ^*_t	$\rho^*_{t+1} = [11]$	$\rho^*_{t+1} = [12]$	$\rho^*_{t+1} = [21]$	$\rho^*_{t+1} = [22]$
[11]	0.9576	0.0424	0.0000	0.0000
[12]	0.0000	0.0000	0.2112	0.7888
[21]	0.9576	0.0424	0.0000	0.0000
[22]	0.0000	0.0000	0.2112	0.7888

Table 2.14: Regime transition parameters under the MET$-\mathbb{Q}$ measure for the RSLN2 model.

To compute the option price using the FFT method in (2.4.27), we need the value of $\mathcal{L}(v)$ in (2.4.26), in which we need the characteristic function $\psi^{\mathbb{Q}}_{\mathbf{Z}}(\mathbf{u})$ with $\mathbf{u} = (\frac{1}{3}(v - ia - i), \frac{1}{3}(v - ia - i), \frac{1}{3}(v - ia - i))'$. $\psi^{\mathbb{Q}}_{\mathbf{Z}}(\mathbf{u})$ is obtained through $\psi^{\mathbb{Q}}_{\mathbf{Z}}(\mathbf{u}|\{\rho^*_t\}_{t=1}^T)$ defined in (2.4.21), based on (2.4.22). Let N_{ij} represents the number of $[ij]$ in a path of $\{\rho^*_t\}_{t=1}^T$. We have

$$\psi^{\mathbb{Q}}_{\mathbf{Z}}(\mathbf{u}|\{\rho^*_t\}_{t=1}^T) = \sum_{i=1}^{2}\sum_{j=1}^{2}\left[\psi^{\mathbb{Q}}_{\mathbf{Y}_{t,\bullet}}(\mathbf{u}|\rho^*_t = [ij])\right]^{N_{ij}}. \tag{2.5.31}$$

By plugging $\mathbf{u} = (\frac{1}{3}(v - ia - i), \frac{1}{3}(v - ia - i), \frac{1}{3}(v - ia - i))'$ into the characteristic functions $\psi^{\mathbb{Q}}_{\mathbf{Y}_{t,\bullet}}(\mathbf{u}|\rho^*_t = [ij])$ of multivariate normal under the MET-$\mathbb{Q}$ measure is

$$\begin{aligned} & \psi^{\mathbb{Q}}_{Y_{t,\bullet}}(\mathbf{u}|\rho^*_t = [i1]) \\ = \;& \exp\left(i\mathbf{u}'\boldsymbol{\mu}^*_{[i1]} - \frac{1}{2}\mathbf{u}'\boldsymbol{\Sigma}_1\mathbf{u}\right) \\ = \;& \exp\left((a+1+iv)\frac{1}{3}\sum_{l=1}^{3}\boldsymbol{\mu}^*_{t,l} - \frac{1}{18}(v - ia - i)^2\mathbf{1}'\boldsymbol{\Sigma}_1\mathbf{1}\right), \quad i = 1, 2, \end{aligned} \tag{2.5.32}$$

where $\mathbf{1} = (1, 1, 1)'$. Similarly, we plug $\mathbf{u}$ into the characteristic function of multivariate Laplace distribution under the MET-$\mathbb{Q}$ measure, with $\lambda = 2$, to obtain

$$\psi^{\mathbb{Q}}_{\mathbf{Y}_{t,\bullet}}(\mathbf{u} \,|\, \rho^*_t = [i2]) = \frac{2 - 2\mathbf{h}'_{t,\bullet}\boldsymbol{\Sigma}_2\mathbf{h}_{t,\bullet}}{2 + 2(\mathbf{u} - i\mathbf{h}_{t,\bullet})'\,\boldsymbol{\Sigma}_2\,(\mathbf{u} - i\mathbf{h}_{t,\bullet})}. \tag{2.5.33}$$

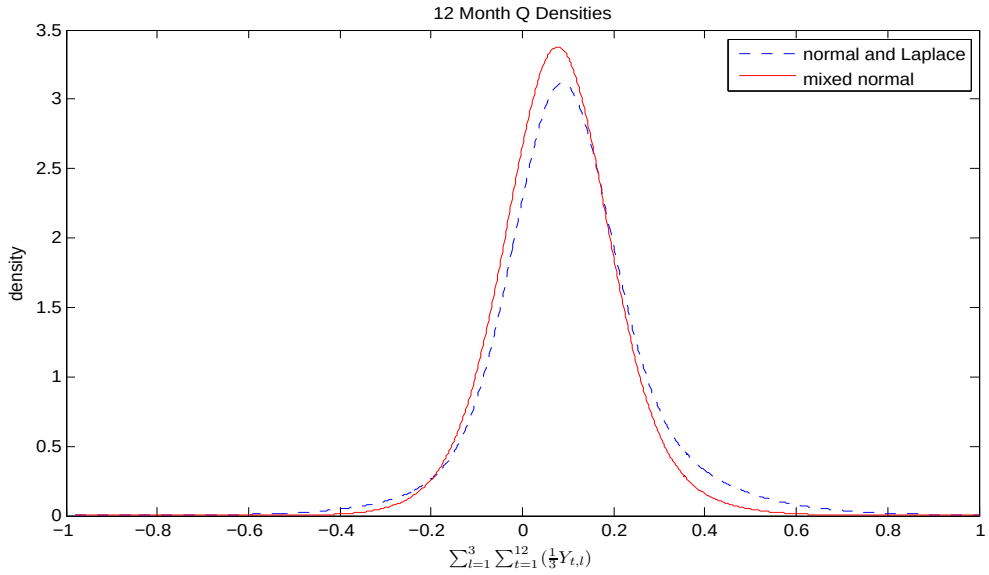

Figure 2.4: Densities under Q-measure: Normal and Laplace vs. Two Normal

Figure 2.4 shows the densities of the 12-month cumulative log-return $\sum_{l=1}^{3}\sum_{t=1}^{12}(\frac{1}{3}Y_{t,l})$ of the geometric average, under the MET-$\mathbb{Q}$ measure. In the figure, the solid line is the density under the multivariate RSLN2 model, and the dashed line is the density under the regime switching model with multivariate normal and Laplace distributions. It shows that the density of the latter has fatter tails than the multivariate RSLN2 models.

The pricing is carried out using the fast Fourier Transform (see, for example, Paolella (2007)). Table 2.15 displays the European Put Option Prices on Geometric Averages. Compared with those of the multivariate regime switching log-normal models given in Table 2.7–2.12, in our case study, the prices are higher under the regime switching models with multivariate normal and Laplace distributions.

K	$T = 120$	24	12	4
50	0.2868	0.0342	0.0320	0.0476
100	7.3723	5.5198	4.2649	2.6079
150	18.0414	34.5417	41.5187	47.0559
200	33.2960	77.5515	88.3712	96.0410

Table 2.15: European put option prices on geometric averages, for multivariate Laplace-normal regime switching models, with geometric weights (1/3, 1/3, 1/3) and positive covariance

Remark 2.5.1. The Fourier transform method is usually accurate in obtaining density functions, as the tails of density functions decay, while its application in the computation of tail expectation is much worse, as the values may not decay in both tails. See, for example, Čížek et al. (2005). As discussed in Carr and Madan (1999), if we choose a value α with $\alpha < 0$ in (2.4.24) for computing option prices, we enlarge the computing errors for using $\tilde{P}_c(k)$ instead of $P_c(k)$ when $k > 0$. In the option pricing using the FFT methods, different α may result in different part of pricing errors. Thus, the choice of the parameter α in (2.4.24) plays an important role. Unfortunately, to the best of my knowledge, there is no uniformly best choice available for α. The method used by Carr and Madan (1999) to choose α is based on the observation of the price curves. Figure 2.5 displays some price curves based

on different choice of α. Based on the observation, we choose α between 0.15 to 0.2.

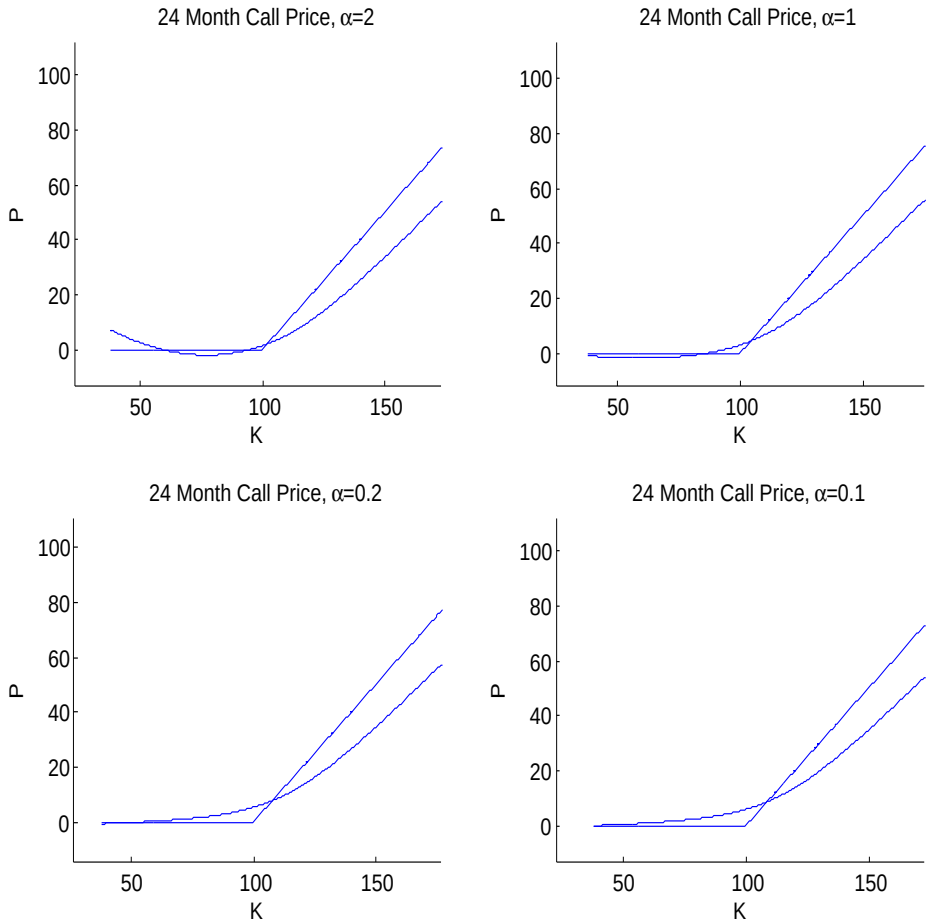

Figure 2.5: Price (curve) vs. Payoff when $S_T = 100$ (straight lines) under different choice of α (K: strike prices; $S_0 = 100$)

Remark 2.5.2. After obtaining the prices for the geometric average European options, we can use them to evaluate the European options written on the arithmetic average of stock prices, which is called the basket option with payoff $H(S_{T,\bullet}) = (\sum_{l=1}^{N} \omega_l S_{t,l} - K)^+$. The basket option is priced using the same approaching as

Asian options, since these two options are both written on the arithmetic average of the underlying asset prices. The commonly used pricing approaches for the geometric average European options include the following two. The first one uses Monte Carlo simulation with control variate method. As commented by Boyle et al. (1997), the control variate method is the most efficient compared with other variance reduction methods. The second one is an approximation approach suggested by Vorst (1992).

2.6 Conclusion

In this chapter, we apply the Esscher transform to identify the risk neutral pricing measure for derivatives written on multiple assets under a discrete time regime switching model, and calculate the prices of the geometric average European options. The pricing is through a double expectation, with the inner expectation calculated conditional on a given regime transition path while the outer expectation is with respect to the probabilities over each path. For the inner expectation, there is no uncertainty associated with regime transition involved and hence we can borrow many well-developed pricing methods available in literature. Moreover, since the prices of all underlying assets are assumed to follow a same regime switching process, the techniques developed in Chapter 1 to reduce the computation time is still applicable to calculate the outer expectation. Derivative pricing often come along with the hedging strategies, to make the pricing more meaningful. In the later part of this thesis, we will investigate more on hedging which is of particular interest for regime switching models.

Chapter 3

Comparison of Hedging Performance among the 3 Risk-neutral Methods along with MV Hedging

3.1 Introduction

In Chapter 1, we developed the ET-$\mathbb{Q}$ method to price European options in an incomplete market consisting of two assets: a bond and a stock, with stock prices (S_t) following the RSLN2 model. We also introduced two other pricing methods and compared their prices. The goal of this chapter is to investigate hedging using the ET-$\mathbb{Q}$ method, through a comparative study based on simulation. We focus on discrete time hedging for European options written on a single underlying risky asset. The comparison is organized in two parts. The first part compares discrete time delta hedging from the three risk-neutral methods: the Black–Scholes, the NEMM methods, and the ET-$\mathbb{Q}$ methods. The second part, section 3.3 conducts the comparative analysis of the 3 risk-neutral methods with the mean-variance method in terms of their hedging performance. It is worth noting that in the study, the

hedging of loss is from the option's issuer point of view.

Our hedging comparison is conducted based on the analysis of hedging loss for the writer of the option. The comparison is separate for single-period and multiperiod settings. Without loss of generality, let the single period be $[0, 1]$. Based on this single period, we measure and compare the delta hedging loss at maturity, denoted by $L(Y_1)$, as a function of the log-return Y_1 as follows:

$$L(Y_1) = P_1 - (\Delta_0 \, S_0 e^{Y_1} + B_0 \, e^r), \tag{3.1.1}$$

where P_1 represents the maturity value of the option (or the payoff), Δ_0 and B_0 respectively represent the units of stock and the value of bonds in the delta hedging portfolio constructed at $t = 0$. As a result, $L > 0$ represents a loss.

For multiperiod options, we measure and compare the present value of the cumulative hedging errors. Assume hedging is implemented over a set of discrete time points $t = 0, 1, \ldots, T$. Let P_t denote option values, and ζ_t denote hedging portfolio values at time t. The hedging portfolio is constructed at time $t = 0$ with $\zeta_0 = P_0$, and is rebalanced at $t = 1, \ldots, T-1$ to achieve $\zeta_t = P_t$. At any intermediate time, say s for $t - 1 < s < t$, $\zeta_s = \Delta_{t-1} \, S_s + B_{t-1} \, e^{r(s-t+1)}$, in which Δ_{t-1} and B_{t-1} representing the units of stocks and the value of bonds in the portfolio after rebalancing at time $t - 1$ for a delta hedging. As a result, the hedging error for each period, denoted by ϵ_t for the period $(t - 1, t)$, is

$$\epsilon_t = P_t - \zeta_{t-} \tag{3.1.2}$$

where ζ_{t-} represents the value of the portfolio immediately before rebalancing at t, and $\zeta_{t-} = \Delta_{t-1} \, S_t + B_{t-1} \, e^r$ for delta hedging. In the study for multiperiod hedging, the present value of cumulative hedging errors, denoted by $PVHL$, is

$$PVHL = \sum_{t=1}^{T} \epsilon_t \, e^{-rt}. \tag{3.1.3}$$

Based on the distribution of $L(Y_1)$ or $PVHL$, we conduct the hedging effects

analysis. To analyze the effects for the single period setting, we employ a tool of effective hedging range, denoted by the interval $[D, U]$ of the continuous random variable, the asset price S_1 or its log-return $Y_1 = \log(S_1/S_0)$, defined as follows.

Definition 3.1.1. Let $L(Y_1) : \Omega \to \mathbb{R}$ as defined in (3.1.1). Then, an interval $[D, U]$ is called the effective hedging range (EHR) of Y_1, if $L(Y_1) \leq 0$ if and only if $Y_1 \in [D, U]$.

We may also define the EHR of S_1 similar to Definition 3.1.1, with $[0, D)$ and (U, ∞) representing the left and right ranges of S_1 generating a loss. It is worth noting that, the EHR may not exist for $PVHL$ on the cumulative yield $\sum_{t=1}^{T} Y_t$ in multiperiod dynamic hedging, because the $PVHL$, defined in (3.1.3), is not only dependent on the value of $\sum_{t=1}^{T} Y_t$, but may also dependent on the path of $Y_1, \ldots, Y_T$. That is, for the same value of $\sum_{t=1}^{T} Y_t$, two different paths of $Y_1, \ldots, Y_T$ may result in different hedging losses. As a result, we may not have a EHR defined only on $\sum_{t=1}^{T} Y_t$.

However, single period EHRs could still be interesting information for comparing hedging difference between different methods, and helpful in interpreting the difference in multiperiod hedging results. In section 3.2, we will verify the existence of EHRs of Y_1 in discrete time hedging for a single period under three risk neutral methods: the Black–Scholes, the NEMM methods, and the ET-$\mathbb{Q}$ methods, and compare their values. The locations and length of the effective hedging range is of interest for hedging analysis. Indeed, from the hedging case study in the following two sections, we will see that among the three risk-neutral approaches, the ET-$\mathbb{Q}$ method has the widest EHR, covering the EHRs of the two other methods. We also observe that the mean-variance method tends to shift both boundaries of $[D, U]$ to the right compared to the risk-neutral approaches, implying a different hedging strategy with a weaker protection for downside loss. We may also analyze other risk measures based on EHRs if the risk measures on the ranges are comparable. For example, in the period $[0, 1]$ under regime switching models, let $[D_i, U_i]$ denote the EHR for hedging in the period given $\rho_1 = i$. Then, we can compute and compare hedging loss probabilities

$\mathbb{P}(L > 0|\rho_1 = i)$:

$$\mathbb{P}(L > 0|\rho_1 = i) = 1 - \int_{[D_i, U_i]} f^{\mathbb{P}}(y_1|\rho_1 = i)\, dy_1, \tag{3.1.4}$$

where $f^{\mathbb{P}}(y_1|\rho_1 = i)$ is the conditional physical density of $Y_1 = y_1$. As an example, since ET-$\mathbb{Q}$ method has the widest EHR, it has the lowest loss probability in either side of tails. However, the hedging probabilities are more complicated to compare between mean-variance methods and risk neutral methods.

Besides EHRs, we also compute risk measures such as the Value at Risk (VaR) and the Conditional Tail Expectation (CTE) under both single period and multiperiod settings.

Definition 3.1.2. (**McNeil et al., 2005**) The Value at Risk (VaR) at the confidence level α of the loss L is defined as

$$VaR_\alpha = \inf\{l \in \mathbb{R} : \mathbb{P}(L > l) \leq 1 - \alpha\}$$

Definition 3.1.3. (**McNeil et al., 2005**) The Conditional Tail Expectation (CTE) at the confidence level α of the loss L is defined as

$$CTE_\alpha = \frac{1}{1-\alpha} \int_\alpha^1 VaR_u(L) du$$

The CTE can be interpreted as "the expected loss given that the loss falls in the worst $(1 - \alpha)$ part of the loss distribution" (Hardy, 2006). We use the confidence-level $\alpha = 95\%$, at which the values of VaR_α and CTE_α can be compared for different methods.

The organization of the remaining content of this chapter is as follows. In section 3.2, we obtain analytical results of the single period EHRs $[D, U]$ for the three risk-neutral methods we mentioned above; compare their EHRs and risk measures such as probabilities of having a loss and the $\text{CTE}_{95\%}$ of the loss distributions for hedging a European put option. In section 3.3, we compute the mean-variance hedging cost and compare hedging loss between mean-variance methods and the ET-$\mathbb{Q}$ methods.

At the end of this section, we specifically discuss the difference of the effective hedging ranges and its impact on the associated risk measures between these two methods.

3.2 Hedging Comparison for Risk Neutral Methods

The objective of this section is to compute and compare hedging difference, in terms of effective hedging ranges and some risk measures of hedging loss, among three risk-neutral methods: the Black–Scholes, the NEMM methods, and the ET-$\mathbb{Q}$ methods.

We first compute and compare EHRs for hedging a European put option in the single period $[0, 1]$. We assume the put option is expired in one period, instead of assuming it is expired after the period. The result of the study for one period options also provides useful information for hedging a multiperiod option.

3.2.1 Single Period EHR for the Black–Scholes Method

In this section, we compute the effective hedging range $[D, U]$ for the Black–Scholes method. The hedging portfolio is constructed at $t = 0$ for a put option. At $t = 0$ the value of the delta hedging portfolio is

$$\zeta_0 = B_0 - S_0\Delta_0,$$

where $B_0 = e^{-r}K\Phi(-d_2)$ and $\Delta_0 = -\Phi(-d_1)$, with $\Phi(\cdot)$ denoting the standard normal distribution function,

$$d_1 = \frac{\log(S_0/K) + (r + \frac{\sigma^2}{2})}{\sigma}, \quad \text{and} \quad d_2 = d_1 - \sigma. \tag{3.2.5}$$

At $t = 1$ before making payoff, the portfolio value becomes

$$\zeta_{1^-} = K\Phi(-d_2) - S_0\, e^{Y_1}\Phi(-d_1).$$

Then, the loss function $L(Y_1)$ is

$$L(Y_1) = \begin{cases} L_L(Y_1), & \text{if } Y_1 < \log(K/S_0) \\ L_U(Y_1), & \text{if } Y_1 \geq \log(K/S_0) \end{cases} \tag{3.2.6}$$

where $L_L(Y_1)$ denotes the hedging loss when the put option expires in the money, and $L_U(Y_1)$ denotes the hedging loss function when the option expires out of the money. More specifically,

$$L_L(Y_1) \;=\; K - S_0\, e^{Y_1} - (\, K\, \Phi(-d_2) - S_0\, e^{Y_1}\, \Phi(-d_1)\,),$$

and

$$L_U(Y_1) \;=\; -(\, K\, \Phi(-d_2) - S_0\, e^{Y_1}\, \Phi(-d_1)\,).$$

Based on L, we can have the result of $[D, U]$ given in Proposition 3.2.1. To proceed, we first define the term *U–shaped* as follows.

Definition 3.2.1. Let $T(x) : \mathbb{R} \to \mathbb{R}$. We say T is U–shaped against x, if and only if the following two conditions are met:

1. T is a continuous function of x;
2. $T(x)$ is a continuous increasing function of x over (a, ∞) and a continuous decreasing function over $(-\infty, a)$

As a result, there $\exists\, a \in \mathbb{R}$ satisfying $a = \arg\min_{x \in \mathbb{R}} T(x)$.

Proposition 3.2.1. *(**CQ**) There exists $D, U \in \mathbb{R}$ such that $L \leq 0$, for L defined in (3.2.6), if and only if $Y_1 \in [D, U]$. Moreover, $\min_{Y_1} L$ is obtained at $Y_1 = \log(K/S_0)$ and*

$$[D, U] = \left[\log\left(\frac{K\, \Phi(d_2)}{S_0\, \Phi(d_1)} \right),\; \log\left(\frac{K\, \Phi(-d_2)}{S_0\, \Phi(-d_1)} \right) \right].$$

Proof. To show the existence of $[D, U]$, we show L is U–shaped against the value of Y_1, and $\min_{Y_1} L \leq 0$, obtained at $Y_1 = \log(K/S_0)$; then, we can compute $[D, U]$ by letting $L = 0$ in equation (3.2.6). Indeed, from (3.2.6), we have

$$\frac{\partial L}{\partial Y_1} = \begin{cases} -S_0\, e^{Y_1}\,(1 - \Phi(-d_1)) < 0 & \text{if } Y_1 < \log(K/S_0) \\ S_0\, e^{Y_1}\,\Phi(-d_1) > 0 & \text{if } Y_1 > \log(K/S_0) \end{cases}.$$

In addition, $L_L(Y_1)$ and $L_U(Y_1)$ in (3.2.6) are continuous functions of Y_1, and be equal at $Y_1 = \log(K/S_0)$. As a result, L is U–shaped against Y_1. Thus, L achieves the minimum at $Y_1 = \log(K/S_0)$.

To show $\min_{Y_1} L \leq 0$, from (3.2.5), it is clear that $d_2 < d_1$, i.e., $-d_2 > -d_1$, i.e., $\Phi(-d_2) > \Phi(-d_1)$. Thus, at $Y_1 = \log(K/S_0)$, we have

$$\begin{aligned} \min_{Y_1} L = & \quad (K - S_1)^+ - (K\,\Phi(-d_2) - S_0\, e^{Y_1}\,\Phi(-d_1))\big|_{Y_1 = \log(K/S_0)} \\ = & \quad -K\,(\Phi(-d_2) - \Phi(-d_1)) < 0. \end{aligned} \tag{3.2.7}$$

□

Remark 3.2.1. Based on the loss function (3.2.6), we can compute the CTE_α of hedging loss. Conditional on the initial regime $\rho(0) = i$ for $i = 1, \ldots, R$, the CTE_α of the hedging loss is

$$\text{CTE}_\alpha = \int_{(-\infty, y_1') \bigcup (y_2', \infty)} L(y_1)\, f^{\mathbb{P}}(y_1 | \rho_0 = i)\, dy_1,$$

where y_1' and y_2', with $y_1' < y_2'$, are determined by

$$1 - \alpha = \mathbb{P}(Y_1 \leq y_1' | \rho_0 = i) + \mathbb{P}(Y_1 > y_2' | \rho_0 = i) \tag{3.2.8}$$

and

$$L_L(y_1') = L_U(y_2'). \tag{3.2.9}$$

Equation (3.2.9) implies $y_1' < \log(K/S_0) < y_2'$. The reason is as follows. Since L is U–shaped against Y_1, and $Y_1 = \log(K/S_0)$ is the unique minimizer of the loss

function L, the minimum point must locate between any two y_1' and y_2' which result in a same value for L. Regarding the length of the range $[y_1', y_2']$, the interval $[y_1', y_2']$ determined in the above equations (3.2.8) and (3.2.9) may not have the smallest length among all the α–level intervals of Y_1. The reason is as follows. The equality $f^{\mathbb{P}}(y_1'|\rho_0 = i) = f^{\mathbb{P}}(y_2'|\rho_0 = i)$ is a necessary condition for the confidence interval to be smallest at a fixed α–level significance. However, $L_L(y_1') = L_U(y_2')$ for an asymmetric loss function L may imply $f^{\mathbb{P}}(y_1'|\rho_0 = i) \neq f^{\mathbb{P}}(y_2'|\rho_0 = i)$.

3.2.2 Single Period EHR for the NEMM Method

The NEMM pricing method under the RSLN2 models is introduced in Section 1.4.3. In this method and the ET-$\mathbb{Q}$ method, we assume that the current regime $\rho_0 = i$ is known and the process in $[0, 1]$ switches to regime j with probability p_{ij}. Based on its pricing formula, the effective hedging ranges can be obtained similarly as for the Black–Scholes method. The hedging portfolio, conditional on ρ_0, at $t = 0$ is the mixture of two Black–Scholes delta hedging portfolios as follows:

$$\zeta_0 = p_{i1}(K\, e^{-r}\, \Phi(-d_2^{\sigma_1}) - S_0\, \Phi(-d_1^{\sigma_1})) + p_{i2}(K\, e^{-r}\, \Phi(-d_2^{\sigma_2}) - S_0\, \Phi(-d_1^{\sigma_2})),$$

where $d_1^{\sigma_j}$ and $d_2^{\sigma_j}$ are the d_1 and d_2 values dependent on σ_j specified by $\rho_1 = j$. The hedging–loss function $L(Y_1)$, given $\rho_0 = i$, becomes $L_L(Y_1)$ or $L_U(Y_1)$, with

$$\begin{cases} L_L(Y_1) &= K - S_0 e^{Y_1} - p_{i1}\left[K\Phi(-d_2^{\sigma_1}) - S_0 e^{Y_1}\Phi(-d_1^{\sigma_1})\right] \\ &\quad\quad -p_{i2}\left[K\Phi(-d_2^{\sigma_2}) - S_0 e^{Y_1}\Phi(-d_1^{\sigma_2})\right], \qquad Y_1 < \log(K/S_0), \\ L_U(Y_1) &= -p_{i1}\left[K\Phi(-d_2^{\sigma_1}) - S_0 e^{Y_1}\Phi(-d_1^{\sigma_1})\right] \\ &\quad\quad -p_{i2}\left[K\Phi(-d_2^{\sigma_2}) - S_0 e^{Y_1}\Phi(-d_1^{\sigma_2})\right], \qquad Y_1 \geq \log(K/S_0). \end{cases} \tag{3.2.10}$$

Proposition 3.2.2. *(**CQ**) There exist real values D, U such that $L \leq 0$, if and only*

if $Y_1 \in [D, U]$, *and* $[\,D, U\,]$ *is*

$$\begin{cases} D &= \log\left\{\dfrac{K\,(1-p_{i1}\,\Phi(-d_2^{\sigma_1})-p_{i2}\,\Phi(-d_2^{\sigma_2}))}{S_0\,(1-p_{i1}\,\Phi(-d_1^{\sigma_1})-p_{i2}\,\Phi(-d_1^{\sigma_2}))}\right\} \\ \\ U &= \log\left\{\dfrac{K\,(p_{i1}\,\Phi(-d_2^{\sigma_1})+p_{i2}\,\Phi(-d_2^{\sigma_2}))}{S_0\,(p_{i1}\,\Phi(-d_1^{\sigma_1})+p_{i2}\,\Phi(-d_1^{\sigma_2}))}\right\} \end{cases}$$

Proof. The proof is based on similar argument as in the proof of Proposition 3.2.1. The existence of $[D, U]$ is based on the U–shape of the loss function L against the value of Y_1 and the fact that $\min_{Y_1} L < 0$. First, because $0 < p_{i1}\,\Phi(-d_1^{\sigma_1}) + p_{i2}\,\Phi(-d_1^{\sigma_2})) < 1$, the slope of the loss function L satisfies

$$\frac{\partial L}{\partial Y_1} = \begin{cases} -S_0\,e^{Y_1}\;(1-p_{i1}\,\Phi(-d_1^{\sigma_1})-p_{i2}\,\Phi(-d_1^{\sigma_2}))<0, & Y_1 < \log(K/S_0), \\ \\ S_0\,e^{Y_1}\;(p_{i1}\,\Phi(-d_1^{\sigma_1})+p_{i2}\,\Phi(-d_1^{\sigma_2})>0, & Y_1 > \log(K/S_0). \end{cases}$$

In addition, L is continuous in Y_1. Thus, L is U–shaped against Y_1. As a result, L achieve its unique global minimum at $Y_1 = \log(K/S_0)$. Second, since $[K\Phi(-d_2^{\sigma_1}) - S_0 e^{Y_1}\Phi(-d_1^{\sigma_1})] > 0$ at $Y_1 = \log(K/S_0)$, from (3.2.10), we have $\min_{Y_1} L < 0$. Based on these two properties of L, the values of D, U can be computed by letting $L_L(Y_1) = 0$ and $L_U(Y_1) = 0$ in (3.2.10). □

3.2.3 Single Period EHR for the ET-$\mathbb{Q}$ Method

The ET-$\mathbb{Q}$ method pricing is described in section 1.3 in Chapter 1. Based on the pricing formula, we compute its discrete time delta hedging ranges $[D, U]$ in this section. Let $\eta_j = e^{-r+\mu_{ij}+\frac{\sigma_j^2}{2}}, j = 1, 2$. For notational convenience, let $d_1^{[ij]}$ and $d_2^{[ij]}$ represent the parameters d_1 and d_2 in (1.3.62), respectively, given the single period transition $\{\rho_0 = i, \rho_1 = j\}$. Recall the transition probability under ET-$\mathbb{Q}$ measure,

q_{ij}, is given in (1.3.53). Then, the loss function $L(Y_1)$, given $\rho_0 = i$, is

$$\begin{cases} L_L(Y_1) &= K - S_0\, e^{Y_1} - q_{i1}\left(K\,\Phi(-d_2^{[i1]}) - S_0\, e^{Y_1}\,\eta_1\,\Phi(-d_1^{[i1]})\right) \\ &\quad -q_{i2}\left(K\,\Phi(-d_2^{[i2]}) - S_0\, e^{Y_1}\,\eta_2\,\Phi(-d_1^{[i2]})\right) \qquad Y_1 < \log(K/S_0) \\ L_U(Y_1) &= -q_{i1}\left(K\,\Phi(-d_2^{[i1]}) - S_0\, e^{Y_1}\,\eta_1\,\Phi(-d_1^{[i1]})\right) \\ &\quad -q_{i2}\left(K\,\Phi(-d_2^{[i2]}) - S_0\, e^{Y_1}\,\eta_2\,\Phi(-d_1^{[i2]})\right) \qquad Y_1 \geq \log(K/S_0) \end{cases}$$

Proposition 3.2.3. *(**CQ**) There exist real values D, U such that $L(Y_1) \leq 0$ if and only if $Y_1 \in [D, U]$, where $[\,D, U\,]$ is*

$$\begin{cases} D &= \log\left\{\dfrac{K\,\left(1 - q_{i1}\,\Phi(-d_2^{[i1]}) - q_{i2}\,\Phi(-d_2^{[i2]})\right)}{S_0\,\left(1 - q_{i1}\,\eta_1\,\Phi(-d_1^{[i1]}) - q_{i2}\,\eta_2\,\Phi(-d_1^{[i2]})\right)}\right\}, \\ U &= \log\left\{\dfrac{K\,\left(q_{i1}\,\Phi(-d_2^{[i1]}) + q_{i2}\,\Phi(-d_2^{[i2]})\right)}{S_0\,\left(q_{i1}\,\eta_1\,\Phi(-d_1^{[i1]}) + q_{i2}\,\eta_2\,\Phi(-d_1^{[i2]})\right)}\right\}. \end{cases}$$

Proof. Based on the similar argument as in Proposition 3.2.1. We first show the slope of L against Y_1 satisfying

$$\frac{\partial L}{\partial Y_1} = \begin{cases} -S_0\, e^{Y_1}\,\left(1 - q_{i1}\,\eta_1\,\Phi(-d_1^{[i1]}) - q_{i2}\,\eta_2\,\Phi(-d_1^{[i2]})\right) < 0, & Y_1 < \log(K/S_0), \\ S_0\, e^{Y_1}\,\left(q_{i1}\,\eta_1\,\Phi(-d_1^{[i1]}) + q_{i2}\,\eta_2\,\Phi(-d_1^{[i2]})\right) > 0, & Y_1 < \log(K/S_0). \end{cases} \tag{3.2.11}$$

In (3.2.11), the second expression is positive, since all $q_{ij}, \eta_j, \Phi(\cdot)$ are positive. The

first term is negative, which can be seen as follows. Since

$$\begin{aligned} & q_{i1}\,\eta_1 + q_{i2}\,\eta_2 \\ = \; & \frac{p_{i1}\,e^{\mu_1\,h_1^* + \frac{\sigma_1^2}{2}\,h_1^{*2}}}{\mathsf{E}^{\mathbb{P}}(e^{Y_1\,h_1^*}\,|\,\rho_0 = i)}\,e^{-r+\mu_{i1}+\frac{\sigma_1^2}{2}} + \frac{p_{i2}\,e^{\mu_2\,h_1^* + \frac{\sigma_2^2}{2}\,h_1^{*2}}}{\mathsf{E}^{\mathbb{P}}(e^{Y_1\,h_1^*}\,|\,\rho_0 = i)}\,e^{-r+\mu_{i2}+\frac{\sigma_2^2}{2}} \qquad (3.2.12) \\ = \; & e^{-r}\,\frac{\mathsf{E}^{\mathbb{P}}(e^{Y_1\,(h_1^*+1)}\,|\rho_0 = i)}{\mathsf{E}^{\mathbb{P}}(e^{Y_1\,h_1^*}\,|\rho_0 = i)} \\ = \; & 1. \end{aligned}$$

Also $0 < \Phi(\cdot) < 1$. As a result, we have $1 - q_{i1}\,\eta_1\,\Phi(-d_1^{[i1]}) - q_{i2}\,\eta_2\,\Phi(-d_1^{[i2]}) > 0$. Thus, the first term in equation (3.2.11) is negative. L is a continuous function of Y_t. Thus, the loss L is U–shaped against the value of Y_1. The global minimum of L is obtained at the point $Y_1 = \log(K/S_0)$.

Second, we also have $\min_{Y_1} L < 0$ as follows. $L_L = L_U < 0$ at $Y_1 = k$ if and only if

$$q_{i1}\,\Phi(-d_2^{[i1]}) + q_{i2}\,\Phi(-d_2^{[i2]}) - q_{i1}\,\eta_1\,\Phi(-d_1^{[i1]}) - q_{i2}\,\eta_2\,\Phi(-d_1^{[i2]}) > 0. \qquad (3.2.13)$$

To verify this, let

$$\begin{aligned} F(-\log(S_0/K)) &:= q_{i1}\,\Phi(-d_2^{[i1]}) + q_{i2}\,\Phi(-d_2^{[i2]}) \\ \tilde{F}(-\log(S_0/K)) &:= -q_{i1}\,\eta_1\,\Phi(-d_1^{[i1]}) - q_{i2}\,\eta_2\,\Phi(-d_1^{[i2]}). \end{aligned}$$

Then

$$F(-\log(S_0/K)) = \int_{-\infty}^{-\log(S_0/K)} f_i^{\mathbb{Q}}(y_1)\,dy_1$$

where,with $\phi(z)$ representing the standard normal density function,

$$f_i^{\mathbb{Q}}(y_1) = q_{i1}\,\phi\left(\frac{y_1 - \mu_{[i1]}^{\mathbb{Q}}}{\sigma_1}\right)\frac{1}{\sigma_1} + q_{i2}\,\phi(-d_2^{[i2]})\left(\frac{y_1 - \mu_{[i2]}^{\mathbb{Q}}}{\sigma_2}\right)\frac{1}{\sigma_2}.$$

Also,

$$\tilde{F}(-\log(S_0/K)) \;=\; \int_{-\infty}^{-\log(S_0/K)} g_i^{\mathbb{Q}}(y_1)\, dy_1$$

where $g_i^{\mathbb{Q}}(y_1) = e^{y_1 - r} f_i^{\mathbb{Q}}(y_1)$. As a result of Lemma 1.2.4, the distribution under $g_i^{\mathbb{Q}}(y_1)$ is strictly stochastically larger than the distribution under $f^{\mathbb{Q}}(y_1)$ for Y_1. That is

$$F(-\log(S_0/K)) > \tilde{F}(-\log(S_0/K)).$$

(3.2.13) is proved. □

3.2.4 Numerical Results of Single Period Hedging

In this section, we will compare hedging performance among these aforementioned three pricing methods, from the option issuer's point of view, under a single-period setting. Model parameters are as follows: the parameters of the RSLN2 model, borrowed from Hardy(2003), are given in Table 3.1; $S_0 = 100$; the constant interest rate $r = 0.005$ per month. Numerical results are given for hedging out–of–money

Regime 1	$\mu_1 = 0.012$	$\sigma_1 = 0.035$	$p_{12} = 0.037$
Regime 2	$\mu_2 = -0.016$	$\sigma_2 = 0.078$	$p_{21} = 0.210$

Table 3.1: RSLN2 parameters

and at–the–money European put options.

As assumed, the single period is $[0, 1]$. To compare the hedging results from the three risk-neutral methods, we compute the analytical values of their option prices, effective hedging ranges, loss probabilities, and the CTE_α of hedging loss. Here, loss probability is the probability that a positive loss occurs. The corresponding numerical results are presented in Tables 3.2– 3.6, where we assume the strike price $K = 90$. Based on these results, we have the following three interesting observations.

First, for the out–of–money put option with small values, the price based on the regime switching pricing methods, especially the ET-$\mathbb{Q}$ method, are significantly higher than the price of the Black–Scholes method. This can be seen from Table 3.2, which lists the put option prices (multiplied by 1000) for the three risk-neutral methods, with the average of option prices computed based on the stationary probabilities for the two regimes.

	$\rho_0 = 1$	$\rho_0 = 2$	Average
BS	9.9	9.9	9.9
NEMM	10.4	207.9	39.8
ET-$\mathbb{Q}$	36.6	222.2	64.4

Table 3.2: 1-month put option price $\times 1000$; $S_0 = 100, K = 90$

Second, we see significant differences in option hedging results. The ET-$\mathbb{Q}$ method has the widest effective hedging ranges $[D, U]$, which covers both ranges of the NEMM method and the Black–Scholes method, for hedging the out–of–money put option; see Table 3.3. As a result, the ET-$\mathbb{Q}$ method has the corresponding

	$\rho_0 = 1$	$\rho_0 = 2$
BS	$(89.92, 101.99)$	$(89.92, 101.99)$
NEMM	$(89.95, 103.54)$	$(89.13, 104.10)$
ET-$\mathbb{Q}$	$(89.87, 104.75)$	$(89.08, 104.15)$

Table 3.3: Intervals of EHR for hedging a 1-month put option, with $S_0 = 100$ and $K = 90$

lowest loss probabilities, as given in Table 3.4. In the table, the probability of lower tail loss is the probability of loss occurred when the option expires in the money, and upper tail loss probability is the probability of loss occurred when the option expires out of the money. The average is the expected loss probability: $\mathbb{P}(L > 0) = \sum_{i=1}^{2} \pi_i \, \mathbb{P}(L > 0 \,|\, \rho_0 = i)$, where π_i is the stationary probabilities for the regime process.

Third, based on the empirical distribution of L, Table 3.5 illustrates that the ET-$\mathbb{Q}$ method has the lower values of the $\text{VaR}_{95\%}$ and the $\text{CTE}_{95\%}$ than the Black-

	$\rho_0 = 1$	$\rho_0 = 2$	Average
(two tails, $\rho_1 = 1$ or 2)			
BS	0.414	0.440	0.418
NEMM	0.262	0.311	0.270
ET-$\mathbb{Q}$	0.169	0.307	0.19
(lower tail & $\rho_1 = 1$)			
BS	0.00036	0.00036	
NEMM	0.00037	0.00014	–
ET-$\mathbb{Q}$	0.00034	0.00013	
(upper tail & $\rho_1 = 1$)			
BS	0.4128	0.4127	
NEMM	0.2573	0.2105	–
ET-$\mathbb{Q}$	0.1628	0.2063	
(lower tail & $\rho_1 = 2$)			
BS	0.1236	0.1236	
NEMM	0.1246	0.1021	–
ET-$\mathbb{Q}$	0.1222	0.1007	
(upper tail & $\rho_1 = 2$)			
BS	0.3235	0.3235	
NEMM	0.2574	0.2357	–
ET-$\mathbb{Q}$	0.2118	0.2337	

Table 3.4: Loss probability $\mathbb{P}(L > 0)$ of hedging 1-month put option: $K = 90, S_0 = 100$

Scholes methods, based on the loss on two sides. Based on the loss on the downside only, Table 3.6 also illustrates that the ET-$\mathbb{Q}$ method has the lowest values of the $\text{VaR}_{95\%}$ and the $\text{CTE}_{95\%}$ among the three risk neutral methods under the discrete time hedging for single period put option with $K = 90$. Thus, our results shows that if the RSLN2 model represents the market behavior for the underlying asset, then delta hedging under the ET-$\mathbb{Q}$ measure provides the most effective hedging for a writer of put options, in terms of $\text{VaR}_{95\%}$ and $\text{CTE}_{95\%}$ of hedging loss.

	S_1 values corresponding to $\text{VaR}_{95\%}$ of L	$\text{VaR}_{95\%}$	$\text{CTE}_{95\%}$	$\sigma(L\|L > VaR_{95\%})$
$(\rho_0 = 1)$				
BS	{89.8825, 107.5196}	0.0368	0.355248	1.2724
NEMM	{89.9396, 107.5231}	0.0137	0.333292	1.2902
ET-$\mathbb{Q}$	{89.8470, 107.5174}	0.0240	0.330542	1.2614
$(\rho_0 = 2)$				
BS	{87.3655, 482.7820}	2.5371	5.4062	2.4490
NEMM	{87.3543, 133.1109}	1.6776	4.3827	2.3324
ET-$\mathbb{Q}$	{87.3496, 130.9600}	1.6229	4.3142	2.3240

Table 3.5: Risk measures of hedging loss L for hedging a 1-month put option, with $S_0 = 100$ and $K = 90$ (σ represents standard deviation)

	S_1 corresponding to $\text{VaR}_{95\%}$ of L for one-tail test	$\text{VaR}_{95\%}$	$\text{CTE}_{95\%}$	$\sigma(L\|L > VaR_{95\%})$
$(\ \rho_0 = 1)$				
BS	89.9701	-0.0502	0.3109	1.2830
NEMM	89.9701	-0.0167	0.3153	1.2945
ET-$\mathbb{Q}$	89.9701	-0.0981	0.3054	1.2700
$(\ \rho_0 = 2)$				
BS	87.35724	2.5453	5.4001	2.4592
NEMM	87.35724	1.6748	4.3826	2.3326
ET-$\mathbb{Q}$	87.35724	1.6156	4.3139	2.3243

Table 3.6: Risk measures of one-tail (left-tail) hedging loss, occurred when $S_1 < K$, for hedging a 1-month put option ($S_0 = 100, K = 90$).

Note: In Tables 3.5 and 3.6, no standard errors are associated with $\text{VaR}_{95\%}$ and $\text{CTE}_{95\%}$, because the values are accurately ($\sigma = 0$) computed, not estimated, based on the assumption of the given RSLN2 model.

3.2.5 Simulated Hedging Results for Multiperiod Hedging

In this section, we conduct a simulation study to investigate the hedging loss in a multiperiod case. Recall that P_t represents the option value, and ζ_t represents the hedging portfolio value at time t. In the multiperiod simulation, the hedging portfolio is constructed at time $t = 0$, and rebalanced at $t = 1, \ldots, T-1$ to achieve

$P_t = \zeta_t$ for integer time points $t = 0, \ldots, T-1$. At an intermediate time, say s for $t-1 < s < t$, we have $\zeta_s = \Delta_{t-1}\, S_s + B_{t-1}\, e^{r(s-t+1)}$. To study the multiperiod dynamic hedging effects, we analyze $PVHL$, the present value of the cumulative hedging errors, defined below:

$$PVHL = \sum_{t=1}^{T} e^{-rt} \left(P_t - \zeta_{t-} \right), \tag{3.2.14}$$

where ζ_{t-} represents the hedging portfolio values immediately before the rebalancing at time t for $t = 1, \ldots, T$. Recall that $\zeta_{t-} = \Delta_{t-1}\, S_t + B_{t-1}\, e^r$, with Δ_{t-1} and B_{t-1} respectively representing the units of stocks and the value of bonds in the rebalanced portfolio at time $t-1$.

The simulation is carried out through the following steps. First, simulate regime paths $\{\rho_t\}_{t=0}^{T}$, and the stock prices $\{S_t\}_{t=0}^{T}$ conditional on the simulated regime path, under the RSLN2 models with $S_0 = 100$. Then, the option prices P_t are evaluated and the rebalanced hedging portfolios ζ_t are set up, for each simulated (S_t, ρ_t). Third, at the discrete time t for $1 \le t \le T$, the values of hedging portfolio ζ_{t-1} are updated and the hedging errors ϵ_t are computed based on (3.1.2). Finally, with all $\epsilon_t, 1 \le t \le T$, the value of $PVHL$ is obtained using equation (3.1.3). As a result, risk measures can then be evaluated based on the empirical distribution of $PVHL$. The simulation is based on the same RSLN2 model parameters given in Table 3.1. Other same parameters include $S_0 = 100$ and $r = 0.005$ per month.

Hedging and pricing may not be based on the same information. In hedging a model risk is choosing a wrong initial regime ρ_0, which leads to the risk for hedging design. In our hedging study, if the initial regime cannot be identified, it is assigned an associated probability, and the hedging portfolio may be determined from the combination of two portfolios corresponding to the two possible states. To improve the hedging efficiency, we may improve the accuracy of the probability assigned to each regime. In this study, we apply the recursive approach proposed by Hardy (2003) to estimate these probabilities at each time of setting up the hedging strategy.

The simulated results are given in Tables 3.7 – 3.10 as follows. The results in Table 3.7 are obtained from $10,000$ simulations for a 12 month put option with the

	K	Option Price	$\mathbb{P}(PVHL > 0)$	$\text{CTE}_{95\%}$	σ
BS	90	1.0840	0.3622 (0.0048)	5.5154 (0.1244)	1.9849
NEMM	90	1.008	0.3292 (0.0047)	5.8408 (0.1300)	2.0783
ET-$\mathbb{Q}$	90	1.2449	0.2466 (0.0043)	5.5483 (0.1274)	2.0206
BS	100	3.5983	0.3654 (0.0048)	6.4873 (0.1380)	2.1115
NEMM	100	3.3058	0.3974 (0.0049)	6.9582 (0.1454)	2.2834
ET-$\mathbb{Q}$	100	3.5686	0.3148 (0.0046)	6.1543 (0.1243)	2.1558

note: $\sigma := \sigma(PVHL|PVHL > VaR_{95\%})$

Table 3.7: Option prices and risk measures of hedging loss for hedging 12-month put options, with $S_0 = 100$, based on simulated RSLN2 stock prices (10,000 projections). Standard errors are given in the brackets besides $\mathbb{P}$ and the CTE.

	K	Option Price	$\mathbb{P}(PVHL > 0)$	$\text{CTE}_{95\%}$	σ
BS	90	1.0840	0.3878 (0.0049)	4.9655 (0.1429)	2.0807
NEMM	90	1.0076	0.3483 (0.0048)	5.6911 (0.1569)	2.1539
ET-$\mathbb{Q}$	90	1.2449	0.2444 (0.0043)	5.1429 (0.1528)	2.1654

note: $\sigma := \sigma(PVHL|PVHL > VaR_{95\%})$

Table 3.8: Option prices and risk measures of hedging loss for hedging 12-month put options, with $S_0 = 100$, based on simulation with bootstrapped TSE data (10,000 projections)

strike price $K = 90$; the results in Table 3.8 are simulated using blocked (6 months) bootstrapped TSE data from 1956 to 1999, with $10,000$ simulations; Table 3.9 and 3.10 give the results for options with 120 month maturity, with $10,000$ simulations, regarding the strike prices $K = 90, \ldots, 110$. In the tables, the CTE values are computed for the present values of hedging loss $PVHL$. The variance of the CTE_α is evaluated using the method given by Manistre and Hancock (2005) as follows

$$var(\hat{CTE}_\alpha) \approx \frac{var(PVHL \,|\, PVHL > VaR_\alpha) + \alpha(CTE_\alpha - VaR_\alpha)^2}{n(1-\alpha)},$$

where n is the number of simulations.

	K	Option Price	$\mathbb{P}(PVHL > 0)$	$\text{CTE}_{95\%}$	σ
BS	90	1.1944	0.4131 (0.0049)	2.8032 (0.0708)	1.1041
NEMM	90	1.1017	0.4299 (0.0050)	3.0333 (0.0767)	1.1953
ET-$\mathbb{Q}$	90	1.3924	0.2891 (0.0045)	2.4278 (0.0708)	1.1087
BS	100	1.9842	0.4155 (0.0049)	3.4172 (0.0777)	1.2329
NEMM	100	1.8341	0.4406 (0.0050)	3.6800 (0.0812)	1.2994
ET-$\mathbb{Q}$	100	2.2155	0.3039 (0.0046)	3.1622 (0.0836)	1.2497
BS	110	3.0510	0.4189 (0.0049)	4.0344 (0.0852)	1.3464
NEMM	110	2.8349	0.4515 (0.0050)	4.4419 (0.0900)	1.3606
ET-$\mathbb{Q}$	110	3.3036	0.3164 (0.0047)	3.7874 (0.0902)	1.3982

note: $\sigma := \sigma(PVHL|PVHL > VaR_{95\%})$

Table 3.9: Option prices and risk measures of hedging loss for hedging 120-month puts, with $S_0 = 100$, based on 10,000 projections with simulated RSLN2 stock prices

	K	Option Price	$\mathbb{P}(PVHL > 0)$	$\text{CTE}_{95\%}$	σ
BS	90	51.8013	0.4131 (0.0049)	2.8032 (0.0707)	1.1041
NEMM	90	51.7086	0.5060 (0.0050)	3.2056 (0.0777)	1.1846
ET-$\mathbb{Q}$	90	51.9996	0.2834 (0.0045)	2.5360 (0.0769)	1.1960
BS	100	47.103	0.4155 (0.0049)	3.4172 (0.0777)	1.2328
NEMM	100	46.9529	0.4975 (0.0050)	3.7653 (0.0803)	1.2871
ET-$\mathbb{Q}$	100	47.3346	0.2950 (0.0046)	3.1079 (0.0790)	1.2311
BS	110	42.6817	0.4189 (0.0049)	4.0344 (0.0852)	1.3464
NEMM	110	42.4656	0.4942 (0.0050)	4.4052 (0.0897)	1.4630
ET-$\mathbb{Q}$	110	42.9346	0.3066 (0.0046)	3.6702 (0.0866)	1.3982

note: $\sigma := \sigma(PVHL|PVHL > VaR_{95\%})$

Table 3.10: Call option prices and risk measures of hedging loss for hedging 120-month options based on 10,000 simulations, with $S_0 = 100$ (Hedging results are similar for call and put options)

It is worth noting that the results from the single period study may not be

directly applied in the multiperiod case, because in the single period study, we study the hedging for an out-of-money put option, while in a multiperiod dynamic hedging process, the ratio K/S_t varies at $t = 1, \ldots, T-1$ and the target option may not always be an out–of–money option at $t \neq 0$. Tables 3.7 – 3.10 illustrate that the ET-$\mathbb{Q}$ method developed on the underlying regime switching models provides better hedging than the Black–Scholes method, in terms of lower loss probability and the lower $\text{CTE}_{95\%}$ of loss. The ET-$\mathbb{Q}$ method also performs better than the NEMM method for hedging a put option. The hedging difference is due to the hedging strategies implied by different pricing measures, which is further discussed in chapter 4.

3.3 Comparison with the Mean Variance Hedging

Mean variance hedging (MV) is widely used for hedging in incomplete markets. It was first introduced into finance by Markowitz (1952, 1959), and was introduced to derivative pricing and hedging by Föllmer and Sondermann (1986), followed by many papers such as Föllmer and Schweizer (1991), Zhou and Yin (2004) and others. We are interested in comparing it to the risk-neutral methods to see hedging difference under the RSLN2 models. We compare the probabilities of resulting a loss from the hedging and the $\text{CTE}_{95\%}$ of the hedging loss, for both single-period and multiperiod settings. We will also discuss differences in effective hedging ranges from these two approaches.

The principle of the mean-variance hedging is to minimize the mean squared hedging errors occurred for the remaining periods before expiration, assuming a static hedging (see Föllmer and Schied, 2004). Assume the period is $[t, T]$. The hedging portfolio is constructed at t, and its construction remains untouched during (t, T). Let a_t denote the units of stock, and B_t denote the bond value in the portfolio. Then, the value of the hedging portfolio at time t is $a_t\, S_t + B_t$. Let $Z = \log(S_T/S_t)$, and $H(Z)$ denote the payoff at maturity T. Then, the hedging error is

$$\epsilon(Z) := H(Z) - \left(a_t\, S_t e^Z + B_t e^{r(T-t)}\right). \tag{3.3.15}$$

The determination of a_t and B_t is through the minimization of $\mathsf{E}^{\mathbb{P}}(\epsilon^2)$, as $\mathsf{E}^{\mathbb{P}}(\epsilon) = 0$ under the mean-variance method. It is worth noting that, the distribution of Z is generated based on the multiperiod process S_t under the RSLN2 models.

3.3.1 Hedging Portfolio

This section constructs the mean-variance hedging portfolio for hedging European put options. The market model is $(S_t, B_t)_{0\le t\le T}$, with $B_t = B_{t-1}e^r$ for a constant rate r, and with S_t following the RSLN2 model. That is, the distribution of $Z = \sum_{s=t+1}^{T} Y_s$, where $Y_t = \log(S_t/S_{t-1})$, has the physical density $f(z)$ as follows:

$$f(z) = \sum_l p_l \, \phi\left(\frac{z-\mu_l}{\sigma_l}\right),$$

where l labels the regime switching path with probability p_l, and $\phi(\cdot)$ represents the standard normal density. Parameters μ_l and σ_l are determined by the path l of the switching process. Under the RSLN2 model, the number of regime switching paths is finite within a finite time period.

The hedging loss function ϵ for a European put option is

$$\epsilon(Z) = (K - S_t\, e^Z)^+ - (a_t^{put}\, S_t\, e^Z + B_t^{put}\, e^{r\,(T-t)}), \tag{3.3.16}$$

where a_t^{put} denotes the units of stock and B_t^{put} denotes the bond value in the hedging strategy set up at time t. The target function of the optimization is

$$J \;=\; \int_{-\infty}^{\infty} \epsilon^2(z)\, f^{\mathbb{P}}(z)\, dz \;. \tag{3.3.17}$$

The mean-variance hedging minimizes J, to obtain the optimal portfolio parameters, denoted by $\hat{a}_t^{put}, \hat{B}_t^{put}$, as follows:

$$\left(\hat{a}_t^{put}, \hat{B}_t^{put}\right) = \arg \min_{(a_t^{put}, B_t^{put})} J$$

As a result, we have the following proposition regarding the construction of the optimal hedging portfolio, where we will see that the cost of the mean-variance hedging is

$$\zeta_t = \mathsf{E}^{\mathbb{P}}\left[e^{-r\,(T-t)}(K - S_t\,e^Z)^+\right] + \hat{a}_t^{put}\,S_t\left[1 - \,e^{-r\,(T-t)}\mathsf{E}^{\mathbb{P}}\left(e^Z\right)\right].$$

Proposition 3.3.1. *(**CQ**) The optimal hedging portfolio $(\hat{a}_t^{put}, \hat{B}_t^{put})$ under the mean-variance method is*

$$\begin{aligned} \hat{a}_t^{put} &= \frac{\mathit{Cov}\left(\left[K - S_t\,e^Z\right]^+, S_t\,e^Z\right)}{\mathit{Var}\left(S_t\,e^Z\right)}, \\ \hat{B}_t^{put} &= \mathit{E}^{\mathbb{P}}\left[e^{-r\,(T-t)}(K - S_t\,e^Z)^+\right] - \hat{a}_t^{put}\,S_t\,e^{-r\,(T-t)}\mathit{E}^{\mathbb{P}}\left(e^Z\right), \end{aligned} \tag{3.3.18}$$

with

$$\mathit{Var}\left(S_t\,e^Z\right) = \mathit{E}^{\mathbb{P}}\left[(S_t\,e^Z)^2\right] - \left[\mathit{E}^{\mathbb{P}}(S_t\,e^Z)\right]^2, \tag{3.3.19}$$

$$\mathit{E}^{\mathbb{P}}[(S_t\,e^Z)^2] = S_t^2\sum_l p_l\,e^{2\,\mu_l + 2\,\sigma_l^2}, \quad \mathit{E}^{\mathbb{P}}\left(S_t\,e^Z\right)^2 = S_t^2\left(\sum_l p_l\,e^{\mu_l + \sigma_l^2/2}\right)^2,$$

where l represents a regime path from time t to T, and

$$\begin{aligned} &\mathit{Cov}\left(\left[K - S_t\,e^Z\right]^+, S_t\,e^Z\right) \\ &= K\,S_t\int_{-\infty}^k e^z\,f^{\mathbb{P}}(z)\,dz - S_t^2\int_{-\infty}^k e^{2z}\,f^{\mathbb{P}}(z)\,dz - K\int_{-\infty}^k f^{\mathbb{P}}(z)\,dz\,\mathit{E}^{\mathbb{P}}\left(S_t\,e^Z\right) \\ &\quad + \textstyle\int_{-\infty}^k S_t\,e^z\,f^{\mathbb{P}}(z)\,dz\,\mathit{E}^{\mathbb{P}}\left(S_t\,e^Z\right), \end{aligned}$$

where $k = \log(K/S_t)$, and

$$K\,S_t\int_{-\infty}^k e^z\,f^{\mathbb{P}}(z)\,dz = K\,S_t\sum_l p_l\,e^{\mu_l + \sigma_l^2/2}\,\Phi\left(\frac{k - \mu_l - \sigma_l^2}{\sigma_l}\right)$$

$$S_t^2 \int_{-\infty}^{k} e^{2z}\, f^{\mathbb{P}}(z)\, dz = S_t^2 \sum_l p_l\, e^{2\,\mu_l + 2\,\sigma_l^2}\, \Phi\left(\frac{k - \mu_l - 2\,\sigma_l^2}{\sigma_l}\right)$$

$$K \int_{-\infty}^{k} f^{\mathbb{P}}(z)\, dz\, \mathsf{E}^{\mathbb{P}}(S_t\, e^Z) = S_t \sum_l p_l\, e^{\mu_l + \sigma_l^2/2} \sum_l p_l\, K\, \Phi\left(\frac{k - \mu_l}{\sigma_l}\right)$$

$$\int_{-\infty}^{k} S_t\, e^z\, f^{\mathbb{P}}(z)\, dz\, \mathsf{E}^{\mathbb{P}}(S_t\, e^Z) = S_t^2 \sum_l p_l\, e^{\mu_l + \sigma_l^2/2} \sum_l \left[p_l\, e^{\mu_l + \sigma_l^2/2}\, \Phi\left(\frac{k - \mu_l - \sigma_l^2}{\sigma_l}\right)\right]$$

Proof. In the proof, for notational convenience, let a and B respectively represent a_t^{put} and B_t^{put}. The proof is achieved in two steps. In the first step, we consider the first order optimality conditions:

$$\frac{\partial J}{\partial a} = 0 \quad \& \quad \frac{\partial J}{\partial B} = 0. \tag{3.3.20}$$

In the second step, we verify the global optimality of a and B by showing that the matrix of the second order partial derivatives of J over a and B is positive definite.

In the first step, we need to obtain the function J, based on the double expectation of squared hedging loss. The inner expectation is the expected squared hedging errors, denoted by J_l, conditional on a given path l of regime switching; the external expectation J is the expected J_l over all paths l. To begin with, from the loss function (3.3.16), we have

$$\begin{aligned} J_l \;=\; & \int_{-\infty}^{\infty} \left(a\, S_t\, e^z + B\, e^{r\,(T-t)}\right)^2 \phi(z)\, dz + \\ & \int_{-\infty}^{k} \left[\, (K - S_t\, e^z)^2 - 2\,(K - S_t\, e^z)(a\, S_t\, e^z + B\, e^{r\,(T-t)}\right)\,]\, \phi(z)\, dz. \end{aligned}$$

Then, we obtain

$$\begin{aligned} J &= \mathsf{E}^{\mathbb{P}}(J_l) \\ &= \sum_l p_l \Big\{ a^2\, S_t^2\, e^{2\,\mu_l+\sigma_l^2}(e^{\sigma_l^2}-1) + (a\, S_t\, e^{\mu_l+\sigma_l^2/2} + B\, e^{r\,(T-t)})^2 + \\ &\quad (K^2 - 2\,K\,B\,e^{r(T-t)})\,\Phi\left(\frac{k-\mu_l}{\sigma_l}\right) - \\ &\quad 2\,[K\,S_t(1+a) - B\,S_t\,e^{r(T-t)}]\,e^{\mu_l+\sigma_l^2/2}\,\Phi\left(\tfrac{k-\mu_l-\sigma_l^2}{\sigma_l}\right) + \\ &\quad S_t^2(1+2a)\,e^{2\,\mu_l+2\,\sigma_l^2}\,\Phi\left(\frac{k-\mu_l-2\,\sigma_l^2}{\sigma_l}\right)\Big\}. \end{aligned} \tag{3.3.21}$$

As a result, plugging (3.3.21) into (3.3.20) and solving for a and B, we obtain the results in (3.3.18).

In the second step, we prove that J achieves the global minimum at a and B obtained above. Denote $X = [a,\ B]$. From equations (3.3.21), the target function J is continuously differentiable in X. Let $X_0 = (\hat{a},\, \hat{B})$ represent the values obtained in the first step, and let $\Delta X = (\Delta_a,\, \Delta_B)$ represent the change of the portfolio parameters; then, the target function J can be expanded by Taylor series around X_0 as follows:

$$\begin{aligned} J(X_0+\Delta X) &= J(X_0) + \left[\left.\frac{\partial J}{\partial a}\right|_{a=\hat{a}}\Delta_a + \left.\frac{\partial J}{\partial B}\right|_{B=\hat{B}}\Delta_B\right] \\ &\quad + \frac{1}{2!}(\theta\Delta X)'\,A|_{X_0}\,(\theta\Delta X), \end{aligned}$$

where $0<\theta<1$, and $A = \begin{pmatrix} \dfrac{\partial^2 J}{\partial a^2} & \dfrac{\partial^2 J}{\partial a\,\partial B} \\ \dfrac{\partial^2 J}{\partial B\,\partial a} & \dfrac{\partial^2 J}{\partial B^2} \end{pmatrix}$. If A is positive definite, then $J(X_0)$ is the global minimum. A is positive definite if and only if the determinants of all the leading principal minors of A are positive, i.e.,

$$\frac{\partial^2 J}{\partial a^2} > 0, \quad \text{and} \quad |A| > 0.$$

After taking twice partial derivatives of equation (3.3.21) with respect to a, we have

$$\frac{\partial^2 J}{\partial a^2} = \sum_{i=1}^{n} p_i \left[2 S_t^2 e^{2\mu_i + 2\sigma_i^2} \right] > 0, \tag{3.3.22}$$

where n represent the number of regime paths. In addition,

$$\begin{aligned} |A| &= \frac{\partial^2 J}{\partial a^2} \frac{\partial^2 J}{\partial B^2} - \left(\frac{\partial^2 J}{\partial a \, \partial B} \right)^2 \\ &= 4e^{2r(T-t)} \mathsf{Var}(S_T) \\ &> 0. \end{aligned}$$

i.e., A is strictly positive definite at all points. Therefore, the portfolio with parameters a and B minimizes the expected squared hedging errors globally.

□

3.3.2 Numerical Hedging Study

Based on the mean-variance method described in section 3.3.1, we compute the initial cost for hedging European put options, and conduct hedging study for single period and multiperiod settings. In the study, the RSLN2 model's parameters are given in Table 3.1. As can be seen shortly, the initial hedging costs of the mean-variance method are not no-arbitrage prices. The comparison of hedging is separate for single-period and multiperiod settings. Our numerical study shows that, for hedging a single period out–of–money put option, the mean-variance method has a larger probability for hedging in a loss, larger $\text{CTE}_{95\%}$ of hedging loss given $\rho_0 = 1$, and lower $\text{CTE}_{95\%}$ given $\rho_0 = 2$, compared with ET-$\mathbb{Q}$ methods and NEMM methods. Further discussion on these hedging results are conducted in section 3.3.3, based on the analysis of EHRs. For multiperiod hedging, however, the hedging comparison between the mean-variance method and the ET-$\mathbb{Q}$ method is more complicated.

K	$T = 120$	60	24	12	8	4
10	7.12E-06	1.09E-06	4.36E-10	2.6E-17	5E-25	1.1E-48
40	0.0199	0.0226	0.0062	0.0005	2.62E-05	3.85E-09
70	0.3022	0.5767	0.4809	0.2332	0.1165	0.0179
80	0.5503	1.1561	1.1718	0.7265	0.4601	0.1491
90	0.9175	2.0769	2.4608	1.8447	1.3744	0.6876
100	1.4290	3.4268	4.6236	4.1497	3.6358	2.7443
110	2.1079	5.2827	7.9413	8.3878	8.4625	8.6992
120	2.9748	7.7044	12.5992	14.8414	15.9967	17.7075
150	6.8621	18.6243	33.6250	41.2805	44.1187	47.0298
180	12.8734	34.6415	59.5754	69.5153	72.9418	76.4358
210	21.0545	54.3028	86.2195	97.7702	101.7658	105.8417
240	31.2651	75.9591	112.8526	126.0234	130.5895	135.2477
270	43.2529	98.4330	139.4666	154.2764	159.4131	164.6536
300	56.7175	121.1031	166.0756	182.5294	188.2368	194.0596

Table 3.11: Portfolio cost for hedging put options using the mean-variance method ($S_0 = 100$)

K	$T = 120$	60	24	12	8	4
10	94.5119	95.5918	91.1308	90.5724	90.3921	90.1981
40	78.0675	70.3899	64.5294	62.3299	61.5685	60.7921
70	61.8854	48.7194	38.3964	34.3097	32.8612	31.4040
80	56.6453	41.8906	30.2181	25.3853	23.5970	21.7332
90	51.5245	35.4033	22.6380	17.0859	14.9034	12.4697
100	46.5479	29.3450	15.9316	9.9732	7.5569	4.7244
110	41.7386	23.7927	10.3800	4.7937	2.7756	0.8773
120	37.1174	18.8062	6.1688	1.8296	0.7020	0.0836
150	24.5404	7.5015	0.5870	0.0158	0.0003	-4.3E-05
180	14.0873	1.2942	-0.0703	-0.0023	-0.0003	-4.4E-06
210	5.8040	-1.2690	-0.0338	-0.0035	-2.7E-05	-6.1E-08
240	-0.4497	-1.8373	-0.0083	-4.8E-05	-2.2E-06	-6.3E-10
270	-4.9263	-1.5879	-0.0020	-6.9E-06	-1.8E-07	-6E-12
300	-7.9260	-1.1421	-0.0005	-1.1E-06	-1.5E-08	-2.2E-13

Table 3.12: Portfolio cost for hedging call options using the mean-variance method, with $S_0 = 100$ (Negative values show that the initial costs cannot be no-arbitrage prices.)

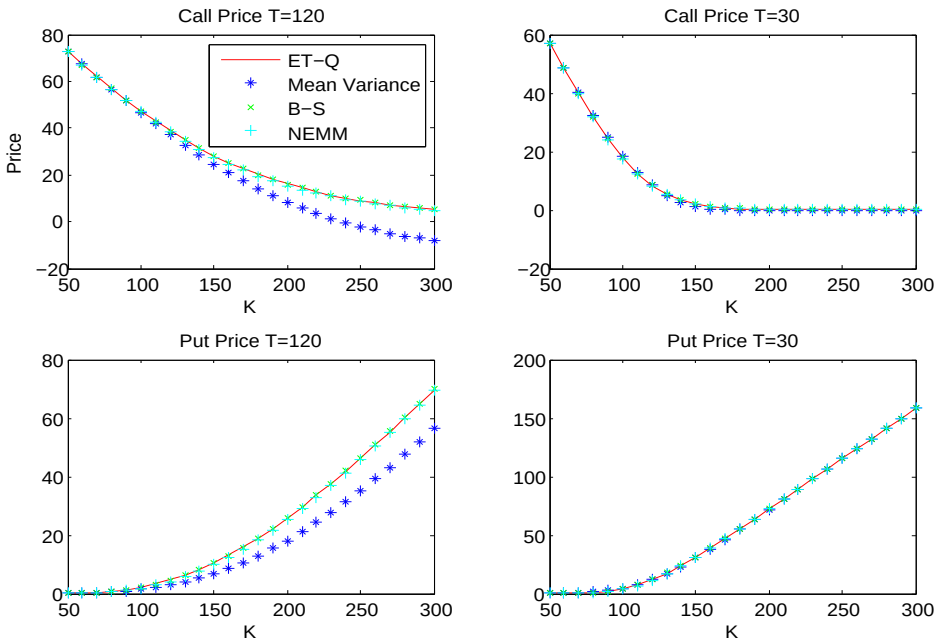

Figure 3.1: Comparison of prices among four methods (Mean variance method prices are significant different from others, and have negative values in the up left plot.)

Arbitrage Prices

The prices of the mean-variance method are given in Table 3.11 and 3.12. Figure 3.1 and 3.2 illustrates the price comparison with the risk-neutral methods. From the given results we have the following three observations.

First, negative values exist in Table 3.12 for the initial hedging cost for call options. Figure 3.1 also displays negative values when K is very large. Since the price of a call option should be positive, if the initial costs under the mean-variance hedging are considered to be the option price, then they are not arbitrage–free prices.

Second, there is a significant gap between the risk-neutral prices and the mean-variance method initial costs, as illustrated in Figure 3.1. When T is small, the price difference is not obvious. The difference is magnified as T increases.

Third, it is worth noting that the initial cost of the mean-variance hedging is

heavily affected by the optimization constraints such as the knowledge of initial regimes. Consider the price of the mean-variance hedging for a put option, given in Table 3.14. Given $\rho_0 = 1$, the put option price is 0.0284; given $\rho_0 = 2$, then the price is 0.2106. However, if we assume $\mathbb{P}(\rho_0 = 1) = \pi_1$ when we price at time zero, then the price is 0.0836. We have the following inequality:

$$0.0284\pi_1 + 0.2106\pi_2 = 0.0557 < 0.0836 \ . \tag{3.3.23}$$

The inequality in equation (3.3.23) illustrates that the knowledge of ρ_0 affects the price and the hedging performance in the mean-variance method. Indeed, in this example, it is consistent with the intuition that, for an optimization, with more knowledge, the prices are lower.

We also compute the hedging cost to minimize the expectation of squared hedging loss in the tail of the distribution of S_1. If the minimization is focused on the left tail, then the optimal hedging strategy for a put option is to sell one share of stock and deposit $K\,e^{-r}$ in the bank. The hedging cost is

$$\zeta_0 = -S_0 + K\,e^{-r}.$$

Consequently, the hedging error is zero when the option expires in the money. However, the hedging error is larger than that of delta hedging with $-1 < \Delta < 0$ when the option expires out of the money. In another case, Table 3.13 illustrates hedging costs for the optimal hedging over intervals $(0, s'] \bigcup [s", \infty)$ with $s' < s"$. The table shows that if the mean-variance hedging is conducted to minimize the tail loss, the hedging cost would be much higher than the cost computed based on the minimization of hedging loss over the entire distribution.

Single Period Hedging Results

In a single period setting with the period $[0, 1]$, the hedging loss L is the same as the ϵ in (3.3.15) with $T = 1$. To compare different methods for a single period hedging, we study three risk measures for hedging loss: the loss probability $\mathbb{P}(L > 0 \,|\, \rho_0)$,

ρ	Different ranges (η) of S_1 within which L is minimized	Price	$\mathsf{E}^{\mathbb{P}}(L\|L \in \eta)$
$\rho_1 = 1$	$\eta = (0, \infty)$	0.0006	-9.7E-13
$\rho_1 = 1$	$\eta = (0, s'] \bigcup [s", \infty)$	0.2517	-1.7E-12
$\rho_1 = 2$	$\eta = (0, \infty)$	0.2393	-1.7E-4
$\rho_1 = 2$	$\eta = (0, s'] \bigcup [s", \infty)$	1.5345	-9.6E-10
$\rho_0 = 1$	$\eta = (0, \infty)$	0.0284	-1.2E-12
$\rho_0 = 1$	$\eta = (0, s'] \bigcup [s", \infty)$	1.2989	-4.5E-11
$\rho_0 = 2$	$\eta = (0, \infty)$	0.2106	-9.7E-12
$\rho_0 = 2$	$\eta = (0, s'] \bigcup [s", \infty)$	1.5228	-9.1E-10

Table 3.13: Option prices and conditional expected hedging loss from minimization of hedging loss over different ranges, for a 1-month put option with $S_0 = 100, K = 90$

1. ρ_0 represents the initial original, while ρ_1 represents the future regime at time one.
2. $s' = 89.8825$ and $s" = 107.5196$, which are given in Table 3.5, corresponding to $VaR_{\alpha=95\%}$ of delta hedging loss using the Black–Scholes method.

the tail expected loss denoted by $\mathsf{E}^{\mathbb{P}}(L|S_1 \in A)$ where A denotes the sets in the tails specified in Table 3.14, and the variance of tail loss $\mathsf{Var}(L|S_1 \in A)$. We numerically compute the quantities for a 1-month out–of–money European put option with strike price $K = 90$. Assume also $S_0 = 100$ and $r = 0.005$ per month.

The results are given in Table 3.14. Some observations are as follows. Let $\mathbb{P}(L^{\mathbb{Q}} > 0)$ and $\mathsf{E}^{\mathbb{P}}(L^{\mathbb{Q}}|A)$ respectively represent the loss probability and the tail loss expectation under $\mathbb{P}$ measure, using the hedging strategies under the $\mathbb{Q}$ measure. Let $\mathbb{P}(L^M > 0)$ and $\mathsf{E}^{\mathbb{P}}(L^M|A)$ respectively represent the corresponding quantities using the mean-variance hedging strategies. From Table 3.14 we can see that, if $\mathbb{Q}$ represents the NEMM method or the ET-$\mathbb{Q}$ method, then for an out–of–money put option or in–the–money call, conditional on $\rho_0 = 1$ or 2

$$\mathbb{P}(L^{\mathbb{Q}} > 0 \,|\, \rho_0) < \mathbb{P}(L^M > 0 \,|\, \rho_0). \tag{3.3.24}$$

The loss probability in the Black–Scholes method is larger, however, with a much

Identities	Values ($\rho_0 = 1$)	Values ($\rho_0 = 2$)
$a =$	-0.0186	-0.0994
$b =$	1.8872	10.1492
Price$\|\rho_0 =$	0.0284	0.2106
Left-tail $\mathbb{P}(L > 0, S_1 < K\|\rho_0) =$	0.0047	0.0705
Two-tail loss $\mathbb{P}(L > 0\|\rho_0) =$	0.4092	0.3761
BS: $\mathbb{P}(L > 0\|\rho_0) =$	0.414	0.440
NEMM: $\mathbb{P}(L > 0\|\rho_0) =$	0.262	0.311
ET-$\mathbb{Q}$: $\mathbb{P}(L > 0\|\rho_0) =$	0.169	0.307
η_1: test range of $S_1 =$	$(0, \infty)$	$(0, \infty)$
MV method: $\mathsf{E}^{\mathbb{P}}(L\|S_1 \in \eta_1, \rho_0) =$	-1.2E-12	-9.7E-12
$\mathsf{Var}(L\|S_1 \in \eta_1, \rho_0) =$	0.0856	1.3161
η_2: test range of $S_1 =$	$(0, 89.8824] \bigcup [107.5260, \infty)$	$(0, 87.3655] \bigcup [482.7820, \infty)$
MV method: $\mathsf{E}^{\mathbb{P}}(L\|S_1 \in \eta_2, \rho_0) =$	0.4169	3.7069
$\mathsf{Var}(L\|S_1 \in \eta_2, \rho_0) =$	1.4633	4.97558
B–S method: $\mathsf{E}^{\mathbb{P}}(L\|S_1 \in \eta_2, \rho_0) =$	0.3551	5.4062
η_3: test range of $S_1 =$	$(0, 89.9396] \bigcup [107.5231, \infty)$	$(0, 87.3534] \bigcup [133.1109, \infty)$
MV method: $\mathsf{E}^{\mathbb{P}}(L\|S_1 \in \eta_3, \rho_0) =$	0.4156	3.7149
$\mathsf{Var}(L\|S_1 \in \eta_3, \rho_0) =$	1.4595	4.9660
NEMM method: $\mathsf{E}^{\mathbb{P}}(L\|S_1 \in \eta_3, \rho_0) =$	0.3333	4.3827
η_4: test range of $S_1 =$	$(0, 89.8470] \bigcup [107.5157, \infty)$	$(0, 87.3496] \bigcup [130.9600, \infty)$
MV method: $\mathsf{E}^{\mathbb{P}}(L\|S_1 \in \eta_4, \rho_0) =$	0.4159	3.7175
$\mathsf{Var}(L\|S_1 \in \eta_4, \rho_0) =$	1.4579	4.9588
ET-$\mathbb{Q}$ method: $\mathsf{E}^{\mathbb{P}}(L\|S_1 \in \eta_4, \rho_0) =$	0.3305	4.1841

Table 3.14: Comparison of 1-month put hedging results: mean-variance method vs. three risk neutral methods ($S_0 = 100, K = 90$, and $r = 0.005$ per month)

- "Left-tail $\mathbb{P}(L > 0, S_1 < K|\rho_0)$" represents the joint probability of loss occurred and the put option expires in-the-money.
- η_1 is the whole range of S_1; η_2, η_3, η_4 corresponds to the ranges determined in Table 3.5 for the Black–Scholes methods, the NEMM methods, and the ET-$\mathbb{Q}$ methods respectively.

	K	Option Price	$\mathbb{P}(PVHL > 0)$	$\text{CTE}_{95\%}$	σ
BS	90	1.0840	0.3622 (0.0048)	5.5154 (0.1244)	1.9849
NEMM	90	1.008	0.3292 (0.0047)	5.8408 (0.1300)	2.0783
ET-$\mathbb{Q}$	90	1.2449	0.2466 (0.0043)	5.5483 (0.1274)	2.0206
MV	90	1.8447	0.1968 (0.0040)	4.0845 (0.0943)	1.7634
BS	100	3.5983	0.3654 (0.0048)	6.4873 (0.1380)	2.1115
NEMM	100	3.3058	0.3974 (0.0049)	6.9582 (0.1454)	2.2834
ET-$\mathbb{Q}$	100	3.5686	0.3148 (0.0046)	6.1543 (0.1243)	2.1558
MV	100	4.4197	0.2519 (0.0043)	5.4806 (0.0954)	1.8333

note: $\sigma := \sigma(PVHL|PVHL > VaR_{95\%})$

Table 3.15: Option prices and risk measures of hedging loss for hedging 12-month put options, with $S_0 = 100$, based on 10,000 simulations

lower cost. In addition, the expected tail loss has the following relationship:

$$\begin{aligned} \mathsf{E}^{\mathbb{P}}(L^{\mathbb{Q}}|A, \rho_0 = 2) &> \mathsf{E}^{\mathbb{P}}(L^{M}|A, \rho_0 = 2) \\ \mathsf{E}^{\mathbb{P}}(L^{\mathbb{Q}}|A, \rho_0 = 1) &< \mathsf{E}^{\mathbb{P}}(L^{M}|A, \rho_0 = 1), \end{aligned}$$

where $\mathbb{Q}$ represents the three risk-neutral methods. That is, the tail loss expectation under the mean-variance hedging method is smaller when $\rho_0 = 2$, and is larger when $\rho_0 = 1$, i.e., the risk measure $\mathsf{E}^{\mathbb{P}}(L^{\mathbb{Q}}|A)$ is not consistently better or worse under the mean-variance method than under the risk neutral methods. We further discuss the results in section 3.3.3.

Multiperiod Hedging Results

In the simulation study for multiperiod hedging, we analyze the random variable $PVHL$, the present value of cumulative hedging errors defined in (3.1.3). Recall P_t

	K	Option Price	$\mathbb{P}(PVHL > 0)$	$\text{CTE}_{95\%}$	σ
BS	90	1.1944	0.4131 (0.0049)	2.8032 (0.0708)	1.1041
NEMM	90	1.1017	0.4299 (0.0050)	3.0333 (0.0767)	1.1953
ET-$\mathbb{Q}$	90	1.3924	0.2891 (0.0045)	2.4278 (0.0708)	1.1087
MV	90	0.9175	0.1444 (0.0035)	5.6363 (0.2178)	3.3031
BS	100	1.9842	0.4155 (0.0049)	3.4172 (0.0777)	1.2329
NEMM	100	1.8341	0.4406 (0.0050)	3.6800 (0.0812)	1.2994
ET-$\mathbb{Q}$	100	2.2155	0.3039 (0.0046)	3.1622 (0.0836)	1.2497
MV	100	1.4290	0.1703 (0.0038)	8.1193 (0.2344)	3.3032

note: $\sigma := \sigma(PVHL|PVHL > VaR_{95\%})$

Table 3.16: Option prices and risk measures of hedging loss for hedging 120-month put options, with $S_0 = 100$, based on 10,000 simulations

denote the option value, and ζ_t denote the hedging portfolio value at time t. Then,

$$PVHL = \sum_{t=1}^{T} e^{-rt} \left(P_t - \zeta_{t-}\right). \tag{3.3.25}$$

where $\zeta_{t-} = a_{t-1} S_t + B_{t-1} e^r$, with a_{t-1} and B_{t-1} representing the units of stocks and the value of bonds in the rebalanced portfolio at time $t-1$. The values of a_{t-1} and B_{t-1} for hedging a European put option are given in (3.3.18). The simulation for $PVHL$ is similar to the simulation for the risk neutral methods in section 3.2.5.

The multiperiod hedging results are given in Table 3.15 for 12–month put options and in Table 3.16 for 120–month put options. The number of simulations is $10,000$. Further results are given in Figures 3.2–3.4. Based on the results obtained for the multiperiod study, we have the following two observations:

i) In our example, compared with the delta hedging results for a put option, the mean-variance method shifts the effective hedging ranges to the right. As a result, the mean-variance method and the risk neutral methods have different results for hedging the left tail and right tail of loss, and the former one has poorer hedging on the left tail and better hedging on the right tail

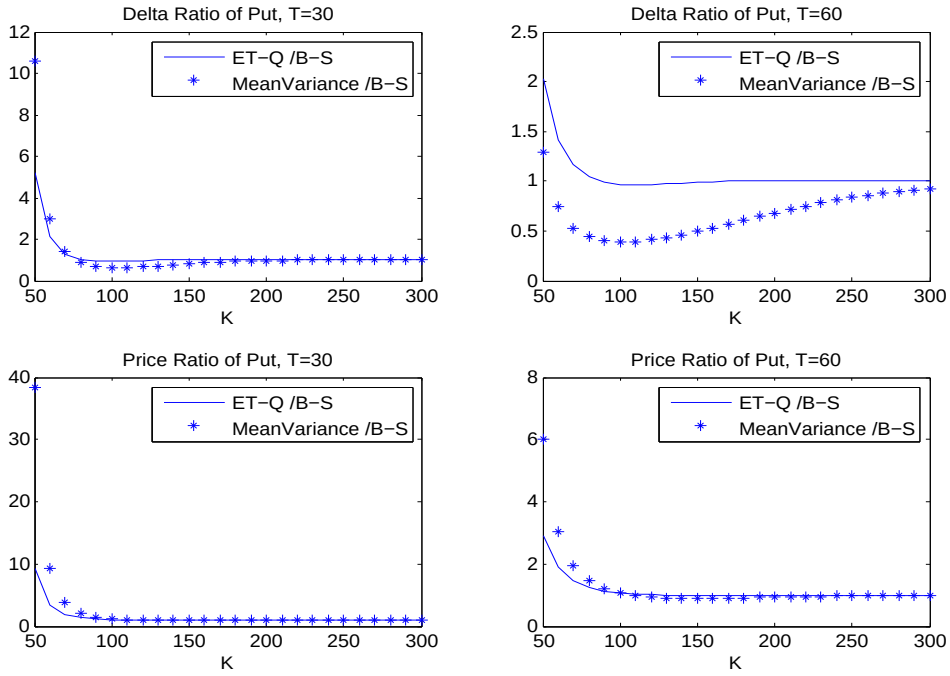

Figure 3.2: Ratios of Delta and Prices. $S_0 = 100$ (The comparison of delta and price between the ET-$\mathbb{Q}$ method and the mean-variance (MV) method, based on the difference of their ratios over the values of the Black-Scholes (B-S) method. The MV method has much smaller delta for options around at-the-money option than the B-S method and the ET-$\mathbb{Q}$ method.)

The points given in (i) can be observed in Figures 3.3 and 3.4. Figure 3.3 displays the values of $PVHL$ from different methods. In the plots, the dashed lines are the hedging errors from the mean-variance method, the solid lines are the hedging errors from the method using the ET-$\mathbb{Q}$. The six figures have different combination of strike prices and the length of maturity, with $K : 90-110$ and maturity $T : 12-24$ months. In five of the six figures, the mean-variance method has the larger loss in the left tail and smaller loss in the right tail, compared with the risk-neutral methods.

The intuition behind the hedging difference described in (i) is the reflection of different hedging targets between the mean variance methods and risk-neutral methods. In our study, the mean-variance method is a quadratic optimization which is to minimize the mean squared hedging errors. As a result, the squared unlimited loss

in the right tail requires more efforts to reduce the loss when the put option expires out-of-money. The hedging can be considered as a zero-sum game. That is, provided that the hedging costs are close and that there are only two assets available in the hedging portfolios, if a hedging strategy hedges more on the right tail, then it is likely to hedge less on the left tail. With this hedging difference, the mean-variance method maybe less useful for hedging put options.

ii) In addition, the overall optimization in the long term hedging effects, in term of $\mathbb{P}(PVHL > 0)$ and $E(PVHL|S_T \in A)$, are quite different from those of the single period, regarding the comparison with the risk-neutral methods. It is more difficult to predict the difference between the mean-variance methods and the risk-neutral methods for the long term hedging. Figure 3.2 displays two graphs about the delta ratios of the mean-variance method and the Black-Scholes method and the delta ratios of the ET-$\mathbb{Q}$ method and the Black-Scholes method. Based on the figure, we can see the delta ratios for the mean variance method and ET-$\mathbb{Q}$ method are not the same over the range of K. Specifically, for hedging a put option, the delta of the mean-variance method, denoted by a^M, is much lower around the center area and gets closer or even higher in the tails than the delta under the risk-neutral method, denoted by $a^{\mathbb{Q}}$. This varying delta ratios makes the comparison complex. In addition, the value of delta implies the volatility of hedging portfolio. This means that using the mean-variance method, hedging will be less volatile for at-the-money options, and more volatile for the out-of-money options, compared with the risk neutral methods. More interesting, based on Table 3.15 for at-the-money options, it appears that the mean-variance method is more attractive to use for short options as it has a higher price and lower loss probability and $\text{CTE}_{95\%}$, while the ET-$\mathbb{Q}$ method for long such options.

Based on Table 3.15 and 3.16, for a 12-month option, the mean-variance method has a higher cost and lower $\text{CTE}_{95\%}$ values, while for a 120-month option, the method has a lower cost and higher $\text{CTE}_{95\%}$ values. This is the evidence that in the long

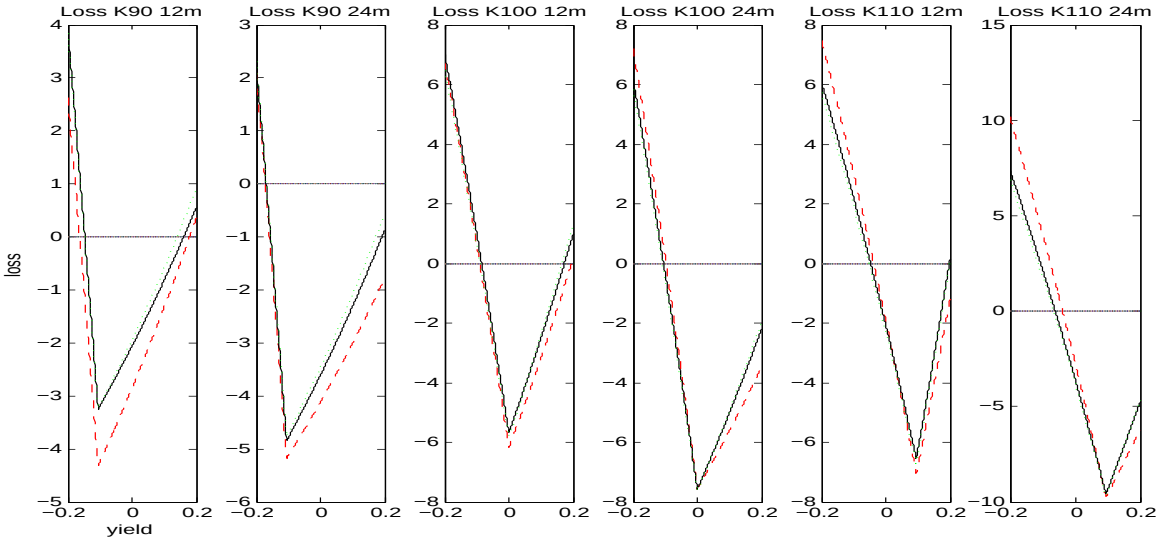

Figure 3.3: Hedging Loss against Log-yield $\log(S_T/S_0)$: ET-$\mathbb{Q}$(–) vs Mean Variance (- -), discussed at page 109.

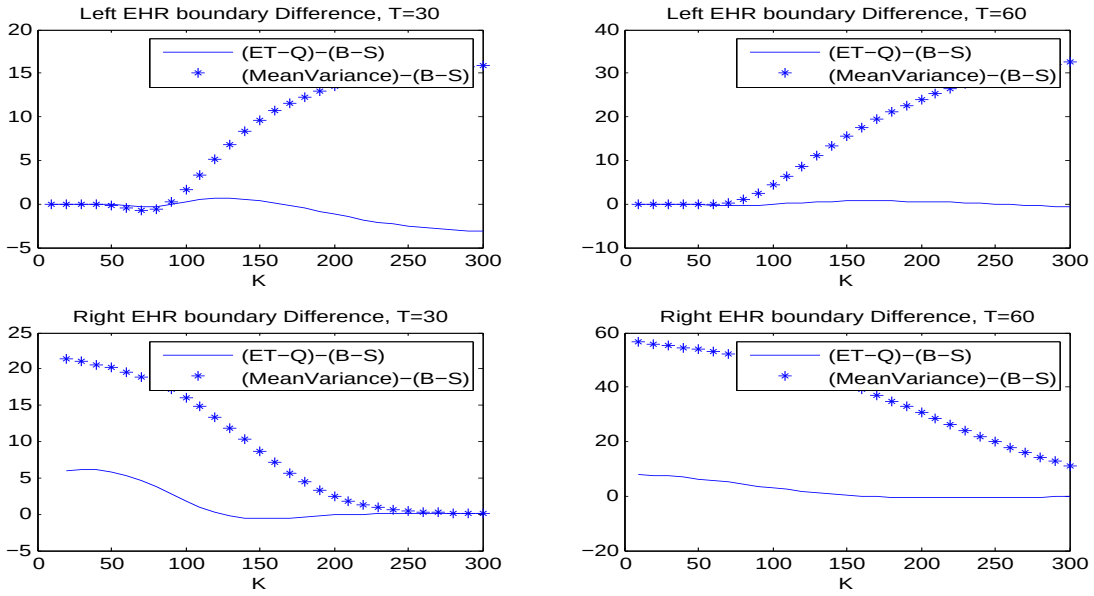

Figure 3.4: Difference of the EHR Boundaries from Hedging: the comparison between ET-$\mathbb{Q}$ method and mean-variance (MV) method, based on difference of their distance over the B-S method ($\left(D^{ET-\mathbb{Q}} - D^{B-S}, U^{ET-\mathbb{Q}} - U^{B-S}\right)$ and $\left(D^{MV} - D^{B-S}, U^{MV} - U^{B-S}\right)$). MV methods has boundaries on the right sides of ET-$\mathbb{Q}$ methods (or B-S methods), discussed at page 109.

run, it is not easy to be predict the hedging difference between the mean-variance method and the risk neutral methods, due to the varying of delta ratios $a^M/a^{\mathbb{Q}}$.

From the comparison of hedging efficiency, the ET-$\mathbb{Q}$ method appears to lie between the Black–Scholes method and the mean-variance method, and much closer to the former one. It may be a more suitable approach for hedging out–of–money put options among the four pricing methods (MV, Black–Scholes, NEMM, ET-$\mathbb{Q}$).

3.3.3 Discussion of Effective Hedging Ranges

As stated in section 3.3.2, we observe from Table 3.14, regarding the loss L for the out-of-money put options, conditional on ρ_0, that

$$\mathbb{P}(L^{\mathbb{Q}} > 0 \,|\, \rho_0) < \mathbb{P}(L^M > 0 \,|\, \rho_0)$$

for $\mathbb{Q}$ representing the NEMM or ET-$\mathbb{Q}$ measures. Moreover, we observe that $\mathsf{E}^{\mathbb{P}}(L^M|A, \rho_0 = 2) < \mathsf{E}^{\mathbb{P}}(L^{\mathbb{Q}}|A, \rho_0 = 2)$ and $\mathsf{E}^{\mathbb{P}}(L^M|A, \rho_0 = 1) > \mathsf{E}^{\mathbb{P}}(L^{\mathbb{Q}}|A, \rho_0 = 1)$ for a tail A specified in Table 3.14. In this section, we discuss these results based on the structure of the hedging portfolio under the regime switching models, for a single period $[0, T]$.

To proceed, we first show the put-call parity of the hedging strategy under the mean-variance methods in the following Proposition 3.3.2. The parity also brings some convenient properties for studying hedging errors. For example, with put call parity, the hedging errors are the same for hedging call and put options, conditional on the same strike price and the same maturity. Let $Z = \log(S_T/S_0)$. Then, in the mean-variance method (see Föllmer and Schied, 2004), for European put and call options, the delta of the hedging portfolio are

$$a_0^{put} = \frac{\mathsf{Cov}([K - S_0\, e^Z]^+, S_0\, e^Z)}{\mathsf{Var}(S_0\, e^Z)}; \quad a_0^{call} = \frac{\mathsf{Cov}([S_0\, e^Z - K]^+, S_0\, e^Z)}{\mathsf{Var}(S_0\, e^Z)}. \tag{3.3.26}$$

The bond values, denoted by B_0^{call}, B_0^{put} for hedging call and put options, are given

by

$$\begin{cases} B_0^{put} &= e^{-rT}[\,\mathsf{E}^{\mathbb{P}}([K - S_0\, e^Z]^+) - a_0^{put}\, S_0 \mathsf{E}^{\mathbb{P}}(e^Z)\,] \\ B_0^{call} &= e^{-rT}[\,\mathsf{E}^{\mathbb{P}}([S_0\, e^Z - K]^+) - a_0^{call}\, S_0 \mathsf{E}^{\mathbb{P}}(e^Z)\,]. \end{cases} \tag{3.3.27}$$

Let ζ^c and ζ^p represent the hedging cost of call and put options. Then,

$$\zeta^c = a_0^{call} S_0 + B_0^{call}, \quad \text{and} \quad \zeta^p = a_0^{put} S_0 + B_0^{put}$$

Proposition 3.3.2. *(**CQ**) For hedging European call and put options, the mean-variance hedging costs ζ^c and ζ^p satisfy the put-call parity, i.e., $\zeta^c - \zeta^p = S_0 - e^{-rT}\, K$.*

Proof. The proof is trivial if we note that $a_0^{call} - a_0^{put} = 1$ and $B_0^{put} - B_0^{call} = e^{-rT}\, K$. □

Here, we discuss the effective hedging ranges defined on S_T for two different hedging approaches. We first carry out the discussion based on two assumed strategies. Then, we extend our discussion on the hedging strategies from the mean-variance method and the risk-neutral method under the RSLN2 models. Let P_c^i, a_i^c and B_i^c represent the hedging portfolio price, delta and bond values for hedging a call option under strategy $i, i = 1, 2$. Similarly, P_p^i, a_i^p and B_i^p can be defined for hedging a put option under strategy i. We further assume the hedging strategies consist of only bonds and stocks, and the following two conditions:

(a) Hedging portfolio prices satisfy put-call parity $P_c^i - P_p^i = S_0 - Ke^{-rT}$.

(b) $\dfrac{P_c^2}{P_c^1} \le \dfrac{a_2^c}{a_1^c}$ and $\dfrac{P_p^2}{P_p^1} \ge \dfrac{a_2^p}{a_1^p}$. This means that, based on the same price, in the hedging portfolios for hedging a call option, strategy two has more units of stock than strategy one; and, for hedging a put option, strategy two short less stock.

Then, based on condition (a), we have that the effective hedging ranges $[D_i, U_i], i = 1, 2$ are the same for hedging call and put options under strategy i. With $0 < a_i^c < 1$,

D_i can be obtained by solving $L_L(S_T) = 0$. That is, from

$$L_L(S_T) = (K - \hat{S}_T) - (a_i^P \hat{S}_T + B_i^p e^{rT}) = 0,$$

we have

$$D_i = (K - B_i^p e^{rT})/(1 + a_i^P).$$

From put-call parity for hedging cost, we have

$$D_i = -B_i^c e^{rT}/a_i^c. \tag{3.3.28}$$

Similarly, by solving right tail loss $L_U = 0$ for hedging call options, we have

$$U_i = -B_i^p e^{rT}/a_i^p.$$

With D_i and U_i obtained and the assumptions (a)-(b) in the above, we have the following result.

Proposition 3.3.3. *(**CQ**) Assume $[D_i, U_i], i = 1, 2$ are the effective hedging ranges of S_T for two hedging strategies with conditions (a) and (b) satisfied. Then, we have*

$$D_1 \leq D_2, \quad \text{and} \quad U_1 \leq U_2.$$

Proof. Before computing the difference $D_2 - D_1$ and $U_2 - U_1$, we establish an inequality as follows. Condition (b) implies that $\dfrac{a_2^c S_t + B_2^c}{a_1^c S_t + B_1^c} \leq \dfrac{a_2^c}{a_1^c}$, which in turn means $\dfrac{B_1^c}{a_1^c} \geq \dfrac{B_2^c}{a_2^c}$. Thus, using (3.3.28), we obtain

$$D_2 - D_1 = \frac{-B_2^c e^{rT}}{a_2^c} - \frac{-B_1^c e^{rT}}{a_1^c} = \left(\frac{B_1^c}{a_1^c} - \frac{B_2^c}{a_2^c}\right) e^{rT} \geq 0.$$

Similarly, based on $P_p^2/P_p^1 \geq a_2^p/a_1^p$, we can obtain $U_1 \leq U_2$. □

Remark 3.3.1. Since the condition (b) is not easy to use, in practice, we can use an alternative but more strict condition as follows:

(b') $1 > a_2^c > a_1^c > 0$, and $P_c^2 = P_c^1$

where $P_c^2 = P_c^1$ can be replaced by $P_c^2 \approx P_c^1$ in practice, which means the option prices obtained from method one and two are very close to each other. Based on (b'), we can make judgement by comparing option prices and deltas, individually. Indeed, if the condition $1 > a_2^c > a_1^c > 0$ in (b') is satisfied, from put–call parity, we have $a_2^p > a_1^p$, and vice versa. It is worth noting that a^c is positive and a^p is negative. Thus, if $a_2^c/a_1^c > 1$, then $a_2^p/a_1^c < 1$. In addition, $P_c^2 \approx P_c^1$ implies $P_p^2 \approx P_p^1$. As a result, the condition (b) is satisfied if condition (b') is satisfied. The application of (b') is indeed the case we will illustrate in the following case study.

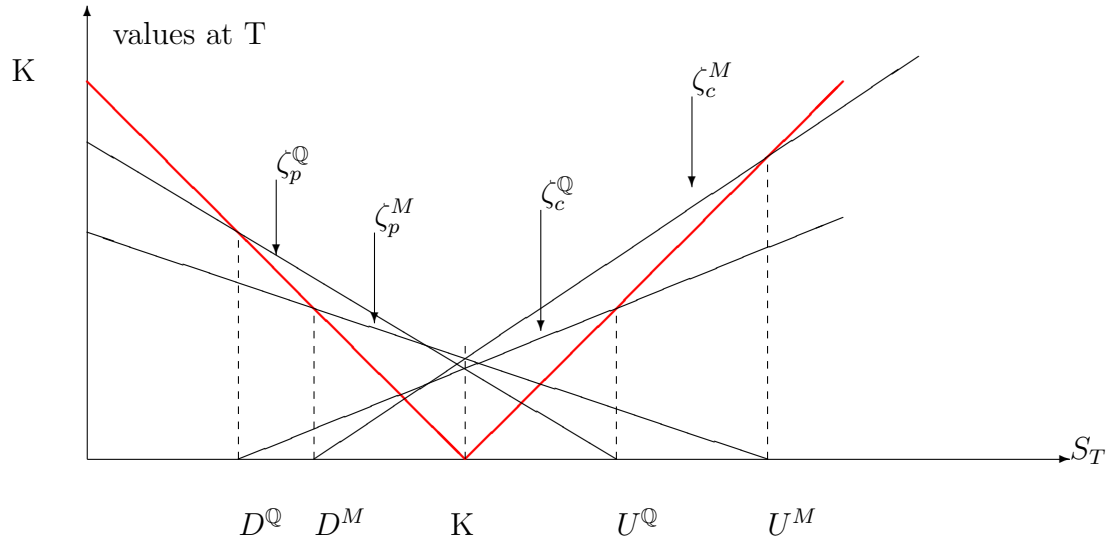

Figure 3.5: Effective hedging ranges of delta hedging call and put options

ζ^M represents the maturity value of the hedging portfolio under the mean-variance method, while $\zeta^{\mathbb{Q}}$ represents the value under the ET-$\mathbb{Q}$ method.

We compare mean-variance methods and the ET-$\mathbb{Q}$ ($\mathbb{Q}$) methods, with (a^M, D^M, U^M) representing the delta and the effective hedging range boundaries in the former method and $(a^{\mathbb{Q}}, D^{\mathbb{Q}}, U^{\mathbb{Q}})$ representing the corresponding quantities in the latter method. Some observations from numerical results are as follows.

a) In Figure 3.2, we observe two curves of delta ratios over the Black-Scholes methods for the two approaches. Let a^B represent the delta of the Black-Scholes methods. For options in a wide range of strike prices, the delta ratio for the ET-$\mathbb{Q}$ method is larger than the ratio for the mean-variance method. That is, $a^{\mathbb{Q}}/a^B > a^M/a^B$. Since a delta for a put option is negative ($a^M, a^{\mathbb{Q}}, a^B < 0$), we have, for a put option,

$$a^M > a^{\mathbb{Q}}.$$

What is more, in the figure, the prices are much closer between these two methods. From remark 3.3.1, conditions (a) and (b') are satisfied. Therefore, from Proposition 3.3.3, we have

$$D^{\mathbb{Q}} \leq D^M, \qquad U^{\mathbb{Q}} \leq U^M.$$

That is, compared with the risk-neutral methods described in Chapter 1, the mean-variance method shifts the boundaries of effective hedging ranges $[D, U]$ to the right, which may not be desirable for hedging put options. Figure 3.4 verifies the results, with the difference $D^M - D^{\mathbb{Q}}$ given in the top two figures and $U^M - U^{\mathbb{Q}}$ given in the bottom two figures.

b) The difference of $[D, U]$ between these two approaches can be used to determine the probability relationship between $\mathbb{P}(L^{\mathbb{Q}} > 0 \,|\, \rho_0)$ and $\mathbb{P}(L^M > 0 \,|\, \rho_0)$, if additional information is given. For example, for the out–of–money put options,

   i) if the physical distribution is skewed to the right so that the range of $(D^M, D^{\mathbb{Q}})$ is close to the central area, where the density function $f(Z)$ is higher, and $(U^M, U^{\mathbb{Q}})$ is far in the right tail, where the density function $f(Z)$ is much smaller, as illustrated in Figure 3.3; and

   ii) if the length of the interval $(D^M, D^{\mathbb{Q}})$ is not too small compared with the length of $(U^M, U^{\mathbb{Q}})$, as illustrated in Figure 3.4 for many K.

   then we could have $\mathbb{P}(L^{\mathbb{Q}} > 0 \,|\, \rho_0) < \mathbb{P}(L^M > 0 \,|\, \rho_0)$.

c) The difference of $[D, U]$ also affects risk measures such as the CTE of loss. Figure 3.3 gives some example of loss L for different methods. The dashed lines represent the loss from the mean-variance method, which is significantly different from the risk-neutral methods. Since the loss in the right tail is significantly less under the mean-variance method, it is reasonable to expect that the tail loss can be lower than the risk-neutral methods under the thick right tail distributions given $\rho_0 = 2$, i.e.,

$$\mathsf{E}^{\mathbb{P}}(L^M|A, \rho_0 = 2) < \mathsf{E}^{\mathbb{P}}(L^{\mathbb{Q}}|A, \rho_0 = 2)$$

for tail event A. While under $\rho_0 = 1$, the order is opposite as the left side loss plays a more important role.

3.4 Conclusion

In this chapter we conducted a simulation study for hedging the out–of–money European put and some call options. We proposed and compared effective hedging ranges under single period hedging setting, and connected them with other risk measures. We also conducted the simulation study for hedging loss in multiple periods, based on risk measures such as the loss probability and $\text{CTE}_{95\%}$. From the study, we can see that the ET-$\mathbb{Q}$ method provides a reasonable cost and more efficient hedging for put options under regime switching models, compared with the Black–Scholes method and the NEMM method.

In addition, we see that the mean-variance method can be less favorable for hedging put options, besides that the measure generated by the mean-variance method is not an equivalent martingale measure and the resulting option prices are not arbitrage free. Based on their different hedging costs and effective hedging ranges, it is of interest to balance these two methods for hedging. In the next chapter, we will extend the analysis to more general models with the different choice of risk neutral measures.

Chapter 4

On Single Period Discrete Time Delta Hedging Errors and Option Prices Analysis Using Tail Ordering

It is well-known that the market is incomplete under regime switching models, due to the uncertainty of regimes. Incompleteness of the market means that there is an infinite number of risk neutral probability measures, and each of them may lead to a different price and different hedging results for a contingent claim. As shown in previous chapters, the difference of hedging performance from two or more risk neutral measures are complicated in comparison. In this chapter, we apply the tool of stochastic ordering to conduct some comparison, and our comparison is focused on discrete time delta hedging errors over one period $(t, T]$ and the resulting option prices.

Stochastic ordering has been widely used to compare two distributions; see, for example, Shaked and Shanthikumar (2007). It has also been widely used in risk theory and management; see, for example, Hadar and Russell (1969), Bawa (1975), Denuit et al. (2005), Kaas et al. (2008), and Höse and Huschens (2011). Some

interesting statistical inference using stochastic order can be found in Ahmad (2001), Ng, et al. (2011) and other references therein. In this chapter, we will propose a new concept of tail ordering to serve our comparison purposes.

This chapter is organized as follows. In section 4.1, we review the strict stochastic ordering and define tail ordering for a random variable under different risk neutral measures. In section 4.2, we recall the effective hedging ranges and discuss relationships between tail ordering and discrete time delta hedging for European call and put options. In section 4.3, we apply tail ordering to study the results of option pricing under different probability measures and its implication on volatility smiles. Finally, this chapter is completed with some applications to models using the discrete time regime switching processes.

4.1 Tail Ordering

We first discuss a property associated with strict stochastic ordering, which implies the limitation of its application on comparing risk neutral measures. This motivates tail ordering as we define in subsection 4.1.2 below.

4.1.1 Strict Stochastic Ordering

Suppose all random variables and probability measures are defined on the same measurable space $(\Omega, \mathcal{F})$ throughout this chapter. In terms of probability measures, the usual strict stochastic ordering is defined through a selected random variable, say Z. Recall that, in definition 1.2.5, a random variable Z is stochastically larger under $\mathbb{Q}_2$ than under $\mathbb{Q}_1$, denoted $\mathbb{Q}_2 \geq_{st} \mathbb{Q}_1$, if

$$\mathbb{Q}_2(Z > a) \geq \mathbb{Q}_1(Z > a), \quad \forall\ a \in \mathbb{R}; \tag{4.1.1}$$

and Z is strictly larger under $\mathbb{Q}_2$ than under $\mathbb{Q}_1$, denoted by $\mathbb{Q}_2 >_{st} \mathbb{Q}_1$, if inequality (4.1.1) holds strictly for some $a \in \mathbb{R}$.

Based on the definition, we have following results regarding the order of $\mathsf{E}^{\mathbb{Q}_1}(Z)$ and $\mathsf{E}^{\mathbb{Q}_2}(Z)$, where $\mathsf{E}^{\mathbb{Q}_i}(Z)$ represent the expectation of Z under $\mathbb{Q}_i$, assuming strict stochastic ordering.

Lemma 4.1.1. *(***Modified from Proposition 9.1.1 Ross, 1996***) If* $\mathbb{Q}_2 >_{st} \mathbb{Q}_1$ *for a random variable* Z*, then* $\mathsf{E}^{\mathbb{Q}_2}(Z) > \mathsf{E}^{\mathbb{Q}_1}(Z)$*.*

Proof. The assumption $\mathbb{Q}_2 >_{st} \mathbb{Q}_1$ implies that

$$\mathbb{Q}_2(Z > z) \geq \mathbb{Q}_1(Z > z), \quad \forall z \in \mathbb{R}$$

and

$$\mathbb{Q}_2(Z > z_0) > \mathbb{Q}_1(Z > z_0), \quad \text{for some } z_o \in \mathbb{R}.$$

Due to the left continuous property of survival function, given $\epsilon > 0$ small enough we must have

$$\mathbb{Q}_2(Z > z) - \mathbb{Q}_1(Z > z) > \epsilon$$

for all $z \in (z_0 - \delta, z_0)$ and some constant $\delta > 0$. Hence

$$\int_{z_0-\delta}^{z_0} [\, \mathbb{Q}_2(Z > z) - \mathbb{Q}_1(Z > z) \,]\, dz > \epsilon\delta > 0. \tag{4.1.2}$$

Noticing that

$$\begin{aligned} \mathsf{E}^{\mathbb{Q}}(Z) &= \int_0^\infty \mathbb{Q}(Z > z)\, dz - \int_{-\infty}^0 \mathbb{Q}(Z \leq z)\, dz \\ &= \int_0^\infty \mathbb{Q}(Z > z)\, dz + \int_{-\infty}^0 [\, \mathbb{Q}(Z > z) - 1]\, dz, \end{aligned}$$

(4.1.2) implies

$$\begin{aligned}
& \mathsf{E}^{\mathbb{Q}_2}(Z) - \mathsf{E}^{\mathbb{Q}_1}(Z) \\
= & \int_{-\infty}^{\infty} [\, \mathbb{Q}_2(Z > z) - \mathbb{Q}_1(Z > z) \,]\, dz \\
= & \int_{-\infty}^{z_0-\delta} [\, \mathbb{Q}_2(Z > z) - \mathbb{Q}_1(Z > z) \,]\, dz + \int_{z_0-\delta}^{z_0} [\, \mathbb{Q}_2(Z > z) - \mathbb{Q}_1(Z > z) \,]\, dz \\
& + \int_{z_0}^{\infty} [\, \mathbb{Q}_2(Z > z) - \mathbb{Q}_1(Z > z) \,]\, dz \\
> & \ 0,
\end{aligned}$$

by which the proof is complete. □

Lemma 4.1.2. *(***Modified from Proposition 9.1.2 Ross, 1996***) For a random variable Z, $\mathbb{Q}_2 >_{st} \mathbb{Q}_1$ if and only if $\mathsf{E}^{\mathbb{Q}_2}[\, g(Z) \,] > \mathsf{E}^{\mathbb{Q}_1}[\, g(Z) \,]$ for any strictly increasing function g defined on the support of Z.*

Proof. Suppose that $\mathbb{Q}_2 >_{st} \mathbb{Q}_1$ for the random variable Z and $g(z)$ is a strictly increasing function of z. We show that $\mathsf{E}^{\mathbb{Q}_2}[\, g(Z) \,] > \mathsf{E}^{\mathbb{Q}_1}[\, g(Z) \,]$. Actually, for any number $a \in \mathbb{R}$,

$$\mathbb{Q}_2(g(Z) > a) = \mathbb{Q}_2(Z > g^{-1}(a)) \geq \mathbb{Q}_1(Z > g^{-1}(a)) = \mathbb{Q}_1(g(Z) > a)$$

for all $a \in \mathbb{R}$, and

$$\mathbb{Q}_2(g(Z) > a_0) = \mathbb{Q}_2(Z > g^{-1}(a_0)) > \mathbb{Q}_1(Z > g^{-1}(a_0)) = \mathbb{Q}_1(g(Z) > a_0)$$

for some $a_0 \in \mathbb{R}$. The above implies that $\mathbb{Q}_2 >_{st} \mathbb{Q}_1$ for the random variable $g(Z)$, which, by Lemma 4.1.1, yields $\mathsf{E}^{\mathbb{Q}_2}[g(Z)] > \mathsf{E}^{\mathbb{Q}_1}[g(Z)]$.

Next, suppose for any strictly increasing function g, $\mathsf{E}^{\mathbb{Q}_2}[g(Z)] > \mathsf{E}^{\mathbb{Q}_1}[g(Z)]$. We show that $\mathbb{Q}_2 >_{st} \mathbb{Q}_1$ for Z. Based on the fact that the strictly increasing function $\tan^{-1}(a) \in (-\pi/2, \pi/2)$ for any $a \in \mathbb{R}$, we construct the following sequence of strictly

increasing functions:

$$g_n(z) = \begin{cases} 1 + (\tan^{-1} z)/n & \text{if } z \geq a \\ (\tan^{-1} z)/n & \text{if } z < a, \end{cases} \tag{4.1.3}$$

for $n = 1, 2, \ldots$ Let $g(z) := \lim_{n\to\infty} g_n(z)$. Then,

$$g(z) = \begin{cases} 1, & \text{if } z \geq a, \\ 0, & \text{if } z < a. \end{cases} \tag{4.1.4}$$

Hence, $\mathsf{E}^{\mathbb{Q}_i}[g(Z)] = \mathbb{Q}_i(Z > a)$ and $\mathsf{E}^{\mathbb{Q}_i}[g(Z)] = \lim_{n\to\infty} \mathsf{E}^{\mathbb{Q}_i}[g_n(Z)]$ for $i = 1, 2$, according to the Dominated Convergence Theorem. Since $g_n(z)$ is strictly increasing, the assumption implies $\mathsf{E}^{\mathbb{Q}_2}[g_n(Z)] > \mathsf{E}^{\mathbb{Q}_1}[g_n(Z)]$ for $n = 1, 2, \ldots$. $\mathsf{E}^{\mathbb{Q}_i}[g_n(z)]$ is also bounded. Consequently, since

$$\mathsf{E}^{\mathbb{Q}_2}[g(Z)] = \lim_{n\to\infty} \mathsf{E}^{\mathbb{Q}_2}[g_n(Z)] \geq \lim_{n\to\infty} \mathsf{E}^{\mathbb{Q}_1}[g_n(Z)] = \mathsf{E}^{\mathbb{Q}_2}[g(Z)]$$

we have $\mathbb{Q}_2(Z > a) \geq \mathbb{Q}_1(Z > a)$ for all $a \in \mathbb{R}$. Moreover, there must exist some $a_0 \in \mathbb{R}$ such that $\mathbb{Q}_2(Z > a_0) > \mathbb{Q}_1(Z > a_0)$. Otherwise, we have $\mathsf{E}^{\mathbb{Q}_2}[g_n(Z)] = \mathsf{E}^{\mathbb{Q}_1}[g_n(Z)]$ for any $n = 1, 2, \ldots$, which contradict to the assumption. Thus, the proof is complete. □

4.1.2 Tail Ordering Under Risk Neutral Measures

Strict stochastic ordering is a partial ordering and hence it is not necessarily applicable to a general pair of probability distributions. In particular, as indicated by the following proposition, it is not applicable when it comes to compare a pair of risk neutral distributions. By risk neutral distribution, we mean the distribution of the log return $Z = \log(S_T/S_t)$ of the underlying asst price under a risk neutral probability measure.

Proposition 4.1.1. *(**CQ**) For the underlying asset price log return random variable Z, a risk neutral distribution can not be strictly stochastically larger than any other risk neutral distribution.*

Proof. Let $\mathbb{Q}_1$ and $\mathbb{Q}_2$ be two risk neutral probability measures associated with Z, the asset-price log return. Assume $\mathbb{Q}_2$ is strictly stochastically larger than $\mathbb{Q}_1$. Then, Lemma 4.1.2 implies

$$\mathsf{E}^{\mathbb{Q}_2}[\, g(Z)\,] > \mathsf{E}^{\mathbb{Q}_1}[\, g(Z)\,] \tag{4.1.5}$$

must hold for any strictly increasing function g. By the definition of equivalent martingale probability measure, the discounted asset price process $(e^{-rt}S_t)_{t=0}^{T}$ is a martingale under either $\mathbb{Q}_1$ or $\mathbb{Q}_2$. This implies that

$$e^{-r(T-t)}\mathsf{E}_t^{\mathbb{Q}_1}[e^Z] = e^{-r(T-t)}\mathsf{E}_t^{\mathbb{Q}_2}[e^Z] = 1,$$

which clearly contradicts to (4.1.5), and hence the proof is complete. □

Remark 4.1.1. A similar result, given in Proposition 3.3.17 of Denuit et al. (2005) can be restated as follows, for a random variable X, if $\mathbb{Q}_1 \leq_{st} \mathbb{Q}_2$ and $\mathsf{E}^{\mathbb{Q}_1}(X) = \mathsf{E}^{\mathbb{Q}_2}(X)$ then $\mathbb{Q}_1 = \mathbb{Q}_2$. Here, we use strict stochastic ordering instead of usual stochastic ordering for comparison purpose.

As a substitute, we can define the so-called tail ordering to compare tail behaviors of two equivalent martingale measures. The definition can be made separately for left and right tails as below.

Definition 4.1.1. (**CQ**) Consider a random variable Z and two probability measures $\mathbb{Q}_1$ and $\mathbb{Q}_2$.

(a) Right Tail Ordering: $\mathbb{Q}_2$ is said to be stochastically larger than (or dominates) $\mathbb{Q}_1$ for the random variable Z on the right tail at a point $k \in \mathbb{R}$, denoted by $\mathbb{Q}_2 >_{RTO} \mathbb{Q}_1$ at k, if and only if both the following two conditions are satisfied:

$$\begin{aligned} &\mathbb{Q}_2(Z > a) \geq \mathbb{Q}_1(Z > a) \quad \forall\, a \geq k, \\ &\mathbb{Q}_2(Z > a_0) > \mathbb{Q}_1(Z > a_0) \quad \text{for some } a_0 \geq k. \end{aligned}$$

(b) Left Tail Ordering: $\mathbb{Q}_2$ is said to be stochastically larger than (or dominates) $\mathbb{Q}_1$ on the left tail at a point $k \in \mathbb{R}$, denoted by $\mathbb{Q}_2 >_{LTO} \mathbb{Q}_1$ at k, if and only

if both the following two conditions are satisfied:

$$\begin{aligned}&\mathbb{Q}_2(Z \le a) \ge \mathbb{Q}_1(Z \le a), \quad \forall\, a \le k,\\ &\mathbb{Q}_2(Z \le a_0) > \mathbb{Q}_1(Z \le a_0) \quad \text{for some } a_0 \le k.\end{aligned}$$

Remark 4.1.2. The introduction of "$>_{RTO}$" and "$>_{LTO}$" is to apply stochastic ordering. Assume Z is a random variable. Let Y denote the left censored Z, i.e., $Y = \max(k, Z)$. Then, Y follows a mixed distribution:

$$\mathbb{Q}_i(Y \le a) = \begin{cases} 0 & \text{if } a < k \\ \mathbb{Q}_i(Z \le k) & \text{if } a = k \\ \mathbb{Q}_i(Z \le k) + \int_k^a f^{\mathbb{Q}_i}(z)\, dz & \text{if } a > k \end{cases}.$$

According to the definition of strictly stochastic larger, $\mathbb{Q}_2 >_{st} \mathbb{Q}_1$ for Y if and only if

$$\begin{aligned}&\mathbb{Q}_2(Y > a) \ge \mathbb{Q}_1(Y > a) \quad \forall\, a \in \mathbb{R},\\ &\mathbb{Q}_2(Y > a_0) > \mathbb{Q}_1(Y > a_0) \quad \text{for some } a_0 \in \mathbb{R}.\end{aligned}$$

Thus, $\mathbb{Q}_2 >_{RTO} \mathbb{Q}_1$ at k for Z is equivalent to that $\mathbb{Q}_2 >_{st} \mathbb{Q}_1$ for Y. Similarly, we often need to consider a random variable $X = \min(k, Z)$. Then,

$$\mathbb{Q}_i(X \le a) = \begin{cases} \mathbb{Q}_i(Z \le a) & \text{if } a < k \\ 1 & \text{if } a \ge k \end{cases}.$$

Recall that $\mathbb{Q}_1 >_{st} \mathbb{Q}_2$ for X if and only if

$$\begin{aligned}&\mathbb{Q}_1(X \le a) \le \mathbb{Q}_2(X \le a) \quad \forall\, a \in \mathbb{R},\\ &\mathbb{Q}_1(X \le a_0) < \mathbb{Q}_2(X \le a_0) \quad \text{for some } a_0 \in \mathbb{R}.\end{aligned}$$

Thus, $\mathbb{Q}_2 >_{LTO} \mathbb{Q}_1$ at k for Z is equivalent to that $\mathbb{Q}_1 >_{st} \mathbb{Q}_2$ for X.

Remark 4.1.3. Tail ordering is similar to the thicker-tailed relationship defined in Definition 7.3.1 in Kaas et al. (2008), which can be restated as follows: $\mathbb{Q}_2$ is thicker-

tailed than $\mathbb{Q}_1$ for a random variable X, if $\mathsf{E}^{\mathbb{Q}_2}(X) = \mathsf{E}^{\mathbb{Q}_1}(X)$, and that a x_0 exists such that $\mathbb{Q}_1(X \leq x) \leq \mathbb{Q}_2(Y \leq x)$ for $x < x_0$ and $\mathbb{Q}_1(X \leq x) \geq \mathbb{Q}_2(Y \leq x)$ for $x > x_0$. Our definition is a modified strict version of the thicker-tailed relationship, without the requirement of the existence of the unique x_0.

4.2 Tail Ordering and Option Hedging

In this section, we apply the tool of tail ordering to compare the hedging of European call and put options under different risk neutral measures in a single period discrete time framework, using discrete time delta hedging strategies. The comparison is based on the EHRs obtained from different pricing measures, which is of great interest for hedging studies as discussed in Chapter 3. In the remaining content of this section, we first discuss the existence of the effective hedging ranges in section 4.2.1. Then, analysis on call and put options is respectively presented in subsections 4.2.2 and 4.2.3.

4.2.1 Existence of Effective Hedging Ranges

The effective hedging range (EHR) is defined as follows. Assume a single period starting at t and ending at T. Let S_T denote the price of the underlying risky asset at maturity, and $L(S_T)$ denote hedging loss for hedging a European option. Then, similar to Definition 3.1.1, we define the interval $[D, U]$ to be the effective hedging range of $L(S_T)$ over S_T, if $L(S_T) \leq 0$ if and only if $S_T \in [D, U]$. In this definition, we define the EHR over S_T instead of Y_T, since it is more convenient to compute the EHRs over the range of S_T.

Before comparison, we first show the existence of the EHRs for hedging European call and put options under a risk neutral measure $\mathbb{Q}_i$, using the single period discrete time delta hedging strategy. Let $k = \log K/S_t$, where K is the strike price in the options; let r denote the risk free rate. Then, the call price evaluated under $\mathbb{Q}_i$,

denoted by $P_c^{\mathbb{Q}_i}$, is

$$P_c^{\mathbb{Q}_i} = e^{-r\,(T-t)}\,\mathsf{E}_t^{\mathbb{Q}_i}\left[(S_T-K)^+\right] = S_t\Delta_i^c - e^{-r\,(T-t)}\,K\left[\,1-F^{\mathbb{Q}_i}(k)\,\right], \quad (4.2.6)$$

where

$$\Delta_i^c = e^{-r\,(T-t)}\int_k^\infty e^z\,f^{\mathbb{Q}_i}(z)\,dz \quad (4.2.7)$$

represents the delta value under $\mathbb{Q}_i$, $f^{\mathbb{Q}_i}(z)$ denotes the density of $Z = \log S_T/S_t$ under $\mathbb{Q}_i$, and $F^{\mathbb{Q}_i}(z)$ represents the corresponding distribution function. Equation (4.2.6) also displays the delta hedging portfolio, denoted by $\zeta^c(t)$, in which the number of stocks held is Δ_i^c and the bond value shorted (or owed at time t) at rate r is $e^{-r\,(T-t)}\,K[\,1-F^{\mathbb{Q}_i}(k)\,]$. Similarly, let $P_p^{\mathbb{Q}_i}, i=1,2$ denote the put option price under $\mathbb{Q}_i$. Then

$$P_p^{\mathbb{Q}_i} = e^{-r\,(T-t)}\,\mathsf{E}_t^{\mathbb{Q}_i}[(K-S_T)^+] = e^{-r\,(T-t)}\,K\,F^{\mathbb{Q}_i}(k) + S_t\Delta_i^p, \quad (4.2.8)$$

where

$$\Delta_i^p = -e^{-r\,(T-t)}\int_{-\infty}^k e^z\,f^{\mathbb{Q}_i}(z)\,dz. \quad (4.2.9)$$

Equation (4.2.8) also displays the delta hedging portfolio for the put option, denoted by $\zeta^p(t)$, and Δ_i^p represents the units of stock short in the portfolio.

A discrete time hedge assumes the hedging portfolio unchanged during the hedging interval (t,T). As a result, the hedging loss at time T is

$$L(S_T) := P_T - (\Delta_t\,S_T + B_t\,e^{r(T-t)}), \quad (4.2.10)$$

where Δ_t and $B_t \in \mathbb{R}$ are the delta and bond value associated the portfolio at time t, and P_T represents the option value at maturity. A positive value of $L(S_T)$ represents a loss for the option writer. To show the existence of EHRs, we recall the U–shaped relationship defined in Definition 3.2.1 as follows. $T(x):\mathbb{R}\to\mathbb{R}$ is U–shaped against x, if $T(x)$ is a continuous function of x and is strictly (or continuously) increasing

in x for $x \in (a, \infty)$ and strictly decreasing in x for $x \in (-\infty, a)$. As a result, there exists a constant a satisfying $a = \arg\min_{x \in \mathbb{R}} T(x)$.

We can see that there exists an EHR, if the following three conditions are satisfied: first, $L(S_T)$ is U–shaped against S_T; second, $\min_{S_T} L(S_T) < 0$; and third, $L(S_T) > 0$ as $S_T \to 0$ and as $S_T \to \infty$. To proceed, we have the following lemma.

Remark 4.2.1. Consider the delta values Δ_i^c and Δ_i^p defined respectively in (4.2.7) and (4.2.9). We have

$$-1 < \Delta_i^p < 0 < \Delta_i^c < 1. \tag{4.2.11}$$

This is trivial, due to the risk neutral equation $S_t = e^{-r\,(T-t)} \mathsf{E}^{\mathbb{Q}_i}(S_T)$. Since

$$1 = e^{-r\,(T-t)} \int_{-\infty}^{+\infty} e^z \, f^{\mathbb{Q}_i}(z)\, dz, \tag{4.2.12}$$

the term $e^{-r\,(T-t)}\, e^z \, f^{\mathbb{Q}_i}(z)$ is an appropriate density function. Thus,

$$0 < \Delta_i^c = \int_k^{+\infty} e^{-r\,(T-t)}\, e^z \, f^{\mathbb{Q}_i}(z)\, dz < 1.$$

Similarly, combining equation (4.2.9) and (4.2.12), we obtain $-1 < \Delta_i^p < 0$.

We now establish the existence of EHRs for delta hedging European call and put options.

Lemma 4.2.1. *(**CQ**) For the hedging loss defined in equation (4.2.10), we have the following results:*

(a). $L(S_T)$ is U-shaped against S_T, and $K = \arg\min_{S_T} L(S_T)$;

(b). $L(S_T) > 0$, as $S_T \to 0$ or $S_T \to \infty$ for $S_T > 0$;

(c). $L(S_T) < 0$ at $S_T = K$.

Proof. (a). Consider the delta hedge of a European call option,

$$L(S_T) \;\; = \;\; (S_T - K)^+ - (\Delta_t^c \, S_T + B_t^c \, e^{r(T-t)}),$$

where Δ_t^c is given in (4.2.7), and $B_t^c = -e^{-r\,(T-t)}\,K\,[\,1 - F^{\mathbb{Q}_i}(k)]$. We have

$$L(S_T) \;=\; \begin{cases} (1-\Delta_t^c)\,S_T + C, & \text{if } S_T \geq K. \\ -\Delta_t^c\,S_T + C', & \text{if } S_T < K. \end{cases} \tag{4.2.13}$$

where C and C' are constants. Based on Remark 4.2.1, it is clear that $L(S_T)$ increases linearly in S_T for $S_T \geq K$, and $L(S_T)$ decreases linearly in S_T if $S_T < K$. In addition, since $L(S_T)$ is continuous at S_T, $L(S_T)$ takes the minimum at $S_T = K$. Thus, $L(S_T)$ is U-shaped against S_T. The result can be proved in the similar way for the hedging loss for a European put option.

(b). For call options, from equation (4.2.13),

$$\lim_{S_T \to 0} L(S_T) = e^{-r\,(T-t)}\,K[\,1 - F^{\mathbb{Q}_i}(k)\,] > 0$$

For put options, we can obtain

$$\lim_{S_T \to 0} L(S_T) = e^{-r\,(T-t)}\,K\,F^{\mathbb{Q}_i}(k) > 0.$$

The results for $S_T \to \infty$ can be obtained in a similar way for both call and put options.

(c). To show $L(S_T) < 0$ at $S_T = K$ is equivalent to showing that

$$L(S_T) = \begin{cases} -\left(\Delta_i^c - \left[\,1 - F^{\mathbb{Q}_i}(k)\right]\right) < 0, & \text{for call options,} \\ -\left(F^{\mathbb{Q}_i}(k) + \Delta_i^p\right) < 0 & \text{for put options.} \end{cases} \tag{4.2.14}$$

We show that it is satisfied for call options. If $k \geq r(T-t)$, then $e^{-r\,(T-t)}e^z > 1$ for $z > k$. Thus,

$$\Delta_i^c = \int_k^{+\infty} e^{-r\,(T-t)}\,e^z\,f^{\mathbb{Q}_i}(z)\,dz \;\;>\;\; \int_k^{+\infty} f^{\mathbb{Q}_i}(z)\,dz = 1 - F^{\mathbb{Q}_i}(k).$$

If $k < r(T-1)$, then $e^{-r\,(T-t)}e^{z} < 1$ for $z < k$. Thus,

$$\Delta_i^c = 1 - e^{-r\,(T-t)} \int_{-\infty}^{k} e^{z}\, f^{\mathbb{Q}_i}(z)\, dz > 1 - F^{\mathbb{Q}_i}(k).$$

That is, we have $-\left(\Delta_i^c - \left[1 - F^{\mathbb{Q}_i}(k)\right]\right) < 0$ at $S_T = K$ for call options. Similarly, we can obtain $-\left(F^{\mathbb{Q}_i}(k) + \Delta_i^p\right) < 0$ at $S_T = K$ for put options, and the proof is complete. □

Lemma 4.2.1 implies the existence of effective hedging ranges for both call and put options as summarized in the following proposition.

Proposition 4.2.1. *(**CQ**) For delta hedging European call and put options, the effective hedging range over S_T exists for hedging loss $L(S_T)$ defined in (4.2.10).*

4.2.2 Right Tail Ordering and One-period Discrete Time Delta Hedging for European Call Options

This subsection compares EHRs resulting from conducting discrete time delta hedging for a European call option under two pricing measures $\mathbb{Q}_1$ and $\mathbb{Q}_2$ over the single period $[t, T]$, through applying right tail ordering. Consider a call option with maturity at T. Assume $\mathbb{Q}_2 >_{RTO} \mathbb{Q}_1$ for $Z = \log(S_T/S_t)$ at the strike yield $k = \log K/S_t$, with $t < T$.

Proposition 4.2.2. *(**CQ**) Assume $\mathbb{Q}_1$ and $\mathbb{Q}_2$ are two risk neutral probability measures satisfying $\mathbb{Q}_2 >_{RTO} \mathbb{Q}_1$ for Z at $k = \log K/S_t$. Let Δ_i^c, defined in (4.2.7), denote the delta of a call option price at a strike price K under $\mathbb{Q}_i$ for $i = 1, 2$. Then, $\Delta_2^c > \Delta_1^c$.*

Proof. Let $Y = \max(k, Z)$ and $\xi(y) = e^{-r(T-t)}\, e^{y}$. Then, by (4.2.7)

$$\begin{aligned}
\Delta_i^c &= \int_k^{+\infty} \xi(z)\, f^{\mathbb{Q}_i}(z)\, dz \\
&= \int_k^{+\infty} \xi(z)\, f^{\mathbb{Q}_i}(z)\, dz + \xi(k)\mathbb{Q}_i(Z \leq k) - \xi(k)\mathbb{Q}_i(Z \leq k) \\
&= \mathsf{E}^{\mathbb{Q}_i}[\xi(Y)] - \xi(k)\mathbb{Q}_i(Z \leq k) \qquad (4.2.15)
\end{aligned}$$

Since $\mathbb{Q}_2 >_{RTO} Q_1$ for Z at k is equivalent to $\mathbb{Q}_2 >_{st} \mathbb{Q}_1$ for Y by Remark 4.1.2, from Lemma 4.1.2 and the strictly increasing property of $\xi(y)$ as a function of y, we have

$$\mathsf{E}^{\mathbb{Q}_2}[\xi(Y)] > \mathsf{E}^{\mathbb{Q}_1}[\xi(Y)] \qquad (4.2.16)$$

Moreover, $\mathbb{Q}_2 >_{st} \mathbb{Q}_1$ for Y implies

$$\mathbb{Q}_2(Z \leq k) = \mathbb{Q}_2(Y \leq k) \leq \mathbb{Q}_1(Y \leq k) = \mathbb{Q}_1(Z \leq k) \qquad (4.2.17)$$

Therefore, combining (4.2.15), (4.2.16) and (4.2.17) we obtain

$$\begin{aligned}
\Delta_2^c &= \mathsf{E}^{\mathbb{Q}_2}[\xi(Y)] - \xi(k)\mathbb{Q}_2(Z \leq k) \\
&> \mathsf{E}^{\mathbb{Q}_1}[\xi(Y)] - \xi(k)\mathbb{Q}_1(Z \leq k) = \Delta_1^c
\end{aligned}$$

□

Next, based on the above results, we study EHRs under $\mathbb{Q}_1$ and $\mathbb{Q}_2$. Recall the call price in (4.2.6) and the corresponding discrete time delta hedging strategies. At maturity T, there are two cash flows. The first one is the option payoff and the second one is the maturity value of the hedging portfolio. Let l_0 label the payoff $V_0(S_T)$, and l_i label the functions of the maturity values $V_i(S_T)$ of the hedging portfolios constructed based on $\mathbb{Q}_i$ for $i = 1, 2$. Then,

$$\begin{aligned}
l_0 : V_0(S_T) &= (S_T - K)^+, \\
l_1 : V_1(S_T) &= \Delta_1^c\, S_T - K\,[1 - F^{\mathbb{Q}_1}(k)], \qquad (4.2.18) \\
l_2 : V_2(S_T) &= \Delta_2^c\, S_T - K\,[1 - F^{\mathbb{Q}_2}(k)].
\end{aligned}$$

We can see that $V_i(S_T)$ is a linear function of S_T for $i = 1, 2$, and a piecewise linear function for $i = 0$. Based on these maturity values, we can compute effective hedging ranges $[D^{\mathbb{Q}_i}, U^{\mathbb{Q}_i}]$ for two hedging strategies under $\mathbb{Q}_1$ and $\mathbb{Q}_2$ respectively. According to Proposition 4.2.1, the EHR over S_T exists for the single period discrete time delta hedging of European call options. With $i = 1, 2$, we compute $D^{\mathbb{Q}_i}$ through solving $l_i = 0$ for S_T, i.e., at $D^{\mathbb{Q}_i}$ the portfolio has zero value at $S_T = D^{\mathbb{Q}_i}$; and $U^{\mathbb{Q}_i}$ is the value of S_T to solve $l_0 = l_i$ conditional on $S_T > K$, i.e. at $U^{\mathbb{Q}_i}$ the portfolio value is the same as the call payoff. As a result, we have

$$\left[D^{\mathbb{Q}_i} = K\frac{1 - F^{\mathbb{Q}_i}(k)}{\Delta_i^c}, \qquad U^{\mathbb{Q}_i} = K\frac{F^{\mathbb{Q}_i}(k)}{1 - \Delta_i^c} \right] \tag{4.2.19}$$

The relative positions of two EHRs are among 9 scenarios, based on the combination of three possible relationship $\{D^{\mathbb{Q}_2} < D^{\mathbb{Q}_1}, D^{\mathbb{Q}_2} = D^{\mathbb{Q}_1}, D^{\mathbb{Q}_2} > D^{\mathbb{Q}_1}\}$, with $D^{\mathbb{Q}_2} \lessgtr D^{\mathbb{Q}_1}$ denoting the set consists of all three cases, and other three relationship $\{U^{\mathbb{Q}_2} < U^{\mathbb{Q}_1}, U^{\mathbb{Q}_2} = U^{\mathbb{Q}_1}, U^{\mathbb{Q}_2} > U^{\mathbb{Q}_1}\}$, with $U^{\mathbb{Q}_2} \lessgtr U^{\mathbb{Q}_1}$ similarly defined. As a result of tail ordering, we can see that the relative positions of EHRs for two portfolios are among five of the nine scenarios, as stated in the following proposition.

Proposition 4.2.3. *(CQ) Assume $\mathbb{Q}_1$ and $\mathbb{Q}_2$ are two risk neutral probability measures satisfying $\mathbb{Q}_2 >_{RTO} \mathbb{Q}_1$ for Z at $k = \log K/S_t$. Then, the relative positions of the EHRs under $\mathbb{Q}_1$ and $\mathbb{Q}_2$ can only be among the following five scenarios.*

(i) $D^{\mathbb{Q}_2} < D^{\mathbb{Q}_1}$ *and* $U^{\mathbb{Q}_2} > U^{\mathbb{Q}_1}$,

(ii) $D^{\mathbb{Q}_2} = D^{\mathbb{Q}_1}$ *and* $U^{\mathbb{Q}_2} > U^{\mathbb{Q}_1}$,

(iii) $D^{\mathbb{Q}_2} > D^{\mathbb{Q}_1}$ *and* $U^{\mathbb{Q}_2} < U^{\mathbb{Q}_1}$,

(iv) $D^{\mathbb{Q}_2} > D^{\mathbb{Q}_1}$ *and* $U^{\mathbb{Q}_2} = U^{\mathbb{Q}_1}$,

(v) $D^{\mathbb{Q}_2} > D^{\mathbb{Q}_1}$ *and* $U^{\mathbb{Q}_2} > U^{\mathbb{Q}_1}$.

Proof. Recall the existence of EHRs is given in proposition 4.2.1. To show that the relative positions of EHRs $[D^{\mathbb{Q}_1}, U^{\mathbb{Q}_1}]$ and $[D^{\mathbb{Q}_2}, D^{\mathbb{Q}_2}]$ are among the five scenarios, it is sufficient to have the following two conditions satisfied.

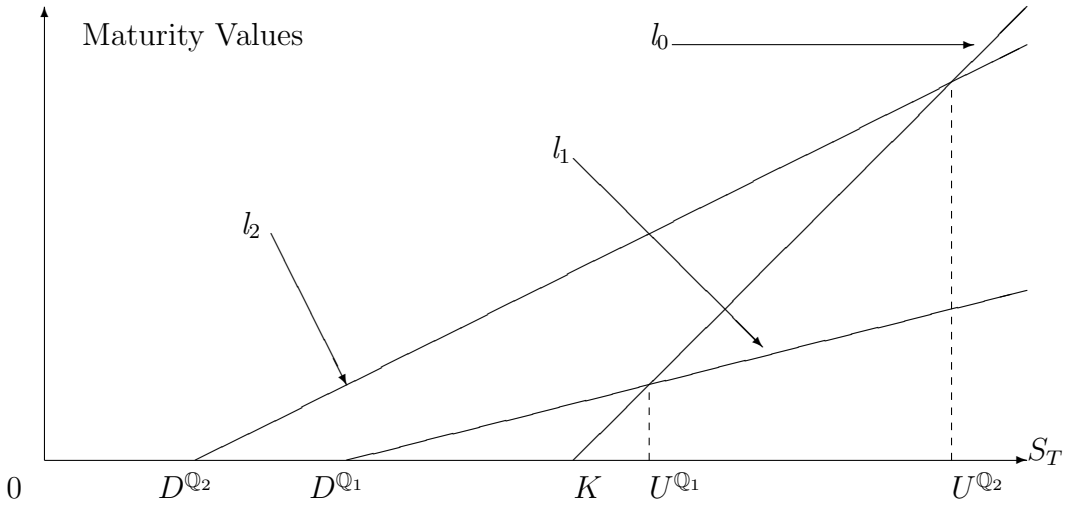

Figure 4.1: Lines of call payoffs and portfolio values, scenario one

Figure 4.1 to 4.5 illustrate relationships between call payoffs and maturity values of two hedging portfolios constructed using $\mathbb{Q}_1$ and $\mathbb{Q}_2$. l_0: call option payoff; $l_i, i = 1, 2$: maturity values of the portfolios; $[D^{\mathbb{Q}_i}, U^{\mathbb{Q}_i}], i = 1, 2$: EHRs, where the portfolio values are greater than option payoffs.

The first is that $0 < D^{\mathbb{Q}_i} < K$ for $i = 1, 2$, which is obvious. Based on the conditions for the existence of the EHR given in Lemma 4.2.1, $L(0) > 0$ and $L(K) < 0$ for $L(S_T)$ defined in (4.2.10). $D^{\mathbb{Q}_i}$ is obtained by letting $L(S_T) = 0$, so there exists $0 < D^{\mathbb{Q}_i} < K$. The second condition is that $0 < \Delta_1^c < \Delta_2^c < 1$, which is satisfied as given in Remark 4.2.1. □

The five scenarios stated in Proposition 4.2.3 are demonstrated in figures 4.1 to 4.5. Figure 4.1 demonstrates $D^{\mathbb{Q}_2} < D^{\mathbb{Q}_1}$ and $U^{\mathbb{Q}_2} > U^{\mathbb{Q}_1}$. That is, hedging with the portfolio constructed using $\mathbb{Q}_2$ is less likely to have a loss as S_T changes and the call option expires in and out of the money. Figure 4.2 demonstrates $D^{\mathbb{Q}_2} = D^{\mathbb{Q}_1}$ and $U^{\mathbb{Q}_2} > U^{\mathbb{Q}_1}$. So the left side hedging are the same for portfolios of $\mathbb{Q}_2$ and $\mathbb{Q}_1$. The portfolio of $\mathbb{Q}_2$, however, has a better hedging positions when S_T goes up. Figure 4.3 to 4.5 demonstrate the three other scenarios associated with $D^{\mathbb{Q}_2} > D^{\mathbb{Q}_1}$. Similar conclusion can be drawn from there.

Remark 4.2.2. Let $Y = \max\{k, Z\}$. We further classify the distributions of Y under $\mathbb{Q}_1$ and $\mathbb{Q}_2$ measures into four types, as demonstrated in Figure 4.6, based on the movement of the ratio of densities $f^{\mathbb{Q}_2}(y)/f^{\mathbb{Q}_1}(y)$ as $y \to \infty$ in the right wing of

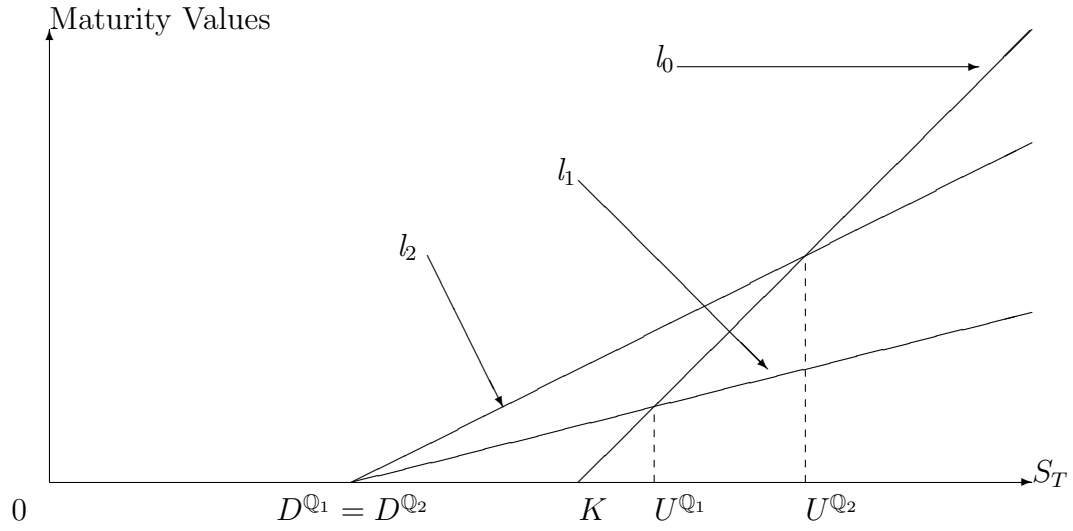

Figure 4.2: Lines of call payoffs and portfolio values, scenario two

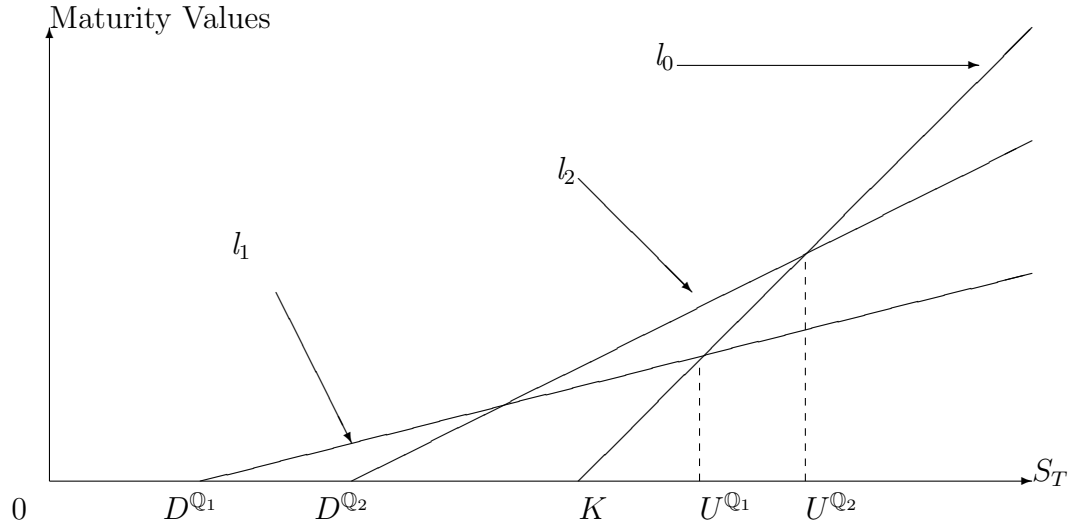

Figure 4.3: Lines of call payoffs and portfolio values, scenario three

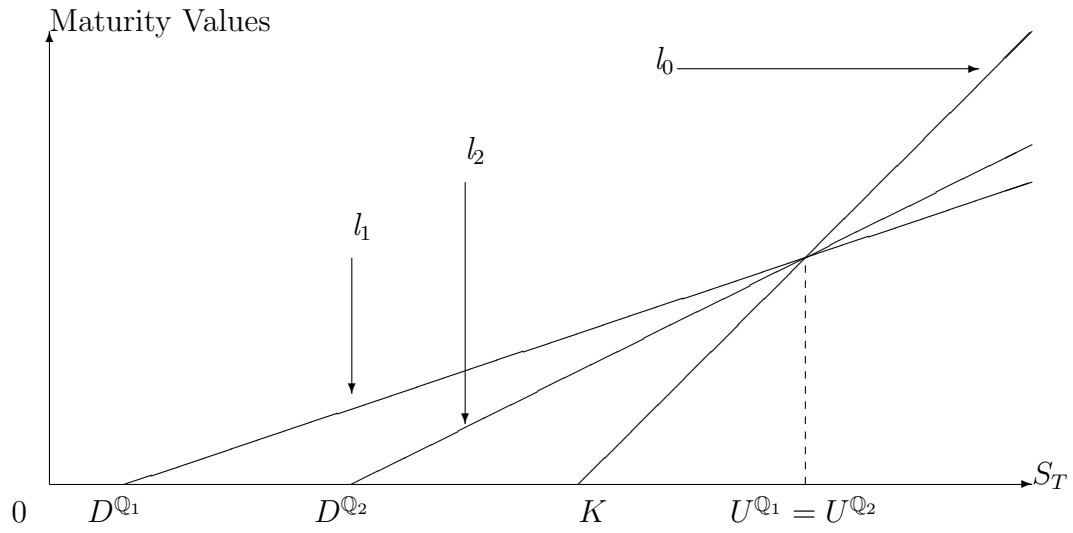

Figure 4.4: Lines of call payoffs and portfolio values, scenario four

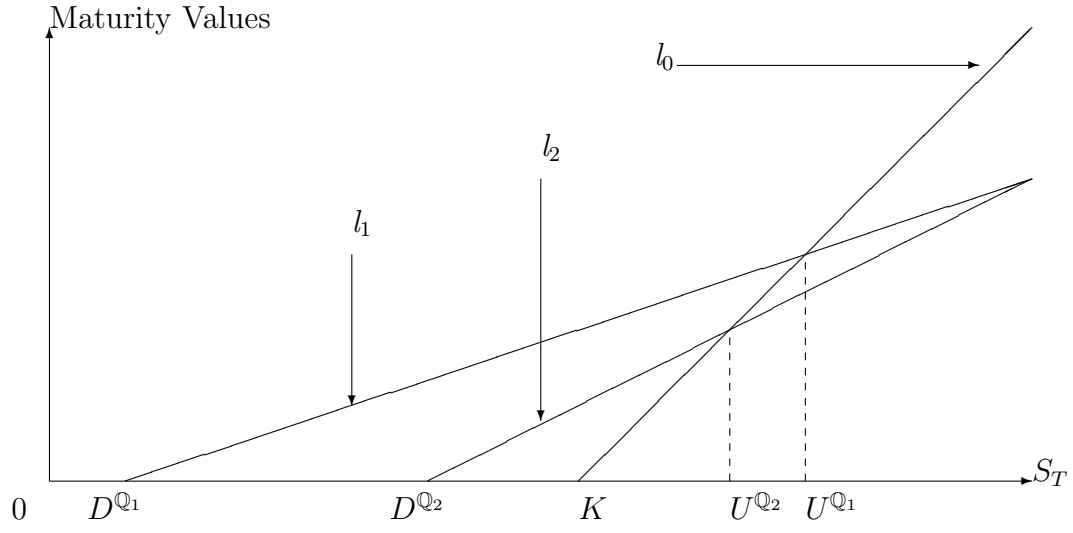

Figure 4.5: Lines of call payoffs and portfolio values, scenario five

the distributions. These four types are defined respectively as follows:

(a) $f^{\mathbb{Q}_2}(y)/f^{\mathbb{Q}_1}(y)$ is decreasing in y, with $f^{\mathbb{Q}_2}(y)/f^{\mathbb{Q}_1}(y) > 1$ for $y > k$;

(b) $f^{\mathbb{Q}_2}(y)/f^{\mathbb{Q}_1}(y) = c$ for $c > 1$ and $y > k$;

(c) $f^{\mathbb{Q}_2}(y)/f^{\mathbb{Q}_1}(y)$ is increasing for $y > k$, and $f^{\mathbb{Q}_2}(y)/f^{\mathbb{Q}_1}(y) > 1$ for $y > k'$ with a $k' > k$;

(d) $f^{\mathbb{Q}_2}(y)/f^{\mathbb{Q}_1}(y)$ has other shapes in the tail. An example is given in graph four, where $f^{\mathbb{Q}_2}(y)/f^{\mathbb{Q}_1}(y)$ fluctuates and becomes greater than one after certain point on the right tail.

In the remaining studies, we will focus on the first three cases (a)-(c) defined in the above.

Proposition 4.2.4. *(**CQ**) Assume two risk neutral measures $\mathbb{Q}_2$ and $\mathbb{Q}_1$ associated with $Z = \log(S_T/S_t)$. Let $D^{\mathbb{Q}_i}$ and $U^{\mathbb{Q}_i}$ denote the EHRs boundaries defined in (4.2.19). Then we have the results summarized in Table 4.1.*

$Y = \max(Z, k)$	$D^{\mathbb{Q}_1}$ vs. $D^{\mathbb{Q}_2}$	$U^{\mathbb{Q}_1}$ vs. $U^{\mathbb{Q}_2}$ ($\mathbb{Q}_2 >_{RTO} \mathbb{Q}_1$* at k)
$\frac{f^{\mathbb{Q}_2}(y)}{f^{\mathbb{Q}_1}(y)}$ is strictly increasing in y	$D^{\mathbb{Q}_2} < D^{\mathbb{Q}_1}$	$U^{\mathbb{Q}_2} > U^{\mathbb{Q}_1}$
$\frac{f^{\mathbb{Q}_2}(y)}{f^{\mathbb{Q}_1}(y)}$ is a constant	$D^{\mathbb{Q}_2} = D^{\mathbb{Q}_1}$	$U^{\mathbb{Q}_2} > U^{\mathbb{Q}_1}$
$\frac{f^{\mathbb{Q}_2}(y)}{f^{\mathbb{Q}_1}(y)}$ is strictly decreasing in y	$D^{\mathbb{Q}_2} > D^{\mathbb{Q}_1}$	$U^{\mathbb{Q}_2} \lessgtr U^{\mathbb{Q}_1}$

Table 4.1: (Proposition4.2.4) EHR positions based on the movement of density ratios

* That is, the condition requires that $\mathbb{Q}_2 >_{RTO} \mathbb{Q}_1$ for $Z = \log(S_T/S_t)$ at $k = \log K/S_t$.

Proof. To determine the relative positions of EHRs, we consider the EHR given in (4.2.19) and focus on the comparison of $D^{\mathbb{Q}_i} = K\,[1 - F^{\mathbb{Q}_1}(k)\,]/\Delta_1^c$. Because

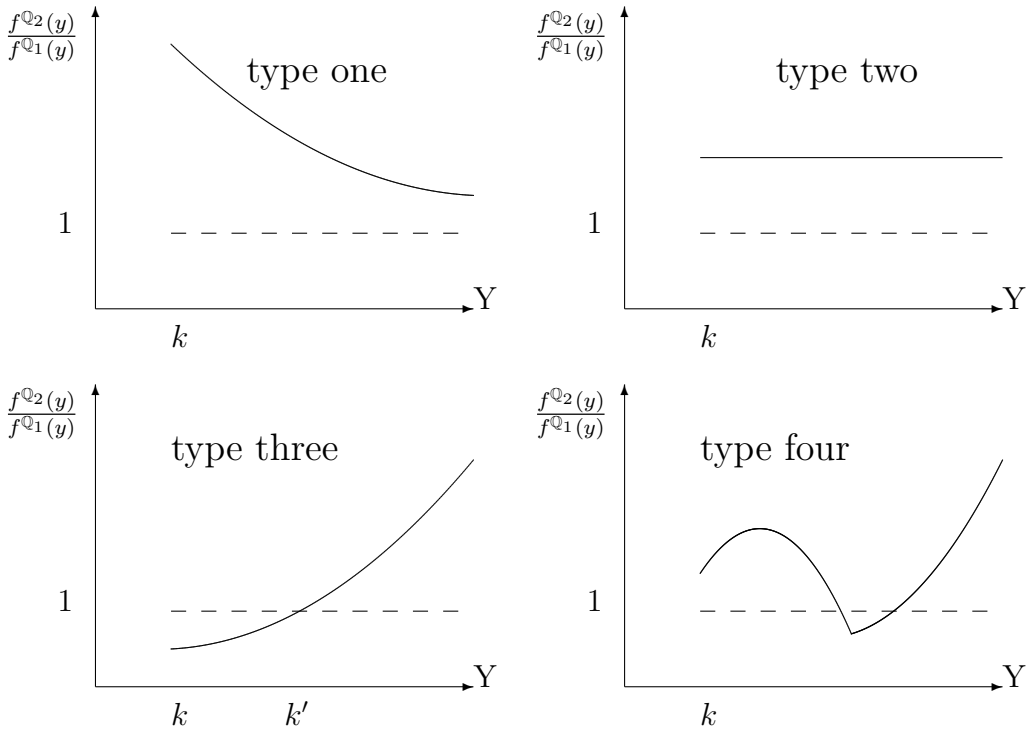

Figure 4.6: Four types of movements of $f^{\mathbb{Q}_2}(y)/f^{\mathbb{Q}_1}(y)$ on the right tail

$1 > \Delta_2^c > \Delta_1^c > 0$ under the assumption $\mathbb{Q}_2 >_{st} \mathbb{Q}_1$, if the relative positions of $D^{\mathbb{Q}_i}$ are given, then the relative positions of $U^{\mathbb{Q}_i}$ can be determined.

(i). If the ratio $f^{\mathbb{Q}_2}(y)/f^{\mathbb{Q}_1}(y)$ is a constant in y, then assume $f^{\mathbb{Q}_2}(y) = C\, f^{\mathbb{Q}_1}(y)$ for all $y > k$ with a positive constant C. Then,

$$\begin{aligned}
\frac{1 - F^{\mathbb{Q}_2}(k)}{\Delta_2^c} &= \frac{\int_k^{+\infty} f^{\mathbb{Q}_2}(y)\, dy}{e^{-r\,(T-t)} \int_k^{+\infty} e^y\, f^{\mathbb{Q}_2}(y)\, dy} \\
&= \frac{\int_k^{+\infty} C\, f^{\mathbb{Q}_1}(y)\, dy}{e^{-r\,(T-t)} \int_k^{+\infty} e^y\, C\, f^{\mathbb{Q}_1}(y)\, dy} \\
&= \frac{1 - F^{\mathbb{Q}_1}(k)}{\Delta_1^c}.
\end{aligned}$$

That is, (4.2.19) implies $D^{\mathbb{Q}_1} = D^{\mathbb{Q}_2}$.

(ii). Assume $f^{\mathbb{Q}_2}(y) = g(y)\, f^{\mathbb{Q}_1}(y)$ for all $y > k$ with some strictly increasing function $g(y)$. We construct two density functions:

$$p_1(y) = \frac{f^{\mathbb{Q}_1}(y)}{\int_k^{+\infty} f^{\mathbb{Q}_1}(y)\, dy} \quad p_2(y) = \frac{f^{\mathbb{Q}_1}(y)\, e^y}{\int_k^{+\infty} f^{\mathbb{Q}_1}(y)\, e^y\, dy}.$$

Note that $p_2(y)/p_1(y) = e^y\, C$, where $C = \int_k^{+\infty} f^{\mathbb{Q}_1}(y)\, dy / \int_k^{+\infty} f^{\mathbb{Q}_1}(y)\, e^y\, dy > 0$ is a constant. Thus, the ratio $p_2(y)/p_1(y)$ is strictly increasing in y. From Lemma 1.2.4, Y is strictly stochastically larger under probability measure with density p_2 than with density p_1. As a result, since $g(y)$ is strictly increasing in y, from Lemma 4.1.2, we have

$$\int_k^{+\infty} g(y) \frac{f^{\mathbb{Q}_1}(y)}{\int_k^{+\infty} f^{\mathbb{Q}_1}(y)\, dy}\, dy < \int_k^{+\infty} g(y) \frac{f^{\mathbb{Q}_1}(y)\, e^y}{\int_k^{+\infty} f^{\mathbb{Q}_1}(y)\, e^y\, dy}\, dy. \tag{4.2.20}$$

That is,

$$\frac{\int_k^{+\infty} f^{\mathbb{Q}_2}(y)\, dy}{\int_k^{+\infty} f^{\mathbb{Q}_2}(y)\, e^y\, dy} < \frac{\int_k^{+\infty} f^{\mathbb{Q}_1}(y)\, dy}{\int_k^{+\infty} f^{\mathbb{Q}_1}(y)\, e^y\, dy},$$

or

$$\frac{1 - F^{\mathbb{Q}_2}(k)}{\Delta_2^c} < \frac{1 - F^{\mathbb{Q}_1}(k)}{\Delta_1^c}$$

From (4.2.19), we have $D^{\mathbb{Q}_2} < D^{\mathbb{Q}_1}$.

(iii). Similarly, if $f^{\mathbb{Q}_2}(y)/f^{\mathbb{Q}_1}(y)$ is strictly decreasing in y, we have $D^{\mathbb{Q}_2} > D^{\mathbb{Q}_1}$. The proof is similar to that of (ii) by assuming $f^{\mathbb{Q}_1}(y) = g(y)\, f^{\mathbb{Q}_2}(y)$ for some strictly increasing function $g(y)$. Then, exchange the notation $f^{\mathbb{Q}_1}(y)$ with $f^{\mathbb{Q}_2}(y)$ in equation (4.2.20) to obtain the result. □

Remark 4.2.3. Under assumption that $\mathbb{Q}_2 >_{st} \mathbb{Q}_1$ for Y at k, i.e. $\mathbb{Q}_2 >_{RTO} \mathbb{Q}_1$ for

Z at k

$$1 - F^{\mathbb{Q}_1}(k) \leq 1 - F^{\mathbb{Q}_2}(k). \tag{4.2.21}$$

Also note that the amount of $e^{-r(T-t)}K[1 - F^{\mathbb{Q}_i}(k)]$ for the bond is shorted in the hedging portfolio. Thus, (4.2.21) implies that the bond shorted under $\mathbb{Q}_1$ is less than or equal to the bond shorted under $\mathbb{Q}_2$.

4.2.3 Left Tail Ordering and Hedging Put Options

Similar to the previous subsection, this subsection compares the EHRs for delta hedging a European put option over single period $[t, T]$, by applying left tail ordering. Consider an option at time t and assume it is written on S_t with the strike price K and the expiry date $T > t$. Assume $\mathbb{Q}_2 >_{LTO} \mathbb{Q}_1$ for $Z = \log(S_T/S_t)$ at $k = \log K/S_t$. Recall the put option prices $P_p^{\mathbb{Q}_i}, i = 1, 2$ in (4.2.8).

Proposition 4.2.5. *(**CQ**) Assume $\mathbb{Q}_1$ and $\mathbb{Q}_2$ are two risk neutral probability measures satisfying $\mathbb{Q}_2 >_{LTO} \mathbb{Q}_1$ for Z at $k = \log K/S_t$. Let Δ_i^p, defined in (4.2.9), denote the delta of a put option price at a strike price K under $\mathbb{Q}_i$ for $i = 1, 2$. Then, $\Delta_2^p < \Delta_1^p$, or equivalently $|\Delta_2^p| < |\Delta_1^p|$.*

Proof. Let $X = \min(k, Z)$ and $\xi(y) = e^{-r(T-t)e^y}$. By (4.2.9)

$$\begin{aligned}
\Delta_i^p &= -\int_{-\infty}^{k} \xi(z) f^{\mathbb{Q}_i}(z) dz \\
&= -\int_{-\infty}^{k} \xi(z) f^{\mathbb{Q}_i}(z) dz - \xi(k)\mathbb{Q}_i(Z > k) + \xi(k)\mathbb{Q}_i(Z > k) \\
&= -\mathsf{E}^{\mathbb{Q}_i}\mathsf{E}[\xi(X)] + \xi(k)\mathbb{Q}_i(Z > k)
\end{aligned} \tag{4.2.22}$$

Since $\mathbb{Q}_2 >_{LTO} \mathbb{Q}_1$ for Z at k is equivalent to $\mathbb{Q}_1 >_{st} \mathbb{Q}_2$ for X by Remark 4.1.2, it follows from Lemma 4.1.2 that

$$\mathsf{E}^{\mathbb{Q}_1}[\xi(X)] < \mathsf{E}^{\mathbb{Q}_2}[\xi(X)] \tag{4.2.23}$$

Moreover, $\mathbb{Q}_1 >_{st} \mathbb{Q}_2$ for X implies

$$\mathbb{Q}_1(Z > k) = \mathbb{Q}_1(X \geq k) \geq \mathbb{Q}_2(X \geq k) = \mathbb{Q}_2(Z > k) \tag{4.2.24}$$

Therefore, combining (4.2.22), (4.2.23) and (4.2.24) we obtain

$$\begin{aligned} \Delta_1^p &= -\mathsf{E}^{\mathbb{Q}_1}[\xi(X)] + \xi(k)\mathbb{Q}_2(Z > k) \\ &> -\mathsf{E}^{\mathbb{Q}_2}[\xi(X)] + \xi(k)\mathbb{Q}_1(Z > k) = \Delta_2^p \end{aligned}$$

□

To proceed, let $\tilde{l}_0$ label the option payoff function with payoff $\tilde{V}_0(S_T)$ and $\tilde{l}_i, i = 1, 2$ label the functions of the maturity values $\tilde{V}_i(S_T)$ of hedging portfolios, constructed based on $\mathbb{Q}_i$, as follows:

$$\begin{aligned} \tilde{l}_0: &\quad \tilde{V}_0(S_T) = (K - S_T)^+, \\ \tilde{l}_1: &\quad \tilde{V}_1(S_T) = K\, F^{\mathbb{Q}_1}(k) + S_T\Delta_1^p, \\ \tilde{l}_2: &\quad \tilde{V}_2(S_T) = K\, F^{\mathbb{Q}_2}(k) + S_T\Delta_2^p. \end{aligned} \tag{4.2.25}$$

Then, $\tilde{V}_1(S_T)$ and $\tilde{V}_2(S_T)$ are linear functions of S_T for $i = 1, 2$, and $\tilde{V}_0(S_T)$ is a piecewise linear function. According to Proposition 4.2.1, the EHR over S_T exist for the discrete time delta hedging of European put options. As a result, $U^{\mathbb{Q}_i}$ is the root to solve $\tilde{l}_i = 0$ for $i = 1, 2$; and $D^{\mathbb{Q}_i}$ is the root to solve $\tilde{l}_i = \tilde{l}_0$ conditional on $S_T < K$. Thus,

$$\left[D^{\mathbb{Q}_i} = K\frac{1 - F^{\mathbb{Q}_i}(k)}{1 + \Delta_i^p} \qquad U^{\mathbb{Q}_i} = K\frac{F^{\mathbb{Q}_i}(k)}{-\Delta_i^p} \right]. \tag{4.2.26}$$

Based on the maturity values, we can compare the EHRs for two delta hedging portfolios. The relative positions of two EHRs are among 9 scenarios, based on the combination of the relationships $\{U^{\mathbb{Q}_2} < U^{\mathbb{Q}_1}, U^{\mathbb{Q}_2} = U^{\mathbb{Q}_1}, U^{\mathbb{Q}_2} > U^{\mathbb{Q}_1}\}$ and $\{D^{\mathbb{Q}_2} < D^{\mathbb{Q}_1}, D^{\mathbb{Q}_2} = D^{\mathbb{Q}_1}, D^{\mathbb{Q}_2} > D^{\mathbb{Q}_1}\}$. As a result of tail ordering, we will see in the following proposition that the relative positions of EHRs for two portfolios.

Proposition 4.2.6. *(CQ) Let $k = \log K/S_t$, and $Z = \log(S_T/S_t)$. Then, Assume*

$\mathbb{Q}_2 >_{LTO} \mathbb{Q}_1$ *for* Z *at* k. *Then,*

(i). If $U^{\mathbb{Q}_2} \geq U^{\mathbb{Q}_1}$ *then* $D^{\mathbb{Q}_2} < D^{\mathbb{Q}_1}$;

(ii). If $U^{\mathbb{Q}_2} < U^{\mathbb{Q}_1}$, *we may have* $D^{\mathbb{Q}_2} < D^{\mathbb{Q}_1}$, $D^{\mathbb{Q}_2} = D^{\mathbb{Q}_1}$, *or* $D^{\mathbb{Q}_2} > D^{\mathbb{Q}_1}$;

(ii). If $D^{\mathbb{Q}_1} \leq D^{\mathbb{Q}_2}$, *then* $U^{\mathbb{Q}_2} \leq U^{\mathbb{Q}_1}$.

Proof. The proof is parallel with the proof in proposition 4.2.3.

□

Remark 4.2.4. Similar to the classification in Remark 4.2.2, we also classify the distributions of Z under $\mathbb{Q}_1$ and $\mathbb{Q}_2$ measures into four types, based on the movement of the density ratios $f^{\mathbb{Q}_2}(z)/f^{\mathbb{Q}_1}(z)$ in the left tail $z \in (-\infty, k)$.

(a) $f^{\mathbb{Q}_2}(z)/f^{\mathbb{Q}_1}(z)$ is increasing in z, with $f^{\mathbb{Q}_2}(z)/f^{\mathbb{Q}_1}(z) > 1$, for $z < k$;

(b) $f^{\mathbb{Q}_2}(z)/f^{\mathbb{Q}_1}(z) = c > 1$ for $z < k$;

(c) $f^{\mathbb{Q}_2}(z)/f^{\mathbb{Q}_1}(z)$ is decreasing in z for $z < k$, and $f^{\mathbb{Q}_2}(z)/f^{\mathbb{Q}_1}(z) > 1$ for $z < k'$ with a $k' \leq k$;

(d) $f^{\mathbb{Q}_2}(z)/f^{\mathbb{Q}_1}(z)$ has other shapes in the tail. An example is given in graph four.

In the remaining studies, we will focus on the first three cases (a)-(c) defined above.

Proposition 4.2.7. ***(CQ)*** *Assume two risk neutral measures* $\mathbb{Q}_2$ *and* $\mathbb{Q}_1$ *associated with* $Z = \log(S_T/S_t)$. *Then we have the results summarized in Table 4.2.*

Proof. (i). Suppose $f^{\mathbb{Q}_2}(z)/f^{\mathbb{Q}_1}(z)$ is constant in z for $z \in (-\infty, k)$. Then, parallel to the proof for part (i) in Proposition 4.2.4, we have $U^{\mathbb{Q}_1} = U^{\mathbb{Q}_2}$.

for $z \in (-\infty, k)$	$D^{\mathbb{Q}_1}$ vs. $D^{\mathbb{Q}_2}$	$U^{\mathbb{Q}_1}$ vs. $U^{\mathbb{Q}_2}$ $(\mathbb{Q}_2 >_{LTO} \mathbb{Q}_1)^*$
$\frac{f^{\mathbb{Q}_2}(z)}{f^{\mathbb{Q}_1}(z)}$ is strictly decreasing in z	$U^{\mathbb{Q}_2} > U^{\mathbb{Q}_1}$	$D^{\mathbb{Q}_2} < D^{\mathbb{Q}_1}$
$\frac{f^{\mathbb{Q}_2}(z)}{f^{\mathbb{Q}_1}(z)}$ is a constant	$U^{\mathbb{Q}_2} = U^{\mathbb{Q}_1}$	$D^{\mathbb{Q}_2} < D^{\mathbb{Q}_1}$
$\frac{f^{\mathbb{Q}_2}(z)}{f^{\mathbb{Q}_1}(z)}$ is strictly increasing in z	$U^{\mathbb{Q}_2} < U^{\mathbb{Q}_1}$	$D^{\mathbb{Q}_2} \lessgtr D^{\mathbb{Q}_1}$,

Table 4.2: EHR positions based on the movement of density ratios

* The right column results assumes that $\mathbb{Q}_2 >_{LTO} \mathbb{Q}_1$ for $Z = \log(S_T/S_t)$ at $k = \log K/S_t$.

(ii). Suppose $f^{\mathbb{Q}_2}(z)/f^{\mathbb{Q}_1}(z)$ is decreasing in z for $z \in (-\infty, k)$. Then, for $X = \max(-k, -Z)$, the ratio $f_X^{\mathbb{Q}_2}(x)/f_X^{\mathbb{Q}_1}(x)$ is increasing in x. Assume

$$f_X^{\mathbb{Q}_2}(x) = g(x) f_X^{\mathbb{Q}_1}(x), \quad \text{for all } x > -k,$$

with a strictly increasing function $g(x)$. Construct two densities

$$p_1(x) = \frac{f_X^{\mathbb{Q}_1}(x)}{\int_{-k}^{+\infty} f_X^{\mathbb{Q}_1}(x)\, dx}, \quad \text{and} \quad p_2(x) = \frac{e^{-x} f_X^{\mathbb{Q}_1}(x)}{\int_{-k}^{+\infty} e^{-x} f_X^{\mathbb{Q}_1}(x)\, dx}.$$

Since e^{-x} is positive and decreasing in x, the ratio $p_1(x)/p_2(x)$ is increasing in x for $x > -k$. From Lemma 1.2.4, Y is strictly stochastically larger under probability measure with density p_1 than with density p_2. In addition, since $g(x)$ is a strictly increasing function of x, from Lemma 4.1.2, we have

$$\int_{-k}^{+\infty} \frac{e^{-x} f_X^{\mathbb{Q}_1}(x)\, g(x)}{\int_{-k}^{+\infty} e^{-x} f_X^{\mathbb{Q}_1}(x)\, dx}\, dx < \int_{-k}^{+\infty} \frac{f_X^{\mathbb{Q}_1}(x)\, g(x)}{\int_{-k}^{+\infty} f_X^{\mathbb{Q}_1}(x)\, dx}\, dx \tag{4.2.27}$$

That is,

$$\frac{\int_{-\infty}^{k} f^{\mathbb{Q}_1}(z)\, dz}{e^{-r(T-t)} \int_{-\infty}^{k} e^z f^{\mathbb{Q}_1}(z)\, dz} < \frac{\int_{-\infty}^{k} f^{\mathbb{Q}_2}(z)\, dz}{e^{-r(T-t)} \int_{-\infty}^{k} e^z f^{\mathbb{Q}_2}(z)\, dz},$$

i.e.,

$$\frac{K\,F^{\mathbb{Q}_1}(k)}{-\Delta_1^p} < \frac{K\,F^{\mathbb{Q}_2}(k)}{-\Delta_2^p}$$

As a result, (4.2.26) implies that $U^{\mathbb{Q}_1} < U^{\mathbb{Q}_2}$, where $U^{\mathbb{Q}_i} = -\left(K\,F^{\mathbb{Q}_i}(k)\right)/\Delta_i^p$ for $i = 1, 2$.

(iii). Suppose $f^{\mathbb{Q}_2}(z)/f^{\mathbb{Q}_1}(z)$ is an increasing function for $z \in (-\infty, k)$. Then, $f_X^{\mathbb{Q}_1}(x)/f_X^{\mathbb{Q}_2}(x)$ is a decreasing function of x. Assume

$$f_X^{\mathbb{Q}_1}(x) = g(x) f_X^{\mathbb{Q}_2}(x), \quad \text{for all } x > -k,$$

with an increasing function $g(x)$. Then, following the step in (ii), with the exchange of $f_X^{\mathbb{Q}_1}(x)$ and $f_X^{\mathbb{Q}_2}(x)$ in (4.2.27), we have $\dfrac{K\,F^{\mathbb{Q}_1}(k)}{-\Delta_1^p} > \dfrac{K\,F^{\mathbb{Q}_2}(k)}{-\Delta_2^p}$, which along with (4.2.26) implies $U^{\mathbb{Q}_1} > U^{\mathbb{Q}_2}$.

Having compared $U^{\mathbb{Q}_1}$ and $U^{\mathbb{Q}_2}$, we can obtain the corresponding results with regard to the comparison of $D^{\mathbb{Q}_1}$ and $D^{\mathbb{Q}_2}$, based on the assumption of $\mathbb{Q}_2 >_{RTO} \mathbb{Q}_1$ for $Z = \log(S_T/S_t)$ at $k = \log K/S_t$. From Proposition 4.2.5, we have $|\Delta_2^p| < |\Delta_1^p|$, and the result in Table 4.2 can be directly obtained. □

4.2.4 Hedging Information between Calls and Puts

In subsection 4.2.2 we applied right tail ordering to compare hedging results for call options under two different risk neutral measures $\mathbb{Q}_1$ and $\mathbb{Q}_2$, and in subsection 4.2.3 we used left tail ordering for the comparison of hedging put options. However, as Proposition 4.1.1 claims, no risk neutral measure can be stochastically strictly larger than another, and thus right and left tail ordering does not hold for the parameter k over the entire support of Z. As a result, the analysis for hedging a call or a put option can be conducted only when the strike price K belongs to a particular range. In this section, we shall use put-call parity to develop more insight into the hedging results for call and put options. Indeed, as we can see shortly, the information we

obtained in the previous subsections for a call option can be used to analyze a put option at the same strike price and expiry date, and vice versa.

Let P_s and S_s represent the option price and stock price at time s for $t < s < T$, and Δ_t and B_t represent the delta and bond values at time t. Then, the interim hedging error, denoted by $\epsilon(S_s)$, for an option at time s is

$$\epsilon(S_s) = P_s - (\Delta_t\, S_s + B_t\, e^{r(s-t)}). \tag{4.2.28}$$

We further define the put-call parity for delta hedging strategies as follows.

Definition 4.2.1. (**CQ**) Let $\zeta^c(t)$ and $\zeta^p(t)$ denote the values of the hedging portfolios for call and put options with the same strike price K. $\zeta^c(t)$ and $\zeta^p(t)$ are said to satisfy put–call parity if and only if

$$\zeta^c(t) - \zeta^p(t) = S_t - Ke^{-r(T-t)}. \tag{4.2.29}$$

Remark 4.2.5. Delta hedging strategies under a risk neutral measure $\mathbb{Q}$ satisfy put-call parity. Other strategies such as mean variance hedging strategies for call and put options, consisting with bonds and stocks, also satisfy the put–call parity.

Lemma 4.2.2. *(**CQ**) If P_p and P_c and their associated hedging strategies $\zeta^c(t)$ and $\zeta^p(t)$ satisfy put-call parity, then the hedging errors defined in (4.2.28) are equal for hedging a European call and a put option, based on the same strike price and expiry date.*

Proof. The proof is trivial by Definition 4.2.1 and put-call parity. □

Based on Lemma 4.2.2, the delta hedging error expressed in (4.2.28) is the same for a European call and a put option under a $\mathbb{Q}_i$-measure, provided that the univariate options have the same K and expiry dates. This fact implies that to analyze the hedging error and the corresponding EHRs from a call option, we can investigate the EHRs for a put option, and vice versa. Indeed, the EHRs $[D^{\mathbb{Q}_i}, U^{\mathbb{Q}_i}]$ are the same

for hedging a univariate European call and a European put option, as in Corollary 4.2.1 as below.

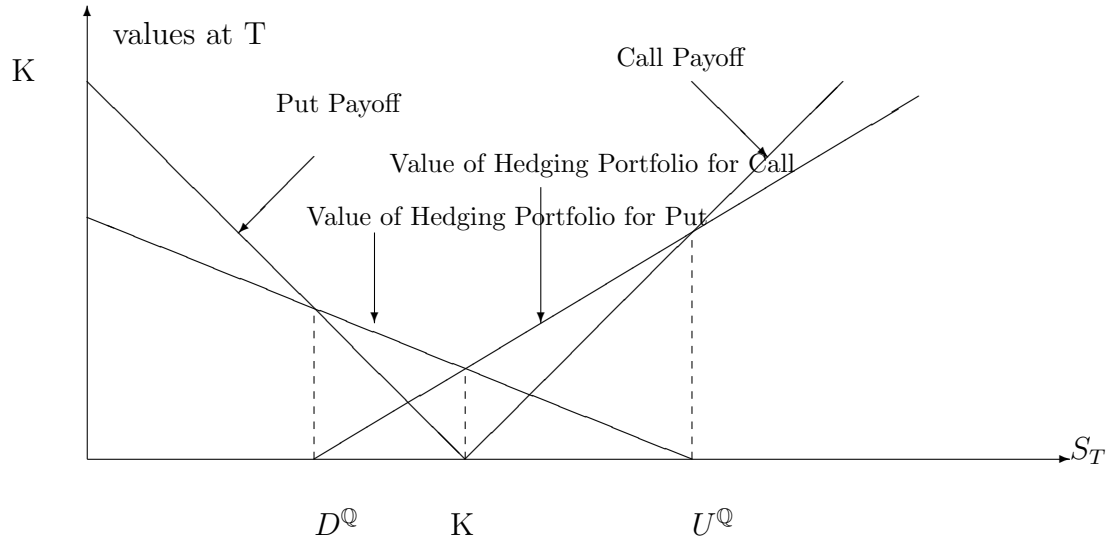

Figure 4.7: Delta hedging intervals of call and put options

Corollary 4.2.1. *Denote* $D^{\mathbb{Q}_i}(\text{put})$ *and* $U^{\mathbb{Q}_i}(\text{put})$ *the EHR boundaries of discrete time delta hedging for a European put option, given in* (4.2.26)*, and* $D^{\mathbb{Q}_i}(\text{call})$ *and* $U^{\mathbb{Q}_i}(\text{call})$ *denoted the EHR boundaries for hedging a European call option, given in* (4.2.19)*. Then, with the same strike prices* K *and expiry dates* T*, we have*

$$D^{\mathbb{Q}_i}(\text{put}) = D^{\mathbb{Q}_i}(\text{call}) \quad \& \quad U^{\mathbb{Q}_i}(\text{put}) = U^{\mathbb{Q}_i}(\text{call}) \tag{4.2.30}$$

Corollary 4.2.1 can be easily verified based on equations (4.2.19) and (4.2.26) and the condition $1 = -\Delta^{put} + \Delta^{call}$. The results of (4.2.30) are illustrated in Figure 4.7.

4.2.5 Examples

In this section, we apply the hedging results based on tail ordering to some option pricing models, including the discrete time regime switching models investigated in previous chapters.

Example 8. In this example, we compare the hedging positions of EHRs for call and put options under two risk neutral Gaussian distributions having $\sigma_i, i = 1, 2$. Let $G_i(r - \sigma_i^2/2, \sigma_i)$, with $\sigma_1 < \sigma_2$, denote the Gaussian distribution function of Z under risk neutral probability measures. Then, the ratio of densities is

$$\frac{f^{G_2}(z)}{f^{G_1}(z)} = \exp\left(\frac{\sigma_2^2 - \sigma_1^2}{2\sigma_1^2\sigma_2^2}(z-r)^2 + \log\sigma_1 - \log\sigma_2 + \frac{1}{8}(\sigma_1^2 - \sigma_2^2)\right)$$

The terms in the exponential function form a upward parabolic curve of z, with the minimum at $z = r$. That is, the above density ratio is increasing as z goes to $\pm\infty$, and

$$G_2(Z \le r) = G_1(Z \le r)$$

Let $k = \log(K/S_t)$. We have $G_2 >_{LTO} G_1$ for Z at $k < r$ and $G_2 >_{RTO} G_1$ at $k > r$. Based on Propositions 4.2.3 and 4.2.6 and Corollary 4.2.1, the positions of EHRs, denoted by $[D^{G_i}, U^{G_i}]$, for hedging European call and put options using discrete time delta hedging, are compared in Table 4.3.

options	D	U
call	$D^{G_2} < D^{G_1}$	$U^{G_2} > U^{G_1}$
put	$D^{G_2} < D^{G_1}$	$U^{G_2} > U^{G_1}$

Table 4.3: Comparison of EHRs between two Gaussian distributions

Example 9. This example investigates the delta hedging difference between the Black–Scholes method and the ET-$\mathbb{Q}$ methods discussed in chapter 1. Figure 4.8 illustrates their underlying densities and the density ratios for multiple periods—60 and 120 month period. Let $f^{ET-\mathbb{Q}}(z)$ and $f^{G}(z)$ denote the densities under the

ET-$\mathbb{Q}$ measure and of the Gaussian distributions. We can see the density ratio $f^{ET-\mathbb{Q}}(z)/f^{G}(z)$ increases as $z \to -\infty$. Based on the tail ordering in the left tails, we expect the ET-$\mathbb{Q}$ method has higher prices and delta values for out-of-money put options, as well as the wider EHRs according to Proposition 4.2.6.

The results of one-period delta values of put options are displayed in Figure 4.9, where the ET-$\mathbb{Q}$ method has larger delta values for the out-of-money put options, and smaller delta values for some in-the-money options. The hedging difference for the put options between the ET-$\mathbb{Q}$ method and the Black–Scholes method is displayed in Figure 4.10. The ET-$\mathbb{Q}$ method has a wider EHRs for out-of-the-money put options, but the ET-$\mathbb{Q}$ methods do not always have a wider EHR. For some in-the-money put options, the EHRs are smaller for the ET-$\mathbb{Q}$ methods. This is possible since the densities from the ET-$\mathbb{Q}$ measure and the Gaussian measure does not satisfy left or right tail ordering at these strike prices. The hedging results are the same for call options.

Example 10. This example compares the one-period delta hedging between the NEMM method and the ET-$\mathbb{Q}$ method. Figure 4.12 compares their option prices with maturity $T = 60$ but no rebalancing, and shows that the ET-$\mathbb{Q}$ method has higher prices for put options, while the NEMM method has higher prices for the out-of-money call options with $K > 220$.

Figure 4.12 further illustrates that the ET-$\mathbb{Q}$ method and the NEMM methods have different hedging performance, with regard to options with different strike price K. In the figure, the hedging comparison is based on the difference of the EHR boundaries. Let $D^{NEMM} - D^{ET-\mathbb{Q}}$ and $U^{NEMM} - U^{ET-\mathbb{Q}}$ denote the differences respectively for left (D) and right (U) EHR boundaries between the NEMM methods and the ET-$\mathbb{Q}$ methods. It shows that the ET-$\mathbb{Q}$ method has a better hedging performance, in terms of wider EHRs, when $K < 150$, which is consistent with the results in Proposition 4.2.7. If K is very large, the NEMM method has a better hedging performance. This hedging difference is due to the difference of the distribution under these two risk neutral measures, as the ET-$\mathbb{Q}$ measure has thicker left tails, while the NEMM measure has thicker right tails, as shown in Figure 4.11.

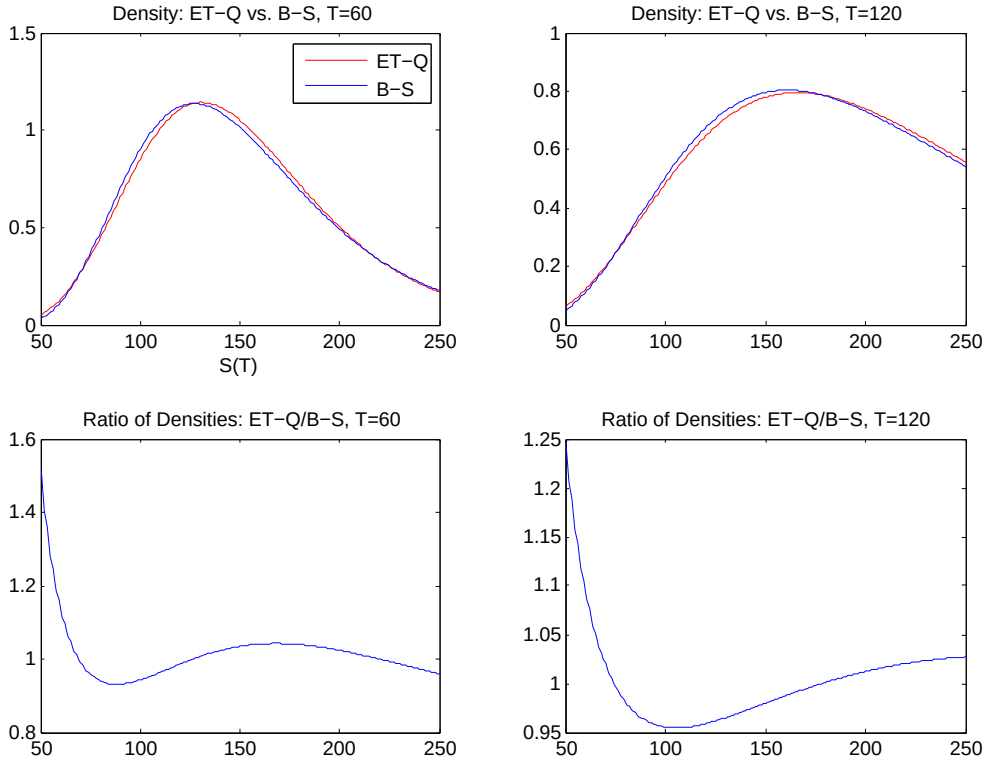

Figure 4.8: Risk neutral densities and density ratios between the ET-$\mathbb{Q}$ measure and the Gaussian measure)

In Figure 4.8, Y-axis in the top two graphs represents the density values under the ET-$\mathbb{Q}$ measure (ET-Q) and risk neutral Gaussian Distributions (B-S), identified under the RSLN2 model in chapter 1. In the bottom two graphs, Y-axis represents the density ratio $f^{ET-\mathbb{Q}}/f^{G}$ under the two measures. X–axis in the figure represents the stock price $S_T = 50, \ldots, 250; S_0 = 100$.

4.3 Tail Ordering and Option Pricing

In this section, we apply right and left tail ordering to compare the prices of European options calculated under two different risk neutral measures.

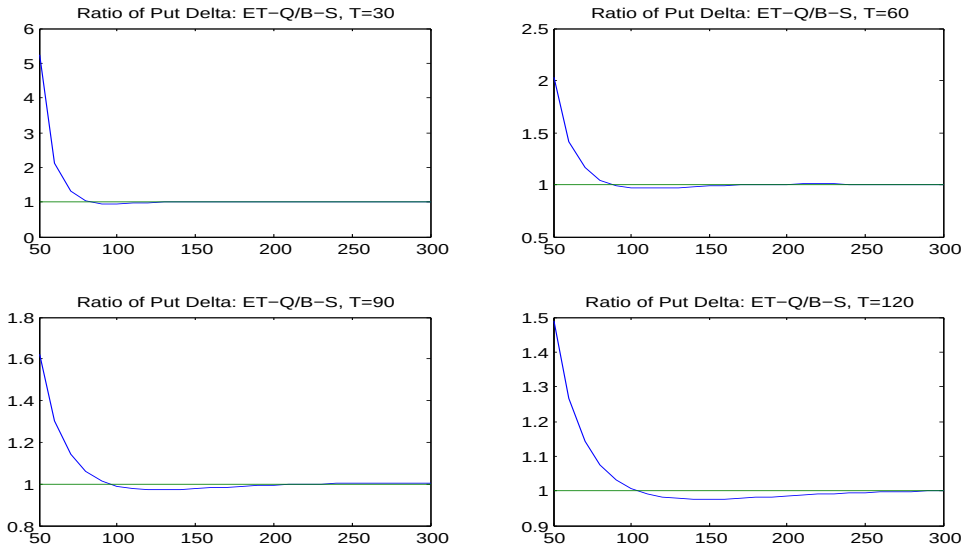

Figure 4.9: Ratio of put delta: ET-$\mathbb{Q}$/Black-Scholes

Denote $\Delta^{ET-\mathbb{Q}}$ and Δ^{B-S} the delta values from the ET-$\mathbb{Q}$ method and the Black-Scholes methods. In Figure 4.9, Y–axis represents the ratio $\dfrac{\Delta^{ET-\mathbb{Q}}}{\Delta^{B-S}}$, and X–axis represents the strike price $K = 50, \ldots, 300; S_0 = 100$.

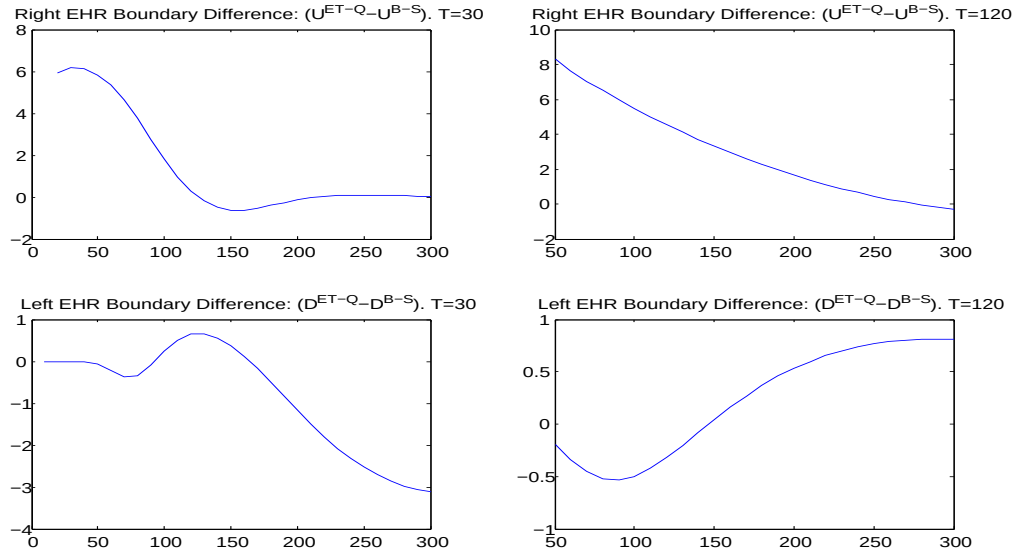

Figure 4.10: EHR boundary difference between the ET-$\mathbb{Q}$ and the B-S method

In Figure 4.10, Y-axis is the difference of the left EHR boundaries $D^{ET-\mathbb{Q}} - D^{B-S}$ and right EHR boundaries $U^{ET-\mathbb{Q}} - U^{B-S}$; X–axis is the strike price $K = 0, \ldots, 300; S_0 = 100$.

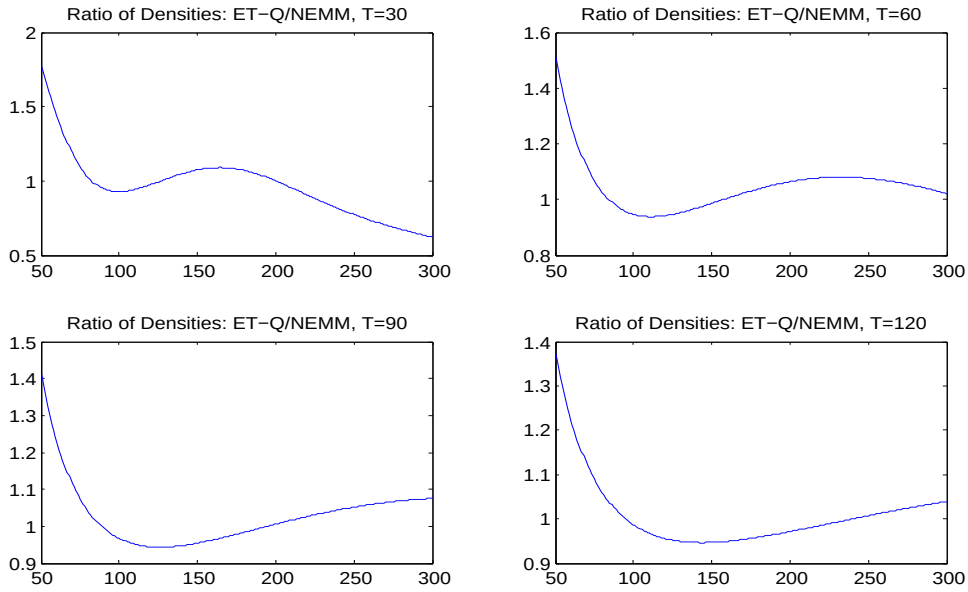

Figure 4.11: Ratio of densities: ET-$\mathbb{Q}$ / NEMM

In Figure 4.11, Y-axis measures the densities under the ET-$\mathbb{Q}$ measure and the NEMM measure and density ratios; X–axis is the stock price $S_T = 50, \ldots, 300; S_0 = 100$.

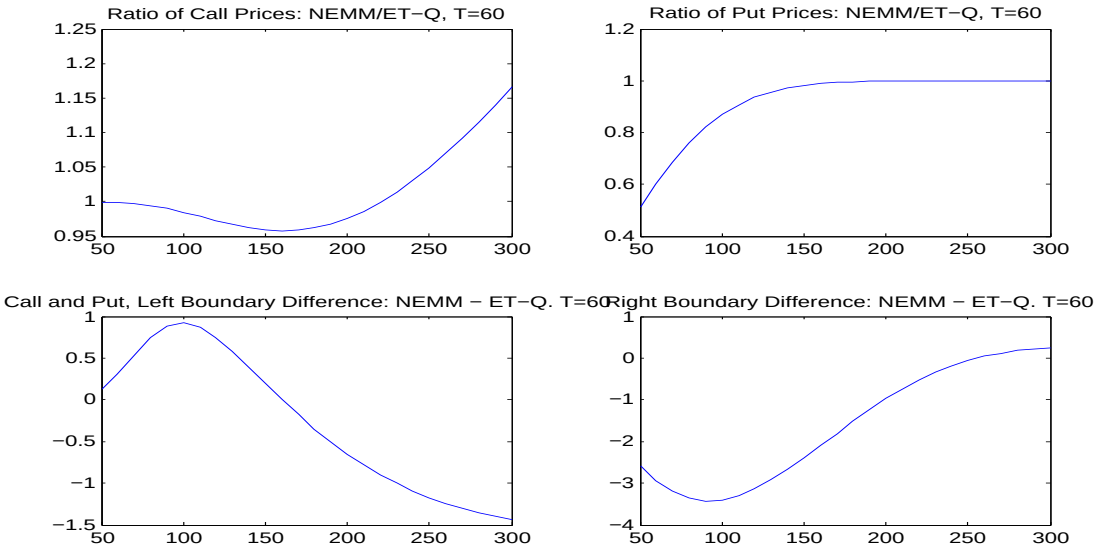

Figure 4.12: Price ratios and boundary difference of EHRs: NEMM - ET-$\mathbb{Q}$

In Figure 4.12, Y-axis is the difference $D^{NEMM} - D^{ET-\mathbb{Q}}$ and $U^{NEMM} - U^{ET-\mathbb{Q}}$; X–axis is the strike price $K = 50, \ldots, 300; S_0 = 100$.

4.3.1 Option Price Difference

An immediate result on the difference of call and put prices under $\mathbb{Q}_1$ and $\mathbb{Q}_2$ obtained from the tail ordering is as follows. Recall $Z = \log(S_T/S_t)$, $k = \log(K/S_t)$, and $P_p^{\mathbb{Q}_i}$ and $P_c^{\mathbb{Q}_i}$ represent, respectively, the put and call option price determined under $\mathbb{Q}_i$.

Proposition 4.3.1. **(CQ)** *For call and put options with the same strike price $K = S_t e^k$ and the same maturities,*

(a). If $\mathbb{Q}_2 >_{RTO} \mathbb{Q}_1$ for Z at k, then $P_c^{\mathbb{Q}_2} > P_c^{\mathbb{Q}_1}$.

(b). If $\mathbb{Q}_2 >_{LTO} \mathbb{Q}_1$ for Z at k, then $P_p^{\mathbb{Q}_2} > P_p^{\mathbb{Q}_1}$.

(c). $P_p^{\mathbb{Q}_2} - P_p^{\mathbb{Q}_1} = P_c^{\mathbb{Q}_2} - P_c^{\mathbb{Q}_1}$.

Proof. (a). The assumption $\mathbb{Q}_2 >_{RTO} \mathbb{Q}_1$ for Z at k implies that $\mathbb{Q}_2 >_{st} \mathbb{Q}_1$ for $Y = \max(Z, k)$ according to Remark 4.1.2. Since the payoff function $S_t\, e^Y - K$ is strictly increasing function in the support of Y, it follows from Lemma 4.1.2 that

$$\mathsf{E}_t^{\mathbb{Q}_2}[\, S_t\, e^Y - K\,] > \mathsf{E}_t^{\mathbb{Q}_1}[\, S_t\, e^Y - K\,],$$

i.e.

$$e^{-r\,(T-t)}\, \mathsf{E}_t^{\mathbb{Q}_2}[\, (S_t\, e^Z - K)^+\,] > e^{-r\,(T-t)}\, \mathsf{E}_t^{\mathbb{Q}_1}[\, (S_t\, e^Z - K)^+\,],$$

That is, the call price is larger under $\mathbb{Q}_2$.

(b). Let $X = \min(k, Z)$. The put option can be expressed as follows:

$$e^{-r\,(T-t)}\mathsf{E}_t^{\mathbb{Q}_2}[\, (K - S_t\, e^Z)^+\,] \;\; = \;\; e^{-r\,(T-t)}\, \mathsf{E}_{X,t}^{\mathbb{Q}_1}[\, K - S_t\, e^X\,],$$

The functoin $-(K - S_t\, e^x)$ is a strictly increasing in x. Since $\mathbb{Q}_2 >_{LTO} \mathbb{Q}_1$ for Z implies $\mathbb{Q}_1 >_{st} \mathbb{Q}_2$ for X according to Remark 4.1.2, it follows from Lemma 4.1.2 that

$$\mathsf{E}_{X,t}^{\mathbb{Q}_1}(\, K - S_t\, e^{-X}\,) < \mathsf{E}_{X,t}^{\mathbb{Q}_2}(\, K - S_t\, e^{-X}\,),$$

which implies

$$e^{-r\,(T-t)}\,\mathsf{E}_t^{\mathbb{Q}_1}[\,(K - S_t\,e^Z)^+\,] < e^{-r\,(T-t)}\,\mathsf{E}_t^{\mathbb{Q}_2}[\,(K - S_t\,e^Z)^+\,],$$

i.e., $P_p^{\mathbb{Q}_2} > P_p^{\mathbb{Q}_1}$ as desired.

(c). This is a direct result of the put-call parity under the $\mathbb{Q}$ measure. □

Let $P^{\mathbb{Q}_i}$ denote the European call or put option prices under $\mathbb{Q}_i$ measure. Then, we further investigate the shape of $P^{\mathbb{Q}_2} - P^{\mathbb{Q}_1}$, the price difference, under two different $\mathbb{Q}_i$-measures. Without loss of generality, assume options are priced at $t = 0$. Proposition 4.3.2 below describes the movement of the price difference along the strike price K, and Remark 4.3.2 describes the movement of price difference along the increasing of S_t. To proceed, we need the following lemma.

Lemma 4.3.1. *(**CQ**) Under two risk neutral measures $\mathbb{Q}_1$ and $\mathbb{Q}_2$ for a continuous random variable Z, there exists k such that $\mathbb{Q}_1(Z \le k) = \mathbb{Q}_2(Z \le k)$.*

Proof. The proof is a direct result from Proposition 4.1.1 as follows: if no such k exists, then $\mathbb{Q}_1$ and $\mathbb{Q}_2$ satisfy strict stochastic ordering, in contradiction to Proposition 4.1.1. □

Remark 4.3.1. The existence of k in Lemma 4.3.1 makes it possible to construct a simple relationship between $\mathbb{Q}_1$ and $\mathbb{Q}_2$, where we assume a k satisfying $\mathbb{Q}_2 >_{LTO} \mathbb{Q}_1$ and $\mathbb{Q}_2 >_{RTO} \mathbb{Q}_1$ for the random variable $Z = \log(S_T/S_t)$ at k. We give an illustration in Example 11 in section 4.3.4.

Proposition 4.3.2. *(**CQ**) Assume $\mathbb{Q}_2 >_{LTO} \mathbb{Q}_1$ and $\mathbb{Q}_2 >_{RTO} \mathbb{Q}_1$ at a $k' \in \mathbb{R}$ for the random variable $Z = \log(S_T/S_t)$. Let $k = \log(K/S_t)$. Then,*

(a). $k' = \arg\max_k P^{\mathbb{Q}_2} - P^{\mathbb{Q}_1}$ with k' satisfying $\mathbb{Q}_1(Z \le k') = \mathbb{Q}_2(Z \le k')$;

(b). $P^{\mathbb{Q}_2} - P^{\mathbb{Q}_1}$ is monotonically decreasing in k for $k > k'$, and monotonically increasing in k for $k < k'$, assuming other parameters are fixed for the options.

Proof. (a.) It is obvious that k' satisfies $\mathbb{Q}_1(Z \le k') = \mathbb{Q}_2(Z \le k')$ from the assumption. Next, we show that $k' = \arg\max_k P^{\mathbb{Q}_2} - P^{\mathbb{Q}_1}$. We note that $P^{\mathbb{Q}_i}$ depends on the strike price K and hence on k. For put options, if $k \le k'$, or $K \le S_t e^{k'}$, we have

$$\begin{aligned} \frac{\partial(\, P_p^{\mathbb{Q}_2} - P_p^{\mathbb{Q}_1}\,)}{\partial K} &= \frac{\partial}{\partial K} e^{-r} \int_{-\infty}^{\log K/S_t} (K - S_t e^z)(f^{\mathbb{Q}_2}(z) - f^{\mathbb{Q}_1}(z))\, dz \\ &= e^{-r} \int_{-\infty}^{\log K/S_t} (f^{\mathbb{Q}_2}(z) - f^{\mathbb{Q}_1}(z)) dz \\ &\ge 0. \end{aligned} \tag{4.3.31}$$

Therefore, $P_p^{\mathbb{Q}_2} - P_p^{\mathbb{Q}_1}$ is monotonically increasing in k for $k \le k'$. Noticing $P_p^{\mathbb{Q}_2} - P_p^{\mathbb{Q}_1} = P_c^{\mathbb{Q}_2} - P_c^{\mathbb{Q}_1}$ from Proposition 4.3.1, we know $P_c^{\mathbb{Q}_2} - P_c^{\mathbb{Q}_1}$ is also increasing in k for $k \le k'$. Similarly, for call options, if $k \ge k'$, we have

$$\begin{aligned} \frac{\partial(\, P_c^{\mathbb{Q}_2} - P_c^{\mathbb{Q}_1}\,)}{\partial K} &= \frac{\partial}{\partial K} e^{-r} \int_{\log K/S_t}^{\infty} (S_t e^z - K)(f^{\mathbb{Q}_2}(z) - f^{\mathbb{Q}_1}(z)) dz \\ &= e^{-r} \int_{\log K/S_t}^{\infty} (f^{\mathbb{Q}_1}(z) - f^{\mathbb{Q}_2}(z)) dz \\ &\le 0. \end{aligned}$$

Therefore, $P_c^{\mathbb{Q}_2} - P_c^{\mathbb{Q}_1}$ is decreasing in k for $k \ge k'$. Again, from Proposition 4.3.1, $P_p^{\mathbb{Q}_2} - P_p^{\mathbb{Q}_1}$ is also decreasing in k for $k \ge k'$.

Combining the above, as a continuous function of k, $P^{\mathbb{Q}_2} - P^{\mathbb{Q}_1}$ is increasing for $k \le k'$ and decreasing for $k \ge k'$. Thus, k' is its minimizer.

(b). It is the direct result from the proofs in (a) that the option-price difference $P^{\mathbb{Q}_2} - P^{\mathbb{Q}_1}$ monotonically decreases as k moves away from k'. □

Remark 4.3.2. We can also investigate the price difference $P^{\mathbb{Q}_2} - P^{\mathbb{Q}_1}$ against a sequence of S_t, which is useful for analyzing option prices at a future initial time point t, over the range of S_t. Recall that the option deltas are denoted by Δ_i^c and Δ_i^p under $\mathbb{Q}_i$. We have

$$\frac{\partial(\, P_c^{\mathbb{Q}_2} - P_c^{\mathbb{Q}_1}\,)}{\partial S_t} = \Delta_2^c - \Delta_1^c, \quad \text{and} \quad \frac{\partial(\, P_p^{\mathbb{Q}_2} - P_p^{\mathbb{Q}_1}\,)}{\partial S_t} = \Delta_2^p - \Delta_1^p.$$

In addition, $\Delta_2^c - \Delta_1^c = \Delta_2^p - \Delta_1^p$. That is, the changing rates of the price differences are the same for call and put options, based on the same strike price and maturity.

According to Proposition 4.2.3, if $\mathbb{Q}_2 >_{RTO} \mathbb{Q}_1$, then $\Delta_2^c > \Delta_1^c$ for call options. That is, $\Delta_2^c - \Delta_1^c > 0$, and the price difference $P^{\mathbb{Q}_2} - P^{\mathbb{Q}_1}$ increases as S_t increases. As an example, assume K is larger than S_t. In other words, for a fixed K, S_t is assumed to be smaller. Then, the price difference $P^{\mathbb{Q}_2} - P^{\mathbb{Q}_1}$ increases in S_t, assuming $\mathbb{Q}_2 >_{RTO} \mathbb{Q}_1$.

In addition, $\Delta_2^p < \Delta_1^p$ under $\mathbb{Q}_2 >_{LTO} \mathbb{Q}_1$. That is, the price difference $P^{\mathbb{Q}_2} - P^{\mathbb{Q}_1}$ decreases in S_t. In this case, the strike price K is on the left tail of S_t, and S_t is larger than K. As an example, for a fixed K, assume S_t is larger than K. Then, the option price difference $P^{\mathbb{Q}_2} - P^{\mathbb{Q}_1}$ decreases in S_t, assuming $\mathbb{Q}_2 >_{LTO} \mathbb{Q}_1$. As a result of these two examples, the option price difference may show a bell shape along the range of S_t. We given an illustration in Example 15 in section 4.3.4.

4.3.2 Option Price Ratios and Volatility Smiles

This section investigates the impact on the option price ratios from the movement of $f^{\mathbb{Q}_2}(z)/f^{\mathbb{Q}_1}(z)$ in the tails. We will apply the obtained results to discuss volatility smiles. Let $f^{\mathbb{Q}_i}(z)$ denote the density function of Z under $\mathbb{Q}_i$. Proposition 4.3.3 describes the movement of the price ratios for the European call and put options, dependent on the behavior of $f^{\mathbb{Q}_2}(z)/f^{\mathbb{Q}_1}(z)$.

Proposition 4.3.3. *(**CQ**) Let $f^{\mathbb{Q}_i}$ denote the density functions of $Z = \log S_T/S_t$ (or $Y = \max[k, Z]$) under $\mathbb{Q}_i$ measure, and $k = \log K/S_t$. Let $\nearrow, \rightarrow$ and $\searrow$ denote the behavior of increasing, being constant, and decreasing. Then, we have the relationship between the behavior of option price ratios and the density ratios given in Tables 4.4 and 4.5 below.*

Proof. We prove the results given in the table for call and options separately. For put options, we consider the behavior of the option price ratios as strike price K

Movement of Density Ratios for $Z\|Z < k$	Corresponding Movement of Price Ratios (Put options) for $K < S_0 e^k$
$\frac{f^{\mathbb{Q}_2}(z)}{f^{\mathbb{Q}_1}(z)} \nearrow$ as z decreases	$\frac{P_p^{\mathbb{Q}_2}}{P_p^{\mathbb{Q}_1}} \nearrow$ as K decreases
$\frac{f^{\mathbb{Q}_2}(z)}{f^{\mathbb{Q}_1}(z)} \rightarrow$ as z decreases	$\frac{P_p^{\mathbb{Q}_2}}{P_p^{\mathbb{Q}_1}} \rightarrow$ as K decreases
$\frac{f^{\mathbb{Q}_2}(z)}{f^{\mathbb{Q}_1}(z)} \searrow$ as z decreases	$\frac{P_p^{\mathbb{Q}_2}}{P_p^{\mathbb{Q}_1}} \searrow$ as K decreases

Table 4.4: Put option price ratios vs left tail density ratios

Movement of Density Ratios for $Y = \max[k, Z]$	Corresponding Movement of Price Ratios (Call options) for $K > S_0 e^k$
$\frac{f^{\mathbb{Q}_2}(y)}{f^{\mathbb{Q}_1}(y)} \nearrow$ as y increases	$\frac{P_c^{\mathbb{Q}_2}}{P_c^{\mathbb{Q}_1}} \nearrow$ as K increases
$\frac{f^{\mathbb{Q}_2}(y)}{f^{\mathbb{Q}_1}(y)} \rightarrow$ as y increases	$\frac{P_c^{\mathbb{Q}_2}}{P_c^{\mathbb{Q}_1}} \rightarrow$ as K increases
$\frac{f^{\mathbb{Q}_2}(y)}{f^{\mathbb{Q}_1}(y)} \searrow$ as y increases	$\frac{P_c^{\mathbb{Q}_2}}{P_c^{\mathbb{Q}_1}} \searrow$ as K increases

Table 4.5: Call option price ratios vs right tail density ratios

decreases. From equation (4.2.8) and (4.3.31), we have

$$\begin{aligned}
&\frac{\partial(P_p^{\mathbb{Q}_2}/P_p^{\mathbb{Q}_1})}{\partial K} \\
= \;& \frac{(P_p^{\mathbb{Q}_2})' P_p^{\mathbb{Q}_1} - P_p^{\mathbb{Q}_2}(P_p^{\mathbb{Q}_1})'}{(P_p^{\mathbb{Q}_1})^2} \\
= \;& \left\{ e^{-rT} \int_{-\infty}^{\log(K/S_t)} f^{\mathbb{Q}_2}(z)dz \, P_p^{\mathbb{Q}_1} - P_p^{\mathbb{Q}_2} \, e^{-rT} \int_{-\infty}^{\log(K/S_t)} f^{\mathbb{Q}_1}(z)dz \right\} \Big/ (P_p^{\mathbb{Q}_1})^2
\end{aligned} \tag{4.3.32}$$

According to Proposition 4.2.7, if $f^{\mathbb{Q}_2}(z)/f^{\mathbb{Q}_1}(z)$ increases as z decreases in the left tail for $z < k$, then

$$\frac{KF^{\mathbb{Q}_1}(k)}{-\Delta_1} < \frac{KF^{\mathbb{Q}_2}(k)}{-\Delta_2}.$$

We then have

$$e^{-rT}\int_{-\infty}^{\log(K/S_t)} f^{\mathbb{Q}_2}dz\, P_p^{\mathbb{Q}_1} < P_p^{\mathbb{Q}_2}\, e^{-rT}\int_{-\infty}^{\log(K/S_t)} f^{\mathbb{Q}_1}dz.$$

As a result, equation (4.3.32) is negative. Thus, $P_p^{\mathbb{Q}_2}/P_p^{\mathbb{Q}_1}$ increases as K decreases towards 0. Similarly, we can obtain the results for the movement of the ratio $P_p^{\mathbb{Q}_2}/P_p^{\mathbb{Q}_1}$ in the cases where $f^{\mathbb{Q}_2}(z)/f^{\mathbb{Q}_1}(z)$ is constant and decreasing in z for $z < k$.

For call options, we consider the behavior of the option price ratios as strike price K increases. Let $Y = \max[k, Z]$. From equation (4.2.6), we have

$$\begin{aligned}&\frac{\partial(P_c^{\mathbb{Q}_2}/P_c^{\mathbb{Q}_1})}{\partial K}\\ =\ &\left\{e^{-rT}\int_{\log(K/S_t)}^{\infty}(-f^{\mathbb{Q}_2}(y))dy\, P_c^{\mathbb{Q}_1} + P_c^{\mathbb{Q}_2}\, e^{-rT}\int_{\log(K/S_t)}^{\infty} f^{\mathbb{Q}_1}(y)dy\right\}\Big/ (P_c^{\mathbb{Q}_1})^2\end{aligned} \tag{4.3.33}$$

According to Proposition 4.2.4,if $f^{\mathbb{Q}_2}(y)/f^{\mathbb{Q}_1}(y)$ increases as y increases, then,

$$\frac{K(1-F^{\mathbb{Q}_2}(k))}{\Delta_2} < \frac{K(1-F^{\mathbb{Q}_1}(k))}{\Delta_1}$$

We then have

$$P_c^{\mathbb{Q}_2}\, e^{-rT}\int_{\log(K/S_t)}^{\infty} f^{\mathbb{Q}_1}(y)dy > e^{-rT}\int_{\log(K/S_t)}^{\infty} f^{\mathbb{Q}_2}(y)dy\, P_c^{\mathbb{Q}_1}.$$

Then, equation (4.3.33) is positive. As a result, $P_c^{\mathbb{Q}_2}/P_c^{\mathbb{Q}_1}$ increases as K increases. Similarly, we can obtain the results for the movement of the ratio $P_c^{\mathbb{Q}_2}/P_c^{\mathbb{Q}_1}$ in the

cases where $f^{\mathbb{Q}_2}(z)/f^{\mathbb{Q}_1}(z)$ is constant and decreasing in y. □

Remark 4.3.3. It is worth noting that the price ratios $P^{\mathbb{Q}_2}/P^{\mathbb{Q}_1}$ are not the same for put and call options, unlike the price difference $P^{\mathbb{Q}_2} - P^{\mathbb{Q}_1}$. As an example, even if $P_c^{\mathbb{Q}_2}/P_c^{\mathbb{Q}_1}$ increases for call options, by assuming $f^{\mathbb{Q}_2}(z)/f^{\mathbb{Q}_1}(z)$ increases in the tail, $P_p^{\mathbb{Q}_2}/P_p^{\mathbb{Q}_1}$ does not necessarily increase for put options. Therefore, according to Proposition 4.3.3, we will separately discusses the movement of $P^{\mathbb{Q}_2}/P^{\mathbb{Q}_1}$ as K increases or decreases, based on call and put options respectively.

Remark 4.3.4. As an application of the results obtained in Proposition 4.3.3, we discuss implied volatilities, which are obtained by inverting the Black-Scholes option pricing formulas on observed option prices. We can use the movement of the price ratio for inferring the shape of implied volatilities at different strike prices K. According to Proposition 4.3.3 and Remark 4.3.3, if K is small, we can use put option prices for the inverting. If K is large, we use call option prices. Nevertheless, it is worth noting that inverting call prices or put prices obtains the same implied volatility. This is because, first, in the Black–Scholes formula, there is one to one relation between $P^{\mathbb{Q}_i}$ and σ, as $\partial P^{\mathbb{Q}_i}/\partial\sigma = S_t\phi(d_1)\sqrt{T} > 0$, where $\phi(\cdot)$ is the density of standard normal distribution. Second, each pair of put and call prices in the put-call parity correspond to a common σ.

To generate the volatility smiles from option prices $P^{\mathbb{Q}_2}$, two conditions need to be satisfied for the distributions of the underlying asset under the risk neutral measure. First, $f^{\mathbb{Q}}(z)/\phi(z)$ is increasing in z moves towards tails, where $f^{\mathbb{Q}}(z)$ denotes the density of the underlying distribution under a $\mathbb{Q}$ measure. According to Proposition 4.3.3, this condition implies that the call or put option price ratio $P^{\mathbb{Q}_2}/P^{BS}$ is increasing as K moves towards ∞ or 0, where P^{BS} denotes the Black-Scholes prices. Second, the function $f^{\mathbb{Q}}(z)$ is not Gaussian density function. Without the second condition, even $f^{\mathbb{Q}_2}(z)/\phi(z)$ satisfies the first condition, the option prices $P^{\mathbb{Q}_2}$ cannot generate volatility smiles. Assume the log return underlying asset prices is generated from a Gaussian distribution with volatility σ. Under risk neutral measures, the distribution of Y_t under a risk neutral measure is normal with volatility equal to σ and the mean equal to the risk-free rate r. That is, all option prices $P^{\mathbb{Q}_2}$ corresponds to a single volatility value. With the second condition satisfied, the increasing ratio

of $f^{\mathbb{Q}}(z)/\phi(z)$ ensures that $f^{\mathbb{Q}}(z)$ interacts with multiple Gaussian distributions with different volatilities. This ends up with volatility uncertainty implied from option prices.

As an example, the distributions under the ET-$\mathbb{Q}$ measures satisfy the two conditions to generate volatility smiles. The ratio of the prices under these two methods increases as K moves towards 0 or ∞. It turns out that, the volatility smiles or smirks may be observed if we invert the Black-Scholes option pricing formulas on the option prices, obtained through the Esscher transform in the pervious chapters, at different strike prices K.

4.3.3 On Discrete Time Delta Hedging for a Single Interim Period Before Maturity

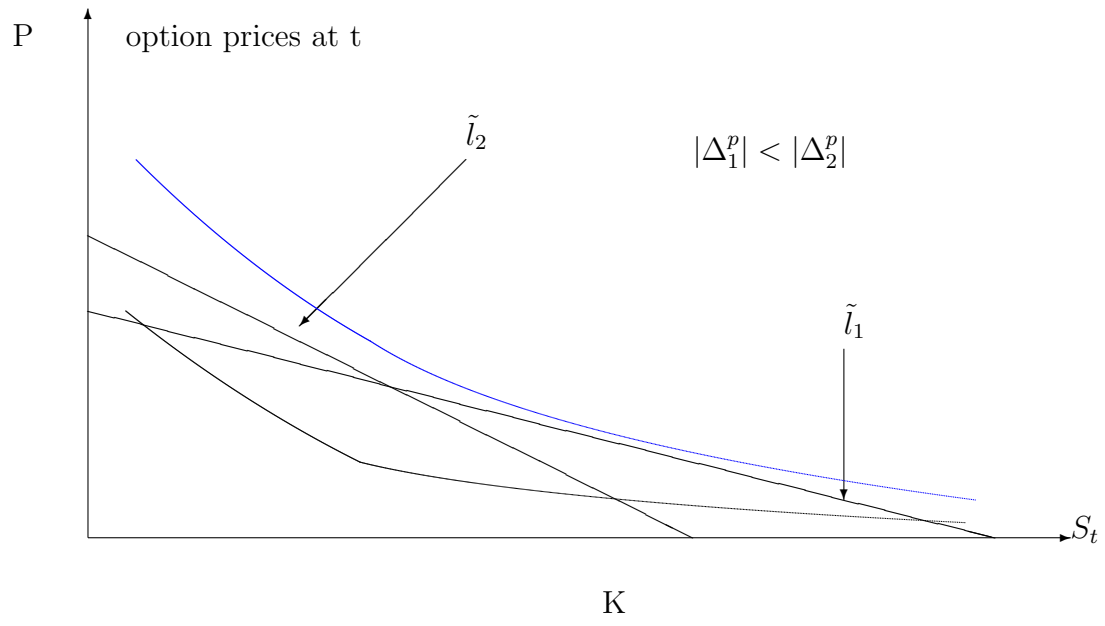

Figure 4.13: The relative positions of possible realized option prices (two curves) and the values of two hedging portfolios (straight line segments $\tilde{l}_1, \tilde{l}_2$) at time t

In this section, we discuss a single interim period hedging for a multi-period European option, with regard to the positions of EHRs. We focus on a put option. Nevertheless, the hedging for a call option will have similar loss results based on the equivalence of hedging error stated in Lemma 4.2.2. Suppose we set up a single period hedging at time $t-1$ for $t < T$, to hedge the time t value of a European put option with the expiry date at T, under a two-state regime switching models. The interim hedging error, denoted by ϵ_t, for a European put option is

$$\epsilon_t = P_t - (\Delta_{t-1}\, S_t + B_{t-1}\, e^r),$$

where P_t and S_t represent the option price and the underlying stock price at time t, and Δ_{t-1} and B_{t-1} represent the delta and bond values fixed at time $t-1$. The corresponding P_t, Δ_{t-1} and B_{t-1} are given in (4.2.6) and (4.2.8) for call and put options respectively. Based on ϵ_t, we have the following observations regarding the effective hedging ranges over S_t for hedging ϵ_t from discrete delta hedging.

First, we can see that the EHR over S_t may exist for the discrete delta hedging. The EHR exists if ϵ_t satisfies two conditions. First, there exists a stock price S_t, say, $S_t = \tilde{S}_t$, such that ϵ_t is negative. Second, ϵ_t monotonically increases if S_t moves away from $\tilde{S}_t$, i.e. as S_t moves towards 0 and as S_t increases from $\tilde{S}_t$. Indeed,

$$\partial\epsilon_t/\partial S_t = \Delta_t - \Delta_{t-1}, \tag{4.3.34}$$

where Δ_{t-1} is a constant and $-1 < \Delta_{t-1} < 0$, given $\mathcal{F}_{t-1}$. The value of $\partial\epsilon_t/\partial S_t$ depends on the value of Δ_t. We have the following results for Δ_t according to (4.2.9). First, $-1 < \Delta_t < 0$; second, Δ_t is increasing in S_t, since Δ_t is computed in (4.2.9) and is decreasing in $k = \log(K/S_t)$ for a fixed K; and third,

$$\lim_{S_t \to 0} \Delta_t = -1, \quad \& \quad \lim_{S_t \to \infty} \Delta_t = 0. \tag{4.3.35}$$

As a result of the second point, $\partial\epsilon_t/\partial S_t$ is monotonically increasing in S_t. From Equations (4.3.35) and (4.3.34), and the monotonic increasing property of $\partial\epsilon_t/\partial S_t$ in S_t, we see that $-1 - \Delta_{t-1} < \partial\epsilon_t/\partial S_t < 0 - \Delta_{t-1}$ and that there exists a value

$\tilde{S}_t \in (0, \infty)$ satisfying

$$\text{sgn}(\partial \epsilon_t / \partial S_t) = \begin{cases} - & \text{if } S_t < \tilde{S}_t \\ + & \text{if } S_t > \tilde{S}_t \end{cases}$$

where $\text{sgn}(\cdot)$ is the sign function. Thus, the hedging error ϵ_t is decreasing in S_t as $S_t < \tilde{S}_t$ and increasing in S_t as $S_t > \tilde{S}_t$. As a result, the second condition of the existence of EHR satisfied.

However, the first condition may not be satisfied for the existence of the EHR. That is, we may not have $\min_{S_t} \epsilon_t < 0$. We illustrate this issue in Figure 4.13, where the curves represent option prices and the straight line segments represent the value of hedging portfolio at time t. In the figure, the EHR exists if there is a range of S_t at which the portfolio values are greater than option prices. However, in the figure, if the curve in the above represents option prices, then the portfolio value is smaller than the option price for each S_t. That is, no EHR exists.

In the content of regime switching models, two curves illustrated in Figure 4.13 may represent different realized option prices at time t given different regimes ρ_t. If the option price is always higher than the value of the hedging portfolio in one regime, the hedging is insufficient. This ia an extra risk under the regime switching models. To set up an investment portfolio, we need to balance the earning in one regime and reducing the risk of insufficient hedging in other regimes.

4.3.4 Examples

In this section, we illustrate the results obtained in this section with examples under the discrete time regime switching models investigated in previous chapters.

Example 11. This example discusses the simplest relationship between density functions, say, $f^{\mathbb{Q}_1}(z)$ and $f^{\mathbb{Q}_2}(z)$, under two risk neutral measures displayed in Figure 4.14. In the figure, $f^{\mathbb{Q}_1}(z)$ and $f^{\mathbb{Q}_2}(z)$ intersect at k_1 and k_2.

Lemma 4.3.2. *(**CQ**) Let $\tilde{N}$ denote the number of intersections between densities under two risk neutral measures $\mathbb{Q}_1$ and $\mathbb{Q}_2$ for a continuous random variable $Z =$*

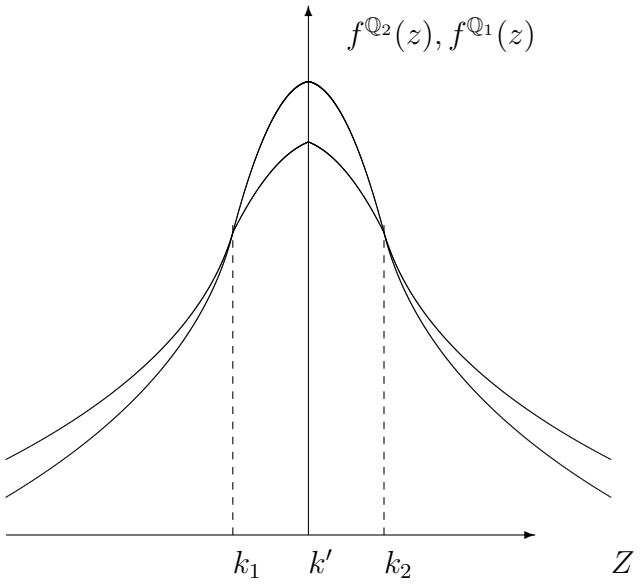

Figure 4.14: Risk neutral densities $f^{\mathbb{Q}_2}(z), f^{\mathbb{Q}_1}(z)$ under the thick-tailed relationship
Assume $f^{\mathbb{Q}_2}(z) > f^{\mathbb{Q}_1}(z)$ in tails and $f^{\mathbb{Q}_2}(z) < f^{\mathbb{Q}_1}(z)$ in the center.

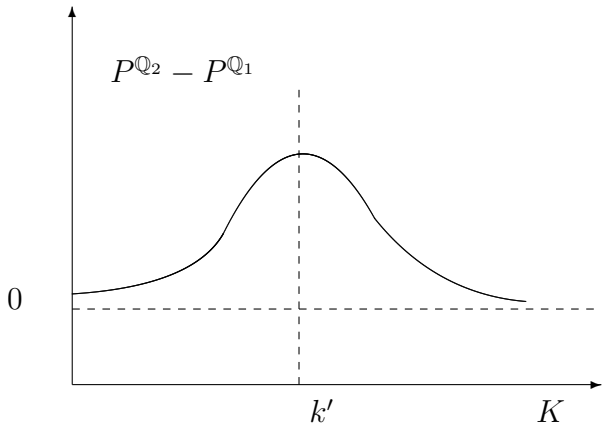

Figure 4.15: Price difference

$\log S_T/S_t$,

(a). $\tilde{N} \geq 2$;

(b). *If* $\tilde{N} = 2$, *say* k_1 *and* k_2, *then there exists a unique* $k', k_1 < k' < k_2$ *satisfies* $\mathbb{Q}_1(Z \leq k') = \mathbb{Q}_2(Z \leq k')$ *for two risk neutral measures* $\mathbb{Q}_1$ *and* $\mathbb{Q}_2$ *with two cross points in their densities (illustrated in Figure 4.14).*

Proof. (a). $\tilde{N} \neq 0$; otherwise, one density curve is always above the other. As a result, one of them is not a proper probability density functions. If $\tilde{N} = 1$, then $\mathbb{Q}_1$ and $\mathbb{Q}_2$ satisfy the strict stochastic ordering, a contradiction to Proposition 4.1.1 regarding two risk neutral measures.

b). From Lemma 4.3.1, there exists $k = k'$ such that $\mathbb{Q}_1(Z \leq k') = \mathbb{Q}_2(Z \leq k')$. It is obvious that $k_1 < k' < k_2$. The uniqueness of k' in Figure 4.14 can be proved if $\tilde{N} = 2$, say $Z = k_1$ and $Z = k_2$ as the only two cross points of the two density functions. In this case, $\mathbb{Q}_2(Z \leq k) - \mathbb{Q}_1(Z \leq k)$ is strictly positive or negative

$$\begin{cases} \mathbb{Q}_2(Z > k) - \mathbb{Q}_1(Z > k) < 0, & \forall k < k' \\ \mathbb{Q}_2(Z > k) - \mathbb{Q}_1(Z > k) > 0, & \forall k > k', \end{cases} \tag{4.3.36}$$

which is obvious. □

Based on $f^{\mathbb{Q}_2}$ and $f^{\mathbb{Q}_1}$ in Figure 4.14, with $f^{\mathbb{Q}_2}$ assumed to be higher in the tails, we have $\mathbb{Q}_2 >_{LTO} \mathbb{Q}_1$ and $\mathbb{Q}_2 >_{RTO} \mathbb{Q}_1$ at a $k' \in \mathbb{R}$ for Z. According to Proposition 4.3.2, $P^{\mathbb{Q}_2} - P^{\mathbb{Q}_1}$ has a bell shape as displayed in Figure 4.15 for European call or put options.

Example 12. In this example, we study the price difference between the ET-$\mathbb{Q}$ method and the Black–Scholes method, based on the comparison of their risk neural measures. Let $\mathbb{Q}^{ET-\mathbb{Q}}$ represent the ET-$\mathbb{Q}$ probability measure, and $f^{ET-\mathbb{Q}}(z)$ represent the density of the random variable Z; let $\Phi(\cdot)$ represent the standard normal distribution function, with density function $\phi(\cdot)$. The density functions $f^{ET-\mathbb{Q}}(z)$ and $\phi\left(\frac{z-r}{\sigma}\right)$ are illustrated in Figure 4.16 for $T = 30$ months. Compared with $\phi\left(\frac{z-r}{\sigma}\right)$, the density $f^{ET-\mathbb{Q}}(z)$ has a higher kurtosis, which means it is higher in the tails and around the center area.

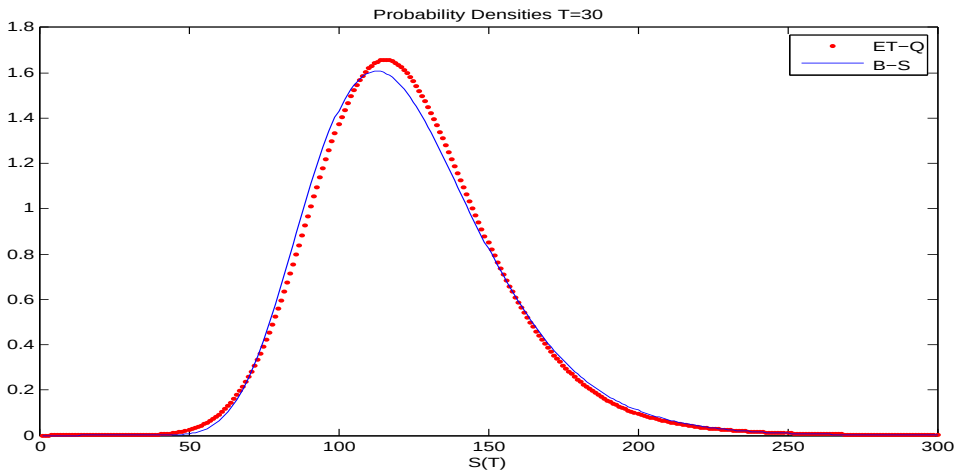

Figure 4.16: $\mathbb{Q}$ Densities of $T = 30$ (ET-$\mathbb{Q}$: dotted line, Black–Scholes: solid line)

The two densities are illustrated by Figure 4.17. In the figure, based on the results in Lemma 4.3.2, there exists k_1, k_2, k_3 to divide the range of z into four regions: A, B, C, and D, with $\mathbb{Q}^{ET-\mathbb{Q}}(Z \leq k_i) = \Phi\left(\frac{z-k_i}{\sigma}\right)$ for $i = 1, 2, 3$. Thereby, the probabilities of Z falling within each of the four regions are the same under ET-$\mathbb{Q}$ measure and under the risk neutral Gaussian measure; thus, the probability of Z in each region can be normalized to one. Let $W_A^{ET-\mathbb{Q}} = ZI_{(Z\in A)}$, where $I_{(\cdot)}$ is an indicator function and $W_A^{ET-\mathbb{Q}}$ has the density function

$$f(W^A = w) = \begin{cases} f^{ET-\mathbb{Q}}(z)/\mathbb{Q}^{ET-\mathbb{Q}}(Z \leq k_1) & w \in A \\ 0 & o.w. \end{cases}$$

Similarly, we can define $W_i^{ET-\mathbb{Q}}$ for $i = B, C, D$ and W_i^{LN} for $i = A, B, C$, and D. Then, we have the stochastic ordering relationships given in Table 4.6.

Based on these stochastic orders for W, we can infer the price difference, approximated by Figure 4.18, according to Proposition 4.3.2. It is worth noting again that in the relationship the density under the ET-$\mathbb{Q}$ measure has a larger kurtosis

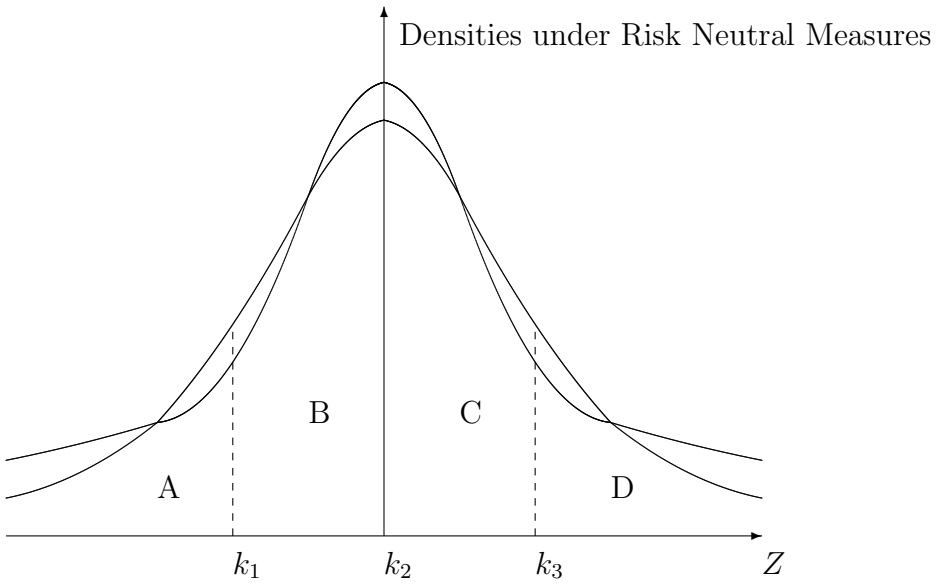

Figure 4.17: Densities of $\phi\left(\frac{z-r}{\sigma}\right)$ and $f^{ET-\mathbb{Q}}(z)$, which is higher in the tails and in the center.

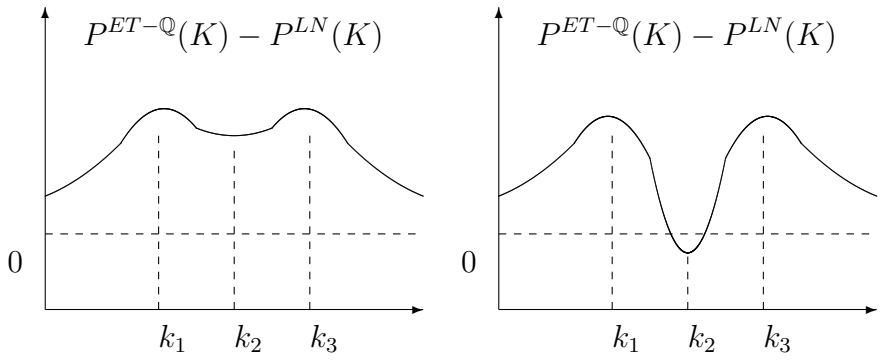

Figure 4.18: Option price difference

stochastic ordering
$-W_A^{ET-\mathbb{Q}} >_{st.} -W_A^{LN}$
$-W_B^{ET-\mathbb{Q}} <_{st.} -W_B^{LN}$
$W_C^{ET-\mathbb{Q}} <_{st.} W_C^{LN}$
$W_D^{ET-\mathbb{Q}} >_{st.} W_D^{LN}$

Table 4.6: Stochastic ordering in 4 regimes

compared with the normal density. This property is consistent with the observations based on market prices, and it implies the volatility smiles (see Hull, 2006). More specifically, let $P^{ET-\mathbb{Q}}(K)$ represent the option price under the ET-$\mathbb{Q}$ method, and P^{LN} represent the Black–Scholes prices. Let $\mathcal{D} := P^{ET-\mathbb{Q}}(K) - P^{LN}(K)$. Then, $\mathcal{D}$ increases with K in region A, decreases in region B, increases in region C, and decreases in region D.

Example 13. This example illustrates the volatility smiles or smirks implied by the ET-$\mathbb{Q}$ prices. Figures 4.19 and 4.20 illustrate that the price ratio $P^{ET-\mathbb{Q}}(K)/P^{LN}(K)$ increases as K moves towards zero for put options, and increases or decreases for call options as K increases. As a result, according to Remark 4.3.4, the prices $P^{ET-\mathbb{Q}}(K)$ generate the volatility smiles or volatility smirks as shown in Figure 4.21

Example 14. Figure 4.22 illustrates the bell shape of option price differences $P^{\mathbb{Q}_2} - P^{\mathbb{Q}_1}$ against the strike prices K, with two risk neutral measures $\mathbb{Q}_1$ and $\mathbb{Q}_2$ satisfying $\mathbb{Q}_2 >_{LTO} \mathbb{Q}_1$ and $\mathbb{Q}_2 >_{RTO} \mathbb{Q}_1$ at a $k \in \mathbb{R}$. In the RSLN2 model, the risk neutral distribution of S_T conditional on $\rho_0 = 2$ has thicker tails than the distribution conditional on $\rho_0 = 1$. If $\mathbb{Q}_{\rho_0=i}$ denotes the pricing measure under $\rho_0 = i$, we have $\mathbb{Q}_{\rho_0=2} >_{RTO} \mathbb{Q}_{\rho_0=1}$ and $\mathbb{Q}_{\rho_0=2} >_{LTO} \mathbb{Q}_{\rho_0=1}$ at a $k \in \mathbb{R}$. Thus, the price differences $P_{\rho_0=2} - P_{\rho_0=1}$ has a bell shape for both calls and puts, according to Proposition 4.3.2.

In Figures 4.22, the difference $P_{\rho_0=2} - P_{\rho_0=1}$ is smaller if the option maturity is longer. This can be explained by that the two underlying distributions in the RSLN2 model get closer to each other when T gets longer (see, for example, Lawler 2006). Let $R_{[ij]}, i, j \in \{1, 2\}$ denote the sojourn of regime $[ij]$. Then, we can see that the expectation $\mathsf{E}^{\mathbb{P}}(R_{[ij]}|\rho_0 = j)$ converges to the stationary probability π_{ij} for

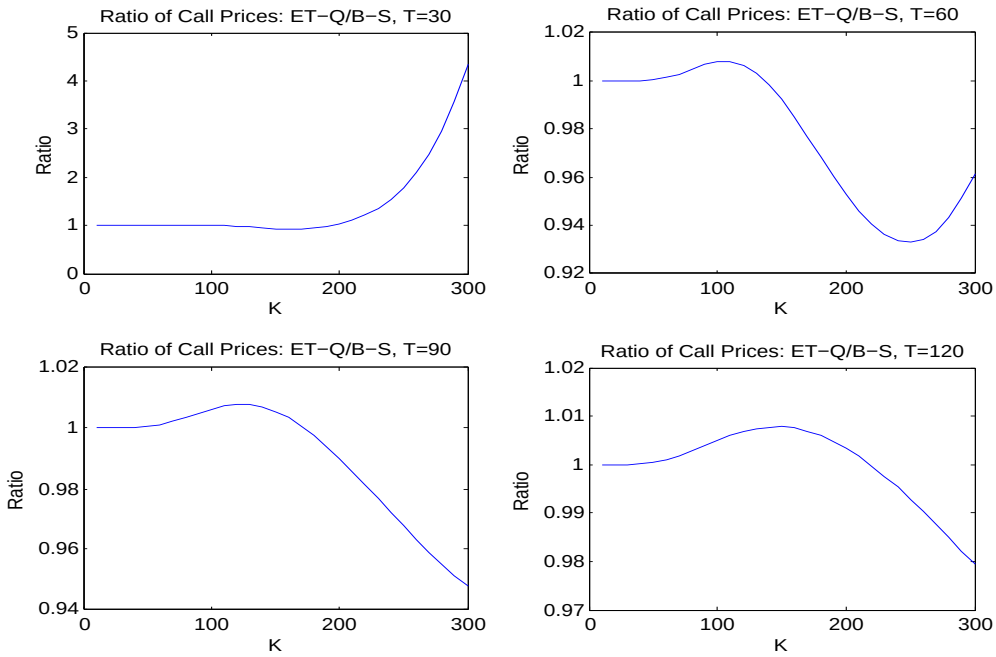

Figure 4.19: Call Option Price Ratio: ET-$\mathbb{Q}$/B-S

Y-axis: call price ratios $P_c^{ET-\mathbb{Q}}/P_c^{B-S}$; X–axis: strike prices $K = 0, \ldots, 300; S_0 = 100$.

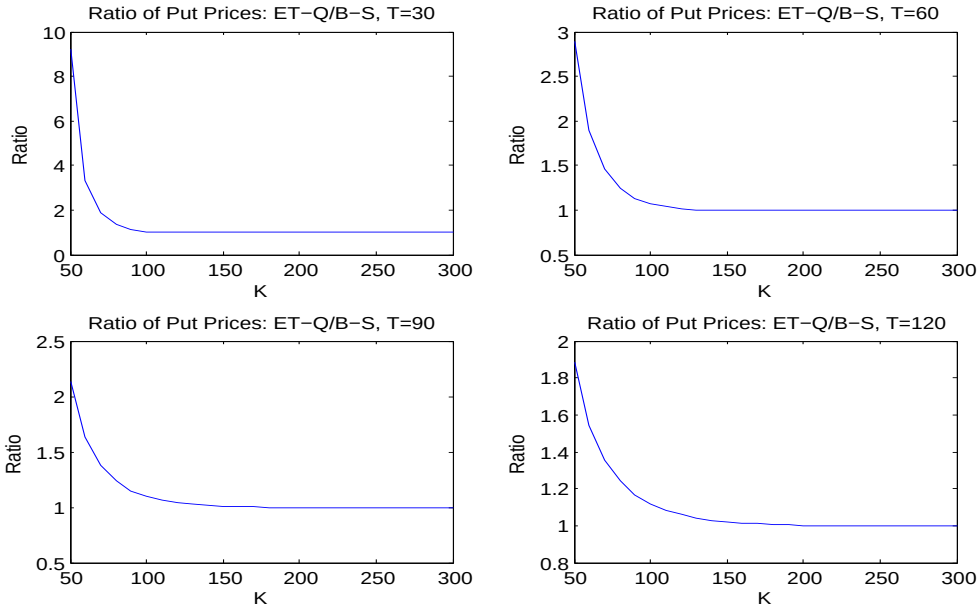

Figure 4.20: Put Option Price Ratio: ET-$\mathbb{Q}$/B-S

Y-axis: put price ratios $P_p^{ET-\mathbb{Q}}/P_p^{B-S}$; X–axis: strike prices $K = 0, \ldots, 300; S_0 = 100$.

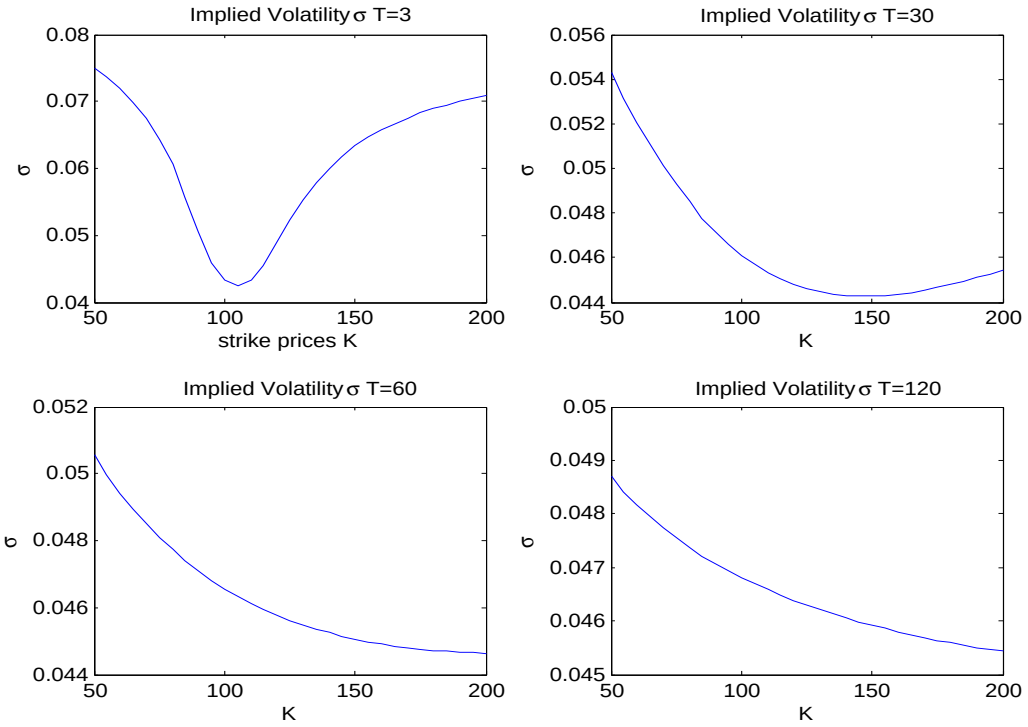

Figure 4.21: Volatility Smile Implied from the Option Prices under ET-$\mathbb{Q}$ Method

all regimes, i.e., in the long run,

$$\lim_{T\to\infty}\left[\mathsf{E}^{\mathbb{P}}\left(R_{[ij]}|\rho_0=1\right),\mathsf{E}^{\mathbb{P}}\left(R_{[ij]}|\rho_0=2\right)\right]=\left[\pi_{[ij]},\pi_{[ij]}\right].$$

Consequently, in the long term, the underlying distributions converges to each other, and the option price difference diminishes with regard to different ρ_0.

Example 15. Figure 4.23 illustrates the bell shapes of $P^{\mathbb{Q}_2}-P^{\mathbb{Q}_1}$ against the initial underlying asset price S_0, with the two risk neutral measures $\mathbb{Q}_1$ and $\mathbb{Q}_2$ satisfying $\mathbb{Q}_2 >_{LTO} \mathbb{Q}_1$ and $\mathbb{Q}_2 >_{RTO} \mathbb{Q}_1$ at a $k\in\mathbb{R}$. More specifically, under the RSLN2 models, the risk neutral distribution of S_T conditional on $\rho_0=2$ has thicker tails than the distribution conditional on $\rho_0=1$. As a result, $\mathbb{Q}_i$ refers to the pricing measure conditional on $\rho_0=i$, and satisfies the claimed tail ordering relationship. According to the Remark 4.3.2, the option prices obtained from $\mathbb{Q}_1$ and $\mathbb{Q}_2$ are different and their difference has a bell shape against S_0. This result is observed in

Figure 4.23, for both call and put options.

4.4 Summary and Conclusion

In this chapter, we show the restriction of applying strict stochastic ordering for comparing distributions under different risk neutral measures. As a result, we define right and left tail ordering as a tool. With this tool, we study the hedging results, by comparing the defined effective hedging ranges for European call and put options for single period discrete time delta hedging errors. We also investigate the option prices using the tail ordering, and use the results of option price ratios to deduct the implication of implied volatility smiles. In a conclusion, the difference in the tail thickness under different risk neutral measures can be represented by tail ordering. This ordering may be an effective tool for pricing and hedging analysis.

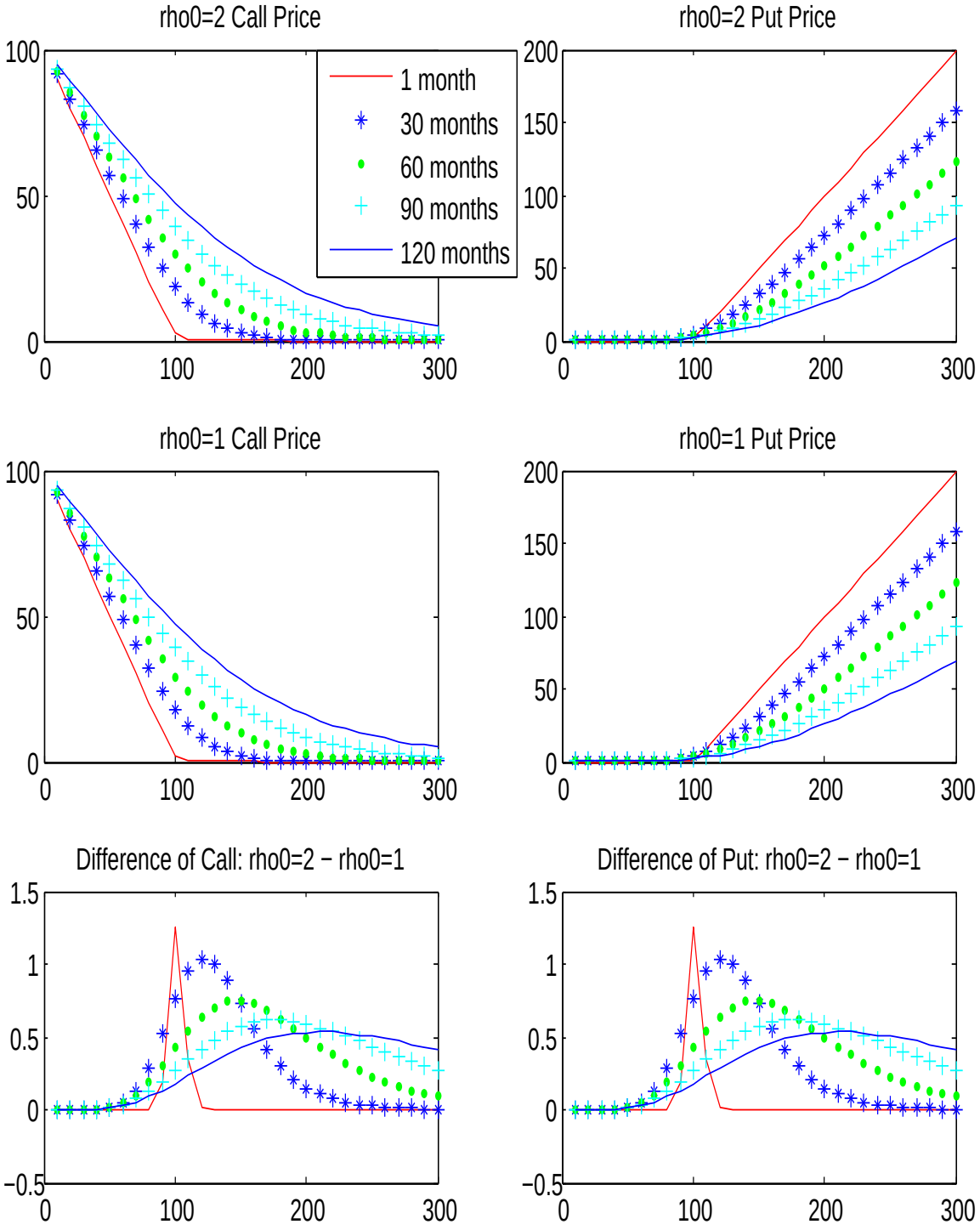

Figure 4.22: Bell shapes of price difference $P_{\rho_0=2} - P_{\rho_0=1}$ against K under the RSLN2 models, with different maturities (1 month - 120 months) at Example 14.

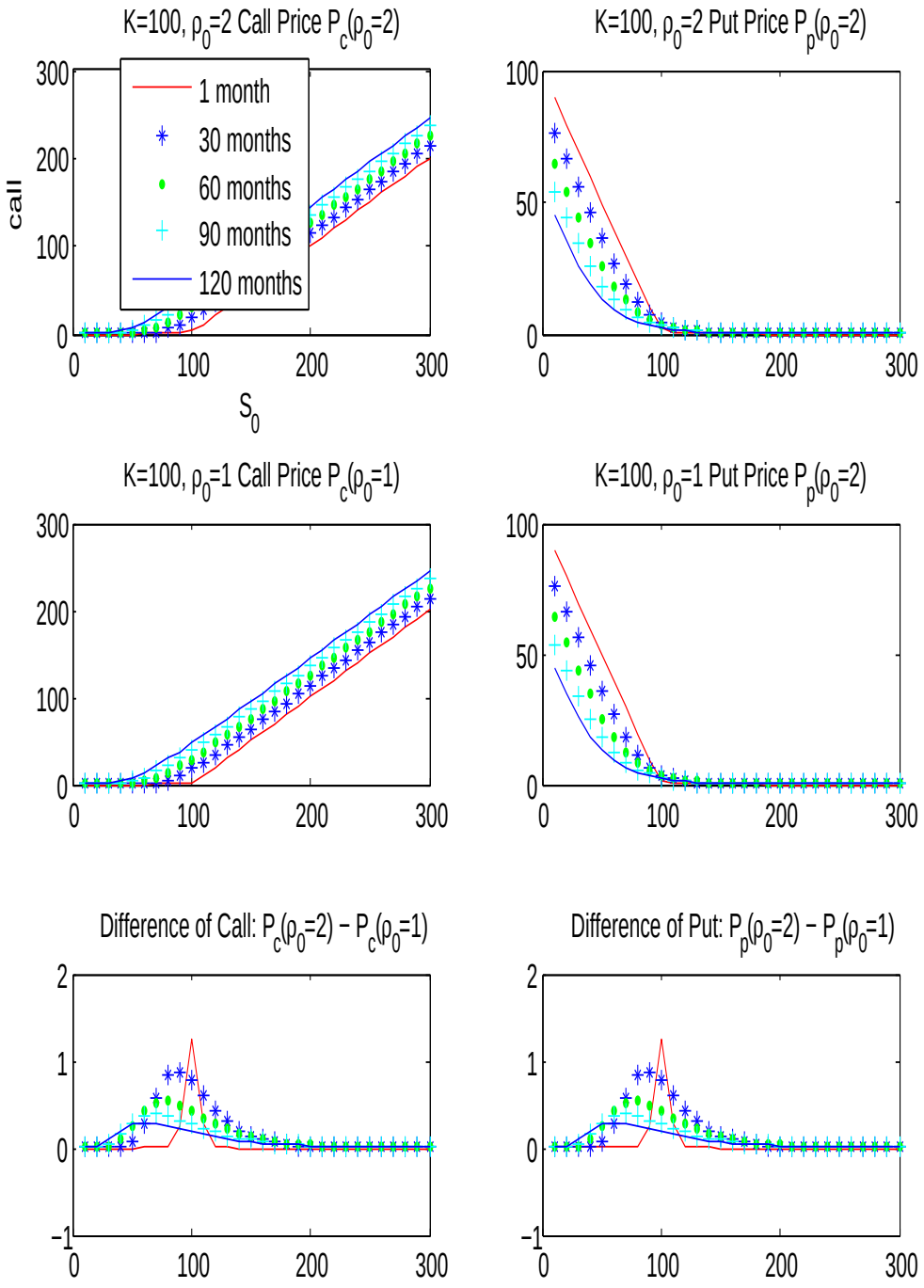

Figure 4.23: Bell shapes of price difference $P_{\rho_1=2} - P_{\rho_1=1}$ against S_0 under the RSLN2 models, with different maturities (1 month - 120 months) at Example 15.

Chapter 5

Conclusion and Future Works

The regime switching lognormal model is widely used to model the asset price processes in an incomplete market. Pricing and hedging derivative under such a model is of great interest. To price under the no arbitrage condition, we need an equivalent martingale measure. However, under regime switching models, the market is incomplete, and hence there is an infinite number of equivalent martingale measures. In my thesis, I adopted the risk neutral conditional Esscher transform to determine an equivalent martingale measure (ET-$\mathbb{Q}$), and formally proved that the market will not admit arbitrage opportunity if options are priced under such a equivalent martingale measure.

In my research up to now, I have focused on European options. The resulting pricing formula developed based on the ET-$\mathbb{Q}$ is expressed as a double expectation, where the inner expectation can be calculated by the usual Black-Scholes formula conditional on the regime paths, while the outer expectation is the average over all possible regime paths. As the number of the regime paths increases exponentially with the length of the expiration, I developed an iteration algorithm to efficiently reduce the number from an exponential time to a polynomial time. Moreover, I also conducted some comparison between the prices for European options obtained by our ET-$\mathbb{Q}$ method with those by the Black–Scholes method and the NEMM method. The ET-$\mathbb{Q}$ method captures interesting characteristics for option prices and displays

its advantage in a preliminary hedging study.

We apply the Esscher transform to risk neutral pricing for derivatives on multiple assets under the discrete time regime switching processes. The option prices are calculated using double expectations, with the inner expectation calculated conditional on a fixed regime transition path. For the inner expectation, there is no uncertainty for regime transition involved and hence we can borrow many developed pricing methods available in literature. Through the study on multivariate options, we investigated various multivariate pricing issues such as the impact of different dependence structure.

Besides pricing, we analyzed hedging by comparing delta hedging performance from three different risk neutral methods (the Black-Scholes method, the NEMM method and the ET-$\mathbb{Q}$ method) along with the study of hedging performance from the mean variance hedging method, under the regime switching lognormal models. The study shows that the ET-$\mathbb{Q}$ method provides consistent better protection, at extra costs, for out–of–money put options with different length of maturities, in terms of hedging loss probabilities, expected hedging loss, and the positions of effective hedging ranges.

We further study delta hedging for more general incomplete markets with the choice of different risk neutral measures. By exploiting the so-called tail stochastic ordering, and more specifically the monotonic behavior of the ratio of two probability densities in the tails, we study the pricing and delta hedging difference for European options under two different risk neutral pricing measures. The analysis also helps to better understand some practical issues, such as volatility smiles.

5.1 Future Work

Capitalizing on the momentum of my research program, I plan to explore further in directions of both hedging and pricing options under regime switching models. For example, I plan to explore the application of the Esscher transform to more complex derivatives, and for dynamic hedging strategies in the incomplete markets

models incorporating the regime switching process. Some of my future plans are listed below.

5.1.1 Bermudan and Other Path-dependent Options

Our pricing method is developed for long term options; thus it is of interest to apply it to the embedded options in insurance and annuity products. Many of these are path-dependent. It may be difficult to directly apply the regime path reduction developed in chapter 1. We may instead use simulation, with variance reduction, for pricing. We plan to start with the Bermudan option.

A Bermudan option gives the owner the right to exercise the option at a set of discrete times. The free exercising time raises difficulty in determining the no-arbitrage price. Motivated by prevalent tools in pricing the American put options, I plan to explore the value of the Bermuda put option by solving a discrete time optimal stopping problem.

Assume a discrete time line $t = 0, \ldots, T$, and consider the time 0 price of a Bermudan put option with maturity date at T. Let $\hat{\tau}$ represent the optimal exercising time. Then, $\hat{\tau}$ is the solution to the following optimization problem:

$$\hat{\tau} = \arg\max_{\tau} \mathsf{E}^{\mathbb{Q}}[e^{-r\tau}(K - S_\tau)^+], \tag{5.1.1}$$

and the option price is

$$\mathsf{E}^{\mathbb{Q}}[e^{-r\hat{\tau}}V_{\hat{\tau}}]. \tag{5.1.2}$$

To determine $\hat{\tau}$, we solve the optimization by the backward dynamic programming, which is a sequence of optimizations from $t = T - 1$ to $t = 0$, and achieve a sequence of values, denoted by $V_t, 0 \le t \le T$, as follows:

$$\begin{cases} V_T = (K - S_T)^+ \\ V_t = \max[\,(K - S_t)^+, e^{-r}\mathsf{E}^{\mathbb{Q}}(V_{t+1}|\mathcal{F}_t)\,], \qquad 0 \le t \le T-1, \end{cases} \tag{5.1.3}$$

where $(K - S_t)^+$ is called the intrinsic value at time t and $e^{-r}\mathsf{E}^{\mathbb{Q}}(V_{t+1}|\mathcal{F}_t)$ is called the continuing value, which is denoted by ξ_t and is $\mathcal{F}_t$–measurable. In dynamic programming, the value V_T, is the payoff of a put option. The value $V_t, 0 \leq t < T$ is the maximum of the intrinsic value and the continuing value. The value V_0 is the resulting option price. Based on backward dynamic programming, the optimal stopping time $\hat{\tau}$ is

$$\hat{\tau} = \min(t, t \in (0, 1, \ldots, T)|(K - S_t)^+ \geq \xi_t), \tag{5.1.4}$$

To determine the dynamic program under the RSLN2 models, we try to employ the risk neutral measure obtained by the Esscher transform, as described in chapter one, and to develop the no–arbitrage pricing methods. The no–arbitrage pricing should be feasible based on the extension of the pricing for European options, with additional consideration of all possible exercising times.

5.1.2 Alternative Multivariate Esscher Transforms

Based on different information of market data, it is also of interest to investigate alternative multivariate Esscher transforms to identify the unique risk neutral pricing measure. The following are some examples.

The Esscher Transform on the Returns of Asset Prices

Let $\eta_{s,l} = S_{s,l}/S_{s-1,l}$ and $\eta_{s,\bullet} = (\eta_{s,1}, \ldots, \eta_{s,N})$. Then, an alternative Esscher transform is defined on $\eta_{s,l}$ (Mcleish, 2005) as follows

$$\left.\frac{d\mathbb{Q}}{d\mathbb{P}}\right|_{\mathcal{F}_t} = \prod_{s=1}^{t} \frac{e^{\mathbf{h}'_{s,\bullet}\eta_{s,\bullet}}}{\mathsf{E}^{\mathbb{P}}(e^{\mathbf{h}'_{s,\bullet}\eta_{s,\bullet}}|\,\mathcal{F}_{s-1})}, \tag{5.1.5}$$

for $t = 1, \ldots, T$, and the Esscher transform parameters $h_{s,k}, k = 1, \ldots, N$ satisfies the following N equations

$$e^r = \frac{\mathsf{E}^{\mathbb{P}}[\eta_{s,l}\, e^{\mathbf{h}'_{s,\bullet}\eta_{s,\bullet}} | \mathcal{F}_{s-1}]}{\mathsf{E}^{\mathbb{P}}[e^{\mathbf{h}'_{s,\bullet}\eta_{s,\bullet}} | \mathcal{F}_{s-1}]} = \mathsf{E}^{\mathbb{Q}}\left[e^{Y_{s,l}} | \mathcal{F}_{s-1}\right], \; l = 1, \ldots, N, \tag{5.1.6}$$

for all $s = 1, \ldots, t$, where $\mathbb{Q}$ is identified by the Radon-Nikodym derivative (5.1.5). We denote the resulting $\mathbb{Q}$ as METS-$\mathbb{Q}$.

Based on the Esscher transform defined in (5.1.5), we can obtain the $\mathcal{F}_{t-1}$-measurability of $\mathbf{h}_{t,\bullet}$ (based on, say, the results of Corollary 2.5 in Brown (1986)). However, a disadvantage of using this approach is the existence of the moment generating function of $\eta_{t,\bullet} = (e^{Y_{t,1}}, \ldots, e^{Y_{t,N}})$ conditional on $\mathcal{F}_{t-1}$. However, this model is still worth being investigated for certain models, and has potential interest due to its relationship with entropy optimization.

Lemma 5.1.1. *The METS-$\mathbb{Q}$ measure identified through the Radon-Nikodym derivative (5.1.5) and conditions (5.1.6) is a risk neutral measure.*

Proof. As $\mathbf{h}_{s,\bullet} \in \mathcal{F}_{t-1}$ for $s \leq t$, we apply $\frac{d\mathbb{Q}}{d\mathbb{P}}\big|_{\mathcal{F}_t}$ defined in (5.1.5) as follows:

$$\begin{aligned}
\mathsf{E}^{\mathbb{Q}}\left(\frac{S_{t,l}}{S_{t-1,l}}\middle| \mathcal{F}_{t-1}\right) &= \mathsf{E}^{\mathbb{P}}\left[e^{Y_{t,l}} \frac{\frac{d\mathbb{Q}}{d\mathbb{P}}|_{\mathcal{F}_t}}{\frac{d\mathbb{Q}}{d\mathbb{P}}|_{\mathcal{F}_{t-1}}}\middle| \mathcal{F}_{t-1}\right] \\
&= \mathsf{E}^{\mathbb{P}}\left[\eta_{t,l} \frac{e^{\mathbf{h}'_{t,\bullet}\eta_{t,\bullet}}}{\mathsf{E}^{\mathbb{P}}[e^{\mathbf{h}'_{t,\bullet}\eta_{t,\bullet}}|\mathcal{F}_{t-1}]}\middle| \mathcal{F}_{t-1}\right] \\
&= e^r,
\end{aligned} \tag{5.1.7}$$

where $\eta_{s,l} = S_{s,l}/S_{s-1,l}$, and the last equation is given in the conditions (5.1.6) with $s = t$. Thus, the METS-$\mathbb{Q}$ measure is a risk neutral measure. □

Alternative Risk Neutral Conditions

Another alternative method to obtain the uniqueness of $\mathbf{h}_{t,\bullet}$ is based on the modification of the risk neutral conditions as follows. The Radon-Nikodym derivative

$d\mathbb{Q}/d\mathbb{P}|_{\mathcal{F}_t}$ defined as follows

$$\left.\frac{d\mathbb{Q}}{d\mathbb{P}}\right|_{\mathcal{F}_t} = \prod_{s=1}^{t} \frac{e^{\mathbf{h}'_{s,\bullet} y_{s,\bullet}}}{\mathsf{E}^{\mathbb{P}}(e^{\mathbf{h}'_{s,\bullet} Y_{s,\bullet}} | \, \mathcal{F}_{s-1})}, \quad t = 1, \ldots, T, \tag{5.1.8}$$

where the Esscher transform parameter $\mathbf{h}_{s,\bullet}$ satisfies the following N equations

$$r = \frac{\mathsf{E}^{\mathbb{P}}[\, Y_{s,l} e^{\mathbf{h}'_{s,\bullet} Y_{s,\bullet}} | \, \mathcal{F}_{s-1}\,]}{\mathsf{E}^{\mathbb{P}}[e^{\mathbf{h}'_{s,\bullet} Y_{s,\bullet}} | \, \mathcal{F}_{s-1}]} = \mathsf{E}^{\mathbb{Q}}\left[Y_{s,l} | \, \mathcal{F}_{s-1}\right], \; l = 1, \ldots, N, \tag{5.1.9}$$

for a constant risk free rate r and for $s = 1, \ldots, t$. The equivalent martingale measure identified by (5.1.8) is denoted by METY-$\mathbb{Q}$. Using this approach, we can achieve the $\mathcal{F}_{t-1}$-measurability of $\mathbf{h}_{t,\bullet}$. It is, however, a great challenge to develop the risk neutral pricing based on the new numeraire, the martingale process of $(Y_{t,\bullet})_t$, instead of stock prices.

Alternative Risk Neutral Conditions II

We may represent the underlying assets $Y_1, \ldots, Y_N$, using other random variables $Z_1, \ldots, Z_N$, as follows.

$$\begin{aligned} Y_{t,1} &= a_{1,0} + a_{11} Z_1 \\ Y_{t,2} &= a_{2,0} + a_{21} Z_1 + a_{22} Z_2 \\ &\cdots \\ Y_{t,N} &= a_{N,0} + a_{N1} Z_1 + a_{N2} Z_2 + \cdots + a_{NN} Z_N \end{aligned} \tag{5.1.10}$$

This representation is possible when $Y_{t,1}, \ldots, Y_{t,N}$ is multivariate normal. As a result, the Esscher transform parameters may be determined one by one, from $h_{t,1}$ associated with the risk neutral condition of $S_{t,1}$, to $h_{t,N}$ associated with that of $S_{t,N}$.

5.1.3 Other Topics

The following are some examples.

1. Consider optimal hedging under the RSLN2 model. In the RSLN2 model, the exact replicating function for $V(S_{t+1})$ is uncertain and dependent on ρ_{t+1}. As a result, the hedging may not be simply obtained from pricing, due to the lack of replicating process for regime switching. Thus, the hedging may use a dynamic optimization process. The hedging strategy at time t may be optimized based on the analysis of prices and hedging effects for different ρ_{t+1} according to results in chapter 4.

2. It may be of interest to investigate the more general form of univariate and multivariate Esscher transforms, and the possibility of representing an ad hoc risk neutral measure through the Esscher transform. In the literature, Kajima (2006) and Wang (2007) have studied the links between distortion and the Esscher transform; Monfort and Pegoraro (2012) have studied second moment Esscher transforms for asset pricing. We plan to incorporate other forms of transform on the underlying random variables into the Esscher transform to fit the selected risk neutral measures.

References

Ahmad, I. A. (2001). Testing stochastic ordering in tails of distribution. *Journal of Nonparametric Statistics*, *13*, 775-790.

Bawa, V. S. (1975). Optimal rules for ordering uncertain prospects. *Journal of Financial Economics*, *2*, 95-121.

Bertholon, H., Monfort, H., & Pegoraro, F. (n.d.). Econometric asset pricing modelling. *Journal of Financial Econometrics*, *6*(4), 407-458.

Bollen, N. P. B. (1998). Valuing options in regime–switching models. *Journal of Derivatives*, *6*(1), 38–49.

Boyle, P., Broadie, M., & Glasserman, P. (1997). Monte Carlo methods for security pricing. *Journal of Economic Dynamic and Control*, *21*(8-9), 1267-1321.

Boyle, P., & Liew, S. S. (2007). Asset allocation with hedging funds on the menu. *North American Actuarial Journal*, *11*(4), 1-21.

Brown, L. D. (1986). *Fundamentals of statistical exponential families with applications in statistical decision theory*. Hayward, CA: Institute of Mathematical Statistics, Lecture Notes-Monograph Series.

Bühlmann, H. (1980). An economic premium principle. *ASTIN Bulletin*, *11*, 52–60.

Bühlmann, H. (1983). The general economic premium principle. *ASTIN Bulletin*, *14*, 13–21.

Bühlmann, H., Delbaen, F., Embrechts, P., & Shiryaev, A. N. (1998). On Esscher transforms in discrete finance models. *ASTIN Bulletin*, *28*(2), 171–183.

Bühlmann, H., Delbaen, F., Embrechts, P., & Shiryaev, V. (1996). No–arbitrage, change of measure and conditional Esscher transforms. *CWI Quarterly*, *9*(4), 291–317.

Carr, P., & Madan, D. (1999). Option pricing and the fast Fourier transform. *Journal of Computational Finance*, *2*(4), 61–73.

Čížek, P., Härdle, W., & Weron, R. (2005). *Statistical tools for finance and insurance*. Berlin: Springer.

Christoffersen, P., Elkamhi, R., Feunou, B., & Jacobs, K. (2010). Option valuation with conditional heteroskedasticity and nonnormality. *Review of Financial Studies*, *23*(5), 2139-2183.

Denuit, M., Dhaene, J., Goovaerts, M., & Kaas, R. (2005). *Actuarial theory for dependent risks: Measures, orders and models*. New York: John Wiley & Sons, Ltd.

Duan, J. C. (1995). The Garch option pricing model. *Mathematical Finance*, *5*(1), 13–32.

Duan, J. C., Popova, I., & Ritchken, P. (2002). Option pricing under regime switching. *Quantitative Finance*, *2*(2), 116–132.

Elliott, R., Chan, L., & Siu, T. K. (2005). Option pricing and Esscher transform under regime switching. *Annals of Finance*, *1*(4), 423-432.

Elliott, R., & Madan, D. B. (1998). A discrete time equivalent martingale measure. *Mathematical Finance*, *8*(2), 127–152.

Eltoft, T., Kim, T., & Lee, T. W. (2006). On the multivariate Laplace distribution. *IEEE Signal Pocessing Letters*, *13*(5), 300-303.

Föllmer, H., & Schied, A. (2004). *Stochastic finance: An introduction in discrete time*. Berlin: Walter de Gruyter GmbH & Co. KG.

Föllmer, H., & Schweizer, M. (1991). Hedging of contingent claims under incomplete information. In M. H. A. Davis & R. J. Elliott (Eds.), *Applied stachastic analysis* (pp. 389–414). Gordon and Breach, London.

Föllmer, H., & Sondermann, D. (1986). Hedging of non-redundant contingent claims. In W. Hildenbrand & A. Mas-Colell (Eds.), *Contribution to mathematical economics. in honor of G. Debreu* (p. 205-223). Elsevier Science Publ., North-Holland (1986).

Gerber, H. U., & Shiu, E. S. W. (1994). Option pricing by Esscher transforms. *Transactions of the Society of Actuaries*, *46*, 99–140. (Discussions 141–91)

Goldfeld, S. M., & Quandt, R. E. (1973). A markov model for switching regressions. *Journal of Econometrics*, *1*, 3–16.

Gourieroux, C., & Monfort, A. (2007). Econometric specifications of stochastic discount factor models. *136*, 509-530.

Hadar, J., & Russell, W. R. (1969). Rules for ordering uncertain prospects. *American Economic Review*, *59*, 25-34.

Hamilton, J. D. (1989). A new approach to the economic analysis of nonstationary time series and the business cycle. *Econometrica*, *57*, 357–384.

Hardy, M. R. (2001). A regime switching model of long term stock returns. *North American Actuarial Journal*, *5*(2), 41–53.

Hardy, M. R. (2003). *Investment guarantees: Modeling and risk management for equity–linked life insuarance*. Hoboken, NJ: John Wiley & Sons, Inc.

Hardy, M. R. (2006). *An introduction to risk measures for actuarial applications*. Schaumburg, IL: Society of Actuaries - Study Notes.

Hardy, M. R., Freeland, R. K., & Till, M. C. (2006). Bootstrap validation of long term equity models. *North American Actuarial Journal*, *10*(4), 28-47.

Harrison, J. M., & Kreps, D. M. (1979). Martingales and atbitrage in multiperiod securities markets. *Journal of Economic Theory*, *20*, 381–408.

Harrison, J. M., & Pliska, S. R. (1981). Matingale and stochastic integrals in the theory of continuous trading. *Stochastic Processes and Their Applications*, *11*, 215–260.

Heston, S. L. (1993). A closed–form solution for options with stochastic volatility with applications to bond and currency options. *The Review of Financial Studies*, *6*(2), 327–43.

Hogg, R. V., Craig, A., & McKean, J. W. (2004). *Introduction to mathematical statistics* (6 ed.). Englewood Cliffs, NJ: Prentice Hall.

Höse, S., & Huschens, S. (2013). Stochastic orders and non-Gaussian risk factor models. *Review of Managerial Science*, *7*(2), 99-140.

Hull, J. C. (2006). *Options, futures, and other derivatives* (6 ed.). Englewood Cliffs, NJ: Prentice Hall.

Jarvis, S., Southall, F., & Varnell, E. (2001). *Modern valuation techniques*. Unpublished paper, presented to Stape Inn Actuarial Society, 6 February 2001.

Kaas, R., Goovaerts, M., Dhaene, J., & Denuit, M. (2008). *Modern actuarial risk theory using R* (2 ed.). Berlin: Springer.

Kahn, P. M. (1962). An introduction to collective risk theory and its application to stop–loss reinsurance. *Transactions of the Society of Actuaries*, *14*(40), 400-449.

Kajima, M. (2006). A multivariate extension of equilibrium pricing transforms: The multivariate Esscher and Wang transforms for pricing financial and insurance risks. *ASTIN Bulletin*, *36*(1), 269–283.

Kremer, E. (1982). A characterization of the Esscher transformation. *ASTIN Bulltin*, *13*(1), 57-59.

Lawler, G. F. (2006). *Introduction to stochastic processes*. Boca Ration, FL: Chapman & Hall/CRC.

Liew, C. C., & Siu, T. K. (2010). A hidden markov regime–switching model for option valuation. *Insurance: Mathematics and Economics*, *47*, 374–384.

Liu, Y. (2010). *Pricing and hedging the gurantanteed minimum withdrawal benefits in variable annuities*. PhD Thesis, University of Waterloo.

Mamon, R. S., & Rodrigo, M. R. (2005). Explicit solutions to european options in a regime–switching economy. *Operations Research Letters*, *33*, 581–586.

Manistre, B. J., & Hancock, G. H. (2005). Variance of the cte estimator. *North American Actuarial Journal*, *9*(2), 129–156.

Markowitz, H. M. (1952). Portfolio selection. *The Journal of Finance*, *7*(1), 77-91.

Markowitz, H. M. (1959). *Portfolio selection: Efficient diversification of investments*. New York: John Wiley & Sons.

McLeish, D. L. (2005). *Monte carlo simulation and finance*. Hoboken, NJ: John Wiley & Sons, Inc.

McNeil, A. J., Frey, R., & Embrechts, P. (2005). *Quantitative risk management*. Princeton, NJ: Princeton University Press.

Merton, R. C. (1976). Option pricing when the underlying stock returns are discontinuous. *Journal of Financial Economics*, *3*, 125-144.

Modigliani, F., & Miller, M. G. (1958). The cost of capital, corporation finance and the theory of investment. *The American Economic Review*, *48*(3), 261–97.

Monfort, A., & Pegoraro, F. (2010). Asset pricing with second-order Esscher transform. *Journal of Banking and Finance*, *36*, 1678-1687.

Musiela, M., & Rutkowski, M. (2004). *Martingale methods in financial modelling*. Berlin: Springer.

Naik, V. (1993). Option valuation and hedging strategies with jumps in the volatiity of asset returns. *The Journal of Finance*, *48*, 1969-1984.

Ng, A. C. Y., & Li, J. S. (2011). Valuing variable annuity guarantees with the multivariate Esscher transform. *Insurance, Mathematics and Economics*, *49*, 393–400.

Ng, C. T., Lim, J., & Hahn, K. S. (2011). Testing stochastic orders in tails of contingency tables. *Journal of Applied Statistics*, *38*(6), 1133-1149.

Panjer, H. (Ed.). (1998). *Financial economics with applications to investment, insurance and pensions*. Schaumburg, IL: The Actuarial Foundation.

Paolella, M. S. (2007). *Intermediate probability: A computational approach*. West Sussex, England: John Wiley & Sons, Inc.

Pennacchi, G. (2007). *Theory of asset pricing*. Englewood Cliffs, NJ: Prentice Hall.

Resnick, S. I. (1999). *A probability path*. New York: Birkhäuser Boston.

Ross, S. M. (1996). *Stochastic processes*. New York: John Wiley & Sons, Inc.

Shaked, M., & Shanthikumar, J. G. (2007). *Stochastic orders*. New York: Springer.

Siu, T. K. (2011). Regime–switching risk: to price or not to price? *International Journal of Stochastic Analysis*.

Song, N., Ching, W. K., Siu, T. K., Fung, E. S., & Ng, M. K. (2010). Option valuation under a multivariate markov chain model. *Third International Joint conference on Computational Science and Optimization, May 28-31, Huangshan, China*.

Stuart, A., & Ord, J. K. (1994). *Kendall's advanced theory of statistics*. Edward Arnold.

Till, M. C. (2011). *Actuarial inference and applications of hidden markov models*. PhD Thesis, University of Waterloo.

Vorst, T. (1992). Price and hedge ratios of average exchange rate options. *International Review of Financial Analysis*, *1*(3), 179–193.

Wang, S. (2007). Normalized exponential tilting: Pricing and measuring multvariate risks. *North American Actuarial Journal*, *11*(3), 89–99.

Yang, H. L. (2004). Esscher transform. In *Encyclopedia of actuarial science* (pp. 617–621). New York: John Wiley & Sons.

Yuen, F. L., & Yang, H. (2009). Option pricing in a jump–diffusion model with regime switching. *ASTIN Bulletin*, *39*(2), 515–539.

Zhou, X. Y., & Yin, G. (2004). Dynamic mean-variance portfolio selection with regime switching: A continuous-time model. *IEEE Transactions on Automatic Control*, *49*, 349-360.